

https://dspace.org/

Defining virus-antibody interplay during the development of HIV-1 neutralization breadth to inform vaccine design

Bhiman, Jinal Nomathemba

2016

http://hdl.handle.net/10539/22283

Bhiman, Jinal Nomathemba (2016) Defining virus-antibody interplay during the development of HIV-1 neutralization breadth to inform vaccine design, University of the Witwatersrand, Johannesburg, <http://hdl.handle.net/10539/22283>

Downloaded from a DSpace repository. https://dspace.org/

Defining virus-antibody interplay during the development of HIV-1 neutralization breadth to inform vaccine design

Jinal Nomathemba Bhiman

A thesis submitted to the School of Pathology, Faculty of Health Sciences, University of the Witwatersrand, Johannesburg, in fulfilment of the requirements for the degree of Doctor of Philosophy.

Johannesburg, 2016

Declaration

I **Jinal Nomathemba Bhiman** (Student number: 0408743N) am a student registered for the degree of Doctor of Philosophy in the academic year 2016.

I hereby declare the following:

- I am aware that plagiarism (the use of someone else's work without their permission and/or without acknowledging the original source) is wrong.
- I confirm that the work submitted for assessment for the above degree is my own unaided work except where I have explicitly indicated otherwise.
- I have followed the required conventions in referencing the thoughts and ideas of others.
- I understand that the University of the Witwatersrand may take disciplinary action against me if there is a belief that this is not my own unaided work or that I have failed to acknowledge the source of the ideas or words in my writing.
- I have included as an appendix a report from "Turnitin" (or other approved plagiarism detection) software indicating the level of plagiarism in my research document.

Signature: _____ Date: 4 June 2016

For Jinny, my saddest *dead-end*.

For Alex, Joy, Teresa, Faith and Brian, my *ancestors*.

For Amilcar, Alika, Tasanya, Melisha, Duane and Bentley, who take me *off* the science *track*.

For Penny and Lynn, for *developing* and *maturing* me into a scientist.

For Bradley, who *initiated* my scientific curiosity.

For Constantinos Kurt, who is *co-evolving* with me through this journey.

Presentations

Bhiman JN, Doria-Rose NA, Moore PL, Nonyane M, Khoza T, Abdool Karim SS, Kwong PD, Mascola JR and Morris L.
Interplay between broadly cross-neutralizing V2 monoclonal antibodies and autologous viral evolution.
Oral
AIDS Vaccine Conference. Barcelona, Spain. 2013.

Bhiman JN, Doria-Rose NA, Wibmer CK, Sheward DJ, Williamson C, Abdool Karim SS, Kwong PD, Mascola JR, Morris L and Moore PL.
Maturation of broadly neutralizing anti-HIV antibodies in the context of autologous viral escape.
Oral
WITS Research Day and Postgraduate Expo. Johannesburg, South Africa. 2014

Bhiman JN, Doria-Rose NA, Wibmer CK, Sheward DJ, Williamson C, Abdool Karim SS, Kwong PD, Mascola JR, Morris L and Moore PL.
Maturation of broadly neutralizing anti-HIV antibodies in the context of autologous viral escape.
Oral
HIV Research for Prevention, Cape Town, South Africa. 2014

Bhiman JN, Doria-Rose NA, Roark RS, Pancera M, Abdool Karim SS, Kwong PD, Mascola JR, Morris L and Moore PL.
Persistence of a broadly neutralizing antibody family despite complete viral escape.
Oral and poster
6th Infectious Diseases in Africa Symposium, Cape Town, South Africa. 2015

Bhiman JN. Anthony CA, Doria-Rose NA, Karimanzira O, Schramm CA, Khoza T, Kitchin D, Botha G, Gorman J, Garrett NJ, Abdool Karim SS, Shapiro L, Williamson C, Kwong PD, Mascola JR, Morris L and Moore PL.
Viral variants that initiate and drive maturation of V1V2-directed HIV-1 broadly neutralizing antibodies.
Oral
5th HIV Prevention Workshop, KwaZulu Natal, South Africa. 2015

Publications from this thesis

Doria-Rose NA*, Schramm CA*, Gorman J*, Moore PL*, **Bhiman JN**, DeKosky BJ, Ernandes MJ, Georgiev IS, Kim HJ, Pancera M, Staupe RP, Altae-Tran HR, Bailer RT, Crooks ET, Cupo A, Druz A, Garrett NJ, Hoi KH, Kong R, Louder MK, Longo NS, McKee K, Nonyane M, O'Dell S, Roark R, Rudicell RS, Schmidt SD, Sheward DJ, Soto C, Wibmer CK, Yang Y, Zhang Z, NISC Comparative Sequencing Program, Mulkin JC, Binley JM, Sanders RW, Wilson IA, Moore JP, Ward AB, Georgiou G, Williamson C, Adbool-Karim SS, Morris L, Kwong PD, Shapiro L and Mascola JR.

Developmental pathway for potent V1V2-directed HIV-neutralizing antibodies.

Nature. 2014: 509: 55-62.

PMID: 24590074; PMCID: PMC4395007.

*Joint first authors

Doria-Rose NA, **Bhiman JN**, Roark RS, Schramm CA, Gorman J, Chuang G-Y, Pancera M, Cale EM, Ernandes MJ, Louder MK, Asokan M, Bailer RT, Druz A, Fraschilla IR, Garrett NJ, Jarosinski M, Lynch RM, McKee K, O'Dell S, Pegu A, Schmidt SD, Staupe RP, Sutton MS, Wang K, Wibmer CK, Haynes BF, Abdool-Karim S, Shapiro L, Kwong PD, Moore PL, Morris L, Mascola JR.

New member of the V1V2-directed CAP256-VRC26 lineage that shows increased breadth and exceptional potency.

Journal of Virology. 2016: 90: 76–91. doi:10.1128/JVI.01791-15.

PMID: 26468542

Bhiman JN, Anthony C, Doria-Rose NA, Karimanzira O, Schramm CA, Khoza T, Kitchin D, Botha G, Gorman J, Garrett NJ, Abdool Karim SS, Shapiro L, Williamson C, Kwong PD, Mascola JR, Morris L, Moore PL.

Viral variants that initiate and drive maturation of V1V2-directed HIV-1 broadly neutralizing antibodies.

Nature Medicine. 2015: 21(11): 1332-6.

PMID: 26457756; PMCID: PMC4637988 [Available on 2016-05-01].

Other publications

Moore PL, Gray ES, Wibmer CK, **Bhiman JN**, Nonyane M, Sheward DJ, Hermanus T, Bajimaya S, Tumba NL, Abrahams MR, Lambson BE, Ranchobe N, Ping L, Ngandu N, Abdool Karim Q, Abdool Karim SS, Swanstrom RI, Seaman MS, Williamson C, Morris L.
Evolution of an HIV glycan-dependent broadly neutralizing antibody epitope through immune escape.
Nature Medicine. 2012: 18(11): 1688-92.
PMID: 23086475; PMCID: PMC3494733.

Wibmer CK, **Bhiman JN**, Gray ES, Tumba N, Abdool Karim SS, Williamson C, Morris L and Moore PL.
Viral escape from HIV-1 neutralizing antibodies drives increased plasma neutralization breadth through sequential recognition of multiple epitopes and immunotypes.
PLoS Pathogens. 2013: October 9(10):e1003738. doi: 10.1371/journal.ppat.1003738.
PMID: 24204277; PMCID: PMC3814426.

Bradley T*, Fera D*, **Bhiman J**, Eslamizar L, Lu X, Anasti K, Zhang R, Sutherland LL, Scearce RM, Bowman CM, Stolarchuk C, Lloyd KE, Parks R, Eaton A, Foulger A, Nie X, Karim SS, Barnett S, Kelsoe G, Kepler TB, Alam SM, Montefiori DC, Moody MA, Liao HX, Morris L, Santra S, Harrison SC, Haynes BF.
Structural Constraints of Vaccine-Induced Tier-2 Autologous HIV Neutralizing Antibodies Targeting the Receptor-Binding Site.
Cell Reports. 2016: January 5;14(1): 43-54. doi:10.1016/j.celrep.2015.12.017.
PMID: 26725118
*Joint first authors

Abstract

Human Immunodeficiency Virus Type 1 (HIV-1) infects approximately two million people annually, highlighting the need for a preventative vaccine. An effective HIV-1 vaccine will likely need to elicit broadly neutralizing antibodies (bNAbs), which arise naturally in some infected individuals and recognize the envelopes (Env) of multiple HIV-1 strains. Understanding the molecular events that contribute to bNAb development during infection may provide a blueprint for vaccine strategies. Here we investigated the development of a V1V2-directed bNAb lineage in the context of viral co-evolution in an HIV-1 superinfected participant (CAP256). For this, clonally-related monoclonal antibodies (mAbs), with a range of neutralization breadth, were isolated. We determined their developmental pathway from strain-specificity towards neutralization breadth and identified viral variants responsible for initiating and maturing this bNAb lineage.

MAbs were isolated by memory B cell culture or trimer-specific single B cell sorting and extensively characterized by Env-pseudotyped neutralization, cell surface-expressed Env binding, electron microscopy and epitope-predictive algorithms. Antibody next-generation sequencing (NGS) at multiple time-points enabled the inference of the unmutated common ancestor (UCA) of this lineage. Viral co-evolution was investigated using Env single genome amplification and V1V2 NGS.

A family of 33 clonally-related mAbs, CAP256-VRC26.01-33, was isolated from samples spanning four years of infection. The UCA of this lineage possessed an unusually long heavy chain complementarity determining region 3 (CDRH3), which resulted from a unique recombination event. Surprisingly, this UCA potently neutralized later viral variants that had evolved from the superinfecting virus, which we termed bNAb-initiating Envs. Viral diversification, which peaked prior to the development of neutralization breadth, created multiple immunotypes at key residues in the V1V2 epitope. Exposure to these immunotypes allowed adaptation of some mAbs to tolerate this variation and thus mature towards neutralization breadth.

Based on these data, we proposed a four-step immunization strategy which includes priming with bNAb-initiating Envs to engage rare B cells with a long CDRH3; followed by three sequential boosts (including select V1V2 immunotypes) to drive antibody maturation. In conclusion, this study has generated a testable HIV-1 vaccine immunization strategy through the delineation of mAb-virus co-evolution during the development of neutralization breadth.

Acknowledgements

I would like to acknowledge:

- My supervisor Prof Penny Moore, who has been more than simply a mentor to a "terrible student" and who has given so selflessly of her time and energy to developing my confidence, scientific thinking and career.

- My co-supervisor, Prof Lynn Morris, for her positive encouragement, gentle prodding (which despite my protests, is always in the right direction) and for teaching me to aim high.

- Dr John Mascola and all the members of the Vaccine Research Center Humoral Immunology Section for hosting me during my Fogarty traineeships in 2012 and 2014. I would especially like to thank Dr Nicole Doria-Rose for her guidance, mentorship, friendship and random purple M&M deliveries.

- Past and present members of the Morris Lab for constant encouragement, advice, help with experiments and corridor conversations. In particular I would like to thank: Dr Bronwen Lambson for proof-reading my integrated narrative and all included publications; Sheila Doig and Carina Kriel for organizing all my funding and WITS-related admin and for downloading numerous articles for my literature review; Sue Hermann and Michelle Reddy for processing all my reagent and consumable orders; Jaymati Patel for resolving all my equipment-related problems.

- The Center for the AIDS Programme of Research in South Africa (CAPRISA) and the participants of the CAPRISA 002 cohort, without whom this study would not have been possible.

- The Poliomyelitis Research Foundation for grant and bursary funding (grant numbers 14/17 and 13/43 respectively), a University of the Witwatersrand Post-graduate Merit Award, a National Research Foundation (NRF) Innovation Doctoral Scholarship, a Department of Science NRF Women in Science PhD Fellowship and a L'Oreal-UNESCO For Women In Science PhD Fellowship. (Opinions expressed and conclusions arrived at, are those of the author and are not necessarily to be attributed to the NRF.)

- The Columbia University-Southern African Fogarty AIDS International Training and Research Program (AITRP) through the Fogarty International Centre, National Institutes of Health (NIH) (grant number: 5 D43 TW000231) for funding two short-term traineeships to the Vaccine Research Center, NIAID/NIH.

- My friends, Natasha, Zaida and Sherwin for much needed breaks, countless celebrations and "Ctrl Alt Delete."

- The Bhiman, Peter and Bickford-Wibmer families, because each of you has played a role in shaping my life and bringing me this far. With special thanks to my father, Alex Bhiman, for understanding when I could not visit and for supporting me through every important decision; my siblings, Amilcar and Alika Bhiman for the love, fun and much needed distractions; my husband Kurt for being my confidant, chauffeur, chef, biggest fan and personal trainer and for suffering my grumpiness during stressful periods.

Table of Contents

Declaration ii
Dedication iii
Presentations iv
Publications from this thesis v
Other publications vi
Abstract vii
Acknowledgements ix
Table of Contents xi
List of Figures xiii
Abbreviations xiv
General Abbreviations xiv
Symbols and Units xvii
Amino Acid Abbreviations xvii
Part 1: Integrated narrative 1
1. The global HIV-1 epidemic 2
2. HIV-1 prevention 2
2.1. Antiretroviral drugs as prevention tools 2
2.2. HIV-1 vaccines 3
3. HIV-1 5
3.1 The origins of HIV-1 5
3.2. HIV-1 genome and virion organization 6
4. The HIV-1 envelope (Env) 7
4.1. HIV-1 Env structure and function 7
4.2. HIV-1 Env biosynthesis 11
5. B cell responses to the HIV-1 Env 12
5.1. B cell diversity 12
5.2. Anti-HIV-1 neutralizing antibodies and HIV-1 Env immune evasion 15
5.3. Role of NAb responses in HIV-1 prevention 16
6. Anti-HIV-1 broadly neutralizing antibodies (bNAbs) 17
6.1. BNAb targets 17

6.2. Broadly neutralizing plasma antibodies in CAPRISA participant, CAP256 20
6.3. Anti-HIV-1 bNAb isolation 22
7. V1V2-directed bNAbs 26
7.1 The conformational V1V2 Env epitope 26
7.2. Origin of the long CDRH3 29
8. Virus-antibody co-evolution: a blueprint for vaccine design 30
8.1. Viral escape from NAbs 30
8.2 Tracking bNAb repertoires 31
8.3 Virus-antibody co-evolution and the development of neutralization breadth 32
8.4. Initiation of bNAb precursors 35
8.5. The role of viral evolution in driving neutralization breadth 36
8.6 Caveats and implications for vaccine design 38
8.7. Conclusion 40
9. References 41
Part 2: Publications 59
1. Developmental pathway for potent V1V2-directed HIV-neutralizing antibodies 60
Paper 1: Supplementary Information 85
2. New member of the V1V2-directed CAP256-VRC26 lineage that shows increased breadth and exceptional potency 110
Paper 2: Supplementary Info 127
3. Viral variants that initiate and drive maturation of V1V2-directed HIV-1 broadly neutralizing antibodies 148
Paper 3: Supplementary Information 156
Appendix 1: Letter of Support 157
Appendix 2: Turnitin Report 158
Appendix 3: Change of Title 159
Appendix 4: Ethics Clearance 160
Appendix 5: Copyright Permissions 161
1. Nature and Nature Medicine 161
2. Journal of Virology 162

List of Figures

Figure 1. Global distribution of antiretroviral use among HIV-1 infected individuals. 3
Figure 2. HIV-1 vaccine phase III efficacy trials. 4
Figure 3. Genome and particle organization of HIV-1. 7
Figure 4. Regions of gp120 and gp41. 8
Figure 5. Structure of the pre- and post-fusion HIV-1 Env. 9
Figure 6. Post-translational processing of N-linked glycans. 12
Figure 7. Antibody structure. 13
Figure 8. Generation of antibody heavy chain diversity and variable region organization. ...14
Figure 9. Broadly neutralizing antibody (bNAb) targets on the prefusion HIV-1 Env trimer. .18
Figure 10. Neutralization of autologous and heterologous viruses by CAP256 plasma. 21
Figure 11. CAP256 viral load and $CD4^+$ T cell count data over 259 weeks of HIV-1 infection. 22
Figure 12. Monoclonal antibody isolation using high-throughput B cell culture and antigen-specific B cell sorting. 24
Figure 13. Structure of the V1V2 broadly neutralizing antibody epitope. 27
Figure 14. Broadly neutralizing V1V2-directed antibody characteristics. 28
Figure 15. Schematic diagram depicting the anti-HIV-1 neutralizing antibody (NAb) response over time. 30
Figure 16. Maturation of the CH103 CD4 binding site mAb lineage towards neutralization breadth. 33
Figure 17. Maturation of the CAP256-VRC26 V1V2-directed mAb lineage towards neutralization breadth. 34
Figure 18. Relationship between CAP256-VRC26 antibody neutralization breadth and tolerance of multiple immunotypes at positions 169 and 166. 38
Figure 19. Recapitulating viral evolution for vaccine design. 39

Abbreviations

General Abbreviations

A:	Adenine
Ad5:	Adenovirus serotype 5
ADCC:	Antibody-dependent cellular cytotoxicity
AID:	Activation-induced cytidine deaminase
AIDS:	Acquired Immunodeficiency Syndrome
APC:	Allophycocyanin
ART:	Antiretroviral therapy
ARV:	Antiretroviral
BCR:	B cell antigen receptor
BLAST:	Basic local alignment search tool
bNAb:	Broadly neutralizing antibody
bp:	Base pairs
C:	Cytosine
C gene:	Constant gene
C1:	Constant region 1
C2:	Constant region 2
C3:	Constant region 3
C4:	Constant region 4
C5:	Constant region 5
CA:	Capsid
CAPRISA:	Centre for the AIDS Programme of Research in South Africa
CCR5:	C-C chemokine receptor type 5
CD4:	Cluster of differentiation 4
CD4bs:	CD4 binding site
CD3:	Cluster of differentiation 3
CD4:	Cluster of differentiation 4
CD8:	Cluster of differentiation 8
CD14:	Cluster of differentiation 14
CD16:	Cluster of differentiation 16
CD19:	Cluster of differentiation 19
CD40L:	Cluster of differentiation 40 ligand
cDNA:	Complementary DNA
CDR:	Complementarity determining region
CDRH3:	Complementarity determining region 3 in the heavy chain
CDRL3:	Complementarity determining region 3 in the light chain
C terminus:	Carboxyl terminus
CRF:	Circulating recombinant form
CXCR4:	C-X-C chemokine receptor type 4
DEAE-dextran:	Diethylaminoethyl dextran
D gene:	Diversity gene
DNA:	Deoxyribonucleic acid

dNTPs:	Deoxynucleoside triphosphates
ddNTPs:	Dideoxynucleoside triphosphates
DMEM:	Dulbecco's Modified Eagle Medium
EBV:	Epstein-Barr virus
EDTA:	Ethylenediaminetetraacetic acid
ELISA:	Enzyme-linked immunosorbent assay
EM:	Electron microscopy
Env:	Envelope
eOD-GT:	engineered outer domain germline targeting
Fab:	Fragment antigen binding region
FBS:	Foetal bovine serum
Fc:	Fragment crystallizable
FcRN:	Neonatal Fc receptor
FDC:	Follicular dendritic cell
FR:	Framework region
FSC:	Forward scatter
G:	Guanine
Gag:	Group associated antigen protein
Glc:	Glucose
GlcNAc:	N-acetyl glucosamine
GnTI, II, IV, V	N-acetylglucosamine transferase I, II, IV, V
gp120:	Glycoprotein 120 kDa
gp41:	Glycoprotein 41 kDa
HEK:	Human embryonic kidney
HEPES:	4-(2-hydroxyethyl)-1-piperazineethanesulfonic acid
HIV-1:	Human Immunodeficiency Virus Type-1
HIV-2:	Human Immunodeficiency Virus Type-2
HIVIG:	HIV immune globulin
HLA:	Human leukocyte antigen
HR1:	Heptad repeat 1
HR2:	Heptad repeat 2
ID_{50}:	50% inhibitory dilution
IC_{50}:	50% inhibitory concentration
Ig:	Immunoglobulin
IgM, D, G, A and E:	Immunoglobulin M, D, G, A and E
IL:	Interleukin
IMGT:	Immunogenetics database
IN:	Integrase
Indels:	Insertions and deletions
J gene:	Joining gene
JH:	Joining gene of the heavy chain
LTR:	Long terminal repeat
MA:	matrix
mAb:	monoclonal antibody
Man:	Mannose
MES:	2-ethanesulfonic acid
MFI:	Median fluorescence intensity
$MgCl_2$:	Magnesium chloride
MPD:	2-Methyl-2,4-pentanediol
MPER:	Membrane proximal external region
NAb:	Neutralizing antibody

NaCl:	Sodium chloride
NC:	Nucleocapsid
Nef:	Negative regulatory factor
NGS:	Next-generation sequencing
NHP:	Non-human primate
N terminus:	Amino terminus
ORF:	Open reading frame
PBMC:	Peripheral blood mononuclear cell
PBS:	Phosphate buffered saline
PCR:	Polymerase chain reaction
PDB ID:	Protein data bank identity
PEG:	Polyethylene glycol
PEI:	Polyethylenimine
p.i:	Post-infection
PI virus:	Primary infecting virus
PNG:	Potential N-linked glycan
Pol:	Polymerase
PR:	Protease
PrEP:	Pre-exposure prophylaxis
PSV:	Pseudovirus
RAG:	Recombination activating gene
Rev:	Regulator of expression of viral proteins
RLU:	Relative light units
RNA:	Ribonucleic acid
R-PE:	R-phycoerythrin
RT:	Reverse transcriptase
RT-PCR:	Reverse transcription polymerase chain reaction
sCD4:	Soluble cluster of differentiation 4
SDS:	Sodium dodecyl sulphate
SGA:	Single genome amplification
SHIV:	Simian-human immunodeficiency chimeric virus
SHM:	Somatic hypermutation
SIV:	Simian Immunodeficiency Virus
SU virus:	Superinfecting virus
T:	Thymine
Tat:	Trans-activator of transcription
TdT:	Terminal deoxynucleotidyl transferase
T/F virus:	Transmitted/founder virus
Tfh:	T follicular helper
Tris:	Tris (hydroxymethyl) aminomethane
UCA:	Unmutated common ancestor
UNAIDS:	United Nations programme on HIV/AIDS
V gene:	Variable gene
V1V2:	Variable regions 1 and 2
V3:	Variable region 3
V4:	Variable region 4
V5:	Variable region 5
VH:	Variable gene of the heavy chain
VL:	Variable gene of the light chain
VLP:	Virus-like particle
Vif:	Viral infectivity factor

Vpr:	Viral protein R
Vpu:	Viral protein U

Symbols and Units

Å:	Angstrom
α:	Alpha
β:	Beta
bp, kb:	Base pairs and kilobases
° C:	Degrees Celsius
Cl:	Chloride
G:	Relative centrifugal force
Mg:	Magnesium
mM, M:	Millimolar and molar
Na:	Sodium
ng, µg, mg:	Nano-, micro- and milligram
nm, µm, cm:	Nano-, micro and centimetre
pmol:	Picomole
rpm:	Revolutions per minute
SO_4:	Sulphate
µl, ml:	Micro- and millilitre
U:	Enzyme units of activity

Amino Acid Abbreviations

Amino Acid	Three-Letter Abbreviations	One-Letter Symbol
Alanine	Ala	A
Arginine	Arg	R
Asparagine	Asn	N
Aspartic acid	Asp	D
Cysteine	Cys	C
Glutamic acid	Glu	E
Glutamine	Gln	Q
Glycine	Gly	G
Histidine	His	H
Isoleucine	Ile	I
Leucine	Leu	L
Lysine	Lys	K
Methionine	Met	M
Phenylalanine	Phe	F
Proline	Pro	P
Serine	Ser	S
Threonine	Thr	T
Tryptophan	Trp	W
Tyrosine	Tyr	Y
Valine	Val	V

Part 1: Integrated narrative

1. The global HIV-1 epidemic

Thirty three years after the discovery of the Human Immunodeficiency Virus Type-1 (HIV-1) as the causative agent for Acquired Immunodeficiency Syndrome (AIDS), and despite numerous prevention and awareness campaigns, approximately 2 million new infections occur globally every year[1]. Of the more than 35 million people infected with HIV-1 worldwide, two thirds reside in sub-Saharan Africa, where young women are disproportionately affected[1]. In areas such as Vulindlela in KwaZulu Natal, South Africa, the HIV-1 prevalence in pregnant women between the ages of 20-24 is strikingly high at 45.5%[2], leading many young individuals to believe that HIV-1 infection is an unavoidable part of life. This resigned mind-set of the most at-risk populations puts into perspective the desperate need for an effective and robust HIV-1 prevention intervention, such as an HIV-1 vaccine.

2. HIV-1 prevention

2.1. Antiretroviral drugs as prevention tools

Since the discovery in 1983 of HIV-1 as the causal agent of AIDS, numerous prevention strategies have been tested. These include male circumcision[3,4] and condom use[5], but the most successful has been the use of antiretroviral (ARV) drugs as pre-exposure prophylaxis (PrEP) to prevent both vertical and horizontal transmission of HIV-1[6]. In South Africa, mother-to-child transmission has declined from 9.6% in 2008 to ~2.7% in 2011[7]. Studies involving discordant couples and homosexual men have shown 67-99% protection through the use of PrEP[8,9]. However while PrEP has been efficacious in clinical trials, its effect at a population level is less clear. Additionally, for HIV-1 infected individuals there is a large unmet need for ARV treatment. This is especially true in resource limited areas, such as South Africa where despite the largest treatment program in the world, only ~55% of HIV-1 infected individuals are on treatment (Figure 1)[1]. In addition, these ARV-based interventions rely on adherence in the absence of illness over an extended period of time. Despite the possibility of slow-release or long-acting ARVs in pills or vaginal ring formulations, other socio-economic barriers may limit the use of these types of strategies in rural communities that are most affected by this disease.

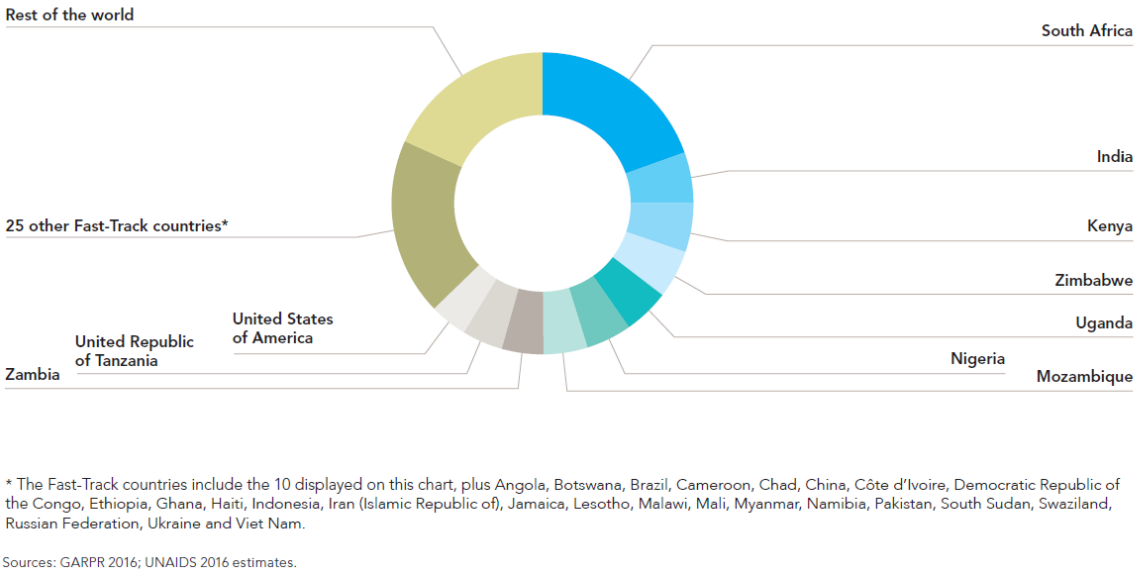


Figure 1. Global distribution of antiretroviral use among HIV-1 infected individuals.
Circular infographic indicating the proportion of HIV-1 infected individuals receiving antiretroviral treatment (ART) in various countries and regions. South Africa has the highest number of individuals on ART globally. Source: Global AIDS Update UNAIDS 2016[1].

2.2. HIV-1 vaccines

Apart from safe water, vaccines have had the largest effect in reducing pathogen-induced mortality[10]. The recent resurgence of measles in the US, largely due to an increase in vaccine hesitancy, highlights the impact of vaccines that rely on the herd effect[11]. Therefore, while a combination of prevention strategies will likely be the most effective solution to limiting the spread of HIV-1, a preventative HIV-1 vaccine is urgently needed.

The first candidate HIV-1 vaccine trial was sanctioned by the US Food and Drug Administration in 1987 and since then more than 218 clinical trials have been conducted[12]. However only 5 of these have progressed to phase III efficacy trials (Figure 2), with one vaccine trial, RV144, conducted in Thailand in 2009, showing 31% efficacy[13].

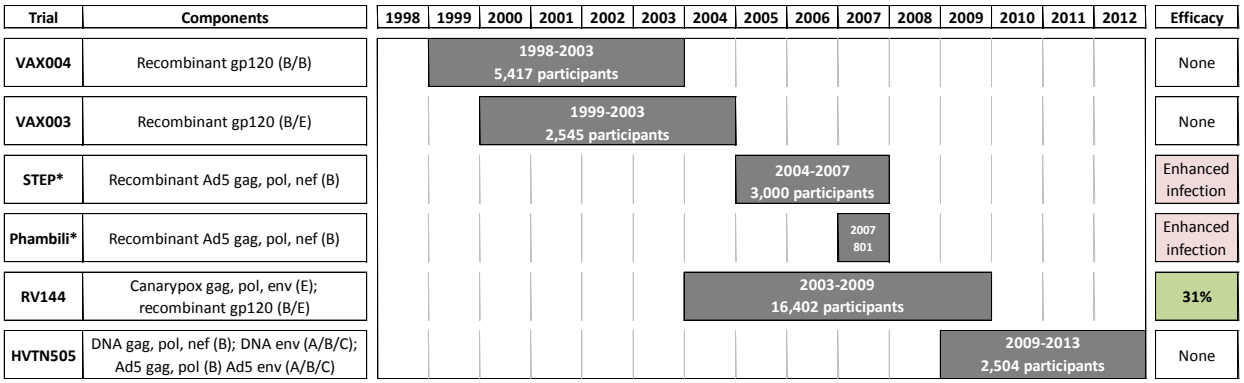


Figure 2. HIV-1 vaccine phase III efficacy trials.
Timeline showing start and end dates for the five HIV-1 vaccine efficacy trials, as well as the components and efficacy of each. Gray blocks show time frames as well as number of participants for each trial. The STEP and Phambili trials (marked by asterisks) tested the same vaccine regimen, but in different geographical areas. Adapted from Esparza 2013[12].

The first trials, VAX003 and VAX004, in North America and Thailand used two distinct gp120 proteins[14] (discussed below in section 3.2) and were conducted amid controversy regarding the scientific rationale for testing these vaccine candidates[15]. While these safe and immunogenic candidates had protected chimpanzees from HIV-1 infection, the strains used were highly sensitive lab-adapted viruses, which were not representative of primary or clinical isolates[16,17]. Therefore the failure of these vaccines[18,19], which aimed to induce antibody responses, in large scale efficacy trials in both populations was unsurprising.

This was followed in 2004 by the STEP trial, which used a recombinant adenovirus serotype 5 (Ad5) vector encoding the HIV-1 *gag*, *pol* and *nef* genes (described in section 3.2) to elicit T-cell responses[20]. Unfortunately, this trial was stopped after approximately 2 years, because an interim analysis showed that vaccinees had an increased rate of HIV-1 infection compared to those individuals who received the placebo[20]. This enhanced risk of infection was later attributed to the presence of a prior Ad5 antibody response and/or the circumcision status of the vaccinees[21]. A sister trial conducted in South Africa, called the HVTN 503/Phambili trial, using the same regimen as the STEP trial was stopped early due to these results[22].

The fifth efficacy trial, the HVTN 505, which included a DNA prime followed by an Ad5-vectored boost, was also stopped two years prior to the expected end date, because interim analysis showed that the vaccine afforded no protection from HIV-1 infection[23-25].

In contrast, the RV144 Thai trial, a prime-boost regimen (combining a canarypox ALVAC-HIV DNA prime, together with the AIDSVAX B/E bivalent gp120 protein boost), showed a modest 31% efficacy[13]. A correlates analysis, which compared the immune response in uninfected vaccinees, infected vaccinees and infected individuals who received the placebo, showed that the presence of V1V2-directed binding antibodies correlated inversely with HIV-1 infection, while IgA binding antibodies correlated directly with HIV-1 infection[26]. In addition low IgA binding antibody levels in association with high levels of antibody-dependent cellular cytotoxicity (ADCC) were inversely correlated with HIV-1 infection. As a result the RV144 trial has reinvigorated current vaccine endeavors and focused attention on the fragment crystallizable (Fc)-mediated effector functions of antibodies, such as ADCC. However a more effective vaccine will likely require the elicitation of broadly cross-neutralizing antibodies which are capable of tolerating the huge diversity among circulating HIV-1 strains.

3. HIV-1

3.1 The origins of HIV-1

HIV-1 is a retrovirus that is closely related to the less pathogenic HIV-2, both of which originated from zoonotic infections transferred to humans via primates. While Simian Immunodeficiency Virus (SIV) that infects sooty mangabeys (*Cercocebus atys*) is the ancestor of HIV-2[27], HIV-1 is derived from the SIV that infects chimpanzees (*Pan troglodytes*)[28-30]. HIV-1 has been sub-divided into 4 groups, which were each the result of a distinct cross-species transmission event, namely M (main), O (outlier), N (non-M, non-O) and P (putative)[31]. Collectively groups N and P infections have been confirmed in less than 20 people, and less than 1% of global infections are caused by group O viruses[32-34]. In contrast HIV-1 group M viruses dominate the current pandemic, having infected over 60 million people[31]. Group M has been further divided into 9 subtypes and more than 40 different circulating recombinant forms (CRFs), highlighting the enormous level of diversity amongst HIV-1 viral strains[31]. The first reports of AIDS in patients in the United States of America[35] and the subsequent identification of HIV-1 as the cause[36-38] occurred in the 1980's. However the earliest samples with confirmed HIV-1 infection date back to 1959[39,40]. In addition, recent epidemiological

studies have suggested that the time of the most recent common ancestor of pre-pandemic HIV-1 group M dates to the 1920s, with the zoonotic transmission from chimpanzees to humans occurring even earlier[41]. This suggests that HIV-1 has been infecting humans for at least 100 years.

3.2. HIV-1 genome and virion organization

HIV-1, a lentivirus of the *Retroviridae* family, has a ~9.8 kb ribonucleic acid (RNA) genome encoding nine open reading frames (ORFs) and a total of 15 viral proteins[42]. The *gag* and *env* ORFs are translated into two polyproteins that are subsequently cleaved into the six structural components that comprise the virion particle (Figure 3A). The *pol* gene encodes three enzymes, which perform four different catalytic activities required for the various stages of the HIV-1 life cycle. In addition the HIV-1 genome codes for six accessory proteins which are involved in various functions including the regulation of replication and virion assembly.

The mature HIV-1 particle, which is between 110 and 128 nm in size[43], is surrounded by the viral membrane (Figure 3B). Embedded within the membrane are the envelope (Env) glycoproteins, the functional form of which is composed of three glycoprotein 120-glycoprotein 41 (gp120-gp41) heterodimers. These functional Env trimers mediate entry into the host cell, however non-functional forms of Env[44] (discussed in section 5.2) are also present in the membrane and act as immunological decoys. Beneath the membrane are the matrix (MA) proteins, which are involved in the budding of new viruses from infected cells[42]. Within the MA is the conical core which is composed of capsid (CA) proteins that are important for transport of the viral genome into the host cell. The CA surrounds two identical viral RNA strands that are closely associated with the nucleocapsid (NC) and three viral enzymes, protease (PR), integrase (IN) and reverse transcriptase (RT), required for viral replication[42]. The viral RT, which possesses both polymerase and RNAse H activities, is extremely error-prone, with a mutation rate of 1 per 1700 nucleotides incorporated[45], contributing to the high level of diversity between and within HIV-1 subtypes.

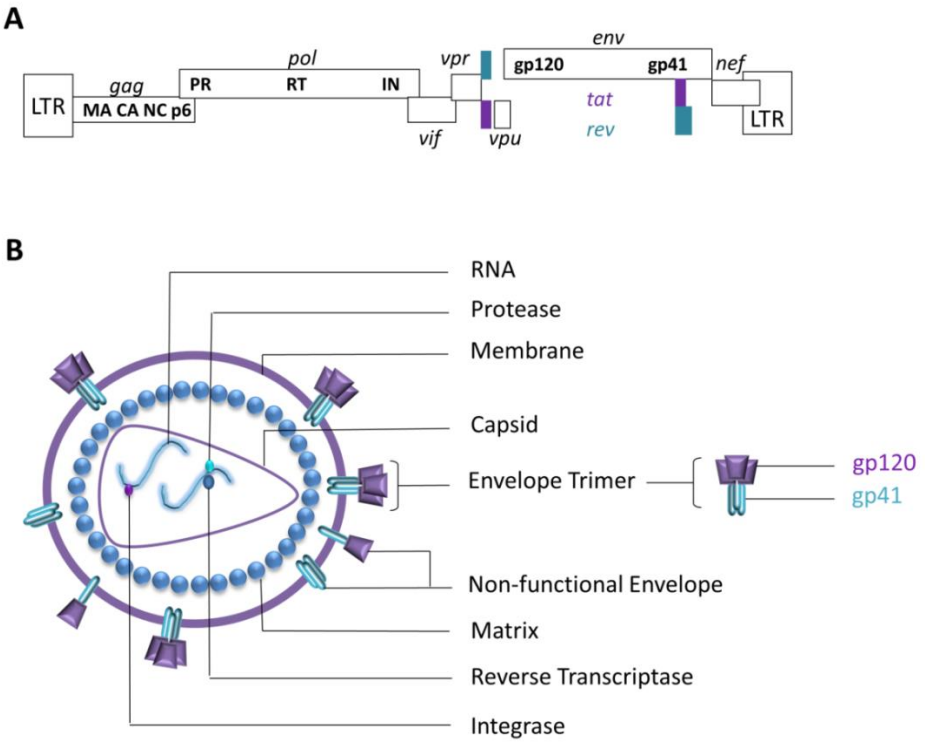


Figure 3. Genome and particle organization of HIV-1.
(A) Schematic diagram showing the location of the genetic elements within the HIV-1 genome. Long terminal repeat (LTR) segments flank nine open reading frames (*gag, pol, vif, vpr, vpu, env, nef, tat* and *rev*), two of which are discontinuous (*tat* in purple and *rev* in turquoise). The *gag* and *env* genes encode the structural components of the virion, namely the matrix (MA), capsid (CA), nucleocapsid (NC), glycoprotein 120 (gp120) and gp41 proteins. The *pol* gene codes for three HIV-1 enzymes, protease (PR), reverse transcriptase (RT) and integrase (IN). The remaining genes, together with a portion of *gag* encode six accessory proteins. Figure adapted from Frankel *et al,* 1998[46]. (B) Schematic showing the HIV-1 virion. Embedded in the lipid membrane that surrounds the HIV-1 virion are the envelope (Env) spikes, each of which is composed of three gp120 and three gp41 proteins. Non-functional Env is also present on the viral surface. The MA proteins surround the CA core that encloses two single RNA strands and three enzymes (PR, IN and RT). Figure adapted from Levy, 1993[42].

4. The HIV-1 envelope (Env)

4.1. HIV-1 Env structure and function

The HIV-1 Env glycoproteins enable viral infection of host cells through two steps. Firstly, gp120 engages the primary host cell receptor cluster of differentiation 4 (CD4)[47,48] and the co-receptor, usually C-C chemokine receptor type 5 (CCR5) and occasionally C-X-C

chemokine receptor type 4 (CXCR4)[49-51]. Secondly, gp41 promotes the fusion of the viral and host membranes.

The cell surface attachment subunit, gp120, which is ~500 amino acids in length, is divided into five constant regions (C1-C5) interspersed with five variable regions (V1-V5)[52,53], as shown in Figure 4. Each variable region, excluding the relatively short V5 region, is bracketed by Cys residues, which covalently bind to form disulfide bridges[54]. The gp120 subunit is heavily glycosylated, with approximately half its mass attributed to glycan residues[55]. The cleavage and fusion peptides mark the C terminus of gp120 and N terminus of gp41 respectively. In contrast to gp120, the ~350 amino acid transmembrane subunit (gp41) is less glycosylated and less variable, a probable consequence of its function[56]. Gp41, a type I fusion protein, is divided into three regions, namely the ectodomain, the membrane-spanning domain and a long cytoplasmic tail[56-58] (Figure 4). Within the ectodomain are two helical regions known as the heptad repeats 1 and 2 (HR1 and HR2)[59-62] as well as the membrane proximal external region (MPER), an approximately 24 amino acid, tryptophan-rich segment that is highly conserved[63,64]. The long cytoplasmic tail (~150 amino acids in length) has conserved motifs that have been implicated in Env incorporation and Gag processing[65,66].

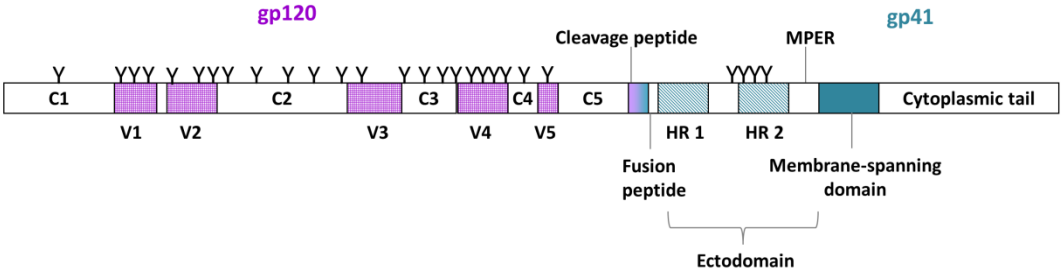


Figure 4. Regions of gp120 and gp41.
Schematic diagram showing that glycoprotein 120 (gp120) is divided into 5 constant regions (C1-C5), interspersed with 5 variable regions (V1-V5). The glycoprotein 41 (gp41) contains an ectodomain, membrane-spanning domain and cytoplasmic tail. The ectodomain is subdivided into the fusion peptide as well as the heptad repeat 1 (HR 1), heptad repeat 2 (HR 2) and the membrane proximal external region (MPER). The positions of potential N-linked glycosylation sequons in both gp120 and gp41 are indicated (Y).

The functional form of Env is a trimer composed of three gp120-gp41 heterodimers or protomers, which are held together by non-covalent protomer-protomer interactions within a trimer association domain[67] and the helical regions of gp41[68-71] (Figure 5). Almost 20 years ago, the first atomic details of the gp120 subunit core, which was stabilized through deglycosylation, truncation of the termini and deletion of the V1V2 and V3 regions, were described[72]. This recombinant Env fragment was further stabilized through interactions with the CD4 receptor and an anti-HIV-1 antibody.

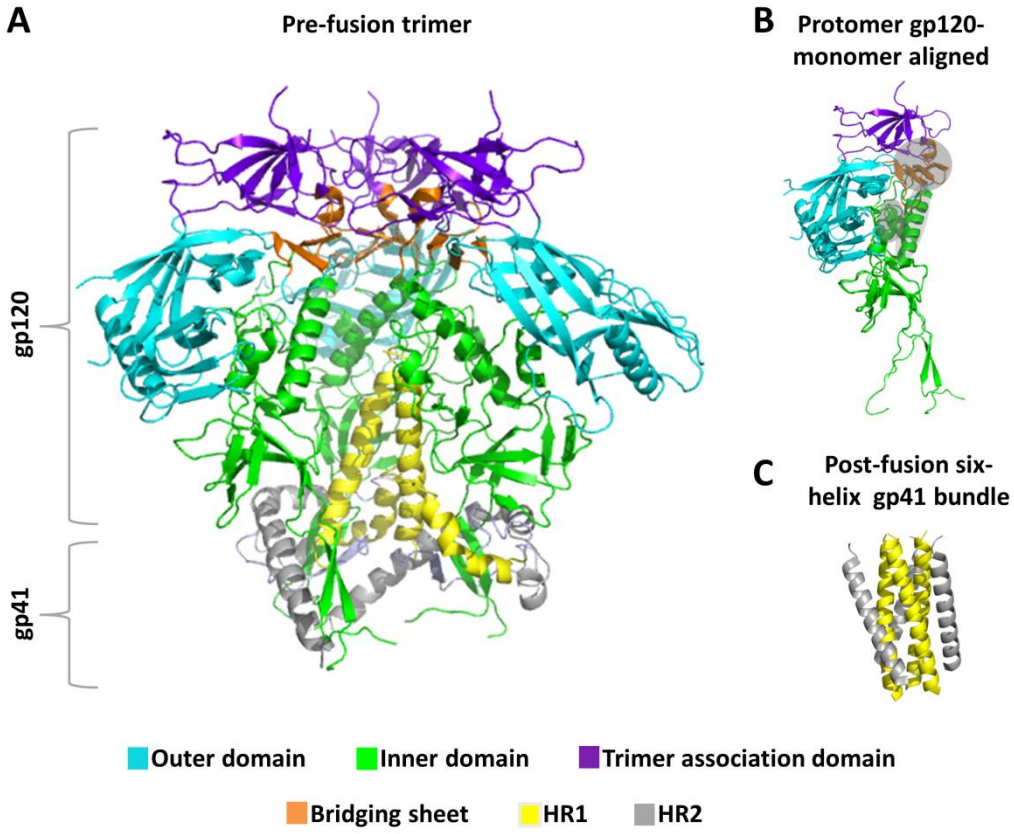


Figure 5. Structure of the pre- and post-fusion HIV-1 Env.
(A) Ribbon representation of the prefusion trimer, with the approximate division between the gp120 and gp41 subunits indicated. The outer domain, inner domain, trimer association domain, bridging sheet, heptad repeat 1 (HR1) and heptad repeat 2 (HR2) are colored according to the key. (B) Ribbon representation of a CD4-bound gp120 monomer, highlighting (in grey shading) the regions of the inner domain, bridging sheet and trimer association domain that undergo the largest structural rearrangements post-CD4 engagement. (C) Rearrangements in gp41 HR1 and HR2 that occur post-fusion and result in the formation of the six-helix bundle. Colors represent different regions as indicated in the key. PBD ID: 4TVP, 3JWD, 1K34.

Since then, numerous crystal structures of recombinant Env (portions of gp120 and gp41) have been obtained[73-79]. In contrast, visualizations of the native trimer were restricted to low resolution electron microscopy, until very recently, when the first cleaved prefusion BG505 SOSIP.664 Env trimer was structurally characterized to 3.5Å resolution[68,69,80]. This recombinant Env protein is truncated at position 664 (before the transmembrane domain in gp41) and deletes most of the MPER, to promote solubility of the protein[81]. An engineered disulfide bond (SOS) between position 501 (in gp120) and 605 (in gp41) covalently links and stabilizes the trimer in the prefusion state, following cleavage[81-85]. An isoleucine mutated to a proline at position 559 (IP) in gp41 strengthens gp41-gp41 interactions which also stabilize the trimer conformation[81]. Through the creation of this recombinant HIV-1 Env trimer, we now have an almost complete structural view of the native HIV-1 Env before CD4 engagement and membrane fusion[68,69,80].

Structurally, the gp120 subunit can be divided into the inner, outer and trimer association domains[67,72] (Figure 5 green, cyan and purple respectively), while the gp41 subunit is divided into HR1 and HR2[59,62] (Figure 5, yellow and grey). The inner domain of gp120 can be further sub-divided into the bridging sheet[72] (which only fully forms post-CD4 binding), an invariant 7-stranded beta sandwich (which maintains its structure pre- and post-fusion) and three topologically flexible layers[74,76]. While the outer domain preserves the same relative conformation prior to and post CD4 engagement, the trimer association and inner domains undergo large structural rearrangements (Figure 5B, grey shading). These include the release of the V3 loop, by V1V2 movements, to expose the co-receptor binding site and conformational changes in the bridging sheet and the first topological layer of gp120[68,69,72,73,80]. In gp41, a prefusion four-helix collar (Figure 5A), that surrounds the gp120 N and C termini[69], transitions into a post-fusion six-helix bundle, which facilitates membrane fusion by releasing energy to overcome this barrier[86,87] (Figure 5C). These conformational rearrangements are only possible in cleaved Env and thus the reason for the metastable nature of the trimer becomes apparent.

4.2. HIV-1 Env biosynthesis

The HIV-1 Env is initially synthesized and simultaneously glycosylated in the rough endoplasmic reticulum as a gp160 polypeptide precursor[88]. At this stage N-linked glycans, transferred onto the free amide of asparagine residues in an N-X-S/T (where X ≠ P) sequon, are oligomannose precursors with three glucose, nine mannose and two *N*-acetylglucosamine residues ($Glc_3Man_9GlcNAc_2$)[89] (Figure 6, Step 1). The terminal glucose and mannose residues of these oligomannose precursors are then trimmed resulting in high mannose, $Man_5GlcNAc_2$, glycoforms (Figure 6, Step 2). Upon oligomerization, predominantly into immature gp160 trimers, the proteins are trafficked to the *trans*-Golgi network, where *N*-acetylglucosamine transferase I (GnTI) creates hybrid glycoforms through the transfer of a GlcNAc moiety to the D1 arm of accessible high mannose glycans[90] (Figure 6, Step 3). Further enzymes, such as mannosidase trimming II, GnTII, GnTIV and GnTV, can convert hybrid glycans into complex forms through the replacement of the D2 and D3 mannose arms with antennae that contain for example galactose and sialic acid residues[89-91] (Figure 6, Step 4 and 5). Due to the high density of glycans on Env, steric hindrance may limit the action of these glycan processing enzymes; therefore three glycoforms (oligomannose, hybrid and complex) can exist on Env[91-94].

In addition to post-translation glycan processing, the Env polypeptide can also be tyrosine sulfated while passing through the Golgi[95]. Finally, within the Golgi apparatus, the immature gp160 trimers are proteolytically cleaved by furin or furin-like enzymes[96] at a highly conserved motif K/R-X-K/R-R[97,98]. The cleaved gp120 and gp41 subunits non-covalently associate to form mature trimers and at lipid rafts in the plasma membrane, 8-14 trimers are incorporated into each budding virus[99].

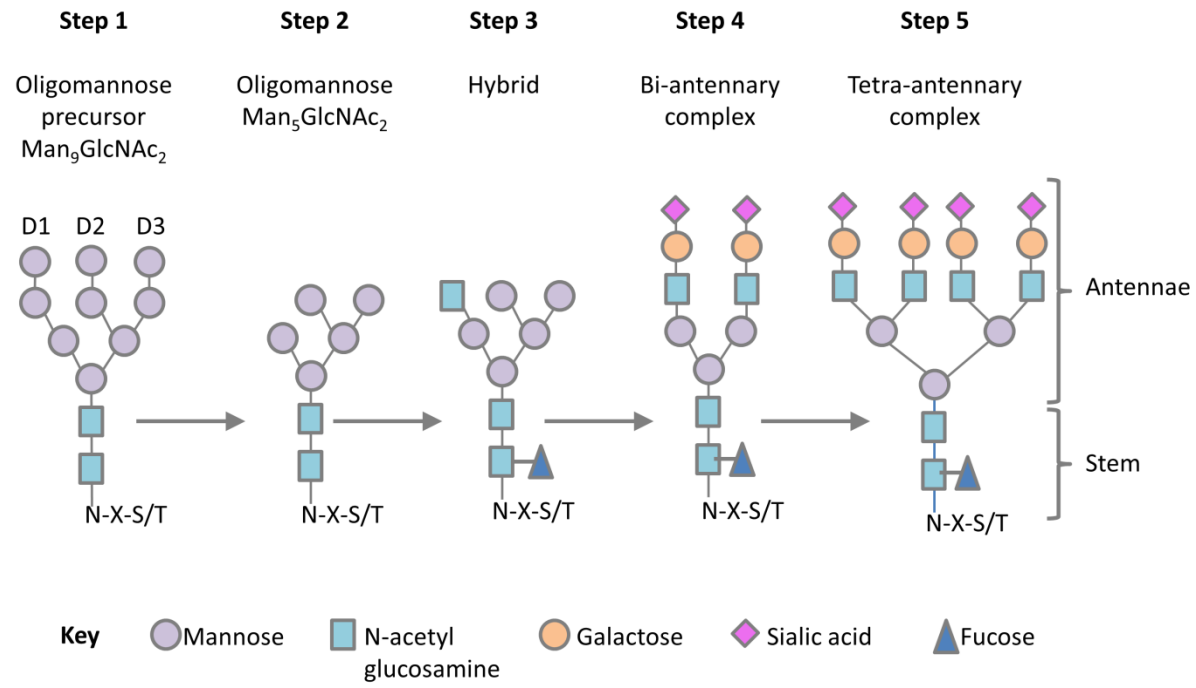


Figure 6. Post-translational processing of N-linked glycans.
Schematic diagram showing the five basic steps of N-linked glycan processing from oligomannose precursors to hybrid and complex glycoforms. The terminal mannose residues on the D1, D2 and D3 arms of oligomannose precursors are trimmed to oligomannose glycoforms (Steps 1 and 2). A subsequent transition to the hybrid glycoform occurs via addition of N-acetyl glucosamine (GlcNAc) residues to the D1 arm (Step 3). Complex glycans are created through replacement of mannose moieties on the D2 and D3 arms with complex antennae that may contain galactose and sialic acid residues (Steps 4 and 5). At all stages following hybrid formation, the oligomannose stems may be fucosylated. Key indicates shapes for each glycan residue. Adapted from Binley *et al,* 2010[100].

5. B cell responses to the HIV-1 Env

5.1. B cell diversity

The year 2015 marked the golden anniversary of the discovery of the B lymphocyte or B cell, named so because of its initial identification in the Bursa of birds[101]. These cells express the B cell antigen receptor (BCR) on their surface and the membrane-free, soluble form of BCRs are known as antibodies[102].

Each BCR or antibody is composed of four disulfide-linked polypeptide chains, two heavy chains and two light chains (Figure 7), which fold into a β-barrel, also known as the immunoglobulin (Ig) fold[102,103]. The relatively conserved, constant region of the heavy chain

forms the Fc region (Figure 7) and determines which of five classes or isotypes (IgM, IgD, IgG, IgA and IgE) the antibody belongs to. In humans the IgG and IgA classes can be further divided into IgG1-4 and IgA1-2 respectively[103]. These isotypes determine the type of effector functions an antibody can initiate, the localization or compartmentalization and the half-life of the antibody. In contrast the more variable portions arrange into two fragment antigen binding (Fab) regions per antibody[102] (Figure 7).

B cell genes have a large repertoire of diversity[104,105], necessary to combat infection caused by a wide spectrum of pathogens. Humans can therefore produce an estimated 10^9-10^{13} unique antibodies[106]. It would be impossible to encode every antigenic response by a single gene; therefore an alternate and efficient way of generating high levels of diversity has evolved.

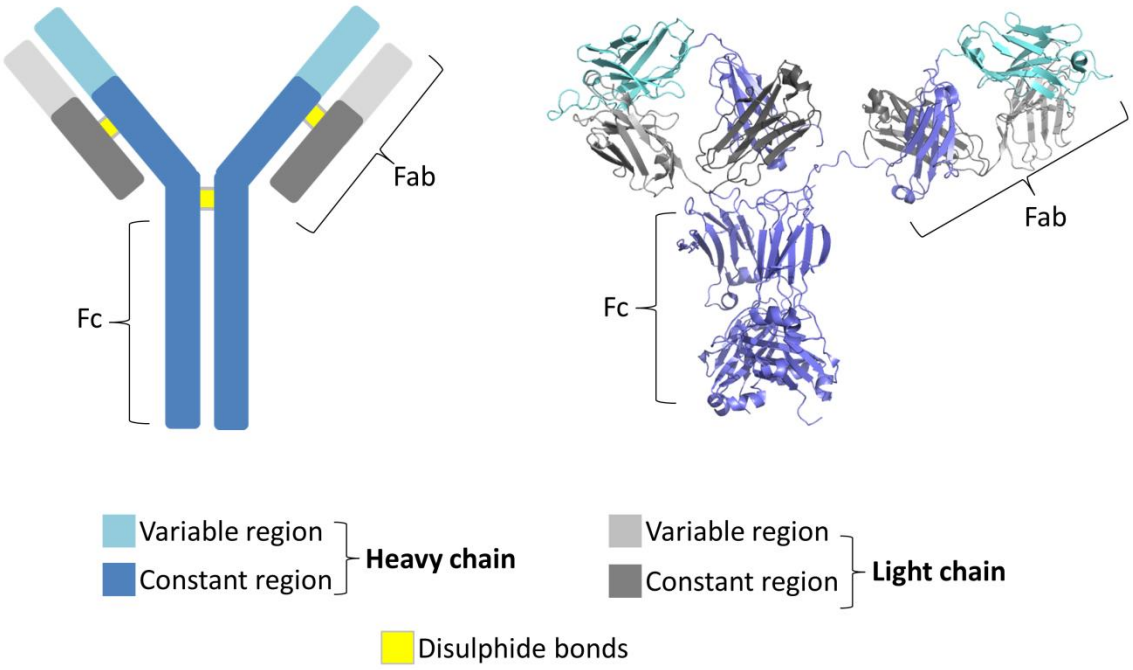


Figure 7. Antibody structure.
Schematic figure (left) and crystal structure (right) of a human immunoglobulin (Ig) monoclonal antibody. Each antibody is composed of two heavy (blue) and two light (grey) chains, which are covalently linked through disulfide bonds (yellow). Each antibody has two fragment antigen binding (Fab) regions, which are composed of the variable regions of each heavy-light chain pair. The single fragment crystallizable (Fc) region per antibody is composed of the constant region of the heavy chains.

The heavy and light chain Ig gene loci are located on three different chromosomes[107]. The single heavy chain Ig locus consists of 48 variable (V), 23 diversity (D), 6 joining (J) and 9 constant (C) functional gene segments [107-109] (Figure 8A). The two light chain loci (kappa and lambda) collectively code for 71 variable, 10 joining and 6 constant gene segments[107] and though they are similar in organization to the heavy chain locus, they do not have D genes.

Primary diversification occurs in the bone marrow early in B cell development, when recombination activating gene (RAG) proteins facilitate the rearrangement of the germline Ig genes[104,105,110]. During this process, single V, (D) and J genes (for both the heavy and light chains) are randomly recombined from the germline gene pool, which creates an ancestor B cell with a unique gene arrangement (Figure 8B). To enhance this range of diversity, insertions between the three gene segments (junctional sites) may also occur, through the action of terminal deoxynucleotidyl transferase (TdT)[111].

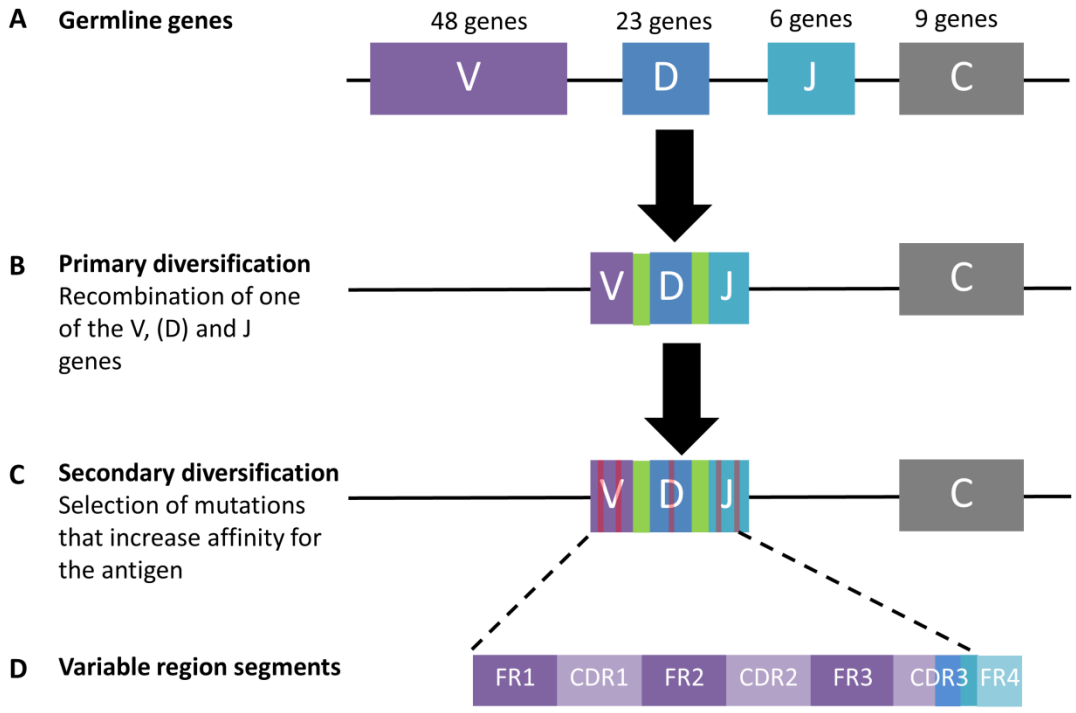


Figure 8. Generation of antibody heavy chain diversity and variable region organization.
Schematic diagram illustrating how antibody diversity is generated through two steps of diversification. (A) Multiple variable (V, purple), diversity (D, blue), joining (J, turquoise) and constant (C, grey) gene segments exist in the B cell germline. (B) Primary diversification occurs through a unique VDJ recombination event. During this process additional residues (green) can be inserted between the V-D and D-J junctions, thereby increasing the diversity. (C) Following antigenic exposure, B cells undergo secondary diversification, whereby somatic hypermutation (SHM) enables the selection of affinity-enhancing mutations (pink lines). (D) The VDJ segment can be divided into

four relatively conserved framework regions (FR1-4) and three hypervariable complementarity determining regions (CDR1-3). The CDR3 contains the entire D gene, as well as portions of the V and J gene, which is discussed further in section 8.4.

Following tolerance checks, these mature B cells migrate to the peripheral organs, where upon exposure to a cognate antigen, a process of secondary diversification begins (Figure 8C)[102]. Somatic hypermutation (SHM) or affinity maturation, one of the mechanisms of secondary diversification, is catalyzed by the enzyme activation-induced cytidine deaminase (AID). AID introduces point mutations into the single-stranded DNA, by deaminating cytosine residues within a W-R-C motif (where W = A/T and R = A/G), thereby producing B cell variants or descendants that differ from the original unmutated common ancestor (UCA) B cell (Figure 8B). These B cell variants then compete for binding to follicular dendritic cell (FDC)-bound antigen and the entire process is repeated until ultimately the B cells with the highest affinity for the antigen are expanded. These two processes alone ensure at least a total 5 x 10^{13} different gene rearrangements[102,103]. Each heavy and light chain variable region is divided into three relatively conserved framework regions (FR1-4), interspersed with three hypervariable complementarity determining regions (CDR1-3) (Figure 8D). Antigen specificity for the most part is conferred by the sequence of the six CDRs, known as CDRH1-3 and CDRL1-3 for those in the heavy and light chains respectively.

5.2. Anti-HIV-1 neutralizing antibodies and HIV-1 Env immune evasion

Neutralizing antibodies (NAbs) block HIV-1 infection by preventing attachment of the virus to the CD4 receptor or by inhibiting the conformational changes required for membrane fusion[72,112]. The native HIV-1 Env is the sole target for NAbs[113] and has thus evolved a number of strategies to combat immune targeting. The simplest immune evasion tactic is the occlusion of the receptor binding sites, through the oligomerization of the trimer[114]. Non-functional or "junk" forms of Env, such as gp41 stumps and gp120-gp41 monomers[44], are present on every HIV-1 virion at a higher frequency than native Env, providing a highly effective way of directing the immune response away from infection-capable Env. Due to the efficiency of these Env decoys, the majority of early HIV-specific antibody responses

target non-neutralizing epitopes that are not accessible in the prefusion native trimer, such as the co-receptor binding site in the V3 loop[115]. The dense glycan cloak of gp120, with host-derived residues, acts as a further immune constraint[112], although multiple studies have now shown that glycan interactions are a component of specific anti-HIV-1 responses discussed below[113,116-119]. Finally, the relatively few native Env spikes on the surface of each virus exacerbates this problem by limiting bivalent binding and therefore decreasing avidity of IgG antibodies[120].

Due to this array of viral immune evasion strategies, the first detectable B cell responses against HIV-1 occur eight days after infection, but are in the form of virus-antibody complexes[121]. The first free antibodies are to gp41 and are present a further five days later; however these antibodies are often cross-reactive with commensal gut bacteria[122,123]. The first HIV-1 specific responses to gp120 only develop ~27 days post-infection (p.i.), but these binding antibodies have no effect on viremia and do not exert selective pressure on the virus. Between 12 and 20 weeks p.i., most HIV-1 infected individuals develop strain-specific neutralizing responses[124-126], which target the more variable regions of the Env trimer, such as the C3V4 region, including the α2-helix of gp120[127]. These responses exert sufficient immune pressure on the viral quasispecies to select for rapid and effective viral escape[124,128-135].

In contrast to these strain-specific responses, between 10-50% of infected individuals develop polyclonal plasma antibodies that are able to neutralize heterologous viruses, including those from multiple subtypes and various geographical areas[117,119,136-141]. These types of responses, termed broadly neutralizing antibodies (bNAbs), are however detected much later, between one and three years after infection[119,139].

5.3. Role of NAb responses in HIV-1 prevention

The induction of neutralizing antibody responses by vaccination mediates protection from multiple human pathogens[142-149], therefore the role of bNAbs in mediating protection from HIV-1 infection has been a focus of many studies.

HIV-1 Envs expressed in SIV backbones to create simian-human immunodeficiency chimeric viruses (SHIVs)[150-153], have enabled non-human primate (NHP) protection studies using human derived anti-HIV-1 bNAbs. High concentrations of two bNAbs and polyclonal HIV immune globulin (HIVIG) administered intravenously offered sterilizing protection following intravenous SHIV challenge[154]. However, HIV-1 infection generally occurs at mucosal surfaces, therefore the same intravenous bNAb-HIVIG cocktail was tested in a vaginal challenge model and showed protection in 4 of 5 macaques[155]. Similarly, a topically administered vaginal gel or saline solution, containing a single bNAb, protected 9 of 12 macaques from SHIV infection[156]. A combination of three bNAbs also prevented infection of neonatal macaques via the oral route, which is representative of mother-to-child transmission. The protection conferred to neonatal NHPs occurred whether transplacental or intravenous bNAbs were administered prior to or after birth respectively[157,158]. Further studies showed that low serum neutralization titers of a single bNAb at the site of infection in NHPs could efficiently provide protection[159-161]. More recently two studies showed 100% protection of vaginally challenged NHPs with intravenous administration of single, more potent bNAbs at concentrations 20 to 40 fold lower than previous studies[162-164], showing that bNAb serum concentrations below 10 µg/ml can mediate sterilizing protection. Finally specific mutations in the Fc region of bNAbs that enhance binding to the neonatal Fc receptor (FcRN) and therefore increased antibody half-life showed improved protection from rectal challenge in NHPs[165]. These proof-of-concept studies have supported the development of bNAbs for HIV-1 prevention and clinical trials to test the efficacy of passively administered bNAbs in humans are underway[166].

6. Anti-HIV-1 broadly neutralizing antibodies (bNAbs)

6.1. BNAb targets

There are five targets for bNAbs on the HIV-1 Env trimer and all but one of these epitopes can include glycan in addition to peptide contacts[113] (Figure 9). The first generation of bNAbs, isolated pre-2009, had limited neutralization breadth, especially against non-subtype B strains[167]. In contrast second generation bNAbs are extremely broad and potent, neutralizing up to 98% of phylogenetically distinct HIV-1 strains[168]. Most anti-HIV-1 bNAbs

possess one or more unusual characteristics, which include exceedingly high levels of SHM, exceptionally short or long CDR loops, insertions or deletions (indels) in the Ig variable regions and autoreactivity against host antigens[169,170]. These uncommon characteristics may result from the B cell dysfunction that is associated with chronic HIV-1 infection, but nonetheless enable bNAbs to neutralize HIV-1 and circumvent viral immune evasion.

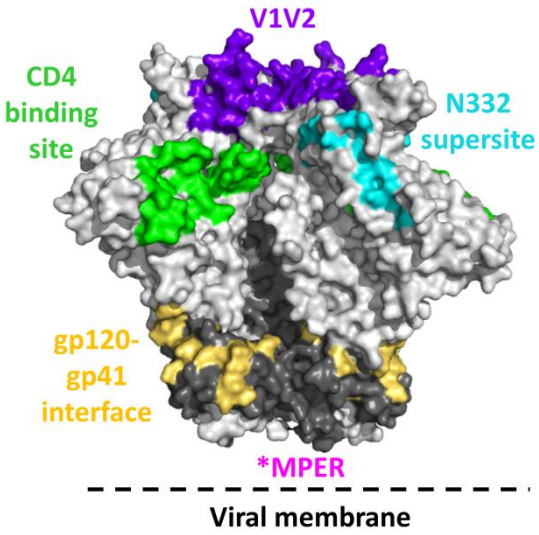


Figure 9. Broadly neutralizing antibody (bNAb) targets on the prefusion HIV-1 Env trimer.
Surface representation of the BG505 SOSIP.664 HIV-1 prefusion trimer. Four of the five bNAb targets are visible in the BG505 SOSIP.664 and are highlighted in purple (V1V2), green (CD4 binding site), cyan (N332 supersite) and yellow (gp120-gp41 interface). The approximate positions of the membrane proximal external region (MPER) and the viral membrane are shown in pink and black respectively. The gp120 and gp41 subunits are shaded in light grey and dark grey respectively. PDB ID: 4TVP.

The first identified[171] and most extensively studied bNAb epitope is the CD4 binding site (CD4bs), which is present on both trimeric, functional Env and also on gp120 monomers (Figure 9, green). Broad antibodies targeting this region can be sub-divided into VH-gene restricted or CDRH3-dominated CD4bs subclasses, categorized according to their mode of binding[172]. VH-gene restricted or VRC01-class antibodies mimic CD4 receptor binding (through interactions with the conserved D368 residue) and have unusually short CDRL3s that avoid steric clashes with the N276 glycan. In contrast, CDRH3-dominated CD4bs bNAbs bind independently of D368 and generally interact directly with the conserved N276 viral

glycan. While antibodies that target the CD4bs have a range in neutralization breadth and potency, the current broadest, VRC07, is able to neutralize 93% of viruses[173]. Although anti-HIV-1 bNAbs generally have unusually high levels of SHM, this is especially true for the heavy chain variable regions of some CD4bs bNAbs, which are close to 30% mutated compared to their germlines[174].

The most recently described bNAb epitope is quaternary (only present on functional Env trimers), discontinuous and involves peptide and glycan residues in both gp120 and gp41 (Figure 9, yellow). These gp120-gp41 interface bNAbs are represented by the antibodies 8ANC195[175], PGT151[176,177], 3BC315[178] and 35O22[179]. These highly glycan dependent antibodies neutralize between 50-66% of globally circulating viruses, but their neutralizing capacity generally does not reach 100% even against viruses that are potently neutralized. These neutralization plateaus have been attributed to the glycan heterogeneity of Env, and though they have been described in all bNAb classes[180], this phenomenon is especially striking in gp120-gp41 interface bNAbs.

The most common bNAb target in chronic HIV-1 infection[119,140,181,182], the N332 glycan supersite, encompasses the V3, V4 and 2G12 sub-epitopes on gp120[183] (Figure 9, cyan). Although these sub-epitopes differ significantly, they all converge on the glycan at position 332 of the C3 region[118,184,185]. These N332 epitopes are present on the outer domain of Env and can therefore be reproduced on monomeric gp120. PGT121 and PGT128, representative of V3 targeting bNAbs, have long CDRH3 loops (20-26 amino acids) which they use to recognize a short linear peptide in V3 together with the glycans at positions N301 and N332/334[79,118]. The V3 loop is closely associated with the V1V2 region and for this reason some V3 targeting bNAbs are also able to interact with the N137 and N156 glycans, which are in V1V2[68,186]. However while the N301 and N332/334 glycan interactions are critical to neutralization by these bNAbs, removal of the V1V2 glycans does not completely abrogate their neutralizing activity[118,186]. PGT135, a V4 domain bNAb, binds to the base of the V4 loop and to glycans at positions N295, N332, N386 and N392[118,183]. While V4 loop bNAbs are also N332 glycan-dependent, they recognize a different face of the glycan compared to the V3 loop bNAbs. The final N332 supersite bNAb subclass is typified by the antibody 2G12, which possesses a unique heavy chain domain exchange used to create a larger paratope[187]. This unusual paratope requirement arises from the glycan-exclusive

mode of recognition by 2G12, which does not contact any protein components of gp120. 2G12 interacts only with terminal glycan moieties at residues N296, N332, N339 and N392[184,185]. The new generation N332 glycan dependent antibodies, isolated after 2G12, are extremely potent and neutralize 30-75% of viruses[169,170].

The MPER is the only epitope located solely on the gp41 subunit of Env, however the location of this epitope within prefusion Env is still unknown (Figure 9, pink asterisk). The MPER is targeted by the broadest anti-HIV-1 mAbs, such as 10E8 which neutralizes 98% of viruses[188]. The breadth of this class of antibodies is associated with the high sequence conservation of the MPER, constrained by its function. This class of bNAbs target overlapping, linear sub-epitopes within the MPER, which is formed by two linked helices between the transmembrane domain and the gp41 ectodomain. However, these bNAbs generally require lipid binding to enhance affinity for the MPER, and are therefore often autoreactive[189].

The fifth epitope, created through the interaction of the three gp120 protomers at the trimer apex and thus only present on the prefusion Env, is the V1V2 region (Figure 9, purple). The quaternary structure-dependent mAbs belonging to this bNAb class are the most potent (with IC_{50} titers in the nanomolar range) and generally depend critically on glycan residues at positions 156 and/or 160 and on amino acids at positions 166 and 169[117,118,190-192]. BNAbs targeting this site include PG9/16[117], the first V1V2 bNAbs isolated, as well as the PGT145[118] and CAP256-VRC26[191,192] antibody families. The V1V2 site and the bNAbs that target it are the focus of this thesis and will therefore be discussed in greater detail below.

6.2. Broadly neutralizing plasma antibodies in CAPRISA participant, CAP256

CAP256, an HIV-1 infected participant from the longitudinal CAPRISA 002 acute infection cohort in Durban, South Africa, was one of seven individuals who developed broadly neutralizing plasma responses (77% of viruses neutralized in a 43 virus panel, Figure 10)[119] by three years p.i.

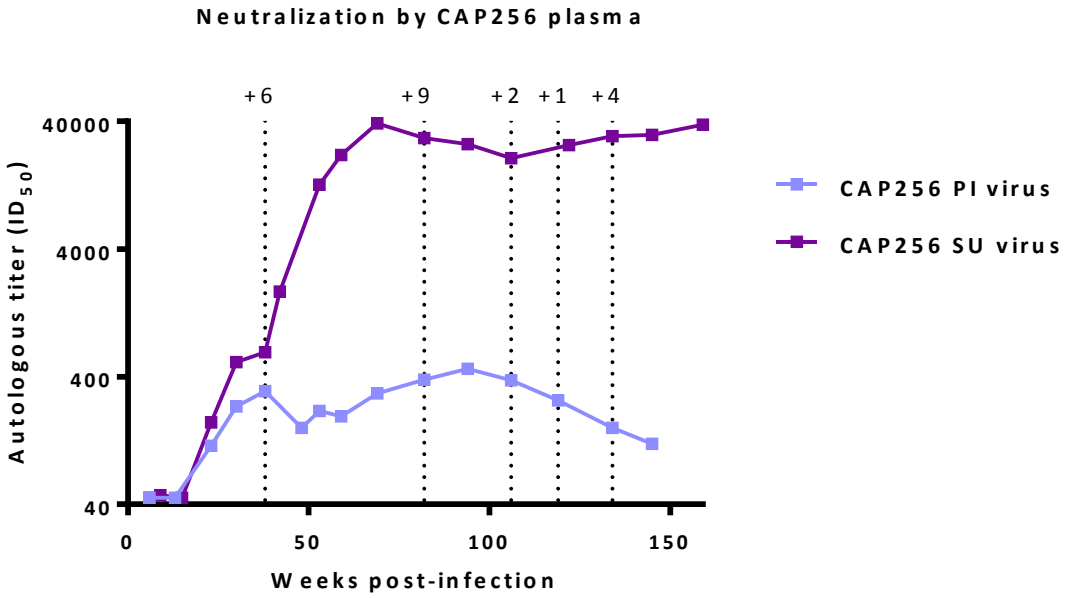


Figure 10. Neutralization of autologous and heterologous viruses by CAP256 plasma.
Longitudinal CAP256 plasma neutralization of the primary infecting (PI, blue) and superinfecting (SU, purple) autologous viruses are shown with ID_{50} titers on the left y-axis and weeks post-infection on the x-axis. The number of heterologous viruses neutralized at each time point after the development of neutralization breadth is indicated above the dashed lines (black). Figure modified from Gray et al, 2011[119] and Moore et al, 2013[193].

CAP256 was infected with a subtype C virus in July 2005 and between 13-15 weeks later was superinfected with a second, but distinct subtype C virus[194] (Figure 10 and 11). She had a median viral load of 105, 000 RNA copies/ml over 219 weeks (~4.5 years) of infection, which peaked at 2,390,000 RNA copies/ml when superinfection was detected. At initial infection she had a $CD4^+$ T-cell count of 689 cells/µL, which had decreased to 267 cells/µL before she initiated ARV treatment in January 2010. Neutralization of heterologous viruses by the CAP256 plasma, first detected at 48 weeks, increased incrementally with each year and finally peaked by 159 weeks. Despite maintaining this neutralization breadth at 219 weeks, the potency of the response began to decrease. Detailed mapping of the CAP256 plasma showed that these bNAbs targeted the V1V2 region of Env[119,194].

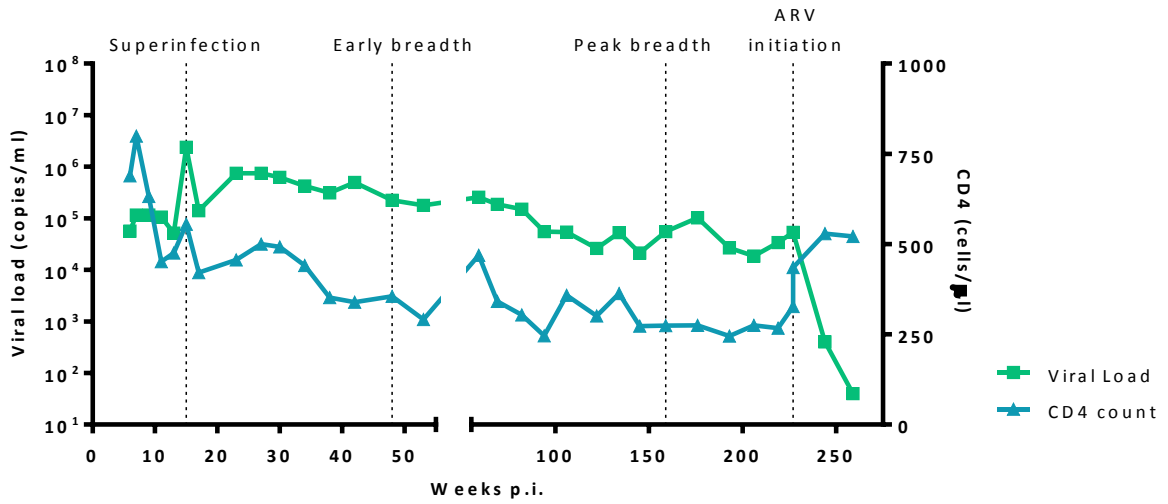


Figure 11. CAP256 viral load and CD4$^+$ T cell count data over 259 weeks of HIV-1 infection.
CAP256 viral loads (RNA copies/ml) in green and CD4+ T cell counts (cells/µL) in blue are shown for all time points from 6 to 259 weeks post infection (p.i.). Dotted lines indicate time of superinfection, early neutralization breadth, peak in neutralization breadth and antiretroviral (ARV) treatment initiation. Viral loads decrease and CD4$^+$ T cell counts increase following ARV initiation. Figure adapted from Moore *et al,* 2011[194].

6.3. Anti-HIV-1 bNAb isolation

Defining and visualizing immune vulnerabilities on the HIV-1 trimer is an important tool to aid rational immunogen design, thus the isolation of monoclonal antibodies (mAb) with neutralization breadth from infected individuals has been a major focus of the HIV-1 vaccine field. Three major strategies have been used to isolate human mAbs against various viral and bacterial pathogens, namely the generation of phage display libraries, B cell immortalization coupled with functional screening and lastly single B cell sorting followed by cloning and expression of the Ig genes. The development of overlapping, multi-primer PCR protocols to amplify the Ig variable heavy and light chain genes from single B cells[192,195-198] provided new avenues for mAb isolation, including B cell culture and antigen-specific B cell sorting. In addition, the identification of potent, broadly neutralizing plasma from chronic HIV-1 infection and the development of high-throughput technologies have greatly aided the anti-HIV-1 bNAb isolation effort.

The first broadly neutralizing anti-HIV-1 antibody, b12[171], was isolated using a phage display library. However, the random pairing of the Ig variable heavy and light chains in this method

may result in antibodies that are not physiologically representative. The next first generation bNAbs 2G12[116], 2F5[199] and 4E10[200] were isolated using B cell immortalization with Epstein-Barr Virus (EBV), a method described in more detail below.

B cell culture

B cell immortalization is advantageous as it allows for screening via neutralization and/or binding and resulted in the recent isolation of bNAbs CH01-04[190] and HJ16[201]. However this method is highly inefficient when using frozen peripheral blood mononuclear cell (PBMC) samples from HIV-1 infected individuals. An adaptation of this method, called B cell culture[117,118,188,201,202], is favored when the antibody response is extremely potent and when the epitope is unknown or not defined on recombinant HIV-1 proteins. In this technique memory B cells isolated as $IgM^-/IgD^-/IgA^-/CD19^+$ by flow cytometry, are negatively selected to limit the activation and subsequent proapoptotic tendencies of the previously frozen B cells (Figure 12, top panel). After dilution, these memory B cells are cultured for two weeks in the presence of CD40 ligand (to activate the B cells), IL-2 (to promote the proliferation, rather than apoptosis of the activated B cells) and IL-21 (to induce expansion of antibody-secreting cells). After 14 days, the supernatants are screened for neutralization and the Ig variable regions of cells with positive neutralization results are PCR amplified. This method has been used to isolate multiple second generation bNAbs, including PG9/16[117], PGT121-123, PGT141-145[118], 10E8[188] and 35O22[179]. In addition, as part of this thesis, we used B cell culture to isolate 25 clonally-related antibodies, named CAP256-VRC26.01-25[191,192], which were derived from the variable heavy 3-30*18 and variable lambda 1-51*02 germline genes. These mAbs targeted the V1V2 epitope and possessed unusually long CDRH3s of between 35-37 amino acids[191,192] (according to Kabat numbering) and are described below in section 7.1.

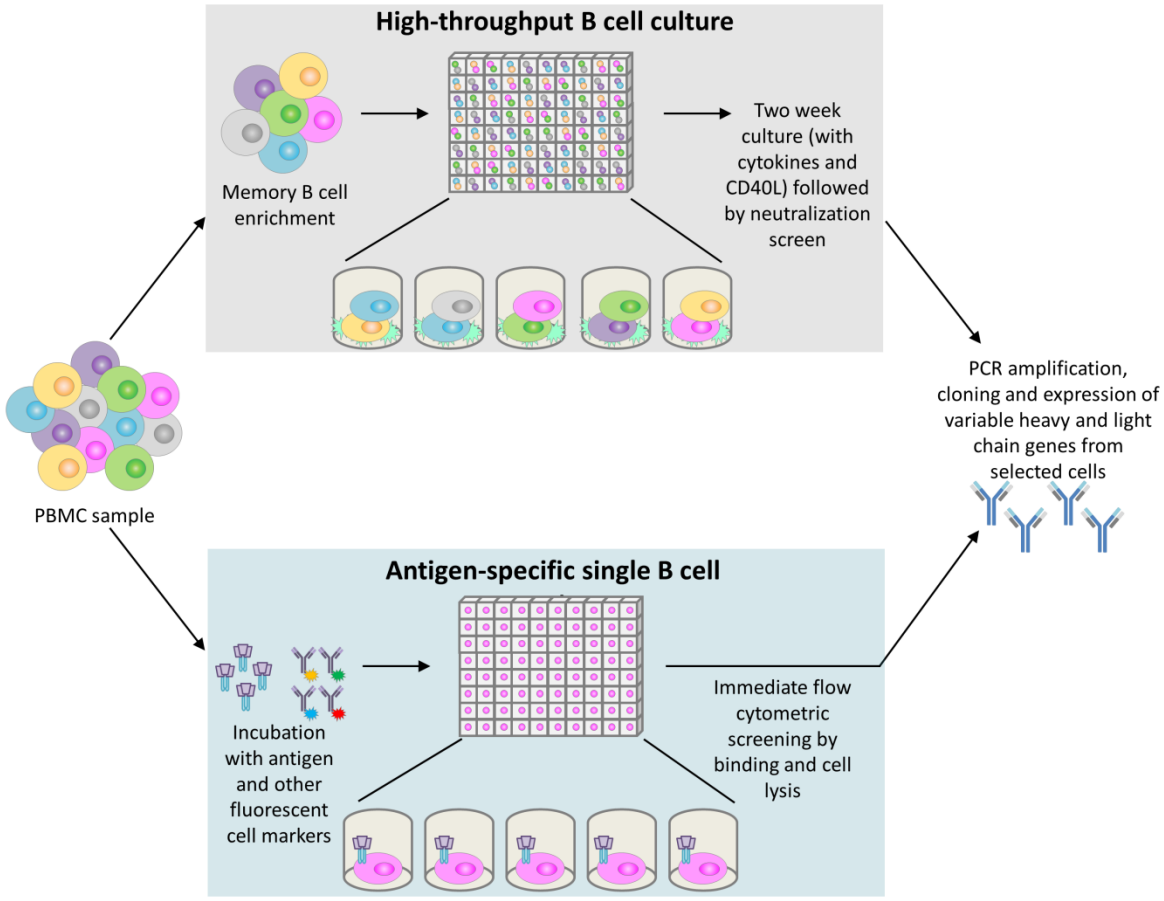


Figure 12. Monoclonal antibody isolation using high-throughput B cell culture and antigen-specific B cell sorting.
During high-throughput B cell culture (top panel), memory B cells are enriched from peripheral blood mononuclear cell (PBMC) samples by flow cytometry or using magnetic bead separation. Subsequently 2 cells/well are cultured in the presence of CD40 ligand and cytokines for B cell activation, proliferation and differentiation. Paired variable heavy and light chain genes from cells that are positive on neutralization screens are then PCR amplified, cloned and expressed as antibodies. In antigen-specific single B cell sorting (bottom panel), PBMC samples are labelled with various cell markers in addition to the engineered antigens. Antigen-specific memory B cells are single sorted (one B cell/well) by flow cytometry. Paired variable heavy and light chain genes from all cells are then PCR amplified, cloned and expressed as antibodies.

Antigen-specific B cell sorting

A second mAb isolation approach is flow cytometry-based antigen-specific B cell sorting (Figure 12, bottom panel), which relies on the rational design of specific antigenic "baits" to select for rare bNAb-producing B cells[197,203,204]. The first anti-HIV-1 bNAb isolated using this method was the CD4bs mAb, VRC01, which bound to a highly specific, rationally engineered resurfaced gp120 core protein[174]. In this method PBMC samples are fluorescently stained

with markers that identify each major cell type circulating in the peripheral blood. While different staining panels are used, the inclusion of CD19, to identify B cells and IgM/IgD, to differentiate naïve B cells, are strict requirements. In terms of antigen-specificity, a fluorescent HIV-1 recombinant Env protein or peptide is used as a "bait" (positive selection) to label memory B cells that express a BCR capable of binding the specifically designed bait. The strategy capitalizes on the high frequency of membrane-bound BCR on the surface of memory B cells, which can therefore be relatively well labelled. Often a differential selection strategy is applied through the use of a "negative bait", which except for engineered epitope-ablating mutations is identical to the positive bait. Monomeric gp120 proteins or MPER peptides have been successfully used to isolate antigen-specific single B cells that produce strain-specific[133,203,205] and broadly neutralizing antibodies[174,197] from HIV-1 infected individuals. In addition, cells expressing HIV-1 Envs on their surface have also been used as antigens and in this way the antibodies 3BC176 and 3BC315 were isolated[206,207].

Until the design and structural characterization of the BG505 SOSIP.664 Env trimer, recombinant Env proteins could not be bound by bNAbs targeting quaternary epitopes. The use of this antigen for specific single memory B cell sorting was first described through the isolation of V1V2 bNAbs belonging to the PGT145 lineage[208]. Although the BG505 SOSIP.664 protein is highly representative of prefusion Env, a portion of the V3 loop is partially exposed[81]. For this reason, a small number of non-neutralizing antibodies, in addition to most bNAbs, are able to bind to this protein[81]. The BG505 SOSIP.664 (positive bait) was therefore used in conjunction with a gp120 monomer, which exposes non-neutralizing sites (negative bait)[208]. This allowed for distinction of cells that bound neutralizing (BG505 single positive cells) and non-neutralizing (gp120/BG505 double positive cells) epitopes.

The use of the BG505 SOSIP.664 trimer as a viable protein for antigen-specific sorting of quaternary dependent V1V2-directed B cells prompted us to adapt the sorting strategy used by Sok and colleagues[208]. We knew from plasma and mAb epitope studies that the bNAb response in CAP256 was extremely sensitive to the K169E mutation[191,194]. We therefore created a negative bait, BG505 SOSIP.664 K169E, which we paired with the wild-type BG505 SOSIP.664[192]. Using this sorting strategy we were able to isolate 11 CAP256-VRC26 B cells, of which 8 had paired heavy-light sequences and were distinct from the 25 B cell culture isolated antibodies. Therefore an epitope-directed differential sorting strategy was 79%

effective at isolating rare bNAb-producing B cells. This was an improvement over the Sok *et al* strategy where only 48% of isolated B cells belonged to the bNAb lineage. Overall, using both binding and neutralization screens, we were able to isolate 33 clonally related antibodies belonging to the CAP256-VRC26 lineage. While culture and sorting methods both yielded mAbs with high levels of neutralization breadth, members of this lineage showed a range of neutralization breadth of between 2 and 63%[191,192]. This provided us with a unique opportunity to investigate the molecular events which shaped the development of breadth in this lineage (discussed in section 8.3).

7. V1V2-directed bNAbs

7.1 The conformational V1V2 Env epitope

The V1V2 region (50-90 amino acids) is located at the apex of the trimer (Figure 13A) and forms part of the trimer association domain[67], which holds the native Env in the prefusion, closed conformation. In native Env, the V3 loop is closely associated with and protected by the V1V2 domain[68,69,209,210] (Figure 13A and B). The role of the V1V2 region in immune evasion, achieved through high levels of sequence variability and glycosylation, is emphasized by the extreme neutralization sensitivity of V1V2-deleted viruses[211-215].

In the prefusion trimer, the most conserved sections of V1V2 fold into five anti-parallel β strands (A, B, C and D) (Figure 13C), while the more variable residues form long, flexible loops that connect the strands[216]. In addition to non-covalent hydrogen bonds, inter-strand disulfide bridges stabilize this five-stranded β-barrel. The C-strand, which forms the short peptide contact zone for most V1V2 bNAbs, is bracketed by the N156 and N160 glycans on the edge and central areas of the trimer cap respectively. Additional contacts for V1V2 bNAbs are located at the highly conserved residues 166 and 169, which are positioned in the central-most area of the trimer apex (Figure 13B).

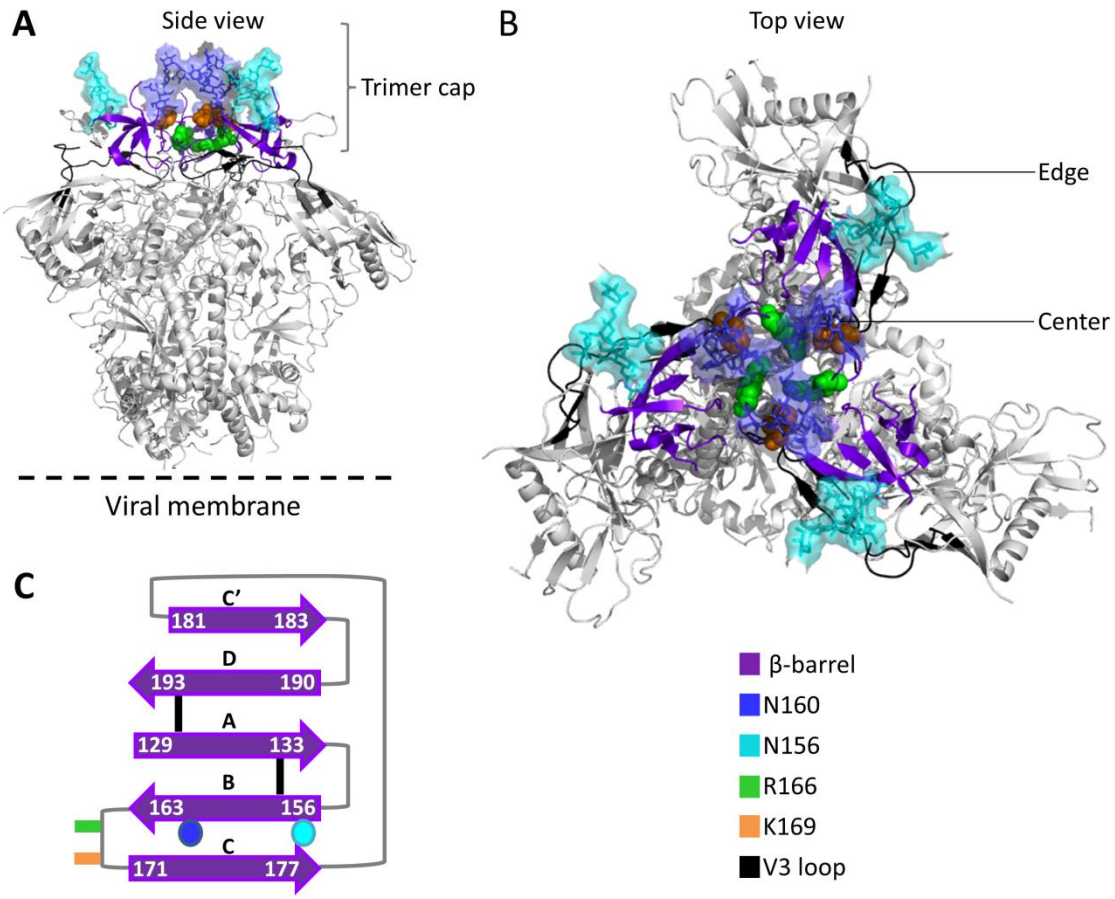


Figure 13. Structure of the V1V2 broadly neutralizing antibody epitope.
(A) Side view ribbon representation of the trimer, highlighting the location of the V1V2 and V3 regions at the trimer apex. As indicated in the key, the five anti-parallel beta strands (beta-barrel) are shown in purple, while stick and surface representations of the N156 and N160 glycans are shown in cyan and blue respectively. The key amino acid residues at position 166 and 169 are shown as spheres in green and orange respectively. The approximate position of the viral membrane is indicated. (B) Ribbon representation of the trimer showing the view from the angle of approach by V1V2 bNAbs. Colors and representations are described in A and the key. (C) Schematic diagram illustrating the five-stranded beta-barrel of the V1V2 region (residues 129-193), together with the connecting loops and positions of glycans and key amino acid residues. Colors are described in A and the key. PDB ID: 4TVP. N-linked glycans were modelled using GlyProt[217].

The first bNAbs targeting the quaternary V1V2 epitope, PG9 and PG16, are second generation bNAbs with excellent breadth (~80%)[117]. To date, V1V2 class bNAbs have been isolated from a total of four HIV-1 individuals, donors IAVI24, IAVI84, CH0219 and CAP256 yielding antibodies PG9/16[117], PGT141-145[118]/PGDM1400-1412[208], CH01-04[190] and CAP256-VRC26.01-33[191,192] respectively (Figure 14). While these bNAbs are derived from multiple heavy and light chain germline genes, they share an unusual characteristic, in that they all

possess long CDRH3s (24-37 amino acids according to Kabat numbering). These long, protruding CDRH3s, the key paratope component of V1V2 bNAbs, are generally anionic and may be sulfated at select tyrosine residues[216,218,219].

Donor	Antibody Family	Ig chain	V gene	D gene	J gene	V mutation (% nt)	CDRH3 length (AA)	CDRH3 tyrosine sulphation	CDRH3 structure	N160 glycan dependence	Breadth (%)
IAVI24	PG9, PG16	Heavy	3-33*05	3-03*01	6*03	12-15	28	Yes		Yes	75-81
		Light	L2-14*01	-	L3*02	8-12					
CAP256	CAP256-VRC26.01-33	Heavy	3-30*18	3.03*01	3*02	4.2-18	35-37	Yes		Partial, potency-dependent	2-63
		Light	L1-51*02	-	L7*01	2.5-15					
CH0219	CH01 - 04	Heavy	3-20*01	3-10*01	2*01	14-16	24	No		Yes	~50
		Light	K3-20*01	-	K1*01	11-14					
IAVI84	PGT 141-145; PGDM1400-1412	Heavy	1-8*01	4-17*01	6*02	18-27	31-32	Yes		Yes	6-83
		Light	K2-28*01	-	K1*01	11-22					

Figure 14. Broadly neutralizing V1V2-directed antibody characteristics.
The donor names, genetic characteristics, complementarity determining region 3 in the heavy chain (CDRH3) features, N160 glycan dependence and breadth of the PG9/16, CAP256-VRC26.01-33, CH01-04 and PGT141-145/PGDM1400-1412 V1V2-directed neutralizing antibodies are shown. CDRH3 structures are shown as surface representations with red and blue shading indicating acidic and basic residues respectively.

Low resolution electron microscopy has shown that this class of bNAbs usually bind with a stoichiometry of one mAb per trimer[83,191,208]. Apart from PG9, V1V2-directed bNAbs are unable to bind to non-native recombinant forms of Env, including gp120 or monomeric V1V2 scaffolds. Although high resolution crystal structures of V1V2 bNAbs bound to the trimer have not been published, their crystal structures with scaffolded V1V2 regions[78,220] and a trimer-V1V2 bNAb model[216] have provided detailed insights about their modes of binding. The long CDRH3s of these bNAbs have been selected because of their ability to reach through the extensive V1V2 glycan shield, and contact the conserved peptide residues beneath. In this way, antibody binding is stabilized through interactions with the N156 or N173 and N160 glycan residues, which can include interactions with sialic acid moieties, terminal mannose residues and the N-acetylglucosamine stems. The extensive length of the CDRH3s of these bNAbs causes the formation of secondary structural β-sheets, which then form strand-strand bonds with the V1V2 C-strand. Lastly, the sulfated tyrosine residues increase their net negative charge of the CDRH3 tips, which in turn forms electrostatic

and/or hydrophobic interactions with the positively charged side chains at V1V2 positions 166 and 169. In contrast to other V1V2-directed bNAbs, the CAP256-VRC26 lineage is affected by N160 glycan mutations in a neutralization potency-dependent manner[192]. This may be dependent on the mode of binding, which is affected by the angle of approach, exact contact residues and the types of interactions involved.

7.2. Origin of the long CDRH3

As previously discussed, all V1V2 class bNAbs possess unusually long CDRH3s, and two hypotheses for their development have previously been proposed[221,222]. Firstly, the insertion of amino acids, by TdT, at junctional sites during the initial V, D and J recombination event (using a limited subset of germline genes[221]), could result in formation of a long CDRH3. Secondly an accumulation of insertions, created by the action of AID, throughout the CDRH3 during affinity maturation could produce a long CDRH3.

We determined the developmental pathway of the CAP256-VRC26 mAb lineage using Ig heavy and light chain variable region next-generation sequencing (NGS) at 9 time points between 15 and 206 weeks after HIV-1 infection[191]. CAP256-VRC26 relatives were detected as early as 34 weeks and this data was used to infer the UCA of this lineage. The inferred UCA possessed a long CDRH3 of 35 amino acids and comparison with 34 week NGS data identified exact sequence matches with this UCA. This study showed that in the CAP256-VRC26 mAb lineage, the long CDRH3 resulted from a unique recombination event, rather than the gradual accumulation of length through SHM. The CAP256-VRC26-UCA was unable to neutralize heterologous viruses, but in a relatively short time period (~14 weeks), acquired neutralization breadth through subsequent SHM. While the developmental pathway for a V1V2 bNAb has only been described in the CAP256-VRC26 lineage, this data is considered a model for the development of all mAbs targeting the V1V2 quaternary epitope, as was originally hypothesized by Briney and colleagues[221,222].

8. Virus-antibody co-evolution: a blueprint for vaccine design

8.1. Viral escape from NAbs

Most HIV-1 infected individuals develop early strain-specific NAbs against the autologous virus after a few months of infection[124-126]. All NAbs, including strain-specific and broad responses, exert sufficient pressure on the virus to select for escape mutations[128-131,134,193,223-229] (Figure 15A). The high mutation rate of HIV-1 ensures that viral escape occurs very rapidly, often via multiple routes or mechanisms, which include amino acid mutations, indels and changes in glycosylation. Generation of viral mutants is so efficient, that even in individuals with relatively low viral loads, escaped viruses are rapidly selected[230]. As a result, contemporaneous viruses are usually less sensitive or resistant to neutralization by autologous NAbs than earlier viruses[130,134,193,228]. In addition, viruses from later in infection are generally resistant to neutralization by early NAb responses. Finally, NAb responses that are completely escaped by the viral quasispecies wane in titer as their antigenic stimuli decreases[130,134] (Figure 15B).

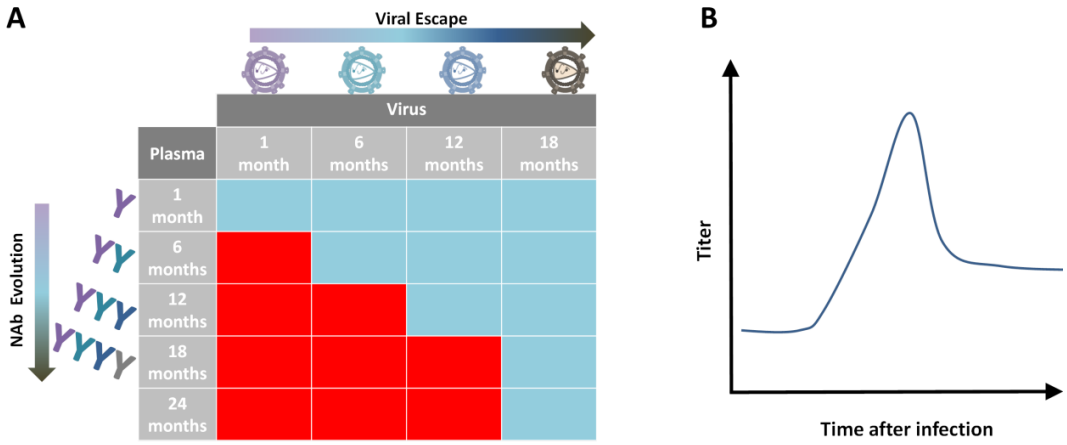


Figure 15. Schematic diagram depicting the anti-HIV-1 neutralizing antibody (NAb) response over time.
(A) "Evolutionary arms race" between the virus and NAb response. Early infection plasma samples are unable to neutralize viruses isolated from any time point as the antibody response only develops after established viral infection. After the development of the initial NAb response, continual viral escape is followed by antibody evolution, with later plasma able to neutralize earlier, but not later or contemporaneous viruses. Eventually complete viral escape is selected for, where all subsequent viruses are resistant to all later plasma. Red and blue squares indicate viral neutralization sensitivity and resistance respectively. (B) NAb response against HIV-1 gradually increases in titer and then wanes over the course of infection, due to viral escape. NAb titer is shown on the y-axis and time after infection is on the x-axis.

8.2 Tracking bNAb repertoires

Antibody isolation, coupled with the recent advances in NGS technologies has provided a platform for interrogating B cell repertoires. The use of variable heavy and light chain gene-specific primers, sequence identifier adapters or indices (to tag individual gene sequences) and fragmentation paired with immobilization of sequences allows for the simultaneous generation of vast numbers of pooled sequences, which can subsequently be deconstructed into individual sequence reads[231]. NGS has been used extensively to track specific antibody repertoires in individuals over time, to compare entire antibody repertoires between individuals and to understand the B cell repertoire prior to and after infection and/or vaccination[231,232]. In the HIV-1 field, cross sectional antibody repertoire studies have shown how antibody maturation circumvents viral immune evasion mechanisms. The PGT121 bNAb lineage, for example, matures over time to lose dependence on glycans and trimer crosslinking[233]. Diversity in bNAb lineages, a direct consequence of SHM, is often high[234,235] and in the VRC01 lineage, this mutation rate is comparable with that of HIV-1[236], enabling this mAb lineage to combat the quickly evolving virus.

These NGS-aided studies have described how SHM generates multiple versions of clonally-related NAbs which form lineages descended from a UCA. Therefore a precursor B cell or UCA gradually evolves through a series of intermediates, sometimes eventually developing the ability to neutralize heterologous viruses. These UCAs and intermediates are inferred, because conventional NGS does not biologically pair heavy and light chains or in the case of cross-sectional studies, due to sample unavailability, actual sequences of the UCAs cannot be acquired. Because the CDR3 of either the heavy or light chain, is created through V(D)J recombination, which may include junctional insertions at the recombination sites, inferring the sequence of the original CDR3 is impossible with cross-sectional samples. Thus, while longitudinal studies can accurately define the UCAs of bNAb lineages, only germline revertants, which contain the mature CDR3 within the backbone of a reverted V gene, can be derived using cross-sectional samples. Despite the inferred status of germline revertants and intermediates on the pathway to the development of neutralization breadth in bNAb lineages, these studies have provided valuable insights for vaccine design, particularly when used with longitudinal samples, which will be discussed below.

8.3 Virus-antibody co-evolution and the development of neutralization breadth

Two landmark studies, one of which forms part of this thesis, used NGS to track mAb evolution over time to accurately infer the UCAs and intermediates on the pathway to the development of a CD4bs[237] and a V1V2[191] bNAb lineage.

The UCA of the CH103 mAb lineage[237], which targeted the CD4bs, was only capable of strain-specific binding to the autologous transmitted/founder virus (Figure 16A). NGS at five time points between 6 and 144 weeks p.i. showed that over the course of 27 weeks a gradual accumulation of mutations in this mAb lineage led to the development of strain-specific neutralizing activity and the subsequent acquisition of broad neutralizing capabilities (Figure 16A and B). However, coupled with the development of breadth, this lineage also developed polyreactive traits. A concomitant accrual of mutations in the viral epitope for these mAbs also occurred, suggesting that co-evolution of the virus and mAbs led to the development of breadth in this antibody lineage.

Similarly, we determined the developmental pathway for the CAP256-VRC26 V1V2-directed mAb lineage using NGS at nine time points between 15 and 206 weeks after infection[191]. However, unlike the CD4bs CH103 UCA, the CAP256-VRC26 lineage possessed a long CDRH3, as a result of a unique recombination event (discussed in section 7.2). A gradual accumulation of mutations occurred in both the CAP256-VRC26 lineage and the virus, with viral diversity in the V1V2 epitope eventually peaking just prior to the development of neutralization breadth (Figure 17). However, while the CH103 UCA was only capable of strain-specific binding to autologous Env, the CAP256-VRC26-UCA was able to weakly neutralize the autologous superinfecting transmitted/founder virus. In addition, development of breadth occurred 14 weeks after the CAP256-VRC26 lineage was first detected by NGS, 13 weeks earlier than the CH103 lineage.

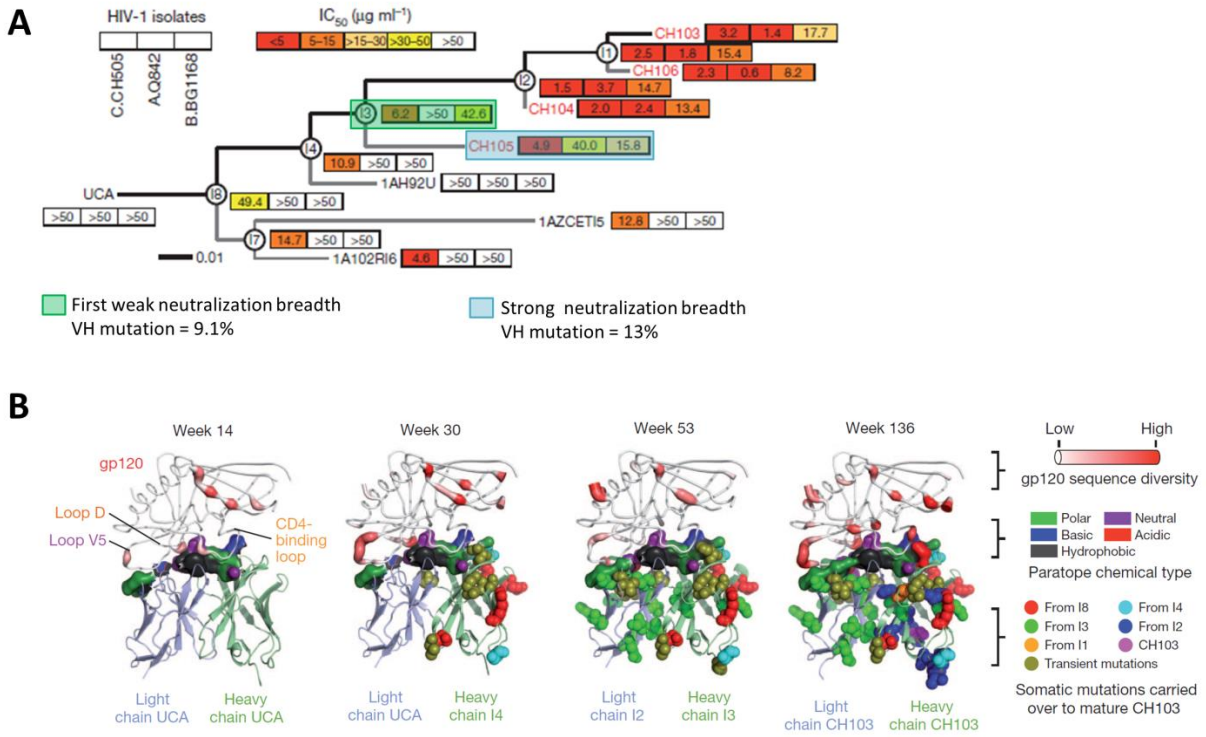


Figure 16. Maturation of the CH103 CD4 binding site mAb lineage towards neutralization breadth. (A) Phylogenetic tree displaying the relationship between the unmutated common ancestor (UCA), developmental intermediates and broadly neutralizing antibodies (bNAbs) within the CH103 lineage. Neutralization of the autologous transmitted/founder virus (CH505) and two heterologous viruses (Q842 and BG168) by each antibody is shown in colored blocks with potency indicated by the key. Binding of the UCA to the transmitted/founder virus is also shown in a block beneath the neutralization data. Intermediate 3 (I3), highlighted in grey, is the first developmental intermediate with weak neutralization breadth. CH103, shaded in green, is the mature bNAb. (B) Antibody-Env binding models displaying the accumulation of mutations in both the virus and antibody from 14 to 136 weeks post-infection. Env residues are shown as tubes, with sequence diversity indicated by the key. Antibody residues are shown as ribbon representations, with spheres (colored according to the key) highlighting mutations. Figure taken from Liao *et al* 2013[237].

CD4bs bNAbs generally arise much later in infection than other bNAb responses and have the highest levels of SHM of all bNAb classes. Together with the fact that the CH103 lineage took twice as long as the CAP256-VRC26 lineage to develop neutralization breadth, may suggest that the V1V2 region may be a more viable vaccine target. In both the CH103 and CAP256-VRC26 lineages however, the acquisition of neutralization breadth occurred with the gradual and concomitant accumulation of mutations in the mAbs and cognate viral epitopes, suggested a role for viral diversification in the development of neutralization breadth.

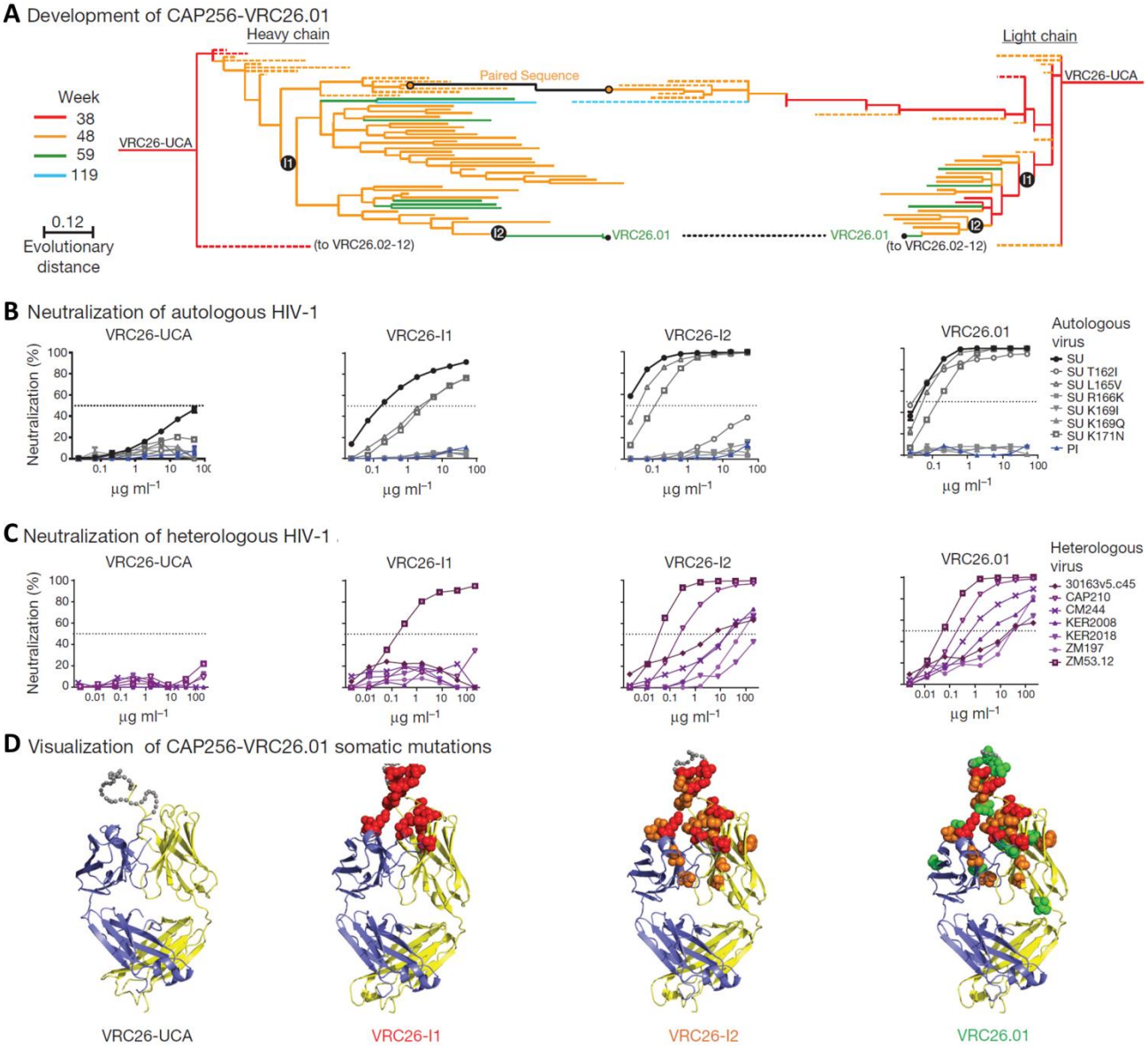


Figure 17. Maturation of the CAP256-VRC26 V1V2-directed mAb lineage towards neutralization breadth.

(A) Maximum likelihood phylogenetic tree showing the pathway of maturation for the heavy (left) and light (right) chain of CAP256-VRC26.01, with the branches to the other CAP256-VRC26 antibodies collapsed. The positions of the inferred intermediates, I1 and I2, are indicated as black dots. Branches are colored by time point when next-generation sequences were first detected as indicated in the key. Scale shows rate of nucleotide change (per site) between nodes. (B) Neutralization of autologous transmitted/founder viruses and V1V2 mutants by the CAP256-VRC26-UCA, -I1, -I2 and .01. (C) Neutralization of heterologous viruses by the CAP256-VRC26-UCA, -I1, -I2 and .01. (D) Ribbon representations of the CAP256-VRC26-UCA, -I1, -I2 and .01 Fab regions, with accumulating mutations highlighted by spheres. Spheres are colored according to when the mutations first appear (red in I1, orange in I2 and green in .01). Figure taken from Doria-Rose *et al* 2014[191].

8.4. Initiation of bNAb precursors

Identification of viruses or recombinant HIV-1 proteins that are reactive with bNAb precursors or UCAs has been challenging and is complicated by the fact that most inferred bNAb precursors are germline revertants, which may not recapitulate the paratope of the actual antibody correctly. Germline reversions of bNAbs targeting four of the five known epitopes on Env (the MPER[238,239], the V1V2 region[190,240], the N332/V3 region[233] and the CD4bs[197,241-243]) show little or no binding to recombinant HIV-1 Env proteins, including those derived from viruses that are well neutralized by their mature bNAb counterparts. This is in contrast to strain-specific NAb germline revertants, which are more promiscuous in their interactions with diverse Envs[244]. Thus, a major hurdle in the elicitation of bNAbs by immunization is the initial interaction between a naïve B cell expressing a bNAb precursor and its cognate antigen.

In addition, longitudinal studies have shown that the epitopes of broadly neutralizing plasma responses in many HIV-1 infected individuals are either absent or less than optimal on the corresponding transmitted/founder viruses[134,227]. This, coupled with the delayed onset of bNAbs, between one and three years after HIV-1 infection[119,139,141] suggests the possibility that later viral variants as well as transmitted/founder viruses may engage bNAb UCAs.

The unusual features of bNAbs suggest that their initiation may be further hampered by the rarity of their precursors in the naïve B cell pool. For example, VH-restricted CD4bs bNAbs generally have an unusually short CDRL3 in the kappa chain, which avoids clashes with the V5 and D loops, however only 0.6-1% of naïve B cells possess these short CDRL3 loops[245]. B cells that produce antibodies with long CDRH3 loops, such as those in V1V2- and N332-directed bNAbs, are generally deleted due to their increased potential for self-reactivity and as such are only present in 0.4% of all naïve B cells[221]. Therefore highly specific immunogens will be required to engage and activate these rare bNAb precursors. Two strategies have been employed to identify such bNAb-initiating Envs or immunogens, namely the identification of naturally occurring viral variants that are engaged by bNAb precursors and structure-guided immunogen design.

The highly conserved CD4bs, for which Env-antibody crystal structures with bNAbs from 14 different donors[172] are available, was used to design[79] and optimize[241,245] engineered outer domain germline targeting (eOD-GT) proteins. To investigate the ability of this immunogen to selectively stimulate expansion of CD4bs bNAb precursors, two groups created humanized mice, which expressed the germline heavy chain of CD4bs bNAbs, VRC01[245] or 3BNC60[246]. eOD-GT8, expressed as 60mers on nanoparticles efficiently and preferentially activated CD4bs bNAb precursors with the VRC01 or 3BNC60 heavy chains and selected for the use of mouse light chains with a short CDRL3. These studies also showed that immunization of the engineered mice with the BG505 SOSIP.664 trimer did not prime CD4bs bNAb precursors.

In this thesis, we studied natural infection to identify authentic bNAb-initiating Envs that primed the V1V2-directed CAP256-VRC26 response by engaging the rare long CDRH3 of the CAP256-VRC26-UCA. While the CAP256-VRC26-UCA was able to weakly neutralize the superinfecting virus, this virus was not detected at 34 weeks after infection, when CAP256-VRC26 sequences were first isolated. However four CAP256 34 week viruses, which were closely related to the superinfecting virus, were 5-17-fold more sensitive to neutralization by the CAP256-VRC-UCA than the superinfecting virus[247]. Although the weak neutralization of the superinfecting virus may suggest that this Env initiated the response and the 34 week Envs boosted the response, the enhanced sensitivity of the 34 week viruses to the CAP256-VRC bNAb precursor suggested that these Envs (rather than the superinfecting virus Env) should be used to create immunogens to prime V1V2-directed responses.

8.5. The role of viral evolution in driving neutralization breadth

Studies using polyclonal and monoclonal bNAb responses have identified a number of factors that are associated with the development of neutralization breadth, including low CD4 T cell count[119], higher frequency of T follicular helper (Tfh) cells in the periphery[248], and HLA genotype[249]. However viral factors, such as high viral loads[119,137,139], inter-clade superinfection[250,251] and higher Env diversity[137] have also been linked with the development of broadly neutralizing responses. In addition, the two longitudinal bNAb ontogeny studies

described an increase in viral diversification within the bNAb epitope prior to the development of neutralization breadth[191,237].

We and others have therefore focused on the role of the autologous viral population in driving neutralization breadth. Recent studies have highlighted three major mechanisms whereby the evolving viral population shapes the development of bNAbs[252]. Firstly, viral escape from other NAb responses can directly create bNAb epitopes by mutating key residues within the bNAb sites[134,227,253]. Secondly, viral escape can induce the exposure of bNAb epitopes[134] through glycan shifting or changing of variable loop lengths. In addition to previous studies which investigated polyclonal plasma responses[134], the third mechanism, of affinity maturation driven by exposure to multiple viral immunotypes, is described in this thesis[247] and will therefore be discussed in greater detail below.

As described in sections 8.3 and 8.4, the CAP256-VRC26-UCA only had the ability to neutralize four closely-related autologous viruses and none of a 196 heterologous virus panel. The development of breadth in the CAP256 plasma occurred 14 weeks after the first detection of the CAP256-VRC26 lineage and just after a peak in viral diversification within the V1V2 epitope. This suggested a role for viral evolution in the development of neutralization breadth. Therefore, to investigate the specific viral changes that occurred during CAP256-VRC26 maturation, we performed viral NGS of the V1V2 region at 28 time points between 6 and 206 weeks after infection[247]. These data showed an accumulation of multiple immunotypes (or amino acids) at two key viral residues in the epitope of the CAP256-VRC26 mAbs. Indeed, just prior to the development of neutralization breadth in CAP256, the autologous viral quasispecies sampled 9 immunotypes at position 169 and approximately 17 weeks later amino acid toggling occurred at position 166. This suggested that early CAP256-VRC26 lineage members exerted strong selection pressure on the autologous virus. Introduction of select immunotypes at positions 169 and 166 into the superinfecting virus showed a correlation between neutralization breadth of the CAP256-VRC26 mAbs and their neutralization of the 169 and 166 mutants (Figure 18). Therefore viral escape created multiple immunotypes at key residues in the CAP256-VRC26 V1V2 epitope. Exposure to this viral variation drove the evolution of CAP256-VRC26 lineage members with the ability to tolerate this diversity and therefore possess neutralization breadth. Thus viral escape generates diversity within the epitope while SHM creates multiple mAb variants, and

affinity-based mAb selection for escaped viruses, results in mAb evolution towards tolerating variability.

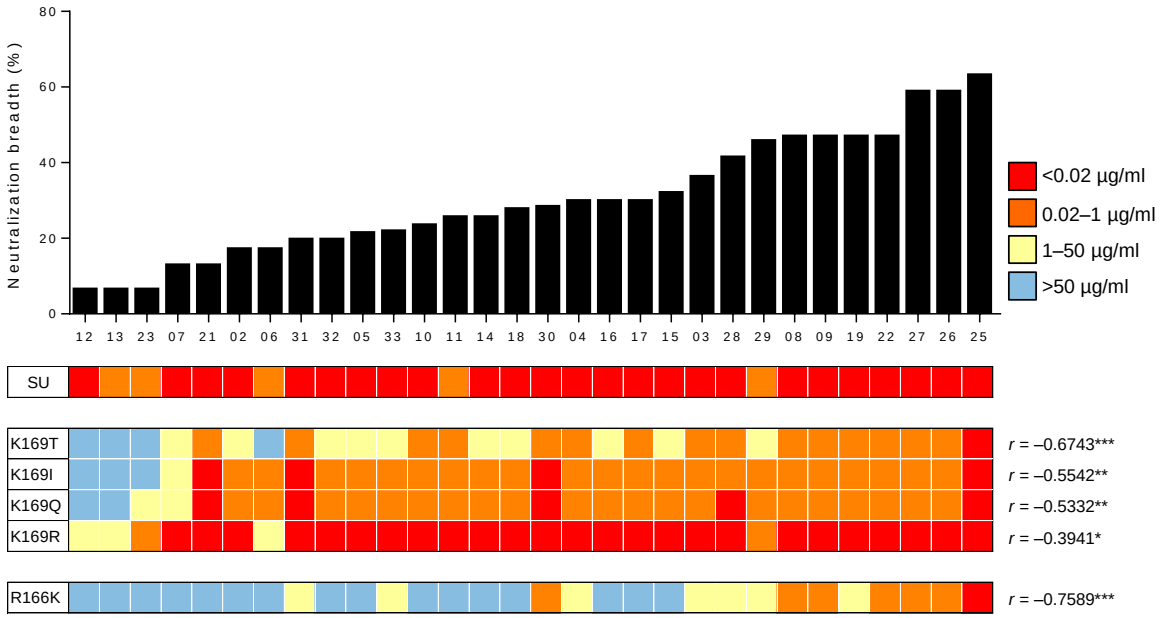


Figure 18. Relationship between CAP256-VRC26 antibody neutralization breadth and tolerance of multiple immunotypes at positions 169 and 166.
Thirty monoclonal antibodies (mAbs) in the CAP256-VRC26 lineage are ranked according to neutralization breadth in the histogram. Neutralization of the superinfecting virus (SU) and 169 or 166 mutant viruses by CAP256-VRC26 mAbs are shown as a heat map, with shading showing neutralization potency, as indicated in the key. Correlations (r) between neutralization breadth and the IC_{50} titers of each mutant virus are indicated on the right of the heat map. *P < 0.05; **P < 0.005; ***P < 0.0001, calculated using a two-tailed non-parametric Spearman correlation. Figure taken from Bhiman *et al* 2015[247].

8.6 Caveats and implications for vaccine design

Anti-HIV-1 bNAb evolution has greatly informed immunization strategies to elicit bNAb responses. Immunogen engineering and validation, based on these studies, has become the new focus of the HIV-1 vaccine field. The use of stabilized trimers as immunogens, including the BG505 SOSIP.664[245,246,254,255], has already begun, however based on the immunodominance of non-bNAb epitopes, it may be necessary to use glycan shielding to limit responses to unwanted regions. In addition, scaffolded bNAb epitope proteins may provide alternate solutions to avoid stimulation of non-bNAb responses[216]. Irrespective of the type of immunogen, multiple rounds of refinement will likely be required to fine tune proposed immunization strategies. These refinements might progress faster through the use

of *in silico* and humanized mice studies. In addition, the concentration of sequential and cocktail immunogens may need to be varied to determine the optimal mixture for the elicitation of bNAb versus strain-specific NAb responses.

The inclusion of all Env diversity generated during bNAb development, either as a cocktail of multiple immunogens or as sequential series of immunogens, has been proposed[237]. However the identification of viral variants present at distinct steps in bNAb development might provide a more rational vaccination strategy. To this end, we have suggested a sequential immunization strategy that mimics the virus-antibody co-evolution which occurred during the development of the CAP256-VRC26 lineage (Figure 19). This regimen begins with a prime, using bNAb-initiating Env derived immunogens, followed by three sequential boosts. The initial boost is designed to act as a bridging between the priming immunogen and the cocktail of immunogens presented in the second boost. While the first two boosts introduce diversity at one site, the final boost generates diversity at a second key site in this bNAb epitope.

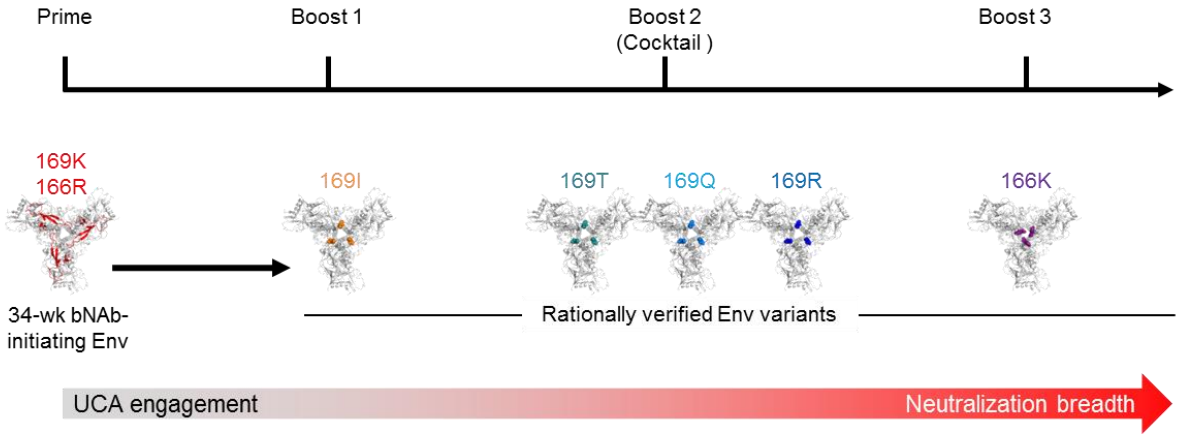


Figure 19. Recapitulating viral evolution for vaccine design.
A proposed prime-sequential boost immunization strategy to elicit V1V2-directed bNAbs, based on the key viral events that initiated and drove neutralization breadth in the CAP256-VRC26 lineage. A CAP256 34-week bNAb-initiating Env (red), which has the 169K and 166R immunotypes, would be used as a prime to engage UCAs with long CDRH3s. This would be followed by three sequential boosts using immunogens with varying immunotypes to mimic the viral diversification in CAP256 that drove bNAb development. The 169I boost (orange) would be administered first, followed by a cocktail of 169T/Q and R immunogens (blue) and a final boost to expose vaccine-induced mAbs to the 166K immunotype (purple). Taken from Bhiman *et al,* 2015[247].

In addition, determining the frequency of bNAb precursors in HIV-1 uninfected, healthy individuals will be required to ascertain feasibility of eliciting bNAb responses. Despite a recent study, showing that HIV-1 infected individuals who develop neutralization breadth and those who do not, have the same Ig germline genetic potential[256], the rare recombination events that lead to development of bNAbs precursors may suggest that not all individuals can make these types of antibodies. NGS screening of the B cell repertoire of greater numbers of healthy individuals, from distinct ethnic backgrounds will be necessary to determine the frequency of these cells. However if all individuals can produce bNAb precursors, this may be a time-dependent occurrence and therefore longitudinal repertoire analysis, in adults and children may be necessary.

8.7. Conclusion

Since the start of this PhD in 2012, the HIV-1 vaccine field has made enormous advancements, big innovations and new discoveries to propel research into an exponential growth phase. These include the identification of a new bNAb target on the HIV-1 Env, elucidation of the developmental pathways of two bNAb lineages and the engineering of an HIV-1 immunogen that preferentially activates CD4bs bNAb precursors in humanized mice. In addition to this, clinical trial approval to test the efficacy of bNAbs for passive, rather than active, vaccination has been granted in countries worst affected by this virus, such as South Africa[166].

While the search for an HIV-1 vaccine still continues, almost 30 years after the very first HIV-1 vaccine trial was performed in 1986[257], the isolation and characterization of bNAbs that target sites of vulnerability on the HIV-1 Env, coupled with the first structural view of the prefusion trimer has moved research towards the rational design of immunogens that can elicit these types of responses.

The findings presented in this thesis show how bNAbs within an HIV-1 infected individual gradually mature to acquire neutralization breadth and how this maturation occurs in direct response to the evolving viral quasispecies. The net result is a testable HIV-1 vaccine

immunization strategy that was identified through the delineation of antibody and virus co-evolution during the development of neutralization breadth.

9. References

1 UNAIDS. Global AIDS Update 2016. (Joint United Nations Programme on HIV/AIDS, Geneva, Switzerland, 2016).

2 Kharsany, A. B. *et al.* Trends in HIV Prevalence in Pregnant Women in Rural South Africa. *J Acquir Immune Defic Syndr* **70**, 289-295, doi:10.1097/QAI.0000000000000761 (2015).

3 Auvert, B. *et al.* Randomized, controlled intervention trial of male circumcision for reduction of HIV infection risk: the ANRS 1265 Trial. *PLoS Med* **2**, e298, doi:05-PLME-RA-0310R1 [pii]10.1371/journal.pmed.0020298 (2005).

4 Gray, R. H. *et al.* Male circumcision and HIV acquisition and transmission: cohort studies in Rakai, Uganda. Rakai Project Team. *AIDS* **14**, 2371-2381 (2000).

5 Pinkerton, S. D. & Abramson, P. R. Effectiveness of condoms in preventing HIV transmission. *Soc Sci Med* **44**, 1303-1312 (1997).

6 Hope, T. J. & Marrazzo, J. M. A Shot in the Arm for HIV Prevention? Recent Successes and Critical Thresholds. *AIDS Res Hum Retroviruses* **31**, 1055-1059, doi:10.1089/AID.2015.0310 (2015).

7 Barron, P. *et al.* Eliminating mother-to-child HIV transmission in South Africa. *Bull World Health Organ* **91**, 70-74, doi:10.2471/BLT.12.106807 (2013).

8 Baeten, J. M. *et al.* Antiretroviral prophylaxis for HIV prevention in heterosexual men and women. *N Engl J Med* **367**, 399-410, doi:10.1056/NEJMoa1108524 (2012).

9 Grant, R. M. Antiretroviral agents used by HIV-uninfected persons for prevention: pre- and postexposure prophylaxis. *Clin Infect Dis* **50 Suppl 3**, S96-101, doi:10.1086/651479 (2010).

10 Plotkin, S. T. & Plotkin, S. A. in *Vaccines* (eds S. A. Orenstein Plotkin, W. A. & A. A. Offit) 1-13 (Elsevier/Saunders, 2013).

11 Prevention, C. f. D. C. a. *Measles Cases and Outbreaks*, <http://www.cdc.gov/measles/cases-outbreaks.html> (Accessed 2 June 2016).

12 Esparza, J. A brief history of the global effort to develop a preventive HIV vaccine. *Vaccine* **31**, 3502-3518, doi:10.1016/j.vaccine.2013.05.018 (2013).

13 Rerks-Ngarm, S. *et al.* Vaccination with ALVAC and AIDSVAX to prevent HIV-1 infection in Thailand. *N Engl J Med* **361**, 2209-2220, doi:NEJMoa0908492 [pii] 10.1056/NEJMoa0908492 (2009).

14 Josefson, D. Approval given for trials of AIDS vaccine. *BMJ* **316**, 1769 (1998).

15 Cohen, J. Planned tests in Thailand spark debate. *Science* **276**, 1197 (1997).

16 Berman, P. W. *et al.* Protection of chimpanzees from infection by HIV-1 after vaccination with recombinant glycoprotein gp120 but not gp160. *Nature* **345**, 622-625, doi:10.1038/345622a0 (1990).

17 Berman, P. W. *et al.* Protection of MN-rgp120-immunized chimpanzees from heterologous infection with a primary isolate of human immunodeficiency virus type 1. *J Infect Dis* **173**, 52-59 (1996).

18 Flynn, N. M. *et al.* Placebo-controlled phase 3 trial of a recombinant glycoprotein 120 vaccine to prevent HIV-1 infection. *J Infect Dis* **191**, 654-665, doi:10.1086/428404 (2005).

19 Pitisuttithum, P. *et al.* Randomized, double-blind, placebo-controlled efficacy trial of a bivalent recombinant glycoprotein 120 HIV-1 vaccine among injection drug users in Bangkok, Thailand. *J Infect Dis* **194**, 1661-1671, doi:10.1086/508748 (2006).

20 Buchbinder, S. P. *et al.* Efficacy assessment of a cell-mediated immunity HIV-1 vaccine (the Step Study): a double-blind, randomised, placebo-controlled, test-of-concept trial. *Lancet* **372**, 1881-1893, doi:10.1016/S0140-6736(08)61591-3 (2008).

21 Duerr, A. *et al.* Extended follow-up confirms early vaccine-enhanced risk of HIV acquisition and demonstrates waning effect over time among participants in a randomized trial of recombinant adenovirus HIV vaccine (Step Study). *J Infect Dis* **206**, 258-266, doi:10.1093/infdis/jis342 (2012).

22 Gray, G. E. *et al.* Recombinant adenovirus type 5 HIV gag/pol/nef vaccine in South Africa: unblinded, long-term follow-up of the phase 2b HVTN 503/Phambili study. *Lancet Infect Dis* **14**, 388-396, doi:10.1016/S1473-3099(14)70020-9 (2014).

23 Catanzaro, A. T. *et al.* Phase 1 safety and immunogenicity evaluation of a multiclade HIV-1 candidate vaccine delivered by a replication-defective recombinant adenovirus vector. *J Infect Dis* **194**, 1638-1649, doi:10.1086/509258 (2006).

24 Catanzaro, A. T. *et al.* Phase I clinical evaluation of a six-plasmid multiclade HIV-1 DNA candidate vaccine. *Vaccine* **25**, 4085-4092, doi:10.1016/j.vaccine.2007.02.050 (2007).

25 Hammer, S. M. *et al.* Efficacy trial of a DNA/rAd5 HIV-1 preventive vaccine. *N Engl J Med* **369**, 2083-2092, doi:10.1056/NEJMoa1310566 (2013).

26 Haynes, B. F. *et al.* Immune-correlates analysis of an HIV-1 vaccine efficacy trial. *N Engl J Med* **366**, 1275-1286, doi:10.1056/NEJMoa1113425 (2012).

27 Hirsch, V. M., Olmsted, R. A., Murphey-Corb, M., Purcell, R. H. & Johnson, P. R. An African primate lentivirus (SIVsm) closely related to HIV-2. *Nature* **339**, 389-392, doi:10.1038/339389a0 (1989).

28 Gao, F. *et al.* Origin of HIV-1 in the chimpanzee Pan troglodytes troglodytes. *Nature* **397**, 436-441, doi:10.1038/17130 (1999).

29 Keele, B. F. *et al.* Chimpanzee reservoirs of pandemic and nonpandemic HIV-1. *Science* **313**, 523-526, doi:10.1126/science.1126531 (2006).

30 Van Heuverswyn, F. *et al.* Genetic diversity and phylogeographic clustering of SIVcpzPtt in wild chimpanzees in Cameroon. *Virology* **368**, 155-171, doi:10.1016/j.virol.2007.06.018 (2007).

31 Sharp, P. M. & Hahn, B. H. Origins of HIV and the AIDS pandemic. *Cold Spring Harb Perspect Med* **1**, a006841, doi:10.1101/cshperspect.a006841 (2011).

32 Plantier, J. C. *et al.* A new human immunodeficiency virus derived from gorillas. *Nat Med* **15**, 871-872, doi:nm.2016 [pii] 10.1038/nm.2016 (2009).

33 Vallari, A. *et al.* Four new HIV-1 group N isolates from Cameroon: Prevalence continues to be low. *AIDS Res Hum Retroviruses* **26**, 109-115, doi:10.1089/aid.2009.0178 (2010).

34 Vallari, A. *et al.* Confirmation of putative HIV-1 group P in Cameroon. *J Virol* **85**, 1403-1407, doi:10.1128/JVI.02005-10 (2011).

35 Gottlieb, M. S. *et al.* Pneumocystis carinii pneumonia and mucosal candidiasis in previously healthy homosexual men: evidence of a new acquired cellular immunodeficiency. *N Engl J Med* **305**, 1425-1431, doi:10.1056/NEJM198112103052401 (1981).

36 Barre-Sinoussi, F. *et al.* Isolation of a T-lymphotropic retrovirus from a patient at risk for acquired immune deficiency syndrome (AIDS). *Science* **220**, 868-871 (1983).

37 Gallo, R. C. *et al.* Isolation of human T-cell leukemia virus in acquired immune deficiency syndrome (AIDS). *Science* **220**, 865-867 (1983).

38 Popovic, M., Sarngadharan, M. G., Read, E. & Gallo, R. C. Detection, isolation, and continuous production of cytopathic retroviruses (HTLV-III) from patients with AIDS and pre-AIDS. *Science* **224**, 497-500 (1984).

39 Zhu, T. *et al.* An African HIV-1 sequence from 1959 and implications for the origin of the epidemic. *Nature* **391**, 594-597, doi:10.1038/35400 (1998).

40 Worobey, M. *et al.* Direct evidence of extensive diversity of HIV-1 in Kinshasa by 1960. *Nature* **455**, 661-664, doi:10.1038/nature07390 (2008).

41 Faria, N. R. *et al.* HIV epidemiology. The early spread and epidemic ignition of HIV-1 in human populations. *Science* **346**, 56-61, doi:10.1126/science.1256739 (2014).

42 Levy, J. A. Pathogenesis of human immunodeficiency virus infection. *Microbiol Rev* **57**, 183-289 (1993).

43 Gentile, M. *et al.* Determination of the size of HIV using adenovirus type 2 as an internal length marker. *J Virol Methods* **48**, 43-52 (1994).

44 Moore, P. L. *et al.* Nature of nonfunctional envelope proteins on the surface of human immunodeficiency virus type 1. *J Virol* **80**, 2515-2528 (2006).

45 Roberts, J. D., Bebenek, K. & Kunkel, T. A. The accuracy of reverse transcriptase from HIV-1. *Science* **242**, 1171-1173 (1988).

46 Frankel, A. D. & Young, J. A. HIV-1: fifteen proteins and an RNA. *Annu Rev Biochem* **67**, 1-25, doi:10.1146/annurev.biochem.67.1.1 (1998).

47 Klatzmann, D. *et al.* T-lymphocyte T4 molecule behaves as the receptor for human retrovirus LAV. *Nature* **312**, 767-768 (1984).

48 McDougal, J. S. *et al.* Binding of HTLV-III/LAV to T4+ T cells by a complex of the 110K viral protein and the T4 molecule. *Science* **231**, 382-385 (1986).

49 Feng, Y., Broder, C. C., Kennedy, P. E. & Berger, E. A. HIV-1 entry cofactor: functional cDNA cloning of a seven-transmembrane, G protein-coupled receptor. *Science* **272**, 872-877 (1996).

50 Deng, H. *et al.* Identification of a major co-receptor for primary isolates of HIV-1. *Nature* **381**, 661-666, doi:10.1038/381661a0 (1996).

51 Alkhatib, G. *et al.* CC CKR5: a RANTES, MIP-1alpha, MIP-1beta receptor as a fusion cofactor for macrophage-tropic HIV-1. *Science* **272**, 1955-1958 (1996).

52 Starcich, B. R. *et al.* Identification and characterization of conserved and variable regions in the envelope gene of HTLV-III/LAV, the retrovirus of AIDS. *Cell* **45**, 637-648 (1986).

53 Willey, R. L. *et al.* Identification of conserved and divergent domains within the envelope gene of the acquired immunodeficiency syndrome retrovirus. *Proc Natl Acad Sci U S A* **83**, 5038-5042 (1986).

54 Leonard, C. K. *et al.* Assignment of intrachain disulfide bonds and characterization of potential glycosylation sites of the type 1 recombinant human immunodeficiency virus envelope glycoprotein (gp120) expressed in Chinese hamster ovary cells. *J Biol Chem* **265**, 10373-10382 (1990).

55 Allan, J. S. *et al.* Major glycoprotein antigens that induce antibodies in AIDS patients are encoded by HTLV-III. *Science* **228**, 1091-1094 (1985).

56 Bosch, M. L. *et al.* Identification of the fusion peptide of primate immunodeficiency viruses. *Science* **244**, 694-697 (1989).

57 Freed, E. O., Myers, D. J. & Risser, R. Characterization of the fusion domain of the human immunodeficiency virus type 1 envelope glycoprotein gp41. *Proc Natl Acad Sci U S A* **87**, 4650-4654 (1990).

58 Freed, E. O., Delwart, E. L., Buchschacher, G. L., Jr. & Panganiban, A. T. A mutation in the human immunodeficiency virus type 1 transmembrane glycoprotein gp41 dominantly interferes with fusion and infectivity. *Proc Natl Acad Sci U S A* **89**, 70-74 (1992).

59 Chan, D. C., Fass, D., Berger, J. M. & Kim, P. S. Core structure of gp41 from the HIV envelope glycoprotein. *Cell* **89**, 263-273 (1997).

60 Dubay, J. W., Roberts, S. J., Brody, B. & Hunter, E. Mutations in the leucine zipper of the human immunodeficiency virus type 1 transmembrane glycoprotein affect fusion and infectivity. *J Virol* **66**, 4748-4756 (1992).

61 Lu, M., Blacklow, S. C. & Kim, P. S. A trimeric structural domain of the HIV-1 transmembrane glycoprotein. *Nat Struct Biol* **2**, 1075-1082 (1995).

62 Weissenhorn, W., Dessen, A., Harrison, S. C., Skehel, J. J. & Wiley, D. C. Atomic structure of the ectodomain from HIV-1 gp41. *Nature* **387**, 426-430 (1997).

63 Munoz-Barroso, I., Salzwedel, K., Hunter, E. & Blumenthal, R. Role of the membrane-proximal domain in the initial stages of human immunodeficiency virus type 1 envelope glycoprotein-mediated membrane fusion. *J Virol* **73**, 6089-6092 (1999).

64 Salzwedel, K., West, J. T. & Hunter, E. A conserved tryptophan-rich motif in the membrane-proximal region of the human immunodeficiency virus type 1 gp41 ectodomain is important for Env-mediated fusion and virus infectivity. *J Virol* **73**, 2469-2480 (1999).

65 Haffar, O. K., Dowbenko, D. J. & Berman, P. W. Topogenic analysis of the human immunodeficiency virus type 1 envelope glycoprotein, gp160, in microsomal membranes. *J Cell Biol* **107**, 1677-1687 (1988).

66 Berman, P. W., Nunes, W. M. & Haffar, O. K. Expression of membrane-associated and secreted variants of gp160 of human immunodeficiency virus type 1 in vitro and in continuous cell lines. *J Virol* **62**, 3135-3142 (1988).

67 Mao, Y. *et al.* Subunit organization of the membrane-bound HIV-1 envelope glycoprotein trimer. *Nat Struct Mol Biol* **19**, 893-899, doi:10.1038/nsmb.2351 (2012).

68 Julien, J. P. *et al.* Crystal structure of a soluble cleaved HIV-1 envelope trimer. *Science* **342**, 1477-1483, doi:10.1126/science.1245625 (2013).

69 Pancera, M. *et al.* Structure and immune recognition of trimeric pre-fusion HIV-1 Env. *Nature* **514**, 455-461, doi:10.1038/nature13808 (2014).

70 Helseth, E., Olshevsky, U., Furman, C. & Sodroski, J. Human immunodeficiency virus type 1 gp120 envelope glycoprotein regions important for association with the gp41 transmembrane glycoprotein. *J Virol* **65**, 2119-2123 (1991).

71 Moore, J. P., Willey, R. L., Lewis, G. K., Robinson, J. & Sodroski, J. Immunological evidence for interactions between the first, second, and fifth conserved domains of the gp120 surface glycoprotein of human immunodeficiency virus type 1. *J Virol* **68**, 6836-6847 (1994).

72 Kwong, P. D. *et al.* Structure of an HIV gp120 envelope glycoprotein in complex with the CD4 receptor and a neutralizing human antibody. *Nature* **393**, 648-659 (1998).

73 Huang, C. C. *et al.* Structure of a V3-containing HIV-1 gp120 core. *Science* **310**, 1025-1028 (2005).

74 Pancera, M. *et al.* Structure of HIV-1 gp120 with gp41-interactive region reveals layered envelope architecture and basis of conformational mobility. *Proc Natl Acad Sci U S A* **107**, 1166-1171, doi:0911004107 [pii]10.1073/pnas.0911004107 (2010).

75 Diskin, R., Marcovecchio, P. M. & Bjorkman, P. J. Structure of a clade C HIV-1 gp120 bound to CD4 and CD4-induced antibody reveals anti-CD4 polyreactivity. *Nat Struct Mol Biol* **17**, 608-613, doi:nsmb.1796 [pii]10.1038/nsmb.1796 (2010).

76 Finzi, A. *et al.* Topological layers in the HIV-1 gp120 inner domain regulate gp41 interaction and CD4-triggered conformational transitions. *Mol Cell* **37**, 656-667, doi:S1097-2765(10)00154-1 [pii]10.1016/j.molcel.2010.02.012 (2010).

77 Kwon, Y. D. *et al.* Crystal structure, conformational fixation and entry-related interactions of mature ligand-free HIV-1 Env. *Nat Struct Mol Biol* **22**, 522-531, doi:10.1038/nsmb.3051 (2015).

78 McLellan, J. S. *et al.* Structure of HIV-1 gp120 V1/V2 domain with broadly neutralizing antibody PG9. *Nature* **480**, 336-343, doi:10.1038/nature10696nature10696 [pii] (2011).

79 Pejchal, R. *et al.* A potent and broad neutralizing antibody recognizes and penetrates the HIV glycan shield. *Science* **334**, 1097-1103, doi:science.1213256 [pii]10.1126/science.1213256 (2011).

80 Lyumkis, D. *et al.* Cryo-EM structure of a fully glycosylated soluble cleaved HIV-1 envelope trimer. *Science* **342**, 1484-1490, doi:10.1126/science.1245627 (2013).

81 Sanders, R. W. *et al.* A next-generation cleaved, soluble HIV-1 Env Trimer, BG505 SOSIP.664 gp140, expresses multiple epitopes for broadly neutralizing but not non-neutralizing antibodies. *PLoS pathogens* **9**, e1003618, doi:10.1371/journal.ppat.1003618 (2013).

82 Sanders, R. W. *et al.* Stabilization of the soluble, cleaved, trimeric form of the envelope glycoprotein complex of human immunodeficiency virus type 1. *J Virol* **76**, 8875-8889 (2002).

83 Julien, J. P. *et al.* Asymmetric recognition of the HIV-1 trimer by broadly neutralizing antibody PG9. *Proc Natl Acad Sci U S A* **110**, 4351-4356, doi:10.1073/pnas.1217537110 (2013).

84 Khayat, R. *et al.* Structural characterization of cleaved, soluble HIV-1 envelope glycoprotein trimers. *J Virol* **87**, 9865-9872, doi:10.1128/JVI.01222-13 (2013).

85 Klasse, P. J. *et al.* Influences on trimerization and aggregation of soluble, cleaved HIV-1 SOSIP envelope glycoprotein. *J Virol* **87**, 9873-9885, doi:10.1128/JVI.01226-13 (2013).

86 Tan, K., Liu, J., Wang, J., Shen, S. & Lu, M. Atomic structure of a thermostable subdomain of HIV-1 gp41. *Proc Natl Acad Sci U S A* **94**, 12303-12308 (1997).

87 Melikyan, G. B. *et al.* Evidence that the transition of HIV-1 gp41 into a six-helix bundle, not the bundle configuration, induces membrane fusion. *J Cell Biol* **151**, 413-423 (2000).

88 Freed, E. O. & Martin, M. A. The role of human immunodeficiency virus type 1 envelope glycoproteins in virus infection. *J Biol Chem* **270**, 23883-23886 (1995).

89 Gagneux, P. & Varki, A. Evolutionary considerations in relating oligosaccharide diversity to biological function. *Glycobiology* **9**, 747-755, doi:cwc089 [pii] (1999).

90 Choi, B. K. *et al.* Use of combinatorial genetic libraries to humanize N-linked glycosylation in the yeast Pichia pastoris. *Proc Natl Acad Sci U S A* **100**, 5022-5027, doi:10.1073/pnas.0931263100 0931263100 [pii] (2003).

91 Kwong, P. D. *et al.* HIV-1 evades antibody-mediated neutralization through conformational masking of receptor-binding sites. *Nature* **420**, 678-682 (2002).

92 Zhu, X., Borchers, C., Bienstock, R. J. & Tomer, K. B. Mass spectrometric characterization of the glycosylation pattern of HIV-gp120 expressed in CHO cells. *Biochemistry* **39**, 11194-11204 (2000).

93 Cutalo, J. M., Deterding, L. J. & Tomer, K. B. Characterization of glycopeptides from HIV-I(SF2) gp120 by liquid chromatography mass spectrometry. *Journal of the American Society for Mass Spectrometry* **15**, 1545-1555, doi:10.1016/j.jasms.2004.07.008 (2004).

94 Crispin, M. D. *et al.* Monoglucosylated glycans in the secreted human complement component C3: implications for protein biosynthesis and structure. *FEBS Lett* **566**, 270-274, doi:10.1016/j.febslet.2004.04.045S0014579304005125 [pii] (2004).

95 Cimbro, R. *et al.* Tyrosine sulfation in the second variable loop (V2) of HIV-1 gp120 stabilizes V2-V3 interaction and modulates neutralization sensitivity. *Proc Natl Acad Sci U S A* **111**, 3152-3157, doi:10.1073/pnas.1314718111 (2014).

96 Hallenberger, S. *et al.* Inhibition of furin-mediated cleavage activation of HIV-1 glycoprotein gp160. *Nature* **360**, 358-361, doi:10.1038/360358a0 (1992).

97 McCune, J. M. *et al.* Endoproteolytic cleavage of gp160 is required for the activation of human immunodeficiency virus. *Cell* **53**, 55-67 (1988).

98 Freed, E. O., Myers, D. J. & Risser, R. Mutational analysis of the cleavage sequence of the human immunodeficiency virus type 1 envelope glycoprotein precursor gp160. *J Virol* **63**, 4670-4675 (1989).

99 Zhu, P. *et al.* Electron tomography analysis of envelope glycoprotein trimers on HIV and simian immunodeficiency virus virions. *Proc Natl Acad Sci U S A* **100**, 15812-15817, doi:10.1073/pnas.2634931100 (2003).

100 Binley, J. M. *et al.* Role of complex carbohydrates in human immunodeficiency virus type 1 infection and resistance to antibody neutralization. *J Virol* **84**, 5637-5655, doi:10.1128/JVI.00105-10 (2010).

101 Cooper, M. D., Peterson, R. D. & Good, R. A. Delineation of the Thymic and Bursal Lymphoid Systems in the Chicken. *Nature* **205**, 143-146 (1965).

102 Murphy, K., Travers, P., Walport, M. & Janeway, C. *Janeway's immunobiology*. 8th edn, (Garland Science, 2012).

103 Bellanti, J. A., Escobar-Gutiérrez, A. & Tsokos, G. C. *Immunology IV : clinical applications in health and disease*. (I Care Press, 2012).

104 Tonegawa, S. Somatic generation of antibody diversity. *Nature* **302**, 575-581 (1983).

105 Brack, C., Hirama, M., Lenhard-Schuller, R. & Tonegawa, S. A complete immunoglobulin gene is created by somatic recombination. *Cell* **15**, 1-14 (1978).

106 Pieper, K., Grimbacher, B. & Eibel, H. B-cell biology and development. *J Allergy Clin Immunol* **131**, 959-971, doi:10.1016/j.jaci.2013.01.046 (2013).

107 Lefranc, M. P. *et al.* IMGT, the international ImMunoGeneTics information system. *Nucleic Acids Res* **37**, D1006-1012, doi:10.1093/nar/gkn838 (2009).

108 Siebenlist, U., Ravetch, J. V., Korsmeyer, S., Waldmann, T. & Leder, P. Human immunoglobulin D segments encoded in tandem multigenic families. *Nature* **294**, 631-635 (1981).

109 Corbett, S. J., Tomlinson, I. M., Sonnhammer, E. L., Buck, D. & Winter, G. Sequence of the human immunoglobulin diversity (D) segment locus: a systematic analysis provides no evidence for the use of DIR segments, inverted D segments, "minor" D segments or D-D recombination. *J Mol Biol* **270**, 587-597, doi:10.1006/jmbi.1997.1141 (1997).

110 Alt, F. W. & Baltimore, D. Joining of immunoglobulin heavy chain gene segments: implications from a chromosome with evidence of three D-JH fusions. *Proc Natl Acad Sci U S A* **79**, 4118-4122 (1982).

111 Bollum, F. J. Terminal deoxynucleotidyl transferase: biological studies. *Adv Enzymol Relat Areas Mol Biol* **47**, 347-374 (1978).

112 Wyatt, R. *et al.* The antigenic structure of the HIV gp120 envelope glycoprotein. *Nature* **393**, 705-711 (1998).

113 Wibmer, C. K., Moore, P. L. & Morris, L. HIV broadly neutralizing antibody targets. *Current opinion in HIV and AIDS* **10**, 135-143, doi:10.1097/COH.0000000000000153 (2015).

114 Kwong, P. D., Wyatt, R., Sattentau, Q. J., Sodroski, J. & Hendrickson, W. A. Oligomeric modeling and electrostatic analysis of the gp120 envelope glycoprotein of human immunodeficiency virus. *J Virol* **74**, 1961-1972 (2000).

115 Davis, K. L. *et al.* High titer HIV-1 V3-specific antibodies with broad reactivity but low neutralizing potency in acute infection and following vaccination. *Virology* **387**, 414-426, doi:10.1016/j.virol.2009.02.022 (2009).

116 Trkola, A. *et al.* Human monoclonal antibody 2G12 defines a distinctive neutralization epitope on the gp120 glycoprotein of human immunodeficiency virus type 1. *J Virol* **70**, 1100-1108 (1996).

117 Walker, L. M. *et al.* Broad and potent neutralizing antibodies from an African donor reveal a new HIV-1 vaccine target. *Science* **326**, 285-289 (2009).

118 Walker, L. M. *et al.* Broad neutralization coverage of HIV by multiple highly potent antibodies. *Nature* **477**, 466-470, doi:nature10373 [pii]10.1038/nature10373 (2011).

119 Gray, E. S. *et al.* The neutralization breadth of HIV-1 develops incrementally over four years and is associated with CD4+ T cell decline and high viral load during acute infection. *J Virol* **85**, 4828-4840, doi:JVI.00198-11 [pii]10.1128/JVI.00198-11 (2011).

120 Klein, J. S. & Bjorkman, P. J. Few and far between: how HIV may be evading antibody avidity. *PLoS pathogens* **6**, e1000908, doi:10.1371/journal.ppat.1000908 (2010).

121 Tomaras, G. D. *et al.* Initial B-cell responses to transmitted human immunodeficiency virus type 1: virion-binding immunoglobulin M (IgM) and IgG antibodies followed by plasma anti-gp41 antibodies with ineffective control of initial viremia. *J Virol* **82**, 12449-12463 (2008).

122 Liao, H. X. *et al.* Initial antibodies binding to HIV-1 gp41 in acutely infected subjects are polyreactive and highly mutated. *J Exp Med* **208**, 2237-2249, doi:jem.20110363 [pii]10.1084/jem.20110363 (2011).

123 Trama, A. M. *et al.* HIV-1 envelope gp41 antibodies can originate from terminal ileum B cells that share cross-reactivity with commensal bacteria. *Cell Host Microbe* **16**, 215-226, doi:10.1016/j.chom.2014.07.003 (2014).

124 Delwart, E. L. *et al.* Slower evolution of human immunodeficiency virus type 1 quasispecies during progression to AIDS. *J Virol* **71**, 7498-7508 (1997).

125 Gray, E. S. *et al.* Neutralizing antibody responses in acute human immunodeficiency virus type 1 subtype C infection. *J Virol* **81**, 6187-6196 (2007).

126 Li, B. *et al.* Evidence for potent autologous neutralizing antibody titers and compact envelopes in early infection with subtype C human immunodeficiency virus type 1. *J Virol* **80**, 5211-5218, doi:80/11/5211 [pii]10.1128/JVI.00201-06 (2006).

127 Moore, P. L. *et al.* The c3-v4 region is a major target of autologous neutralizing antibodies in human immunodeficiency virus type 1 subtype C infection. *J Virol* **82**, 1860-1869, doi:10.1128/JVI.02187-07 (2008).

128 Wei, X. *et al.* Antibody neutralization and escape by HIV-1. *Nature* **422**, 307-312 (2003).

129 Frost, S. D. *et al.* Neutralizing antibody responses drive the evolution of human immunodeficiency virus type 1 envelope during recent HIV infection. *Proc Natl Acad Sci U S A* **102**, 18514-18519 (2005).

130 Moore, P. L. *et al.* Limited neutralizing antibody specificities drive neutralization escape in early HIV-1 subtype C infection. *PLoS pathogens* **5**, e1000598 (2009).

131 Rong, R. *et al.* Escape from autologous neutralizing antibodies in acute/early subtype C HIV-1 infection requires multiple pathways. *PLoS pathogens* **5**, e1000594 (2009).

132 Richman, D. D., Wrin, T., Little, S. J. & Petropoulos, C. J. Rapid evolution of the neutralizing antibody response to HIV type 1 infection. *Proc Natl Acad Sci U S A* **100**, 4144-4149 (2003).

133 Gray, E. S. *et al.* Isolation of a monoclonal antibody that targets the alpha-2 helix of gp120 and represents the initial autologous neutralizing-antibody response in an HIV-1 subtype C-infected individual. *J Virol* **85**, 7719-7729, doi:JVI.00563-11 [pii]10.1128/JVI.00563-11 (2011).

134 Wibmer, C. K. *et al.* Viral escape from HIV-1 neutralizing antibodies drives increased plasma neutralization breadth through sequential recognition of multiple epitopes and immunotypes. *PLoS pathogens* **9**, e1003738, doi:10.1371/journal.ppat.1003738 (2013).

135 Murphy, M. K. *et al.* Viral escape from neutralizing antibodies in early subtype A HIV-1 infection drives an increase in autologous neutralization breadth. *PLoS pathogens* **9**, e1003173, doi:10.1371/journal.ppat.1003173 (2013).

136 Hraber, P. *et al.* Prevalence of broadly neutralizing antibody responses during chronic HIV-1 infection. *AIDS* **28**, 163-169, doi:10.1097/QAD.0000000000000106 (2014).

137 Piantadosi, A. *et al.* Breadth of neutralizing antibody response to human immunodeficiency virus type 1 is affected by factors early in infection but does not influence disease progression. *J Virol* **83**, 10269-10274 (2009).

138 Euler, Z. *et al.* Cross-reactive neutralizing humoral immunity does not protect from HIV type 1 disease progression. *J Infect Dis* **201**, 1045-1053, doi:10.1086/651144 (2010).

139 Sather, D. N. *et al.* Factors associated with the development of cross-reactive neutralizing antibodies during human immunodeficiency virus type 1 infection. *J Virol* **83**, 757-769 (2009).

140 Walker, L. M. *et al.* A limited number of antibody specificities mediate broad and potent serum neutralization in selected HIV-1 infected individuals. *PLoS pathogens* **6**, doi:e1001028 [pii]10.1371/journal.ppat.1001028 (2010).

141 Mikell, I. *et al.* Characteristics of the earliest cross-neutralizing antibody response to HIV-1. *PLoS pathogens* **7**, e1001251, doi:10.1371/journal.ppat.1001251 (2011).

142 Bahmanyar, M., Fayaz, A., Nour-Salehi, S., Mohammadi, M. & Koprowski, H. Successful protection of humans exposed to rabies infection. Postexposure treatment with the new human diploid cell rabies vaccine and antirabies serum. *JAMA* **236**, 2751-2754 (1976).

143 Beasley, R. P. *et al.* Efficacy of hepatitis B immune globulin for prevention of perinatal transmission of the hepatitis B virus carrier state: final report of a randomized double-blind, placebo-controlled trial. *Hepatology* **3**, 135-141, doi:S0270913983000166 [pii] (1983).

144 Gellis, S. S., McGuinnes, A. C. & Peters, M. Study of prevention of mumps orchitis by gamma globulin. *Am. J. Med. Sci.* **210**, 5 (1945).

145 Groothuis, J. R. *et al.* Prophylactic administration of respiratory syncytial virus immune globulin to high-risk infants and young children. The Respiratory Syncytial Virus Immune Globulin Study Group. *N Engl J Med* **329**, 1524-1530, doi:10.1056/NEJM199311183292102 (1993).

146 Janeway, C. A. Use of Concentrated Human Serum gamma-Globulin in the Prevention and Attenuation of Measles. *Bull N Y Acad Med* **21**, 202-222 (1945).

147 Korns, R. F. Prophylaxis of German measles with immune serum globulin. *J Infect Dis* **90**, 183-189 (1952).

148 Ross, A. H. Modification of chicken pox in family contacts by administration of gamma globulin. *N Engl J Med* **267**, 369-376, doi:10.1056/NEJM196208232670801 (1962).

149 Snydman, D. R. *et al.* Use of cytomegalovirus immune globulin to prevent cytomegalovirus disease in renal-transplant recipients. *N Engl J Med* **317**, 1049-1054, doi:10.1056/NEJM198710223171703 (1987).

150 Li, J., Lord, C. I., Haseltine, W., Letvin, N. L. & Sodroski, J. Infection of cynomolgus monkeys with a chimeric HIV-1/SIVmac virus that expresses the HIV-1 envelope glycoproteins. *J Acquir Immune Defic Syndr* **5**, 639-646 (1992).

151 Luciw, P. A., Pratt-Lowe, E., Shaw, K. E., Levy, J. A. & Cheng-Mayer, C. Persistent infection of rhesus macaques with T-cell-line-tropic and macrophage-tropic clones of simian/human immunodeficiency viruses (SHIV). *Proc Natl Acad Sci U S A* **92**, 7490-7494 (1995).

152 Sakuragi, S. *et al.* Infection of macaque monkeys with a chimeric human and simian immunodeficiency virus. *J Gen Virol* **73 (Pt 11)**, 2983-2987 (1992).

153 Shibata, R. *et al.* Generation of a chimeric human and simian immunodeficiency virus infectious to monkey peripheral blood mononuclear cells. *J Virol* **65**, 3514-3520 (1991).

154 Mascola, J. R. *et al.* Protection of Macaques against pathogenic simian/human immunodeficiency virus 89.6PD by passive transfer of neutralizing antibodies. *J Virol* **73**, 4009-4018 (1999).

155 Mascola, J. R. *et al.* Protection of macaques against vaginal transmission of a pathogenic HIV-1/SIV chimeric virus by passive infusion of neutralizing antibodies. *Nat Med* **6**, 207-210 (2000).

156 Veazey, R. S. *et al.* Prevention of virus transmission to macaque monkeys by a vaginally applied monoclonal antibody to HIV-1 gp120. *Nat Med* **9**, 343-346 (2003).

157 Baba, T. W. *et al.* Human neutralizing monoclonal antibodies of the IgG1 subtype protect against mucosal simian-human immunodeficiency virus infection. *Nat Med* **6**, 200-206 (2000).

158 Hofmann-Lehmann, R. *et al.* Postnatal passive immunization of neonatal macaques with a triple combination of human monoclonal antibodies against oral simian-human immunodeficiency virus challenge. *J Virol* **75**, 7470-7480 (2001).

159 Parren, P. W. *et al.* Antibody protects macaques against vaginal challenge with a pathogenic R5 simian/human immunodeficiency virus at serum levels giving complete neutralization in vitro. *J Virol* **75**, 8340-8347 (2001).

160 Hessell, A. J. *et al.* Effective, low-titer antibody protection against low-dose repeated mucosal SHIV challenge in macaques. *Nat Med* **15**, 951-954, doi:nm.1974 [pii]10.1038/nm.1974 (2009).

161 Hessell, A. J. *et al.* Broadly neutralizing human anti-HIV antibody 2G12 is effective in protection against mucosal SHIV challenge even at low serum neutralizing titers. *PLoS pathogens* **5**, e1000433, doi:10.1371/journal.ppat.1000433 (2009).

162 Moldt, B. *et al.* Highly potent HIV-specific antibody neutralization in vitro translates into effective protection against mucosal SHIV challenge in vivo. *Proc Natl Acad Sci U S A* **109**, 18921-18925, doi:10.1073/pnas.1214785109 (2012).

163 Pegu, A. *et al.* Neutralizing antibodies to HIV-1 envelope protect more effectively in vivo than those to the CD4 receptor. *Sci Transl Med* **6**, 243ra288, doi:10.1126/scitranslmed.3008992 (2014).

164 Rudicell, R. S. *et al.* Enhanced potency of a broadly neutralizing HIV-1 antibody in vitro improves protection against lentiviral infection in vivo. *J Virol* **88**, 12669-12682, doi:10.1128/JVI.02213-14 (2014).

165 Ko, S. Y. *et al.* Enhanced neonatal Fc receptor function improves protection against primate SHIV infection. *Nature* **514**, 642-645, doi:10.1038/nature13612 (2014).

166 Maynard, J. *AMP Study - Amping up for HIV Prevention*, <http://www.hvtn.org/en/science/HVTN-studies/AMPstudy.html> (2 June 2016).

167 Gray, E. S., Meyers, T., Gray, G., Montefiori, D. C. & Morris, L. Insensitivity of paediatric HIV-1 subtype C viruses to broadly neutralising monoclonal antibodies raised against subtype B. *PLoS Med* **3**, e255 (2006).

168 Klein, F. *et al.* Antibodies in HIV-1 vaccine development and therapy. *Science* **341**, 1199-1204, doi:10.1126/science.1241144 (2013).

169 Corti, D. & Lanzavecchia, A. Broadly neutralizing antiviral antibodies. *Annu Rev Immunol* **31**, 705-742, doi:10.1146/annurev-immunol-032712-095916 (2013).

170 Kwong, P. D., Mascola, J. R. & Nabel, G. J. Broadly neutralizing antibodies and the search for an HIV-1 vaccine: the end of the beginning. *Nat Rev Immunol* **13**, 693-701, doi:10.1038/nri3516 (2013).

171 Burton, D. R. *et al.* A large array of human monoclonal antibodies to type 1 human immunodeficiency virus from combinatorial libraries of asymptomatic seropositive individuals. *Proc Natl Acad Sci U S A* **88**, 10134-10137 (1991).

172 Zhou, T. *et al.* Structural Repertoire of HIV-1-Neutralizing Antibodies Targeting the CD4 Supersite in 14 Donors. *Cell* **161**, 1280-1292, doi:10.1016/j.cell.2015.05.007 (2015).

173 Yoon, H. *et al.* CATNAP: a tool to compile, analyze and tally neutralizing antibody panels. *Nucleic Acids Res* **43**, W213-219, doi:10.1093/nar/gkv404 (2015).

174 Wu, X. *et al.* Rational design of envelope identifies broadly neutralizing human monoclonal antibodies to HIV-1. *Science* **329**, 856-861, doi:science.1187659 [pii]10.1126/science.1187659 (2010).

175 Scharf, L. *et al.* Antibody 8ANC195 reveals a site of broad vulnerability on the HIV-1 envelope spike. *Cell Rep* **7**, 785-795, doi:10.1016/j.celrep.2014.04.001 (2014).

176 Blattner, C. *et al.* Structural delineation of a quaternary, cleavage-dependent epitope at the gp41-gp120 interface on intact HIV-1 Env trimers. *Immunity* **40**, 669-680, doi:10.1016/j.immuni.2014.04.008 (2014).

177 Falkowska, E. *et al.* Broadly neutralizing HIV antibodies define a glycan-dependent epitope on the prefusion conformation of gp41 on cleaved envelope trimers. *Immunity* **40**, 657-668, doi:10.1016/j.immuni.2014.04.009 (2014).

178 Lee, J. H. *et al.* Antibodies to a conformational epitope on gp41 neutralize HIV-1 by destabilizing the Env spike. *Nat Commun* **6**, 8167, doi:10.1038/ncomms9167 (2015).

179 Huang, J. *et al.* Broad and potent HIV-1 neutralization by a human antibody that binds the gp41-gp120 interface. *Nature* **515**, 138-142, doi:10.1038/nature13601 (2014).

180 McCoy, L. E. *et al.* Incomplete Neutralization and Deviation from Sigmoidal Neutralization Curves for HIV Broadly Neutralizing Monoclonal Antibodies. *PLoS pathogens* **11**, e1005110, doi:10.1371/journal.ppat.1005110 (2015).

181 Tomaras, G. D. *et al.* Polyclonal B Cell Responses to Conserved Neutralization Epitopes in a Subset of HIV-1-infected Individuals. *J Virol*, doi:JVI.05363-11 [pii]10.1128/JVI.05363-11 (2011).

182 Walker, L. M. *et al.* A limited number of antibody specificities mediate broad and potent serum neutralization in selected HIV-1 infected individuals. *PLoS pathogens* **6**, e1001028, doi:10.1371/journal.ppat.1001028 (2010).

183 Kong, L. *et al.* Supersite of immune vulnerability on the glycosylated face of HIV-1 envelope glycoprotein gp120. *Nat Struct Mol Biol* **20**, 796-803, doi:10.1038/nsmb.2594 (2013).

184 Sanders, R. W. *et al.* The mannose-dependent epitope for neutralizing antibody 2G12 on human immunodeficiency virus type 1 glycoprotein gp120. *J Virol* **76**, 7293-7305 (2002).

185 Scanlan, C. N. *et al.* The broadly neutralizing anti-human immunodeficiency virus type 1 antibody 2G12 recognizes a cluster of alpha1-->2 mannose residues on the outer face of gp120. *J Virol* **76**, 7306-7321 (2002).

186 Garces, F. *et al.* Affinity Maturation of a Potent Family of HIV Antibodies Is Primarily Focused on Accommodating or Avoiding Glycans. *Immunity* **43**, 1053-1063, doi:10.1016/j.immuni.2015.11.007 (2015).

187 Calarese, D. A. *et al.* Antibody domain exchange is an immunological solution to carbohydrate cluster recognition. *Science* **300**, 2065-2071 (2003).

188 Huang, J. *et al.* Broad and potent neutralization of HIV-1 by a gp41-specific human antibody. *Nature* **491**, 406-412, doi:10.1038/nature11544 (2012).

189 Haynes, B. F. *et al.* Cardiolipin polyspecific autoreactivity in two broadly neutralizing HIV-1 antibodies. *Science* **308**, 1906-1908 (2005).

190 Bonsignori, M. *et al.* Analysis of a clonal lineage of HIV-1 envelope V2/V3 conformational epitope-specific broadly neutralizing antibodies and their inferred unmutated common ancestors. *J Virol* **85**, 9998-10009, doi:10.1128/JVI.05045-11 (2011).

191 Doria-Rose, N. A. *et al.* Developmental pathway for potent V1V2-directed HIV-neutralizing antibodies. *Nature* **509**, 55-62, doi:10.1038/nature13036 (2014).

192 Doria-Rose, N. A. *et al.* New Member of the V1V2-Directed CAP256-VRC26 Lineage That Shows Increased Breadth and Exceptional Potency. *J Virol* **90**, 76-91, doi:10.1128/JVI.01791-15 (2016).

193 Moore, P. L. *et al.* Multiple pathways of escape from HIV broadly cross-neutralizing V2-dependent antibodies. *J Virol* **87**, 4882-4894, doi:10.1128/JVI.03424-12 (2013).

194 Moore, P. L. *et al.* Potent and broad neutralization of HIV-1 subtype C by plasma antibodies targeting a quaternary epitope including residues in the V2 loop. *J Virol* **85**, 3128-3141, doi:10.1128/JVI.02658-10 (2011).

195 Wardemann, H. *et al.* Predominant autoantibody production by early human B cell precursors. *Science* **301**, 1374-1377 (2003).

196 Tiller, T. *et al.* Efficient generation of monoclonal antibodies from single human B cells by single cell RT-PCR and expression vector cloning. *J Immunol Methods* **329**, 112-124 (2008).

197 Scheid, J. F. *et al.* Sequence and structural convergence of broad and potent HIV antibodies that mimic CD4 binding. *Science* **333**, 1633-1637, doi:10.1126/science.1207227 (2011).

198 Wrammert, J. *et al.* Rapid cloning of high-affinity human monoclonal antibodies against influenza virus. *Nature* **453**, 667-671 (2008).

199 Muster, T. *et al.* A conserved neutralizing epitope on gp41 of human immunodeficiency virus type 1. *J Virol* **67**, 6642-6647 (1993).

200 Buchacher, A. *et al.* Generation of human monoclonal antibodies against HIV-1 proteins; electrofusion and Epstein-Barr virus transformation for peripheral blood lymphocyte immortalization. *AIDS Res Hum Retroviruses* **10**, 359-369 (1994).

201 Corti, D. *et al.* Analysis of memory B cell responses and isolation of novel monoclonal antibodies with neutralizing breadth from HIV-1-infected individuals. *PLoS One* **5**, e8805, doi:10.1371/journal.pone.0008805 (2010).

202 Huang, J. *et al.* Isolation of human monoclonal antibodies from peripheral blood B cells. *Nat Protoc* **8**, 1907-1915, doi:10.1038/nprot.2013.117 (2013).

203 Scheid, J. F. *et al.* Broad diversity of neutralizing antibodies isolated from memory B cells in HIV-infected individuals. *Nature* **458**, 636-640 (2009).

204 Doria-Rose, N. A. *et al.* Frequency and phenotype of human immunodeficiency virus envelope-specific B cells from patients with broadly cross-neutralizing antibodies. *J Virol* **83**, 188-199 (2009).

205 Morris, L. *et al.* Isolation of a human anti-HIV gp41 membrane proximal region neutralizing antibody by antigen-specific single B cell sorting. *PLoS One* **6**, e23532, doi:10.1371/journal.pone.0023532 (2011).

206 Klein, F. *et al.* Broad neutralization by a combination of antibodies recognizing the CD4 binding site and a new conformational epitope on the HIV-1 envelope protein. *J Exp Med* **209**, 1469-1479, doi:10.1084/jem.20120423 (2012).

207 Gaebler, C. *et al.* Isolation of HIV-1-reactive antibodies using cell surface-expressed gp160Deltac(BaL.). *J Immunol Methods* **397**, 47-54, doi:10.1016/j.jim.2013.09.003 (2013).

208 Sok, D. *et al.* Recombinant HIV envelope trimer selects for quaternary-dependent antibodies targeting the trimer apex. *Proc Natl Acad Sci U S A* **111**, 17624-17629, doi:10.1073/pnas.1415789111 (2014).

209 Pinter, A. *et al.* The V1/V2 domain of gp120 is a global regulator of the sensitivity of primary human immunodeficiency virus type 1 isolates to neutralization by antibodies commonly induced upon infection. *J Virol* **78**, 5205-5215 (2004).

210 Wyatt, R. *et al.* Involvement of the V1/V2 variable loop structure in the exposure of human immunodeficiency virus type 1 gp120 epitopes induced by receptor binding. *J Virol* **69**, 5723-5733 (1995).

211 Cao, J. *et al.* Replication and neutralization of human immunodeficiency virus type 1 lacking the V1 and V2 variable loops of the gp120 envelope glycoprotein. *J Virol* **71**, 9808-9812 (1997).

212 Johnson, W. E. *et al.* A replication-competent, neutralization-sensitive variant of simian immunodeficiency virus lacking 100 amino acids of envelope. *J Virol* **76**, 2075-2086 (2002).

213 Stamatatos, L. & Cheng-Mayer, C. An envelope modification that renders a primary, neutralization-resistant clade B human immunodeficiency virus type 1 isolate highly susceptible to neutralization by sera from other clades. *J Virol* **72**, 7840-7845 (1998).

214 Saunders, C. J. *et al.* The V1, V2, and V3 regions of the human immunodeficiency virus type 1 envelope differentially affect the viral phenotype in an isolate-dependent manner. *J Virol* **79**, 9069-9080 (2005).

215 Sanders, R. W. *et al.* Variable-loop-deleted variants of the human immunodeficiency virus type 1 envelope glycoprotein can be stabilized by an intermolecular disulfide bond between the gp120 and gp41 subunits. *J Virol* **74**, 5091-5100 (2000).

216 Gorman, J. *et al.* Structures of HIV-1 Env V1V2 with broadly neutralizing antibodies reveal commonalities that enable vaccine design. *Nat Struct Mol Biol* **23**, 81-90, doi:10.1038/nsmb.3144 (2016).

217 *GlyProt - In Silico Glycosylation of Proteins*, <http://www.glycosciences.de/modeling/glyprot/php/main.php> (2 June 2016).

218 Pancera, M. *et al.* Crystal structure of PG16 and chimeric dissection with somatically related PG9: structure-function analysis of two quaternary-specific antibodies that effectively neutralize HIV-1. *J Virol* **84**, 8098-8110, doi:JVI.00966-10 [pii]10.1128/JVI.00966-10 (2010).

219 Pejchal, R. *et al.* Structure and function of broadly reactive antibody PG16 reveal an H3 subdomain that mediates potent neutralization of HIV-1. *Proc Natl Acad Sci U S A* **107**, 11483-11488, doi:1004600107 [pii]10.1073/pnas.1004600107 (2010).

220 Pancera, M. *et al.* Structural basis for diverse N-glycan recognition by HIV-1-neutralizing V1-V2-directed antibody PG16. *Nat Struct Mol Biol* **20**, 804-813, doi:10.1038/nsmb.2600 (2013).

221 Briney, B. S., Willis, J. R. & Crowe, J. E., Jr. Human peripheral blood antibodies with long HCDR3s are established primarily at original recombination using a limited subset of germline genes. *PLoS One* **7**, e36750, doi:10.1371/journal.pone.0036750 (2012).

222 Gellert, M. V(D)J recombination: RAG proteins, repair factors, and regulation. *Annu Rev Biochem* **71**, 101-132, doi:10.1146/annurev.biochem.71.090501.150203 (2002).

223 Lynch, R. M. *et al.* The B cell response is redundant and highly focused on V1V2 during early subtype C infection in a Zambian seroconverter. *J Virol* **85**, 905-915, doi:JVI.02006-10 [pii]10.1128/JVI.02006-10 (2011).

224 Sagar, M., Wu, X., Lee, S. & Overbaugh, J. Human immunodeficiency virus type 1 V1-V2 envelope loop sequences expand and add glycosylation sites over the course of infection, and these modifications affect antibody neutralization sensitivity. *J Virol* **80**, 9586-9598 (2006).

225 Montefiori, D. C. *et al.* Homotypic antibody responses to fresh clinical isolates of human immunodeficiency virus. *Virology* **182**, 635-643 (1991).

226 Wu, X. *et al.* Selection pressure on HIV-1 envelope by broadly neutralizing antibodies to the conserved CD4-binding site. *J Virol* **86**, 5844-5856, doi:10.1128/JVI.07139-11 (2012).

227 Moore, P. L. *et al.* Evolution of an HIV glycan-dependent broadly neutralizing antibody epitope through immune escape. *Nat Med* **18**, 1688-1692, doi:10.1038/nm.2985 (2012).

228 Sather, D. N. *et al.* Broadly neutralizing antibodies developed by an HIV-positive elite neutralizer exact a replication fitness cost on the contemporaneous virus. *J Virol* **86**, 12676-12685, doi:10.1128/JVI.01893-12 (2012).

229 Lynch, R. M. *et al.* HIV-1 fitness cost associated with escape from the VRC01 class of CD4 binding site neutralizing antibodies. *J Virol* **89**, 4201-4213, doi:10.1128/JVI.03608-14 (2015).

230 Mahalanabis, M. *et al.* Continuous viral escape and selection by autologous neutralizing antibodies in drug-naive human immunodeficiency virus controllers. *J Virol* **83**, 662-672 (2009).

231 Zhu, J. *et al.* Mining the antibodyome for HIV-1-neutralizing antibodies with next-generation sequencing and phylogenetic pairing of heavy/light chains. *Proc Natl Acad Sci U S A* **110**, 6470-6475, doi:10.1073/pnas.1219320110 (2013).

232 Kwong, P. D., Mascola, J. R. & Nabel, G. J. Mining the B cell repertoire for broadly neutralizing monoclonal antibodies to HIV-1. *Cell Host Microbe* **6**, 292-294, doi:10.1016/j.chom.2009.09.008 (2009).

233 Sok, D. *et al.* The effects of somatic hypermutation on neutralization and binding in the PGT121 family of broadly neutralizing HIV antibodies. *PLoS pathogens* **9**, e1003754, doi:10.1371/journal.ppat.1003754 (2013).

234 Wu, X. *et al.* Focused evolution of HIV-1 neutralizing antibodies revealed by structures and deep sequencing. *Science* **333**, 1593-1602, doi:10.1126/science.1207532 (2011).

235 Zhu, J. *et al.* Somatic Populations of PGT135-137 HIV-1-Neutralizing Antibodies Identified by 454 Pyrosequencing and Bioinformatics. *Front Microbiol* **3**, 315, doi:10.3389/fmicb.2012.00315 (2012).

236 Wu, X. *et al.* Maturation and Diversity of the VRC01-Antibody Lineage over 15 Years of Chronic HIV-1 Infection. *Cell* **161**, 470-485, doi:10.1016/j.cell.2015.03.004 (2015).

237 Liao, H. X. *et al.* Co-evolution of a broadly neutralizing HIV-1 antibody and founder virus. *Nature* **496**, 469-476, doi:10.1038/nature12053 (2013).

238 Xiao, X. *et al.* Germline-like predecessors of broadly neutralizing antibodies lack measurable binding to HIV-1 envelope glycoproteins: implications for evasion of immune responses and design of vaccine immunogens. *Biochem Biophys Res Commun* **390**, 404-409, doi:S0006-291X(09)01817-8 [pii]10.1016/j.bbrc.2009.09.029 (2009).

239 Ma, B. J. *et al.* Envelope deglycosylation enhances antigenicity of HIV-1 gp41 epitopes for both broad neutralizing antibodies and their unmutated ancestor antibodies. *PLoS pathogens* **7**, e1002200, doi:10.1371/journal.ppat.1002200 (2011).

240 McGuire, A. T., Glenn, J. A., Lippy, A. & Stamatatos, L. Diverse recombinant HIV-1 Envs fail to activate B cells expressing the germline B cell receptors of the broadly neutralizing anti-HIV-1 antibodies PG9 and 447-52D. *J Virol* **88**, 2645-2657, doi:10.1128/JVI.03228-13 (2014).

241 Jardine, J. *et al.* Rational HIV immunogen design to target specific germline B cell receptors. *Science* **340**, 711-716, doi:10.1126/science.1234150 (2013).

242 Hoot, S. *et al.* Recombinant HIV envelope proteins fail to engage germline versions of anti-CD4bs bNAbs. *PLoS pathogens* **9**, e1003106, doi:10.1371/journal.ppat.1003106 (2013).

243 McGuire, A. T. *et al.* Engineering HIV envelope protein to activate germline B cell receptors of broadly neutralizing anti-CD4 binding site antibodies. *J Exp Med* **210**, 655-663, doi:10.1084/jem.20122824 (2013).

244 McGuire, A. T. *et al.* HIV antibodies. Antigen modification regulates competition of broad and narrow neutralizing HIV antibodies. *Science* **346**, 1380-1383, doi:10.1126/science.1259206 (2014).

245 Jardine, J. G. *et al.* HIV-1 VACCINES. Priming a broadly neutralizing antibody response to HIV-1 using a germline-targeting immunogen. *Science* **349**, 156-161, doi:10.1126/science.aac5894 (2015).

246 Dosenovic, P. *et al.* Immunization for HIV-1 Broadly Neutralizing Antibodies in Human Ig Knockin Mice. *Cell* **161**, 1505-1515, doi:10.1016/j.cell.2015.06.003 (2015).

247 Bhiman, J. N. *et al.* Viral variants that initiate and drive maturation of V1V2-directed HIV-1 broadly neutralizing antibodies. *Nat Med* **21**, 1332-1336, doi:10.1038/nm.3963 (2015).

248 Locci, M. *et al.* Human circulating PD-1+CXCR3-CXCR5+ memory Tfh cells are highly functional and correlate with broadly neutralizing HIV antibody responses. *Immunity* **39**, 758-769, doi:10.1016/j.immuni.2013.08.031 (2013).

249 Landais, E. *et al.* Broadly Neutralizing Antibody Responses in a Large Longitudinal Sub-Saharan HIV Primary Infection Cohort. *PLoS pathogens* **12**, e1005369, doi:10.1371/journal.ppat.1005369 (2016).

250 Cortez, V., Odem-Davis, K., McClelland, R. S., Jaoko, W. & Overbaugh, J. HIV-1 superinfection in women broadens and strengthens the neutralizing antibody response. *PLoS pathogens* **8**, e1002611, doi:10.1371/journal.ppat.1002611 (2012).

251 Powell, R. L., Kinge, T. & Nyambi, P. N. Infection by discordant strains of HIV-1 markedly enhances the neutralizing antibody response against heterologous virus. *J Virol* **84**, 9415-9426, doi:10.1128/JVI.02732-09 (2010).

252 Moore, P. L., Williamson, C. & Morris, L. Virological features associated with the development of broadly neutralizing antibodies to HIV-1. *Trends Microbiol* **23**, 204-211, doi:10.1016/j.tim.2014.12.007 (2015).

253 Gao, F. *et al.* Cooperation of B cell lineages in induction of HIV-1-broadly neutralizing antibodies. *Cell* **158**, 481-491, doi:10.1016/j.cell.2014.06.022 (2014).

254 Cheng, C. *et al.* Immunogenicity of a Prefusion HIV-1-Envelope Trimer in Complex with a Quaternary-Specific Antibody. *J Virol*, doi:10.1128/JVI.02380-15 (2015).

255 Sanders, R. W. *et al.* HIV-1 VACCINES. HIV-1 neutralizing antibodies induced by native-like envelope trimers. *Science* **349**, aac4223, doi:10.1126/science.aac4223 (2015).

256 Scheepers, C. *et al.* Ability to develop broadly neutralizing HIV-1 antibodies is not restricted by the germline Ig gene repertoire. *J Immunol* **194**, 4371-4378, doi:10.4049/jimmunol.1500118 (2015).

257 Zagury, D. *et al.* Immunization against AIDS in humans. *Nature* **326**, 249-250, doi:10.1038/326249a0 (1987).

Part 2: Publications

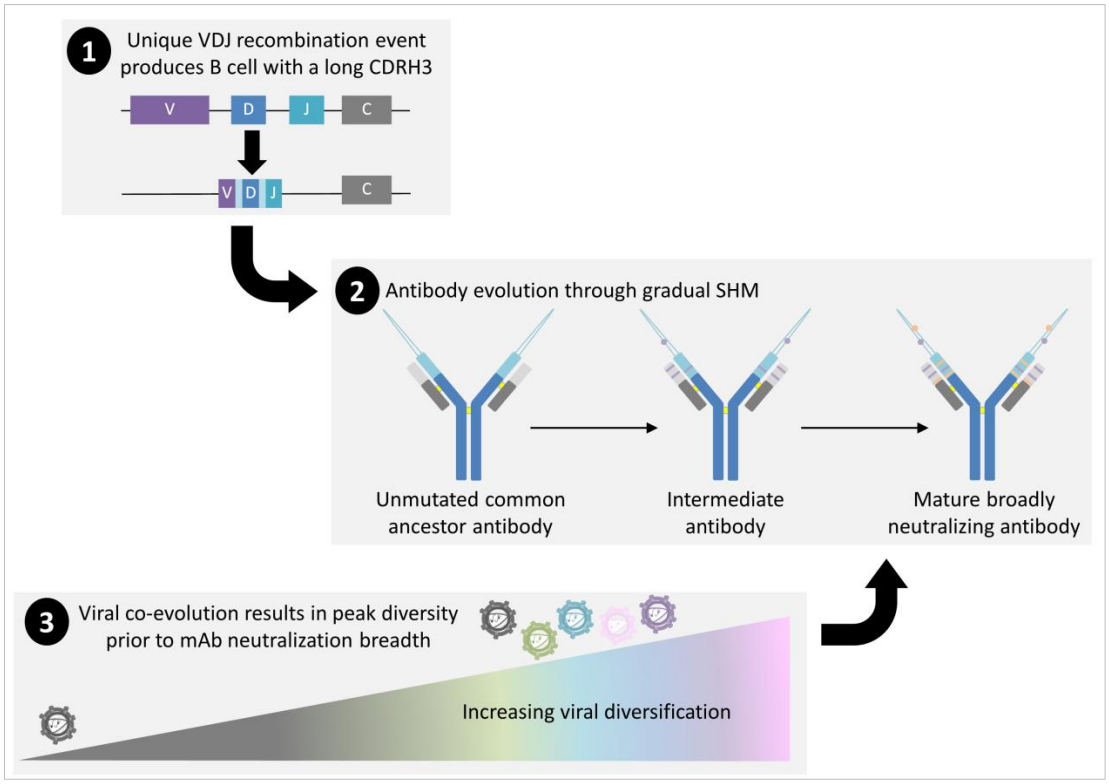
1. Developmental pathway for potent V1V2-directed HIV-neutralizing antibodies

Doria-Rose NA*, Schramm CA*, Gorman J*, Moore PL*, **Bhiman JN**, DeKosky BJ, Ernandes MJ, Georgiev IS, Kim HJ, Pancera M, Staupe RP, Altae-Tran HR, Bailer RT, Crooks ET, Cupo A, Druz A, Garrett NJ, Hoi KH, Kong R, Louder MK, Longo NS, McKee K, Nonyane M, O'Dell S, Roark R, Rudicell RS, Schmidt SD, Sheward DJ, Soto C, Wibmer CK, Yang Y, Zhang Z, NISC Comparative Sequencing Program, Mulkin JC, Binley JM, Sanders RW, Wilson IA, Moore JP, Ward AB, Georgiou G, Williamson C, Adbool-Karim SS, Morris L, Kwong PD, Shapiro L and Mascola JR. *Joint first authors

Nature. 2014: 509: 55-62. PMID: 24590074; PMCID: PMC4395007.

This paper described the development of the V1V2-directed CAP256-VRC26 bNAbs, from strain-specificity to neutralization breadth, in the presence of a concomitantly evolving viral quasispecies.

Graphical Abstract



ARTICLE

doi:10.1038/nature13036

Developmental pathway for potent V1V2-directed HIV-neutralizing antibodies

Nicole A. Doria-Rose[1]*, Chaim A. Schramm[2]*, Jason Gorman[1]*, Penny L. Moore[3,4,5]*, Jinal N. Bhiman[3,4], Brandon J. DeKosky[6], Michael J. Ernandes[1], Ivelin S. Georgiev[1], Helen J. Kim[7,8,9], Marie Pancera[1], Ryan P. Staupe[1], Han R. Altae-Tran[1], Robert T. Bailer[1], Ema T. Crooks[10], Albert Cupo[11], Aliaksandr Druz[1], Nigel J. Garrett[5], Kam H. Hoi[12], Rui Kong[1], Mark K. Louder[1], Nancy S. Longo[1], Krisha McKee[1], Molati Nonyane[3], Sijy O'Dell[1], Ryan S. Roark[1], Rebecca S. Rudicell[1], Stephen D. Schmidt[1], Daniel J. Sheward[13], Cinque Soto[1], Constantinos Kurt Wibmer[3,4], Yongping Yang[1], Zhenhai Zhang[2], NISC Comparative Sequencing Program†, James C. Mullikin[14,15], James M. Binley[10], Rogier W. Sanders[16], Ian A. Wilson[7,8,9,17], John P. Moore[11], Andrew B. Ward[7,8,9], George Georgiou[6,12,18], Carolyn Williamson[5,13], Salim S. Abdool Karim[5,19], Lynn Morris[3,4,5], Peter D. Kwong[1], Lawrence Shapiro[1,2] & John R. Mascola[1]

Antibodies capable of neutralizing HIV-1 often target variable regions 1 and 2 (V1V2) of the HIV-1 envelope, but the mechanism of their elicitation has been unclear. Here we define the developmental pathway by which such antibodies are generated and acquire the requisite molecular characteristics for neutralization. Twelve somatically related neutralizing antibodies (CAP256-VRC26.01–12) were isolated from donor CAP256 (from the Centre for the AIDS Programme of Research in South Africa (CAPRISA)); each antibody contained the protruding tyrosine-sulphated, anionic antigen-binding loop (complementarity-determining region (CDR) H3) characteristic of this category of antibodies. Their unmutated ancestor emerged between weeks 30–38 post-infection with a 35-residue CDR H3, and neutralized the virus that superinfected this individual 15 weeks after initial infection. Improved neutralization breadth and potency occurred by week 59 with modest affinity maturation, and was preceded by extensive diversification of the virus population. HIV-1 V1V2-directed neutralizing antibodies can thus develop relatively rapidly through initial selection of B cells with a long CDR H3, and limited subsequent somatic hypermutation. These data provide important insights relevant to HIV-1 vaccine development.

Developmental pathways of antibodies that neutralize HIV-1 represent potential templates to guide vaccine strategies, if their constituent molecular events were understood and could be reproduced[1–3]. Almost all HIV-1 infected individuals mount a potent antibody response within months of infection, but this response preferentially neutralizes autologous virus, which rapidly escapes[4,5]. Cross-reactive antibodies capable of neutralizing most HIV-1 strains arise in only ~20% of donors after 2–3 years of infection[6–9]. An understanding of the development of broadly neutralizing antibody (NAb) lineages in such donors could provide a roadmap for vaccine design.

One means to obtain such a roadmap is through isolation of broadly cross-reactive neutralizing antibodies, characterization of their genetic sequence and molecular properties, and examination of the B cell genetic record with next-generation sequencing (NGS)[10–14]. The greatest insights can be gained with longitudinal sampling from early after the time of HIV-1 infection[15]. This allows for a genetic delineation of the molecular evolution leading from an unmutated ancestor antibody, through affinity maturation, to acquisition of neutralization breadth. In principle, such a roadmap should link antibody molecular characteristics to the genetic development that a successful vaccine would retrace.

Neutralizing antibodies to the V1V2 region of the HIV-1 viral spike are among the most prevalent cross-reactive antibodies elicited by natural infection[6,16–18] and have been isolated from several donors[19–21]. These antibodies have long heavy-chain complementarity-determining region 3 loops (CDR H3s) that are protruding, anionic and often tyrosine sulphated[22,23]. These CDR H3s penetrate the HIV-1 glycan shield, recognizing a quaternary glycopeptide epitope at the apex of the HIV-1 spike that is formed by V1V2s from at least two gp120 protomers[22–24]. Here we use antibody isolation, B-cell next-generation sequencing, structural characterization, and viral single-genome amplification (SGA) to delineate longitudinal interactions between the developing antibody and autologous virus within donor CAP256, who showed evidence of V1V2-mediated neutralization breadth after one year[18,25,26]. Our results define the molecular requirements and genetic pathways that lead to V1V2-directed neutralization, providing a template for their vaccine elicitation.

[1]Vaccine Research Center, National Institute of Allergy and Infectious Diseases, National Institutes of Health, Bethesda, Maryland 20892, USA. [2]Department of Biochemistry, Columbia University, New York, New York 10032, USA. [3]Center for HIV and STIs, National Institute for Communicable Diseases of the National Health Laboratory Service (NHLS), Johannesburg, 2131, South Africa. [4]Faculty of Health Sciences, University of the Witwatersrand, Johannesburg, 2050, South Africa. [5]Centre for the AIDS Programme of Research in South Africa (CAPRISA), University of KwaZulu-Natal, Congella, 4013, South Africa. [6]Department of Chemical Engineering, University of Texas at Austin, Austin, Texas 78712, USA. [7]Department of Integrative Structural and Computational Biology, The Scripps Research Institute, La Jolla, California 92037, USA. [8]Center for HIV/AIDS Vaccine Immunology and Immunogen Discovery, The Scripps Research Institute, La Jolla, California 92037, USA. [9]IAVI Neutralizing Antibody Center, The Scripps Research Institute, La Jolla, California 92037, USA. [10]Torrey Pines Institute, San Diego, California 92037, USA. [11]Weill Medical College of Cornell University, New York, New York 10065, USA. [12]Department of Biomedical Engineering, University of Texas at Austin, Austin, Texas, USA. [13]Institute of Infectious Diseases and Molecular Medicine, Division of Medical Virology, University of Cape Town and NHLS, Cape Town 7701, South Africa. [14]NISC Comparative Sequencing program, National Institutes of Health, Bethesda, Maryland 20892, USA. [15]NIH Intramural Sequencing Center, National Human Genome Research Institute, National Institutes of Health, Bethesda, Maryland 20892, USA. [16]Department of Medical Microbiology, Academic Medical Center, Amsterdam 1105 AZ, Netherlands. [17]Skaggs Institute for Chemical Biology, The Scripps Research Institute, La Jolla, California 92037, USA. [18]Department of Molecular Biosciences, University of Texas at Austin, Austin, Texas 78712, USA. [19]Department of Epidemiology, Columbia University, New York, New York 10032, USA.

*These authors contributed equally to this work.

†A list of authors and their affiliations appears in the Supplementary Information.

©2014 Macmillan Publishers Limited. All rights reserved

Antibody isolation and characterization

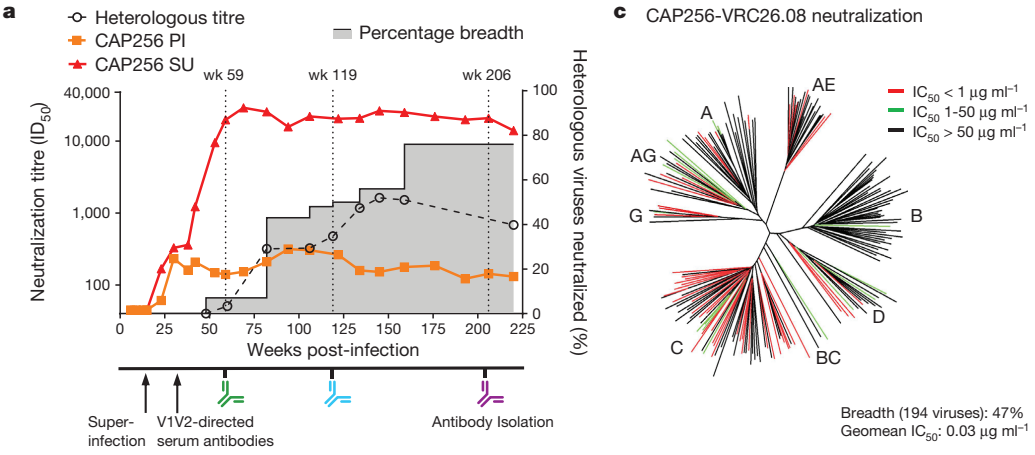
Donor CAP256 peripheral blood mononuclear cells (PBMCs) sampled 59, 119 and 206 weeks post-infection were used to isolate 12 monoclonal antibodies by high-throughput B-cell culture, functional screening by microneutralization, and PCR with reverse transcription (RT–PCR) of antibody variable regions[27,28] (Fig. 1a). All 12 were somatically related and distinguished by long CDR H3s of 35–37 amino acids (Kabat[29] numbering) (Fig. 1b and Extended Data Fig. 1a). The heavy and light chains exhibited somatic mutation of 4–15% from their germline-encoded *V*-genes, VH3-30 and Vλ1-51, respectively (Extended Data Fig 1 and Extended Data Table 1). When these antibodies were reconstituted as IgG1s, they showed varying degrees of heterologous virus neutralization and were extremely potent against many subtype A and C strains (Fig. 1b, c, Extended Data Fig. 2 and Supplementary Fig. 1). The combination of all 12 antibodies recapitulated plasma neutralization (Supplementary Fig. 2), indicating the CAP256-VRC26 antibody lineage to be responsible for the neutralization breadth and potency of donor CAP256.

To map the epitope of the CAP256-VRC26 antibodies, we used neutralization fingerprints[18]; binding assays for HIV-1 Envelope (Env) in soluble, cell surface[30], and viral particle[31] contexts; and negative stain electron microscopy (EM) of Fab CAP256-VRC26.09 bound to a soluble cleaved version of the HIV-1 trimer[24,32,33] (Fig. 2a–c, Supplementary Fig. 3 and Extended Data Figs 3 and 4). Recognition of Env by CAP256-VRC26 antibodies was similar to PG9-class neutralizing antibodies that recognize the trimeric V1V2 cap[24], with high specificity for the Env native quaternary conformation and one Fab bound per trimer (Fig. 2c, left and Extended Data Fig. 4). Neutralization activity of CAP256-VRC26 antibodies was reduced or knocked out by Env mutations in V1V2 strands B and C (Fig. 2d), much like the CAP256 plasma[25,26] and PG9-class neutralizing antibodies[22,23,34]; although unlike PG9, the CAP256-VRC26 antibodies were only partially and variably sensitive to loss of glycans at N160 and N156 (Fig. 2d and Extended Data Fig. 5). Overall, these data indicated the epitope to be at the membrane-distal apex of the HIV-1 spike close to the trimer axis (Fig. 2e), providing a structural explanation for the observed quaternary specificity.

Origin and development of the lineage

To obtain a genetic record of the CAP256-VRC26 antibody lineage, we analysed B cell-immunoglobulin transcripts at eight time points between 15 and 206 weeks post-infection by 454 pyrosequencing. Although no CAP256-VRC26 lineage-related transcripts were detected at 15 and 30 weeks, related heavy chain and light chain transcripts were found at all later time points (Fig. 3a). To track longitudinal prevalence, we used identity-divergence plots[12] of all heavy chain reads assigned to the same VH3-30 germline gene as the isolated antibodies. Using CAP256-VRC26.01 or CAP256-VRC26.08 as the identity referents, segregated islands of related heavy chain sequences first appeared at week 38 (Fig. 3b). For all 12 antibodies, the prevalence and identity of related sequences peaked close to the time of the antibody isolation (Supplementary Fig. 4). To obtain additional antibody lineage data, we performed linked VH:VL paired sequencing[35] at five time points (Fig. 3a and Supplementary Table 1). Of 157 unique CAP256-VRC26 pairs, 7 matched either heavy or light chain sequences present in the 454 pyrosequencing data, including 2 for which both heavy and light chain sequences had previously been captured (Fig. 3c).

Maximum-likelihood phylogenetic trees were constructed using the isolated antibodies and the 454 data (Fig. 3c). The lineage bifurcates early, with one branch leading to CAP256-VRC26.01 and a second developing into CAP256-VRC26.02–12. The unmutated common ancestors (UCAs) for the heavy and light chain were inferred from the phylogenetic trees (Fig. 3c). For the light chain, the UCA had a 12-residue CDR L3, as in CAP256-VRC26.01, and for the heavy chain, the inferred UCA had a 35-residue CDR H3 (Extended Data Fig. 6), probably the result of VDJ recombination with a single *D*-gene, IgHD3-3*01 and non-templated (N)-nucleotide insertions of 34 and 31 nucleotides at each



b

Week	Antibody	Somatic mutations (nt) Vλ1-51*02	Somatic mutations (nt) VH3-30*18	CDR H3 sequence	CDR H3 length (aa)	Neutralization (47 strains) Breadth	Neutralization (47 strains) Potency (IC_{50}, µg ml^{-1})
59	CAP256-VRC26.01	3.9%	8.3%	CAKDVGDYKSDEWGT-EYYDISISYPIQDPRAM--VGAFDLW	35	19%	1.88
119	CAP256-VRC26.02	4.9%	8.7%	CAKDIREYECEYWTS-DYYDFGRPQPCIDSRGV--VGTFDVW	35	17%	0.40
	CAP256-VRC26.03	7.4%	8.7%	CAKDLREDECEEWWS-DYYDFGKQLPCRKSRGV--AGIFDGW	35	36%	0.08
	CAP256-VRC26.04	8.1%	9.0%	CAKDLREDECEEWWS-DYYDFGKQLPCRKSRGV--AGIFDKW	35	30%	0.32
	CAP256-VRC26.05	5.4%	10.1%	CARDQRYYECEEWAS-DYYDFGREQPCLDPRGV--VGIFDLW	35	21%	0.10
	CAP256-VRC26.06	7.4%	10.8%	CARDLRELECEEWTLYNYYDFGSRGPCVDPRGV--AGSFDVW	36	17%	0.38
	CAP256-VRC26.07	7.7%	11.8%	CAKDLREDECEEWWS-DYYDFGKKLPCRKSRGV--AGVFDKW	35	13%	1.51
	CAP256-VRC26.08	9.8%	11.8%	CVRDQREDECEEWWS-DYYDFGRELPCRKFRGLGLAGIFDIW	37	47%	0.11
	CAP256-VRC26.09	9.8%	14.2%	CVKDQREDECEEWWS-DYYDFGRELPCRKSRGLGLAGIFDMW	37	47%	0.07
206	CAP256-VRC26.10	3.9%	11.8%	CAKDMREYECEYWTS-DYYDFGRPQPCIDRRGV--VGIFDMW	35	23%	0.60
	CAP256-VRC26.11	13.7%	11.9%	CVKDMRELECEEWAS-DYYDFGKPQPCLDRRGV--SGISAWW	35	26%	0.94
	CAP256-VRC26.12	8.4%	15.3%	CARDLRESECEEWES-DYYDFGKKGPCVKPRGV--AGGLDLW	35	6%	0.49

Figure 1 | Development of broad neutralization by donor CAP256 and isolation of neutralizing antibodies. **a**, Timing of antibody isolation in relation to plasma neutralization titres against the primary infecting virus (PI), the superinfecting virus (SU), and a panel of 40 heterologous viruses (geometric mean titre shown). Percentage breadth (grey area), percentage of viruses neutralized with plasma median inhibitory dilution (ID_{50}) > 45. **b**, Genetic characteristics and neutralization breadth and potency of the 12 isolated antibodies. Week of antibody isolation and *V*-gene mutation rates are indicated. Residues flanking the Kabat-defined CDR H3 sequences are shown in light grey. Neutralization was assessed against a panel of 47 heterologous viruses. **c**, Breadth and potency of antibody CAP256-VRC26.08 on a panel of 194 Env-pseudoviruses. Dendrogram shows phylogenetic relatedness of Env sequences in the panel.

©2014 Macmillan Publishers Limited. All rights reserved

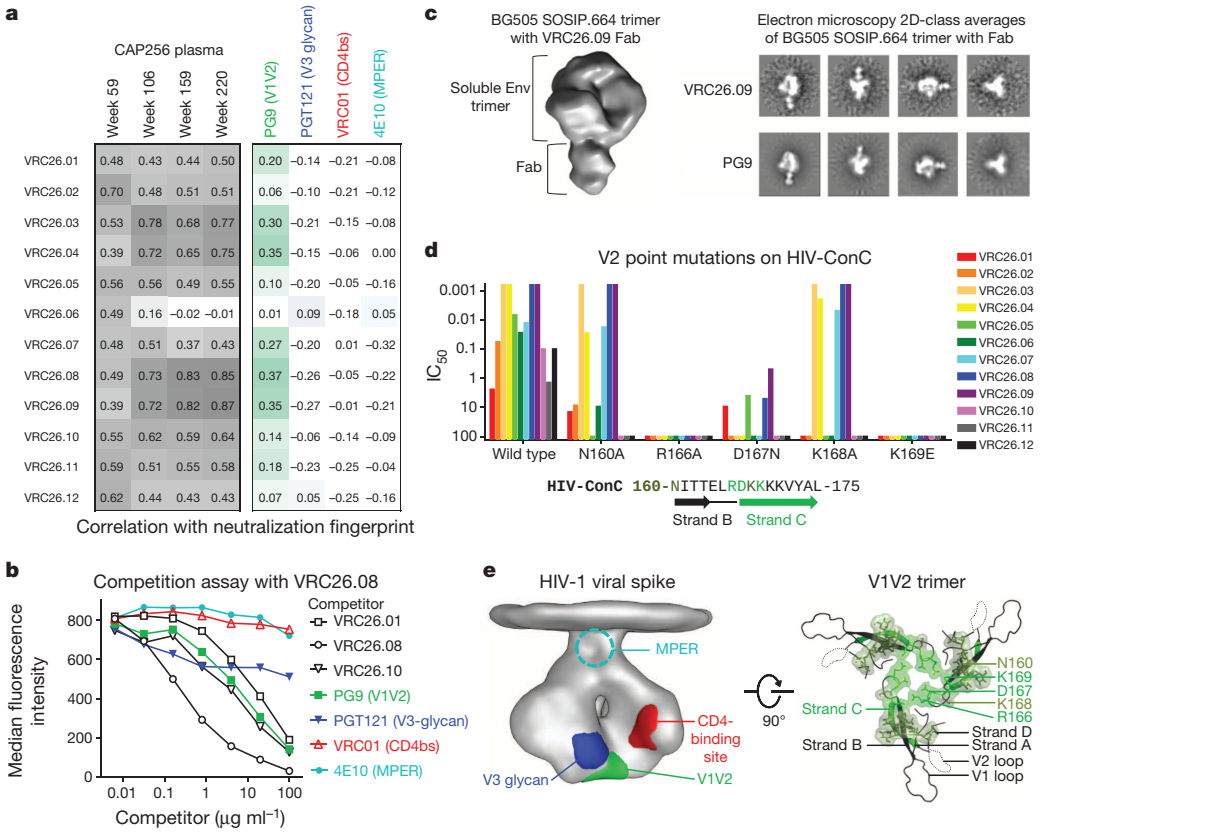


Figure 2 | Mapping of CAP256-VRC26 epitope on the HIV-1 Env spike. **a**, Correlations between neutralization fingerprints (see Methods) of CAP256-VRC26 antibodies and CAP256 plasma (left). Darker grey indicates stronger correlation. Correlations between neutralization fingerprints of CAP256-VRC26 antibodies and representative antibodies targeting the major HIV-1 neutralization epitopes (right). Correlations are colour-coded by antibody; darker shades indicate stronger correlations. **b**, Competition assay. Binding to ZM53-Env-expressing 293T cells by labelled CAP256-VRC26.08 and unlabelled competitor antibodies measured by flow cytometry. Assay shown is representative of three experiments. **c**, Negative stain electron microscopy (EM) 3D reconstruction of CAP256-VRC26.09 Fab in complex with soluble cleaved BG505 SOSIP.664 trimer (left); 2D-class averages of VRC26.09 and PG9 in complex with BG505 SOSIP.664 trimer (right). **d**, Neutralization of Env-pseudoviruses with HIV-ConC and V2 point mutants. Sequence shows amino acids 160–175. **e**, Location of HIV-1 epitopes. EM density of viral spike[50], with viral membrane at top and major sites of vulnerability shown as determined by structural mapping of antibody interactions[24] (left). The gp41 membrane proximal external region (MPER) is shown schematically. Model of V1V2 based on EM structure of BG505 SOSIP.664 trimer[24,32], viewed looking towards the viral membrane along the trimer axis (right). Green ribbon, strand C. V2 mutations from panel **d** are shown with surface representation; brighter green indicates more potent effects on neutralization.

junction (Supplementary Fig. 5). This inferred UCA was further supported by very-low-divergence sequences among the lineage members identified from the week 38 heavy chain data. Five unique sequences were found, all of which had CDR H3s matching the inferred UCA in at least 30 of 35 amino acids while containing three or fewer nucleotide changes in VH and JH combined (Extended Data Fig. 6). Thus, the longitudinal NGS analysis established the first appearance of the CAP256-VRC26 lineage; defined the UCA, the product of gene recombination in the ancestor B cell of the lineage; and provided a genetic record of the development of this lineage over four years.

Structures of CAP256–VRC26 antibodies

To define the structural characteristics of CAP256-VRC26 lineage development, we determined crystal structures for Fabs of the UCA and six antibodies from weeks 59, 119 and 206 (Fig. 4, Supplementary Table 2, and Supplementary Fig. 6a). The mature CDR H3s protruded ~20Å above the antigen-combining surface of the heavy chain and contained a 2-stranded β-sheet, *O*-sulphated tyrosines, and an intra-CDR H3 disulphide bond (Fig. 4a, b). The CDR H3s of the UCA and CAP256-VRC26.01 lacked a CDR H3 disulphide bond, exhibited greater disorder and were positioned more proximal to the light chain (Fig. 4c); the appearance of the disulphide bond correlated with adoption of the mature CDR H3 orientation (Fig. 4c, Supplementary Fig. 6b, and Extended Data Fig. 7a). Mutation to remove the relevant cysteine residues in VRC26.03 resulted in loss of neutralization potency and breadth (Extended Data Fig. 7b, c). Additionally, the appearance of CDR H3 cysteines coincided with a glycine to arginine mutation at the base of the CDR H3, possibly limiting flexibility of the mature antibodies (Extended Data Fig. 7a, b and Supplementary Fig. 7). Overall, the CAP256-VRC26 lineage begins with an anionic protruding CDR H3 with structural properties similar to previously determined V1V2-directed broadly neutralizing antibodies. Development over four years involves the introduction of almost 20 light chain and over 30 heavy chain mutations, including a disulphide bond. The CDR H3 changes its overall orientation while losing negative charge and maintaining tyrosine sulphation (Fig. 4b, c, right).

HIV Env evolution during NAb development

To gain insight into the temporal HIV-1 Env changes driving the development of the CAP256-VRC26 lineage, we used SGA to determine viral sequences over ~3 years. CAP256 Env sequences showed high levels of diversity driven, in part, by recombination between the superinfecting virus (SU) that was first detected 15 weeks post-infection and the primary infecting virus (PI)[26] (Fig. 5a, Supplementary Figs 8, 9). Differences between the primary infecting virus and superinfecting virus Env sequences included V2 residues 165 and 169, and an N160 glycan in the superinfecting virus that was not present in the primary infecting virus (Fig. 5b and Extended Data Fig. 8a, b). Notably, compared to the primary

©2014 Macmillan Publishers Limited. All rights reserved

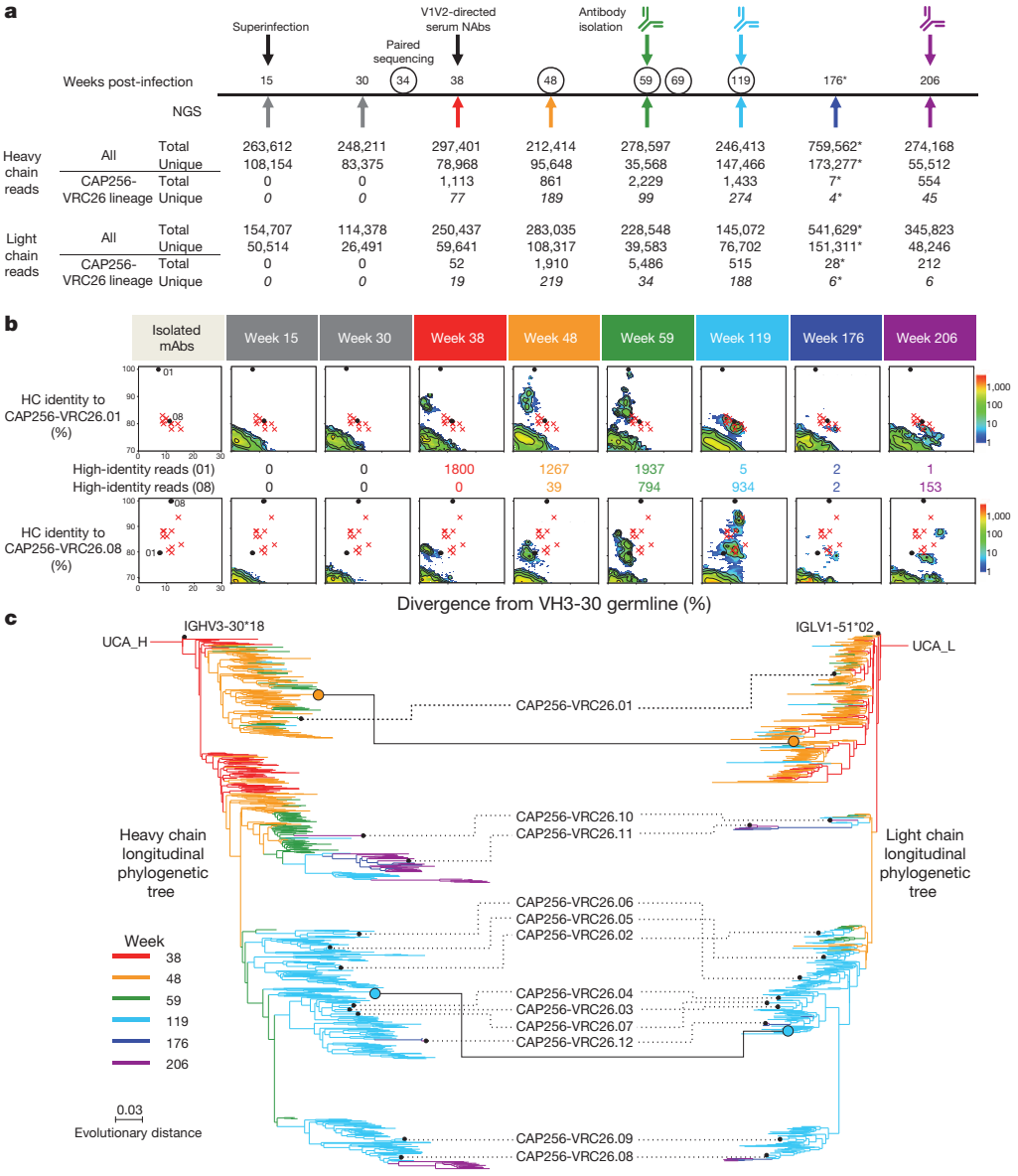


Figure 3 | Maturation of the CAP256-VRC26 lineage revealed by NGS and VH:VL paired sequencing of B cell transcripts. **a**, Timeline of longitudinal peripheral blood samples with quantification of all NGS sequence reads (total and unique), and CAP256-VRC26 lineage-related reads (total and unique). Arrows below the line indicate time points of 454 pyrosequencing for heavy and light chain sequences. Circles indicate time points of paired sequencing of sorted B cells (see Methods). PCR amplifications for pyrosequencing used primers specific for VH3 family sequences (heavy chain) and V lambda sequences (light chain), with the exception of the week 176 sample (asterisk), which was amplified using all-*VH* gene primers, resulting in fewer CAP256-VRC26 specific reads. **b**, Maturation time course for CAP256-VRC26.01 (top) and CAP256-VRC26.08 (bottom panels). Heat map plots show sequence identity (vertical axis) versus germline divergence (horizontal axis) for NGS data. The 12 isolated antibodies are displayed as red 'x' marks for reference, with the exception of the CAP256-VRC26.01 and 08 antibodies which are shown as black dots. Numbers between the top and bottom panels correspond to the number of raw reads with at least 85% identity to the indicated antibody (VRC26.01 (top), VRC26.08 (bottom)). **c**, Phylogenetic trees of the CAP256-VRC26 clonal lineage for heavy chain (left) and light chain (right) were constructed by maximum likelihood using the 454 sequences and the isolated antibodies (black dots, labelled with antibody name). Branches are coloured by time point when NGS sequences were first detected. The orange and blue circles indicate linked heavy and light chain sequences from the paired sequencing data. Scale, rate of nucleotide change (per site) between nodes.

infecting virus, the superinfecting virus contained V2 residues that are more commonly found among circulating viruses (Extended Data Fig. 8a). All 12 antibodies neutralized the superinfecting virus, and, with the exception of CAP256-VRC26.06, failed to neutralize the primary infecting virus, suggesting the superinfecting virus V1V2 initially engaged the naive B cell of the CAP256-VRC26 lineage (Fig. 5d, Extended Data Fig. 8c and Supplementary Fig. 10).

Before the CAP256-VRC26 antibodies developed, most Env sequences had V1V2 regions derived from the primary infecting virus (Fig. 5a–c and Supplementary Figs 8 and 9) and were therefore largely neutralization resistant (Fig. 5d and Supplementary Fig. 10). Among superinfecting-virus-like sequences, a rare K169I mutation arose under strong directional selection (Supplementary Table 3) as the CAP256-VRC26 lineage emerged, which rendered the superinfecting virus resistant to only the earliest antibody (Extended Data Fig. 8d, e), indicating that CAP256-VRC26.01-like antibodies drove this viral escape, followed by maturation of the lineage to tolerate I169. At 48 weeks, the viral population underwent a substantial shift (Fig. 5a and Supplementary Figs 8 and 9), with the

©2014 Macmillan Publishers Limited. All rights reserved

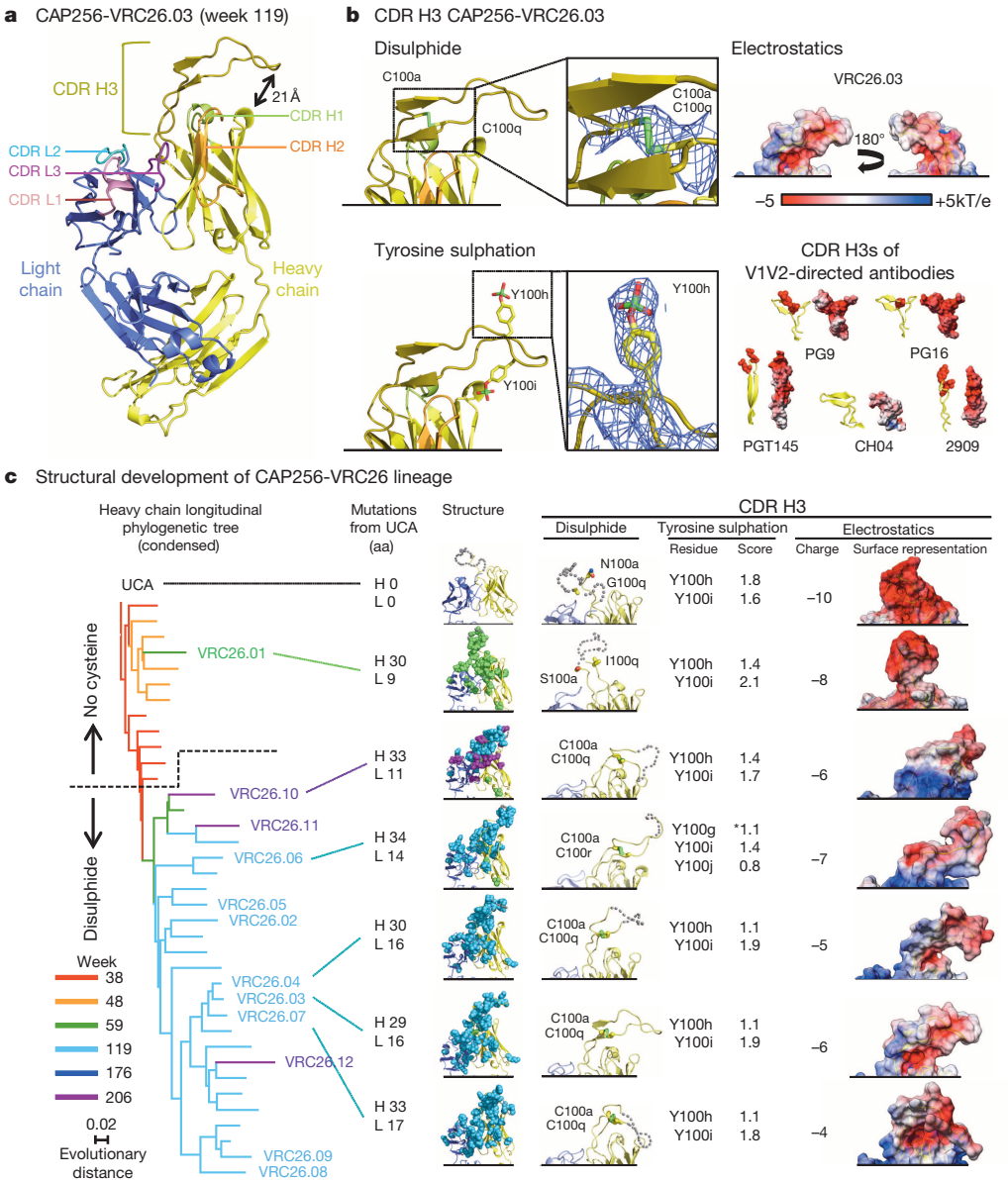


Figure 4 | Structural characteristics of the developing CAP256-VRC26 lineage. **a**, Crystal structure of the antigen-binding fragment (Fab) of CAP256-VRC26.03 shown in ribbon diagram representation. **b**, The intra-loop disulphide bond and tyrosine sulphation are shown in stick representation, and enlarged to show electron density (blue mesh, $2F_o$-F_c at 1σ) (left). Molecular surface, with electrostatic potentials coloured red for acidic and blue for basic (right). CDR H3 regions of broadly neutralizing V1V2-directed antibodies are shown for comparison, with the left image in ribbon representation (tyrosine sulphates highlighted in red) and the right image in electrostatic representation. **c**, A condensed heavy chain phylogenetic tree highlights the isolated antibodies (left). Scale, rate of nucleotide change between nodes. The number of amino acid (aa) mutations to the heavy chain (H) and light chain (L) relative to the UCA are shown. Structures of the variable regions (middle). Mutations from the UCA are represented as spheres coloured according to the week of antibody isolation at which the mutations first appear. CDR H3 details (right). Residues that are (or evolve to become) cysteines are labelled (grey dotted lines indicate modelled disordered regions). The position of tyrosines predicted to be sulphated (scores >1) are noted and were included in the formal charges shown for each CDR H3 and the electrostatic representations (far right). Asterisk denotes Tyr insertion in VRC26.06.

superinfecting-virus-like V1V2 dominating just before the development of neutralization breadth. Neutralization of Env clones by later antibodies (CAP256-VRC26.02-12) tracked with the presence of superinfecting-virus-like V1V2 sequences (black bar, Fig. 5c) until escape occurred through mutations at positions 166 or 169 (Fig. 5c, d and Extended Data Fig. 8d). These mutations resulted in a net charge change in the V2 epitope (+3 to 0, Fig. 5c, Extended Data Fig. 8b) concomitant with the antibody CDR H3s becoming less acidic over time (−10 to −4, Fig. 4 and Extended Data Fig. 9) suggesting co-evolution of the viral epitope and the antibody paratope. Overall, these results highlight the interplay between virus and antibody, with the superinfecting-virus-like V1V2 epitope stimulating expansion of the CAP256-VRC26 lineage.

Rapid development of CAP256-VRC26.01

To gain insight into the development of V1V2-directed neutralization, we focused on the early antibody CAP256-VRC26.01, isolated at week 59, which neutralized 30% of clade C viruses and showed cross-clade neutralization of nearly 20% (Supplementary Fig. 1). Notably, this week 59 time point was 44 weeks after superinfection and only 21 weeks after the CAP256-VRC26 lineage was first detected by NGS. We also inferred heavy and light chains for two developmental intermediates (VRC26-I1 and VRC26-I2) (Fig. 6a and Extended Data Fig. 1) and characterized their function along with the UCA (Fig. 6b–e). The UCA bound and neutralized the superinfecting virus weakly, but did not bind or neutralize heterologous viruses. VRC26-I1, VRC26-I2 and CAP256-VRC26.01 demonstrated progressively greater binding and neutralization, with VRC26-I1 neutralizing 2 of 7 strains and VRC26-I2 neutralizing 6 of 7 strains (Fig. 6e), with dependence on residues in V2 (Fig. 6c). Interestingly, the primary infecting virus was neither bound nor neutralized by the UCA, intermediates, or CAP256-VRC26.01 (Fig. 6c and Supplementary Fig. 11). These data provide further evidence that the CAP256-VRC26 lineage was initiated by interaction with a superinfecting-virus-like V1V2. Subsequent affinity maturation, focused within CDR H3 (Fig. 6f and Extended Data Table 1), allowed for progressively greater binding and neutralization with increased viral diversity preceding the emergence of neutralization breadth. On the basis of the inferred UCA, CAP256-VRC26.01 diverged 11% from germline heavy chain and 7% from germline light chain (Fig. 6f). Thus, once an appropriate gene recombination

©2014 Macmillan Publishers Limited. All rights reserved

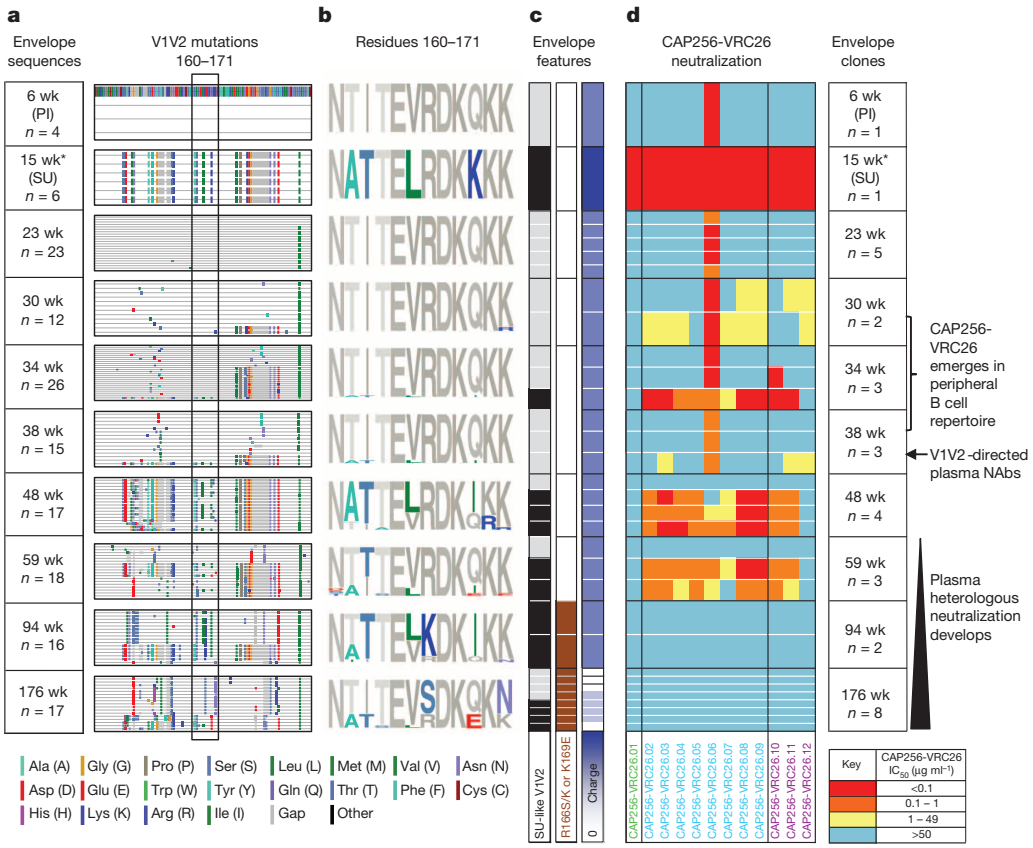


Figure 5 | HIV-1 Env evolution and the development of the CAP256-VRC26 lineage. **a**, V1V2 sequences are shown in highlighter format with the primary infecting virus (PI) designated as master and V2 residues 160 to 171 boxed. Asterisk at week 15 denotes sequences amplified with strain-specific primers matching the superinfecting virus (SU) virus. **b**, Logogram of the V2 epitope for all CAP256 sequences, with mutations away from the PI (master sequence) in colour. **c**, SU-like V1V2 sequences are indicated by black (present) and grey (absent) boxes. Escape mutations (K169E or R166S/K) are indicated by brown boxes. The net charge of the V2 epitope (residues 160 to 171) is shown in purple/white, ranging from +3 to 0. White lines separate clones within a time point; black lines separate time points. **d**, Neutralization by the 12 CAP256-VRC26 monoclonal antibodies of representative longitudinal Env clones isolated between 6 and 176 weeks post-infection (weeks shown at far right). The CAP256 monoclonal antibodies are coloured by time of isolation (as in Fig. 1). The development of the CAP256-VRC26 antibody lineage, V1V2-directed plasma neutralizing antibodies and plasma heterologous neutralization, are indicated on the right.

allows for B-cell receptor recognition of the trimeric V1V2 epitope, development of cross-reactive neutralization can be achieved with moderate somatic mutation in a matter of months.

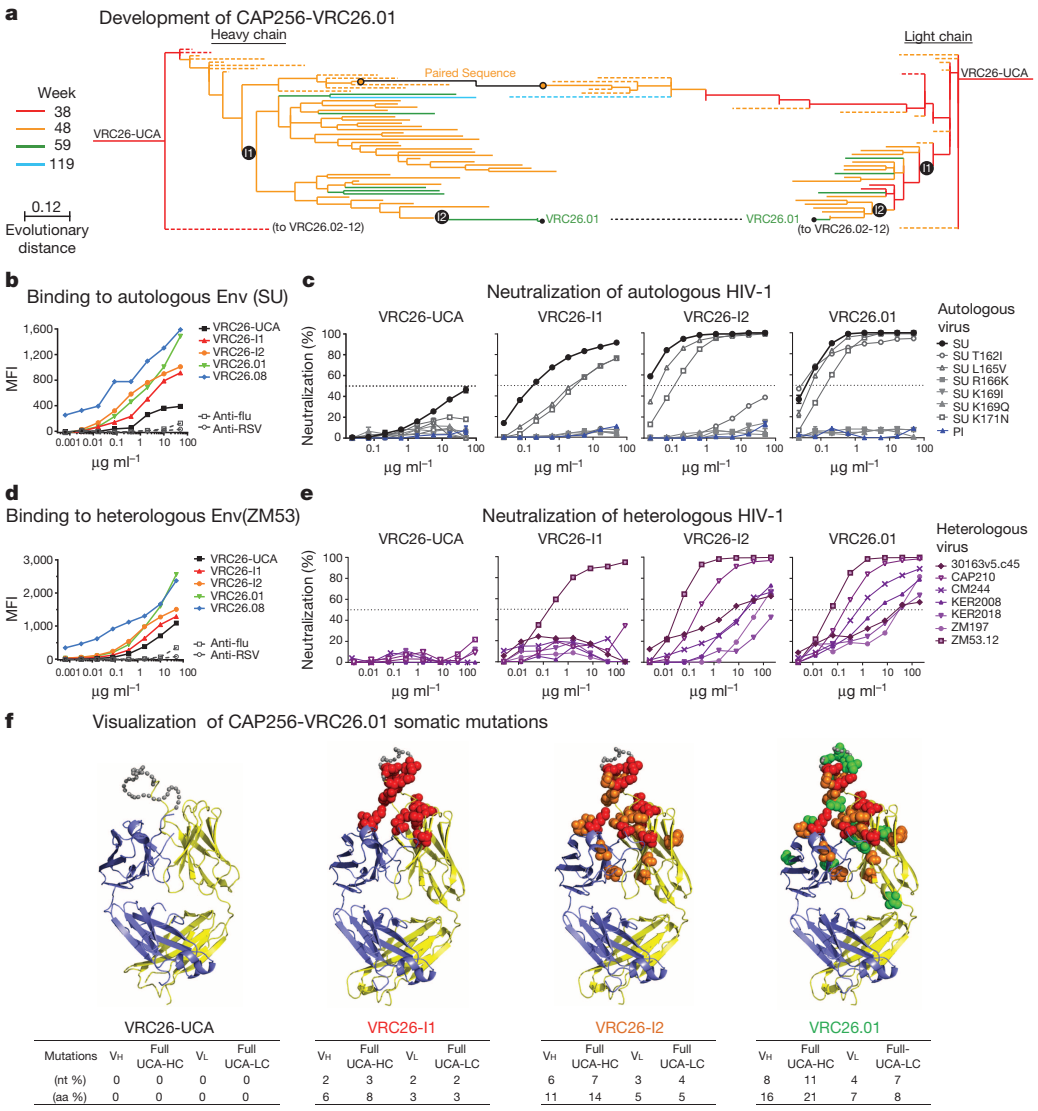
Vaccine implications

The V1V2 region of HIV-1 is a common target of serum neutralizing antibodies[6,16–18]. In the RV144 Thai vaccine trial, an increased level of binding antibodies to the V1V2 region was associated with a reduced risk of infection[36] and viral sieve analysis showed immune pressure in the same region[37]. Although the vaccine in the RV144 trial did not elicit broadly neutralizing V1V2-directed antibodies similar to those described here and elsewhere[19–21], a more effective vaccine would ideally elicit cross-reactive neutralizing antibodies[1–3,38]. Previously described V1V2 neutralizing antibodies, and the CAP256-VRC26 lineage, all have long CDR H3 regions that are necessary to penetrate the glycan shield and engage a V1V2 epitope (Extended Data Table 1). An important unanswered question has been whether these long CDR H3s are fully formed by VDJ recombination, as has been seen in HIV-uninfected donors[39], or emerge by insertions during the process of affinity maturation. We show here that the 35-residue CDR H3 of the CAP256-VRC26 UCA was produced during initial gene rearrangement and therefore existed at the level of the naive B cell receptor.

A potential rate-limiting developmental step in the CAP256-VRC26 lineage is the gene rearrangement that generated its UCA. By one estimate, human B cells with recombined antibody genes encoding long (≥24 amino acids, international immunogenetics database (IMGT)[40] definition) or very long (≥28 amino acids) CDR H3s constitute ~3.5% and 0.4%, respectively, of naive B cells[39]. These long B cell receptors have been associated with autoreactivity, and are subject to both central and peripheral deletion, resulting in an even smaller population of IgG^+ memory B cells[39,41]. We therefore tested the UCA and all 12 CAP256-VRC26 cloned antibodies for autoreactivity[42]. The UCA and mature CAP256-VRC26 antibodies demonstrated little or no reactivity with Hep2 cells or with cardiolipin (Extended Data Fig. 6b, c). In addition, NGS of CAP256 peripheral B cells indicated that <0.4% of sequences had CDR H3s of ≥ 28 amino acids (Extended Data Fig. 6d) suggesting that this donor did not have an unusually high frequency of clonal lineages with long CDR H3 regions.

We also inferred the virological events leading to the stimulation and evolution of the CAP256-VRC26 lineage by the superinfecting virus. Similar to the CH103 CD4-binding site lineage in donor CH505 (ref. 15), the autologous virus in CAP256 showed extensive diversification before the development of breadth. Subsequent antibody–virus interactions appeared to drive somatic mutation and development of cross-reactive neutralization. Finally, the ontogeny of V1V2-directed neutralizing antibodies revealed by the CAP256-VRC26 lineage indicates that neutralization potency and breadth can be achieved without extraordinary levels of somatic hypermutation. Although some neutralizing antibodies appear to require years of maturation[1,3,43,44], we show that a V1V2-directed B cell lineage can acquire HIV-1 neutralization breadth within months rather than years. The critical event appears to be an uncommon gene rearrangement that produces a B-cell receptor

©2014 Macmillan Publishers Limited. All rights reserved



VRC26-UCA				
Mutations	V_H	Full UCA-HC	V_L	Full UCA-LC
(nt %)	0	0	0	0
(aa %)	0	0	0	0

VRC26-I1				
V_H	Full UCA-HC	V_L	Full UCA-LC	
2	3	2	2	
6	8	3	3	

VRC26-I2				
V_H	Full UCA-HC	V_L	Full UCA-LC	
6	7	3	4	
11	14	5	5	

VRC26.01			
V_H	Full UCA-HC	V_L	Full-UCA-LC
8	11	4	7
16	21	7	8

Figure 6 | Development from UCA to CAP256-VRC26.01. **a**, Expanded view of the phylogenetic trees from Fig. 3c, highlighting the maturation pathway of CAP256-VRC26.01. Off-pathway branches were collapsed and are shown as dashed lines. Inferred intermediates VRC26-I1 and VRC26-I2 were expressed for functional analyses. **b**–**e**, Binding and neutralization of antibodies UCA, VRC26-I1, VRC26-I2, VRC26.01. **b**, **d**, Binding to cell-surface expressed Env (SU and ZM53). MFI, median fluorescence intensity. **c**, **e**, Neutralization of PI, SU and point mutants (**c**) and seven heterologous viruses (**e**). Bars, standard error of the mean (triplicates). **f**, Structural models of VRC26.01 lineage antibodies. Affinity matured residues are shown as spheres coloured according to the intermediate at which they first appear: red, VRC26-I1; orange, VRC26-I2; green, VRC26.01. Grey dots, disordered residues in the CDR H3. The number of changes from the UCA to each intermediate are noted for *V* gene only (V_H or V_L), or from the full UCA (UCA-HC or UCA-LC).

with a protruding, tyrosine-sulphated, anionic CDR H3. Identifying features of antigens able to engage naive B cells with such CDR H3s is a critical step in design of vaccines targeting V1V2. Such antigens could be screened for binding to the UCA versions of neutralizing antibodies as an indicator of the ability to engage an appropriate naive B cell receptor. This work also suggests that although an appropriate trimeric V1V2 construct may elicit neutralizing V1V2 antibodies, sequential immunogens that mirror viral evolution may be needed to drive the development of breadth. Overall, the precise delineation of the developmental pathway for the CAP256-VRC26 lineage should provide a basis for attempts to elicit broad V1V2-directed HIV-1-neutralizing antibodies.

METHODS SUMMARY

Serial blood samples were collected from HIV-1-infected subject CAP256 from 6 to 225 weeks after infection. Monoclonal antibodies CAP256-VRC26.01-12 were generated by single-B cell culture, microneutralization screening, RT–PCR, subcloning, and expression as described in[27,28,45]. CDR lengths used Kabat notation[29] except as indicated. Binding of CAP256-VRC26 antibodies to virus-like particles was assessed by ELISA[31] and binding to cell-surface expressed Env was measured by flow cytometry[30]. HIV-1 neutralizing activity of patient plasma and monoclonal antibodies was determined with Env-pseudoviruses using the TZM-bl cell line[46,47]. Neutralization fingerprints are the rank-order of neutralization potencies for an antibody against a set of diverse viral strains, calculated as in ref. 18. A 28Å reconstruction of the BG505 SOSIP.664 gp140 trimer with a single VRC26.09 Fab was obtained by negative stain EM using Appion, Xmipp, IMAGIC, and EMAN software. 454 pyrosequencing was performed as previously described[12,14] on samples from 8 time points after HIV-1 infection. High-throughput V_H:V_L pairing of peripheral blood $CD27^+$ B cells was performed in single cell emulsions generated using a flow focusing apparatus[35]. Phylogenetic analysis, inference of UCA, and identification, synthesis, and expression of clone members were performed as described in the Methods. Epitope mapping onto the spike trimer was performed with the software package UCSF Chimera, using experimental data as described in Methods. Crystallographic analysis of Fab fragments was performed as described in the Methods. Structure modelling of disordered residues in Fab crystal structures was performed using Loopy software. Single-genome amplification and expression of *env* genes was performed as described in Methods and in refs 48, 49.

Online Content Any additional Methods, Extended Data display items and Source Data are available in the online version of the paper; references unique to these sections appear only in the online paper.

Received 13 September 2013; accepted 16 January 2014.
Published online 2 March 2014.

1. Haynes, B. F., Kelsoe, G., Harrison, S. C. & Kepler, T. B. B-cell-lineage immunogen design in vaccine development with HIV-1 as a case study. *Nature Biotechnol.* **30,** 423–433 (2012).
2. Kong, L. & Sattentau, Q. J. Antigenicity and immunogenicity in HIV-1 antibody-based vaccine design. *J. AIDS Clinic. Res.* (Suppl. 8) 003 (2012).
3. Mascola, J. R. & Haynes, B. F. HIV-1 neutralizing antibodies: understanding nature's pathways. *Immunol. Rev.* **254,** 225–244 (2013).
4. Richman, D. D., Wrin, T., Little, S. J. & Petropoulos, C. J. Rapid evolution of the neutralizing antibody response to HIV type 1 infection. *Proc. Natl Acad. Sci. USA* **100,** 4144–4149 (2003).
5. Wei, X. *et al.* Antibody neutralization and escape by HIV-1. *Nature* **422,** 307–312 (2003).

©2014 Macmillan Publishers Limited. All rights reserved

6. Gray, E. S. *et al.* The neutralization breadth of HIV-1 develops incrementally over four years and is associated with CD4$^+$ T cell decline and high viral load during acute infection. *J. Virol.* **85,** 4828–4840 (2011).
7. Piantadosi, A. *et al.* Breadth of neutralizing antibody response to human immunodeficiency virus type 1 is affected by factors early in infection but does not influence disease progression. *J. Virol.* **83,** 10269–10274 (2009).
8. Sather, D. N. *et al.* Factors associated with the development of cross-reactive neutralizing antibodies during human immunodeficiency virus type 1 infection. *J. Virol.* **83,** 757–769 (2009).
9. Doria-Rose, N. A. *et al.* Breadth of human immunodeficiency virus-specific neutralizing activity in sera: clustering analysis and association with clinical variables. *J. Virol.* **84,** 1631–1636 (2010).
10. Glanville, J. *et al.* Precise determination of the diversity of a combinatorial antibody library gives insight into the human immunoglobulin repertoire. *Proc. Natl Acad. Sci. USA* **106,** 20216–20221 (2009).
11. Briney, B. S., Willis, J. R., McKinney, B. A. & Crowe, J. E. Jr. High-throughput antibody sequencing reveals genetic evidence of global regulation of the naive and memory repertoires that extends across individuals. *Genes Immun.* **13,** 469–473 (2012).
12. Wu, X. *et al.* Focused evolution of HIV-1 neutralizing antibodies revealed by structures and deep sequencing. *Science* **333,** 1593–1602 (2011).
13. Zhu, J. *et al.* Mining the antibodyome for HIV-1-neutralizing antibodies with next-generation sequencing and phylogenetic pairing of heavy/light chains. *Proc. Natl Acad. Sci. USA* **110,** 6470–6475 (2013).
14. Zhu, J. *et al.* Somatic populations of PGT135–137 HIV-1-neutralizing antibodies identified by 454 pyrosequencing and bioinformatics. *Front. Microbiol.* **3,** 315 (2012).
15. Liao, H. X. *et al.* Co-evolution of a broadly neutralizing HIV-1 antibody and founder virus. *Nature* **496,** 469–476 (2013).
16. Walker, L. M. *et al.* A limited number of antibody specificities mediate broad and potent serum neutralization in selected HIV-1 infected individuals. *PLoS Pathog.* **6,** e1001028 (2010).
17. Lynch, R. M. *et al.* The B cell response is redundant and highly focused on V1V2 during early subtype C infection in a Zambian seroconverter. *J. Virol.* **85,** 905–915 (2011).
18. Georgiev, I. S. *et al.* Delineating antibody recognition in polyclonal sera from patterns of HIV-1 isolate neutralization. *Science* **340,** 751–756 (2013).
19. Walker, L. M. *et al.* Broad and potent neutralizing antibodies from an African donor reveal a new HIV-1 vaccine target. *Science* **326,** 285–289 (2009).
20. Bonsignori, M. *et al.* Analysis of a clonal lineage of HIV-1 envelope V2/V3 conformational epitope-specific broadly neutralizing antibodies and their inferred unmutated common ancestors. *J. Virol.* **85,** 9998–10009 (2011).
21. Walker, L. M. *et al.* Broad neutralization coverage of HIV by multiple highly potent antibodies. *Nature* **477,** 466–470 (2011).
22. McLellan, J. S. *et al.* Structure of HIV-1 gp120 V1/V2 domain with broadly neutralizing antibody PG9. *Nature* **480,** 336–343 (2011).
23. Pancera, M. *et al.* Structural basis for diverse N-glycan recognition by HIV-1-neutralizing V1–V2-directed antibody PG16. *Nature Struct. Mol. Biol.* **20,** 804–813 (2013).
24. Julien, J. P. *et al.* Asymmetric recognition of the HIV-1 trimer by broadly neutralizing antibody PG9. *Proc. Natl Acad. Sci. USA* **110,** 4351–4356 (2013).
25. Moore, P. L. *et al.* Potent and broad neutralization of HIV-1 subtype C by plasma antibodies targeting a quaternary epitope including residues in the V2 loop. *J. Virol.* **85,** 3128–3141 (2011).
26. Moore, P. L. *et al.* Multiple pathways of escape from HIV broadly cross-neutralizing V2-dependent antibodies. *J. Virol.* **87,** 4882–4894 (2013).
27. Huang, J. *et al.* Broad and potent neutralization of HIV-1 by a gp41-specific human antibody. *Nature* **491,** 406–412 (2012).
28. Tiller, T. *et al.* Efficient generation of monoclonal antibodies from single human B cells by single cell RT–PCR and expression vector cloning. *J. Immunol. Methods* **329,** 112–124 (2008).
29. Kabat, E. A., Wu, T. T., Perry, H. M., Gottesman, K. S. & Foeller, C. *Sequences of Proteins of Immunological Interest* (U.S. Department of Health and Human Services, National Institutes of Health, 1991).
30. Pancera, M. & Wyatt, R. Selective recognition of oligomeric HIV-1 primary isolate envelope glycoproteins by potently neutralizing ligands requires efficient precursor cleavage. *Virology* **332,** 145–156 (2005).
31. Tong, T., Crooks, E. T., Osawa, K. & Binley, J. M. HIV-1 virus-like particles bearing pure env trimers expose neutralizing epitopes but occlude nonneutralizing epitopes. *J. Virol.* **86,** 3574–3587 (2012).
32. Lyumkis, D. *et al.* Cryo-EM structure of a fully glycosylated soluble cleaved HIV-1 envelope trimer. *Science* **342,** 1484–1490 (2013).
33. Julien, J. P. *et al.* Crystal structure of a soluble cleaved HIV-1 envelope trimer. *Science* **342,** 1477–1483 (2013).
34. Doria-Rose, N. A. *et al.* A short segment of the HIV-1 gp120 V1/V2 region is a major determinant of resistance to V1/V2 neutralizing antibodies. *J. Virol.* **86,** 8319–8323 (2012).
35. DeKosky, B. J. *et al.* High-throughput sequencing of the paired human immunoglobulin heavy and light chain repertoire. *Nature Biotechnol.* **31,** 166–169 (2013).
36. Haynes, B. F. *et al.* Immune-correlates analysis of an HIV-1 vaccine efficacy trial. *N. Engl. J. Med.* **366,** 1275–1286 (2012).
37. Rolland, M. *et al.* Increased HIV-1 vaccine efficacy against viruses with genetic signatures in Env V2. *Nature* **490,** 417–420 (2012).
38. Overbaugh, J. & Morris, L. The antibody response against HIV-1. *Cold Spring Harb. Perspect. Med.* **2,** a007039 (2012).
39. Briney, B. S., Willis, J. R. & Crowe, J. E. Jr. Human peripheral blood antibodies with long HCDR3s are established primarily at original recombination using a limited subset of germline genes. *PLoS ONE* **7,** e36750 (2012).
40. Lefranc, M. P. *et al.* IMGT unique numbering for immunoglobulin and T cell receptor variable domains and Ig superfamily V-like domains. *Dev. Comp. Immunol.* **27,** 55–77 (2003).
41. Wardemann, H. *et al.* Predominant autoantibody production by early human B cell precursors. *Science* **301,** 1374–1377 (2003).
42. Haynes, B. F. *et al.* Cardiolipin polyspecific autoreactivity in two broadly neutralizing HIV-1 antibodies. *Science* **308,** 1906–1908 (2005).
43. Kwong, P. D. & Mascola, J. R. Human antibodies that neutralize HIV-1: identification, structures, and B cell ontogenies. *Immunity* **37,** 412–425 (2012).
44. Burton, D. R. *et al.* A blueprint for HIV vaccine discovery. *Cell Host Microbe* **12,** 396–407 (2012).
45. Huang, J. *et al.* Isolation of human monoclonal antibodies from peripheral blood B cells. *Nature Protocols* **8,** 1907–1915 (2013).
46. Shu, Y. *et al.* Efficient protein boosting after plasmid DNA or recombinant adenovirus immunization with HIV-1 vaccine constructs. *Vaccine* **25,** 1398–1408 (2007).
47. Montefiori, D. C. Measuring HIV neutralization in a luciferase reporter gene assay. *Methods Mol. Biol.* **485,** 395–405 (2009).
48. Kraus, M. H. *et al.* A *rev1-vpu* polymorphism unique to HIV-1 subtype A and C strains impairs envelope glycoprotein expression from *rev-vpu-env* cassettes and reduces virion infectivity in pseudotyping assays. *Virology* **397,** 346–357 (2010).
49. Salazar-Gonzalez, J. F. *et al.* Deciphering human immunodeficiency virus type 1 transmission and early envelope diversification by single-genome amplification and sequencing. *J. Virol.* **82,** 3952–3970 (2008).
50. Liu, J., Bartesaghi, A., Borgnia, M. J., Sapiro, G. & Subramaniam, S. Molecular architecture of native HIV-1 gp120 trimers. *Nature* **455,** 109–113 (2008).

Supplementary Information is available in the online version of the paper.

Acknowledgements We thank the participants in the CAPRISA 002 study for their commitment. For technical assistance and advice, we thank: K. Mlisana, S. Sibeko, N. Naicker, the CAPRISA 002 clinical team, N. Samsunder, S. Heeralall, B. Lambson, M. Madzivhandila, T. Khoza, C. Mitchell Scheepers, E. Turk, C.-L. Lin, M. Roederer, J. Stuckey, B. Hartman, G. Loots, J. H. Lee, G. Ippolito, B. Briney, S. Hunicke-Smith and J. Wheeler, and members of the WCMC HIVRAD Core and the NIH Vaccine Research Center HIMS, HIMC, SBS and SBIS sections. We thank J. Baalwa, D. Ellenberger, F. Gao, B. Hahn, K. Hong, J. Kim, F. McCutchan, D. Montefiori, J. Overbaugh, E. Sanders-Buell, G. Shaw, R. Swanstrom, M. Thomson, S. Tovanabutra and L. Zhang for contributing the HIV-1 Envelope plasmids used in our neutralization panel. Funding was provided by the intramural research programs of the Vaccine Research Center and NIAID, the Fogarty International Center, NHGRI, and NIGMS of the National Institutes of Health, USA; the International AIDS Vaccine Initiative; the National Science Foundation; Scripps CHAV-ID; the South African Department of Science and Technology; and fellowships from the Wellcome Trust, Hertz Foundation, Donald D. Harrington Foundation, Poliomyelitis Research Foundation and the National Research Foundation of South Africa. Use of sector 22 (Southeast Region Collaborative Access team) at the Advanced Photon Source was supported by the US Department of Energy, Basic Energy Sciences, Office of Science, under contract number W-31-109-Eng-38.

Author Contributions N.A.D.-R., C.A.S., J.G. and P.L.M. contributed equally to this work. N.A.D.-R., C.A.S., J.G., P.L.M. and J.N.B., designed and performed experiments, analysed data and wrote the manuscript. L.M., P.D.K., L.S. and J.R.M. conceived and designed the experiments, analysed data, and wrote the manuscript. B.J.D., M.J.E., I.S.G, H.J.K., M.P. and R.P.S. conducted experiments and analysed data. H.R.A.-T., B.T.B., E.T.C., A.C., K.H.H., R.K., M.K.L., K.M., M.N., S.O., Ry.S.R., Re.S.R., S.D.S., C.K.W., Y.Y., J.C.M. and NISC conducted experiments. C.W. and A.D. contributed analysis tools and data analysis. S.S.A.K. and N.J.G conceived and managed the CAPRISA cohorts. J.M.B., R.W.S., I.A.W., J.P.M., A.B.W., G.G., N.S.L., D.J.S., C.S. and Z.Z. analysed data.

Author Information Coordinates and structure factors for CAP256-VRC26 lineage Fabs have been deposited with the Protein Data Bank under accession codes 4ODH, 4OCR, 4OD1, 4ORG, 4OCW, 4OD3 and 4OCS. The EM reconstruction density for the CAP256-VRC26.09 complex with BG505 SOSIP.664 trimer has been deposited with the Electron Microscopy Data Bank under accession code EMD-5856. We have also deposited deep sequencing data used in this study to National Center for Biotechnology Information Short Reads Archives (SRA) under accession numbers SRP034555 and SRP017087. Information deposited with GenBank includes: the heavy- and light-chain variable region sequences of cloned antibodies CAP256-VRC26.01-12, UCA, I1 and I2 (accession numbers KJ134860–KJ134889); bioinformatically identified VRC26-related sequences from B cell transcripts: 680 heavy chains and 472 light chains (accession numbers KJ133708 – KJ134387, KJ134388 – KJ134859); and CAP256 Env sequences (accession numbers KF996576 – KF996716). Reprints and permissions information is available at www.nature.com/reprints. The authors declare no competing financial interests. Readers are welcome to comment on the online version of the paper. Correspondence and requests for materials should be addressed for CAPRISA and viral evolution to L.M. (lynnm@nicd.ac.za), for crystallography to P.D.K. (pdkwong@nih.gov), for NGS to L.S. (lss8@columbia.edu), and for isolated antibodies to J.R.M. (jrmascola@nih.gov).

©2014 Macmillan Publishers Limited. All rights reserved

METHODS

Study subject. CAPRISA participant CAP256 was enrolled into the CAPRISA acute infection study[51] that was established in 2004 in KwaZulu-Natal, South Africa for follow-up and subsequent identification of HIV seroconversion. CAP256 was one of the 7 women in this cohort who developed neutralization breadth[6]. The CAPRISA 002 acute infection study was reviewed and approved by the research ethics committees of the University of KwaZulu-Natal (E013/04), the University of Cape Town (025/2004), and the University of the Witwatersrand (MM040202). CAP256 provided written informed consent for study participation. Samples were drawn between 2005–09.

Isolation and expression of CAP256-VRC26 family genes. PBMC isolated from CAP256 blood draws at weeks 59, 119 and 206 were stained and sorted for IgG^+ B cells on a FACS Aria II as described in ref. 18. Cells were plated at two B cells per well in 384-well plates and cultured for 14 days in the presence of IL-2, IL-21, and CD40L-expressing irradiated feeder cells, as described in refs 27 and 45. Culture supernatants were screened by microneutralization as described in ref. 52 against HIV-1 ZM53.12 and either CAP45.G3 or CAP210.E8 Env-pseudoviruses. Kappa and lambda light chain gene and IgG heavy chain gene variable regions were amplified from neutralization-positive wells, subcloned, expressed and purified as described in ref. 18. Heavy chains were reconstituted as IgG1. The efficiency of cloning was as follows. For week 59, a total of 15,000 B cells (7,500 wells) were plated, 8.3% of wells produced IgG, 4 were positive in microneutralization, and one heavy-light chain pair was recovered. For week 119, a total of 45,000 B cells were plated, 48% of wells produced IgG, 49 wells were positive in microneutralization, and 8 heavy-light chain pairs were recovered. For week 206, a total of 42,000 B cells were plated, 29% of wells produced IgG, 34 wells were positive in microneutralization and 3 heavy-light chain pairs were recovered.

The antibodies are numbered CAP256-VRC26.01-.12 in order of the time point of the sample from which they were isolated, and then the degree of heavy-chain somatic mutation.

Neutralization assays. Single round of replication Env-pseudoviruses were prepared, titred and used to infect TZM-bl target cells as described previously[46,47]. Neutralization breadth of CAP256-VRC26.01, .03, .06, and .08 were determined using a previously described[18,53] panel of 194 geographically and genetically diverse Env-pseudoviruses representing the major subtypes and circulating recombinant forms. The remaining antibodies were assayed on a subset of this panel. The data were calculated as a reduction in luminescence units compared with control wells, and reported as half-maximum inhibitory concentration (IC_{50}) in micrograms per microlitre for monoclonal antibodies, or reciprocal dilution (ID_{50}) for plasma samples.

Neutralization fingerprints. Owing to the high sequence variability of HIV-1 Env, different viral strains may exhibit different neutralization sensitivities to the same antibody, and this pattern of neutralization variation can be used to define the neutralization fingerprint for a given antibody. Namely, the neutralization fingerprint of an antibody is defined as the rank-order of neutralization potencies for the antibody against a set of diverse viral strains[18].

The correlations between the neutralization fingerprints of the CAP256-VRC26 antibodies and the neutralization patterns of four longitudinal serum time points (at 59, 106, 159, and 220 weeks post-infection) were computed over a set of 29 HIV-1 strains (6535.3, AC10.29, CAAN.A2, CAP210.E8, CAP244.D3, CAP45.G3, DU156.12, DU172.17, DU422.01, PVO.04, Q168.a2, Q23.17, Q259.d2.17, Q461.e2, Q769.d22, Q842.d12, QH0692.42, REJO.67, RHPA.7, SC422.8, THRO.18, TRJO.58, TRO.11, WITO.33, ZM109.4, ZM135.10a, ZM197.7, ZM233.6, ZM53.12)[18]. The correlations between the neutralization potencies of the CAP256-VRC26 antibodies and a reference set of antibodies targeting the four major sites of vulnerability, with at most two antibodies per unique donor, were computed over a set of 41 HIV-1 strains (6535.3, 0260.v5.c36, 6405.v4.c34, AC10.29, C1080.c3, CAAN.A2, CAP210.E8, CAP244.D3, CAP45.G3, CNE3, DU156.12, DU172.17, DU422.01, KER2008.12, KER2018.11, MB201.A1, MB539.2B7, PVO.04, Q168.a2, Q23.17, Q259.17, Q461.e2, Q769.d22, Q842.d12, QH0692.42, REJO.67, RHPA.7, RW020.2, SC422.8, TH976.17, THRO.18, TRJO.58, TRO.11, UG037.8, WITO.33, ZM109.4, ZM135.10a, ZM197.7, ZM214.15, ZM249.1, ZM53.12). The correlations between the neutralization patterns of the four longitudinal serum time points and the neutralization fingerprints of the reference antibodies were computed over a set of 28 HIV-1 strains (6535.3, AC10.29, CAAN.A2, CAP210.E8, CAP244.D3, CAP45.G3, DU156.12, DU172.17, DU422.01, PVO.04, Q168.a2, Q23.17, Q259.17, Q461.e2, Q769.d22, Q842.d12, QH0692.42, REJO.67, RHPA.7, SC422.8, THRO.18, TRJO.58, TRO.11, WITO.33, ZM109.4, ZM135.10a, ZM197.7, ZM53.12). For the reference antibodies, data from multiple neutralization experiments were averaged and consolidated. All correlations are based on the Spearman's rank correlation coefficient.

Virus-like particle ELISA. VLP ELISAs were performed as described previously[31]. Briefly, VLPs were produced by PEI-based cotransfection of 293T cells with a pCAGGS-based, Env-expressing plasmid and the Env-deficient HIV-1 genomic backbone plasmid pNL-LucR-E. VLPs were coated on ELISA wells at 20× the concentration in transfection supernatants. Monoclonal antibody binding was then assessed by ELISA, omitting detergent in PBS wash buffers and probing with an anti-human Fc alkaline phosphatase conjugate (Accurate, Westbury, NY) and SigmaFAST p-nitrophenyl phosphate tablets (Sigma). Plates were read at 405 nm.

Cell-surface Env binding. 293T cells were transiently transfected with plasmids encoding Env ZM53.12 or CAP256-SU with deletions of the cytoplasmic tail[30]. For binding experiments: after 2 days, the cells were stained with ViVid viability dye (Invitrogen) followed by serial dilutions of antibodies, two washes with PBS/5% FBS, then R-PE-conjugated F(ab) goat anti-human IgG specific for the Fc fragment (Jackson ImmunoResearch) at a 1:200 dilution[54]. For competition assays, the cells were stained with ViVid viability dye followed by biotinylated CAP256-VRC26.08 ($0.8\ \mu g\ ml^{-1}$) premixed with serially diluted unlabelled competitor antibodies. After incubation and 2 washes, cells were stained with streptavidin-PE (Invitrogen) at 1:200 dilution. Cells were analysed on a BD LSRII (Becton Dickinson). Binding was measured as the median fluorescence intensity (MFI) for each sample minus the MFI of cells stained with secondary antibody only.

Polyreactivity analysis of antibodies. Antibody binding to cardiolipin was determined as in ref. 42. Briefly, using the QUANTA Lite ACA IgG III ELISA kit (Zeus Scientific) per manufacturer's protocol, each antibody was diluted to $100\ \mu g\ ml^{-1}$ in the kit sample diluent and tested in threefold serial dilutions. Results shown are representative of at least two independent ELISAs. Positive and negative controls were included on each plate, and values three times above background were considered positive. Antibody reactivity to a human epithelial cell line (HEp-2) was determined with the ANA/HEp-2 Cell Culture IFA Test System (Zeus Scientific) per manufacturer's protocol, as described in ref. 42. Antibodies were diluted to $50\ \mu g\ ml^{-1}$ and $25\ \mu g\ ml^{-1}$ in ZOBRA-NS diluent. Positive and negative controls were included on each slide. Antibodies were scored negative, indeterminate, or positive (1+ to 4+) at each dilution. Results are representative of at least two independent experiments.

Electron microscopy (EM) and image processing. VRC26.09 Fabs in complex with BG505 SOSIP.664 gp140 trimer produced in HEK 293S cells were analysed by negative stain EM. A 3 µl aliquot of $\sim 8\ \mu g\ ml^{-1}$ of the complex was applied for 15 s onto a glow discharged, carbon-coated 400 Cu mesh grid and stained with 2% uranyl formate for 20 s. Grids were imaged using a FEI Tecnai T12 electron microscope operating at 120 kV using a 52,000× magnification and electron dose of 25 $e^-/Å^2$, which resulted in a pixel size of 2.05Å at the specimen plane. Images were acquired with a Tietz 4k × 4k CCD camera in 5° tilt increments from 0° to 50° at a defocus of 1,000 nm using LEGINON[55].

Particles were picked automatically by using DoG Picker and put into a particle stack using the Appion software package[56,57]. Initial reference free 2D class averages were calculated using particles binned by 2 via the Xmipp Clustering 2D Alignment and sorted into 128 classes[58]. Particles corresponding to the complexes were selected into a substack and another round of reference free alignment was carried out with unbinned particles using Xmipp Clustering 2D alignment and IMAGIC softwares[59]. To generate an *ab initio* 3D starting model, a template stack of 44 images of 2D class averages was used without imposing symmetry. The resulting starting model was refined against 2D class averages for 9 cycles and subsequently with 6,763 raw particles for 9 cycles using EMAN[60]. The resolution of the final reconstruction was calculated to be 28Å using an FSC cut-off value of 0.5.

High-throughput sequencing. Amplicon for 454 next-generation sequencing was prepared as described[12,14] with slight modifications as indicated. Briefly, mRNA was prepared from 10–15 million PBMC using an Oligotex kit (Qiagen). cDNA was synthesized using Superscript II reverse transcriptase (Invitrogen) and oligo-dT(12–18) primers. Individual PCR reactions were performed with Phusion polymerase for 30 cycles. Primers (Supplementary Table 4) consisted of pools of 5–7 oligonucleotides specific for all lambda gene families or VH3 family genes, and had adapters for 454 next generation sequencing. For week 176 only, heavy-chain PCR was performed with primers for all VH families, and mixed lambda and kappa primers were used for light chain (Supplementary Table 4). PCR products were gel-purified (Qiagen). Pyrosequencing of the PCR products was performed on a GSFLX sequencing instrument (Roche-454 Life Sciences, Bradford, CT, USA) on a half chip per reaction (full chips for week 176). On average, ~250,000 raw reads were produced.

High-throughput linkage of V_H and V_L transcripts was performed in single cell emulsions generated using a flow focusing apparatus[35] (B.J.D., manuscript in preparation). $CD27^+$ B cells were isolated from CAP256 PBMCs collected at 34, 48, 59, 69, and 119 weeks post-infection by magnetic bead sorting (Miltenyi Biotec, Auburn, CA). Cells from weeks 34 and 119 were divided in two groups and half of the cells were analysed with FR1 primers[35], while the other half were analysed with leader peptide primers[41] (Supplementary Table 5). All other time points were analysed in a single group using only FR1 primers (Supplementary Table 1). Overlap extension RT–PCR was performed as previously reported[35], with extension time increased to 125 s. Nested PCR was performed as described previously with a 23-s

©2014 Macmillan Publishers Limited. All rights reserved

extension time and PCR products were sequenced using the Illumina 2 × 250 bp MiSeq platform. Raw reads were quality-filtered for an Illumina Q-score of 20 in 50% of bases. VRC26-class VH and paired VL sequences were identified via BLAST against CDR-H3 nucleotide sequences of the 12 culture-isolated antibodies.

Antibodyomics pipeline. Raw 454 data was processed using a pipeline implemented in Python, similar to one we reported previously[14]. Briefly, reads were filtered for length, keeping only those between 300 and 600 nucleotides. Germline V genes were then assigned to each read using BLAST with empirically optimized parameters. Reads for which no V gene match was found with an *e*-value $\leq 10^{-10}$ were discarded. For reads assigned to any VH3-30 or Vλ1-51 allele, (the CAP256-VRC26 germline genes), ClustalW2 (ref. 61) was used to calculate the sequence identity to the germline and each isolated antibody. These data were plotted as density heat maps using ggplot2 in R to produce identity-divergence plots (Fig. 3b and Supplementary Fig. 4).

Finding clonally related sequences. Reads that were assigned to the same V genes as CAP256-VRC26, VH3-30 and Vλ1-51, were submitted to IMGT High-Vquest[62] (http://www.imgt.org/IMGTindex/IMGTHighV-QUEST.html), and the results, including automated sequence corrections, were used to further sieve for lineage-related sequences. Reads assigned to *J* genes matching CAP256-VRC26 (JH3 or Jλ1), and having similar divergence (± 15%) in the *V* and *J* genes, similar (± 10%) nucleotide and amino acid divergences in the *V* gene, and containing a continuous open reading frame throughout the entire variable region, were selected for further processing. Next, reads from all time points were pooled and clustered at 97.25% sequence identity (twice the standard deviation of expected 454 sequencing error)[14] using CDHit[63]. For each cluster, a representative sequence was chosen from the earliest possible time point. The choice of cluster representatives from the earliest time points at which they appeared was critical to maintaining information on the chronology of lineage development in subsequent analyses. This procedure yielded 8,485 unique heavy chain and 6,410 unique light chain sequences.

To identify CAP256-VRC26 lineage-member heavy chains, we performed intra-donor phylogenetic analysis[14] on the unique 454 sequence set using the heavy chain sequences of the 12 isolated CAP256-VRC26 antibodies. 707 sequences were identified as likely lineage members, of which 27 were discarded after manual inspection, resulting in a total of 680 unique CAP256-VRC26 lineage heavy chain sequences.

To identify light chain lineage members, a sieve requiring at least 92% sequence identity in CDR L3 to one of the isolated antibodies resulted in 495 sequences. Joinsolver[64] was used to examine the *V-J* junctions of these sequences in detail, to ensure that the recombination points matched those known for the isolated antibodies (Supplementary Fig. 5). This gave a total of 472 unique CAP256-VRC26 lineage light chain sequences.

Paired reads that were identified as members of the CAP256-VRC26 lineage were clustered using CDHit[63] at 95% sequence identity and consensus VH and VL sequences were generated for each cluster containing two or more pairs. Blast was then used to align the resulting sequences to all clonally related sequences identified from the 454 sequencing as described above. Gapless alignments covering at least 190 nucleotides at 97% or greater sequence identity were considered to be matches. Two of the 157 paired sequences determined to be members of the CAP256-VRC26 lineage matched known CAP256-VRC26 lineage sequences in both VH and VL 454 data sets. An additional 4 VH sequences and 1 VL sequence were found in the 454 data, but their light or heavy chain partners were not present.

Computation of phylogenetic trees. Phylogenetic trees were constructed from 454 data and the sequences of antibodies isolated from B cell culture. Raw data are shown in Nexus format in Supplementary Figs 12 and 13. MEGA5 (ref. 65) was used to select the general time-reversible model with a gamma-distributed rate parameter (GTR+G)[66] as the best mathematical model for building a maximum-likelihood tree from the CAP256-VRC26 lineage sequences. FASTML[67] was then used to estimate the gamma parameter and build separate maximum likelihood trees for heavy and light chain sequences (including the isolated antibodies) and these were rooted on the germline *V* gene sequences. Two branches of the light chain tree were manually moved to match their positioning in the heavy chain tree based on the evidence from trees constructed solely with the 12 isolated antibodies. Analysis with DNAML from PHYLIP (Phylogeny Inference Package) version 3.6 (Felsenstein, J. 2005. PHYLIP (Phylogeny Inference Package) version 3.6. Distributed by the author. Department of Genome Sciences, University of Washington, Seattle) (http://cmgm.stanford.edu/phylip/dnaml.html) showed that these rearrangements did not significantly alter the log-likelihood score of the tree.

To create a condensed version of the heavy chain phylogenetic tree (Fig. 4c), CDR H3 sequences were clustered using a 95% sequence identity threshold and requiring that all CDR H3s in a cluster have the same length. Isolated antibodies and monophyletic clusters with at least five members were represented by a single leaf, while all other sequences were removed from the tree. In cases where an internal node was deleted, branch lengths above and below that node were summed, so that the tree depths of all remaining sequences were maintained.

UCA and inferred intermediates. The phylogenetic trees of all heavy and all light chain lineage members calculated above (Fig. 3c and Extended Data Fig. 1) were input into the DNAML maximum likelihood software package to infer ancestral sequences. These are a direct consequence of the input sequences and the mathematical model used to build the trees; the gamma distribution found by FASTML above was used and the topology of the tree was held fixed, so no further information was added. The calculated heavy chain UCA was identical to the germline VH3-30*18 allele. Although the VH3-30*03 allele is only one nucleotide different from *18, germline sequencing of this donor showed that she carries the *18 allele and not the *03 allele (Cathrine Mitchell Scheepers, personal communication). The inferred UCA is very similar to low-divergence sequences found in the week 38 data set (Extended Data Fig. 6).

To test intermediates in the development of CAP256-VRC26.01, two internal nodes were chosen from the phylogenetic trees to be approximately equally spaced in terms of evolutionary distance and the inferred sequences were retrieved using DNAML. Successful complementation of inferred heavy and light chains for each intermediate suggests that the lineage is well sampled by the 454 data and that the calculated phylogenetic trees successfully capture the coupled evolutionary dynamics of heavy and light chains.

Logograms for CDR H3s were made with Weblogo[68].

X-ray crystallography. VRC26.UCA Fab was prepared by digesting purified IgG with Lys-C at 37°C for 2 h. The reaction was then quenched by the addition of cOmplete protease inhibitors (Roche). For VRC26.01, VRC26.03, VRC26.04, VRC26.06, VRC26.07 and VRC26.10 Fab preparation, an HRV3C recognition site (GLEVLFQGP) was inserted after Lys 235 and purified IgG was incubated with HRV3C protease overnight at 4 °C. For all, the digested antibodies were passed over Protein A agarose to remove the Fc fragment. The Fab was further purified over a Superdex 200 gel filtration column and concentrated aliquots were stored at −80 °C. All Fabs were screened against 576 crystallization conditions using a Cartesian Honeybee crystallization robot. Initial crystals were grown by the vapour diffusion method in sitting drops at 20 °C by mixing 0.2 µl of protein complex with 0.2 µl of reservoir solution. Crystals were manually reproduced in hanging drops by mixing 1.0 µl protein complex with 1.0 µl reservoir solution. VRC26-UCA was crystallized with a reservoir solution of 27% PEG 8000 and 0.1 M HEPES pH 7.5 and was flash frozen in liquid nitrogen with 20% PEG 400 as a cryoprotectant. VRC26.01 was crystallized with a reservoir solution of 32% PEG 400, 4% PEG 3350 and 0.1 M sodium acetate pH 5.5 and was flash frozen in liquid nitrogen with 20% ethylene glycol as a cryoprotectant. VRC26.03 was crystallized with a reservoir solution of 22% PEG 8000, 5% MPD and 0.1 M imidazole pH 6.5 and was flash frozen in liquid nitrogen with 20% xylitol as a cryoprotectant. VRC26.04 was crystallized with a reservoir solution of 14% PEG 3350, 25% ispropanol and 0.1 M Tris pH 8.5 and was flash frozen in liquid nitrogen with 20% ethylene glycol as a cryoprotectant. VRC26.06 was crystallized with a reservoir solution of 3 M sodium formate and 0.1 M Tris pH 7.5 and was flash frozen in liquid nitrogen with 20% xylitol as a cryoprotectant. VRC26.07 was crystallized with a reservoir solution of 4% PEG 8000, 0.1 M zinc acetate and 0.1 M MES pH 6 and was flash frozen in liquid nitrogen with 20% glycerol as a cryoprotectant. VRC26.10 was crystallized with a reservoir solution of 22% PEG 4000, 0.4M sodium acetate and 0.1 M Tris pH 7.5 and was flash frozen in liquid nitrogen with no cryoprotectant.

Data for all crystals were collected at a wavelength of 1.00Å at SER-CAT beamlines ID-22 and BM-22 (Advanced Photon Source, Argonne National Laboratory). All diffraction data were processed with the HKL2000 suite[69] and model building and refinement were performed in COOT[70] and PHENIX[71], respectively. For VRC26.03 Fab data, a molecular replacement solution consisting of one Fab molecule per asymmetric unit was obtained using PHASER with a search model from PDB ID 3F12. VRC26.03 then served as a search model for all remaining VRC26 Fabs. Throughout the refinement processes, a cross validation (Rfree) test set consisting of 5% of the data was used and hydrogen atoms were included in the refinement model. Structure validations were performed periodically during the model building/refinement process with MolProbity[72]. Ribbon diagram representations of protein crystal structures were made with PyMOL[73] and electrostatics were calculated and rendered with UCSF Chimera[74].

Structure modelling on trimers. Defined locations of the V1V2, V3-glycan and CD4-binding sites were mapped directly onto EM density of the unliganded HIV-1 BAL spike (EMD-5019)[50] using the software package UCSF Chimera[74]. The CD4-binding site was defined by aligning density of the VRC01-bound BAL spike (EMD-5457)[75] with the unliganded map and fitting a crystal structure of VRC01-bound gp120 (PDB accession number 3NGB)[76] to the density. EM density in close proximity to the Fab structure was colored to highlight the region of contact. The same procedure was used to define the V3-glycan region using a PGT128-bound trimer (EMD-1970) and crystal structure (PDB id 3TYG)[77] and the V1V2

©2014 Macmillan Publishers Limited. All rights reserved

region using the PG9-bound BG505 SOSIP trimer (EMD-2241)[24] and a crystal structure of V1V2-bound PG9 (PDB accession number 3U4E)[22]. The fit of the PG9-V1V2 crystal structure to the SOSIP trimer was used to model the trimeric orientation of V1V2 using the threefold symmetry of the HIV-1 spike. The BG505.664 SOSIP crystal structure[33], PDB 4NCO, was presented to highlight the quaternary location of V1V2 point mutations. Side chains of residues 166 and 167, not seen in the crystal structure, were modelled. The Man5 glycan at N160, also not seen in the crystal structure, is represented as in the crystal structure of the PG9-V1V2 complex (PDB accession code 3U4E).

Loop modelling. Two intermediates were calculated at approximately equal maturation distance along the VRC26-UCA to VRC26.01 pathway. Mutations associated with the intermediates were mapped directly onto the structure of VRC26.01. 14 of the 35 residues in the VRC26.01 structure are disordered and were modelled with Loopy[78] (http://wiki.c2b2.columbia.edu/honiglab_public/index.php/Software:Loopy) and represented as grey dots. Mutations of the intermediates were coloured according to approximate time of occurrence based on the longitudinal phylogenetic tree highlighting the timeline of the structural development. These, and the other antibodies with modelled loops (Fig. 4), were modelled in a single loop prediction involving four steps. In the first step, Loopy was used to predict 10 loop conformations. The number of initial loop conformations to be sampled was set to 50,000 (and the not the default value of 2,000). In the second step, all 10 loop conformations were refined using the Protein Preparation Wizard in Maestro (http://www.schrodinger.com/). In the third step, sulphate groups were added to tyrosine at position 100 of the heavy chain and the entire structure was then subjected to all-atom energy minimization in Maestro. A fourth and final step was needed to ensure a reasonable sampling of the rotameric states for the sulphated tyrosines. The Rapid Torsion Scan module in Maestro was used to sample the chi angle involving the sulphate moiety in steps of 20 degrees. The model with the lowest energy after application of the Rapid Torsion Scan module was considered as the best prediction.

Tyrosine sulphation predictions were carried out in GPS-TPS (Z. Pan *et al.*, http://tsp.biocuckoo.org).

Single genome amplification (SGA), sequencing and cloning. HIV-1 RNA was isolated from plasma using the Qiagen QIAamp Viral RNA kit, and reverse transcribed to cDNA using SuperScript III Reverse Transcriptase (Invitrogen, CA). The envelope genes were amplified from single genome templates[49] and amplicons were directly sequenced using the ABI PRISM Big Dye Terminator Cycle Sequencing Ready Reaction kit (Applied Biosystems, Foster City, CA) and resolved on an ABI 3100 automated genetic analyser. The full-length env sequences were assembled and edited using Sequencher v.4.5 software (Genecodes, Ann Arbor, MI). Multiple sequence alignments were performed using Clustal X (ver. 1.83) and edited with BioEdit (ver. 7.0.9) Sequence alignments were visualized using Highlighter for Amino Acid Sequences v1.1.0 (beta).

For analysis of selection pressure, and to account for recombination between the SU and PI, sequences were partitioned into two alignments (an SU-related, and a PI-related alignment) based on the inferred recombination breakpoints using an in-house script. Breakpoints were identified by a shift in identity from one reference towards the other, and required at least two sequential polymorphisms in common with a corresponding PI/SU-related virus in order to be considered. Phylogenies for both alignments were then reconstructed using FastTree[79] with a GTR+CAT model, and rooted on the PI/SU. Signals of selective pressure were detected with MEME (episodic diversifying selection)[80] and DEPS (directional selection)[81] using the FastTree-generated trees, implemented in Hyphy[82].

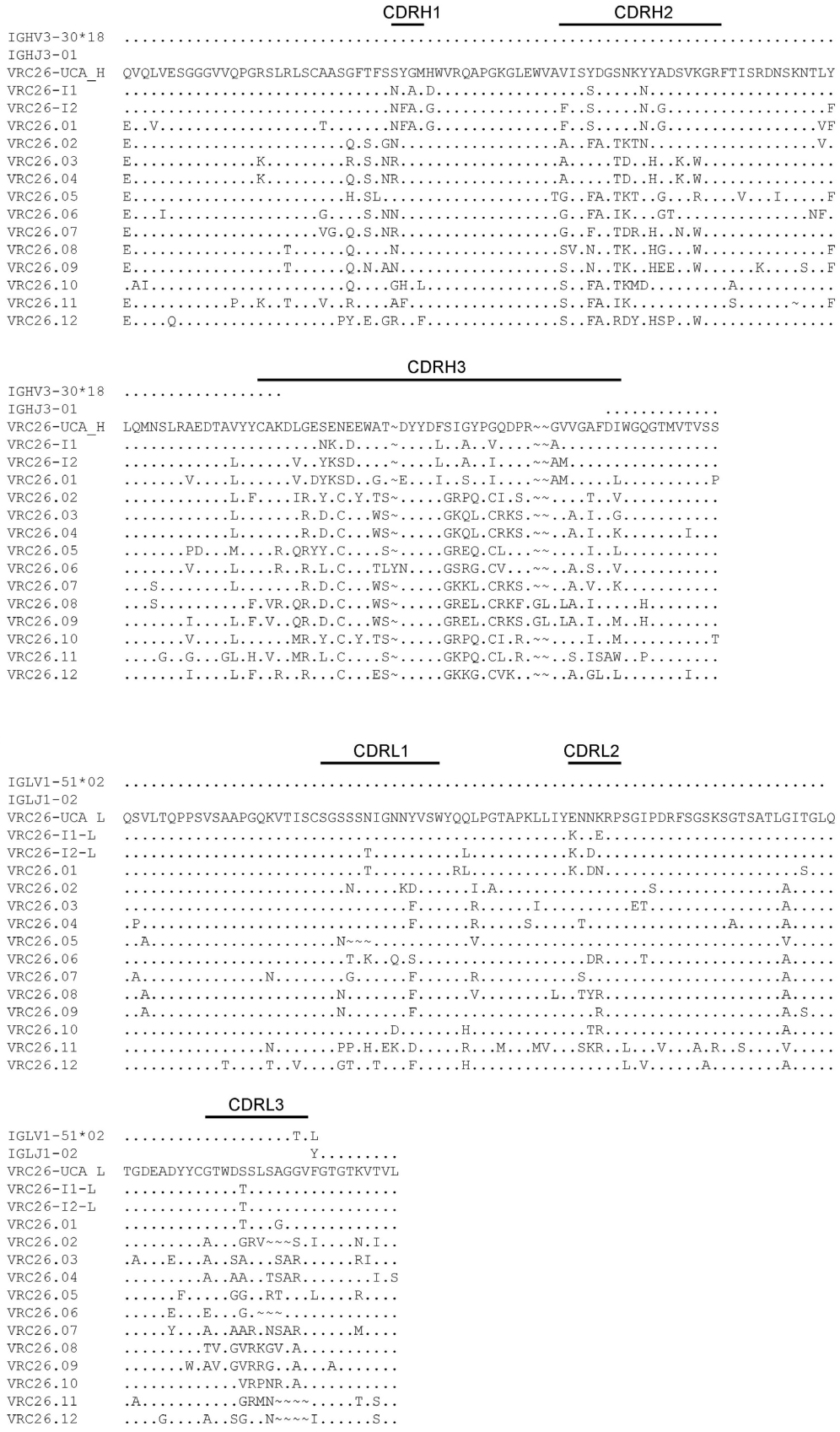
The frequencies of specific amino acids at a site and the distribution of net charges in the V2 epitope were calculated from the 2012 filtered web alignment ($n = 3{,}990$) from the Los Alamos HIV database (http://www.hiv.lanl.gov/).

Selected envelope amplicons were cloned into the expression vector pcDNA 3.1 (directional) (Invitrogen) by re-amplification of SGA first-round products using Pfu Ultra II enzyme (Stratagene) with the EnvM primer, 5′-TAGCCCTTCCAGTCCCCCCTTTTCTTTTA-3′ (ref. 83) and directional primer, EnvAstop, 5′-CACCGGCTTAGGCATCTCCTATGGCAGGAAGAA-3′ (ref. 48). Cloned *env* genes were sequenced to confirm that they exactly matched the sequenced amplicon. Autologous clones were mutated at key residues within the C-strand using the Stratagene QuickChange II kit (Stratagene) as described by the manufacturer. Mutations were confirmed by sequencing. Envelope clones were used to generate single round of replication Env-pseudoviruses as described above.

51. van Loggerenberg, F. *et al.* Establishing a cohort at high risk of HIV infection in South Africa: challenges and experiences of the CAPRISA 002 acute infection study. *PLoS ONE* **3,** e1954 (2008).
52. Doria-Rose, N. *et al.* High throughput HIV-1 microneutralization assay. *Protocol Exchange* http://dx.doi.org/10.1038/protex.2013.069 (2013).
53. Wu, X. *et al.* Rational design of envelope identifies broadly neutralizing human monoclonal antibodies to HIV-1. *Science* **329,** 856–861 (2010).
54. Julien, J. P. *et al.* Broadly neutralizing antibody PGT121 allosterically modulates CD4 binding via recognition of the HIV-1 gp120 V3 base and multiple surrounding glycans. *PLoS Pathog.* **9,** e1003342 (2013).
55. Suloway, C. *et al.* Automated molecular microscopy: the new Leginon system. *J. Struct. Biol.* **151,** 41–60 (2005).
56. Lander, G. C. *et al.* Appion: an integrated, database-driven pipeline to facilitate EM image processing. *J. Struct. Biol.* **166,** 95–102 (2009).
57. Voss, N. R., Yoshioka, C. K., Radermacher, M., Potter, C. S. & Carragher, B. DoG Picker and TiltPicker: software tools to facilitate particle selection in single particle electron microscopy. *J. Struct. Biol.* **166,** 205–213 (2009).
58. Sorzano, C. O. *et al.* A clustering approach to multireference alignment of single-particle projections in electron microscopy. *J. Struct. Biol.* **171,** 197–206 (2010).
59. van Heel, M., Harauz, G., Orlova, E. V., Schmidt, R. & Schatz, M. A new generation of the IMAGIC image processing system. *J. Struct. Biol.* **116,** 17–24 (1996).
60. Ludtke, S. J., Baldwin, P. R. & Chiu, W. EMAN: semiautomated software for high-resolution single-particle reconstructions. *J. Struct. Biol.* **128,** 82–97 (1999).
61. Larkin, M. A. *et al.* Clustal W and Clustal X version 2.0. *Bioinformatics* **23,** 2947–2948 (2007).
62. Alamyar, E., Giudicelli, V., Li, S., Duroux, P. & Lefranc, M. P. IMGT/HighV-QUEST: the IMGT web portal for immunoglobulin (IG) or antibody and T cell receptor (TR) analysis from NGS high throughput and deep sequencing. *Immunome Res.* **8** (2012).
63. Li, W., Jaroszewski, L. & Godzik, A. Clustering of highly homologous sequences to reduce the size of large protein databases. *Bioinformatics* **17,** 282–283 (2001).
64. Souto-Carneiro, M. M., Longo, N. S., Russ, D. E., Sun, H. W. & Lipsky, P. E. Characterization of the human Ig heavy chain antigen binding complementarity determining region 3 using a newly developed software algorithm, JOINSOLVER. *J. Immunol.* **172,** 6790–6802 (2004).
65. Tamura, K. *et al.* MEGA5: molecular evolutionary genetics analysis using maximum likelihood, evolutionary distance, and maximum parsimony methods. *Mol. Biol. Evol.* **28,** 2731–2739 (2011).
66. Waddell, P. J. & Steel, M. A. General time-reversible distances with unequal rates across sites: mixing gamma and inverse Gaussian distributions with invariant sites. *Mol. Phylogenet. Evol.* **8,** 398–414 (1997).
67. Ashkenazy, H. *et al.* FastML: a web server for probabilistic reconstruction of ancestral sequences. *Nucleic Acids Res.* **40,** W580–W584 (2012).
68. Crooks, G. E., Hon, G., Chandonia, J. M. & Brenner, S. E. WebLogo: a sequence logo generator. *Genome Res.* **14,** 1188–1190 (2004).
69. Otwinowski, Z. & Minor, W. Processing of X-ray diffraction data collected in oscillation mode. *Methods Enzymol.* **276,** 307–326 (1997).
70. Emsley, P. & Cowtan, K. Coot: model-building tools for molecular graphics. *Acta Crystallogr. D* **60,** 2126–2132 (2004).
71. Adams, P. D. *et al.* Recent developments in the PHENIX software for automated crystallographic structure determination. *J. Synchrotron Radiat.* **11,** 53–55 (2004).
72. Davis, I. W., Murray, L. W., Richardson, J. S. & Richardson, D. C. MOLPROBITY: structure validation and all-atom contact analysis for nucleic acids and their complexes. *Nucleic Acids Res.* **32,** W615–W619 (2004).
73. DeLano, W. L. The PyMOL Molecular Graphics System. http://www.pymol.org (DeLano Scientific, San Carlos, California, 2002).
74. Pettersen, E. F. *et al.* UCSF Chimera–a visualization system for exploratory research and analysis. *J. Comput. Chem.* **25,** 1605–1612 (2004).
75. Tran, E. E. *et al.* Structural mechanism of trimeric HIV-1 envelope glycoprotein activation. *PLoS Pathog.* **8,** e1002797 (2012).
76. Zhou, T. *et al.* Structural basis for broad and potent neutralization of HIV-1 by antibody VRC01. *Science* **329,** 811–817 (2010).
77. Pejchal, R. *et al.* A potent and broad neutralizing antibody recognizes and penetrates the HIV glycan shield. *Science* **334,** 1097–1103 (2011).
78. Soto, C. S., Fasnacht, M., Zhu, J., Forrest, L. & Honig, B. Loop modeling: Sampling, filtering, and scoring. *Proteins* **70,** 834–843 (2008).
79. Price, M. N., Dehal, P. S. & Arkin, A. P. FastTree 2–approximately maximum-likelihood trees for large alignments. *PLoS ONE* **5,** e9490 (2010).
80. Murrell, B. *et al.* Detecting individual sites subject to episodic diversifying selection. *PLoS Genet.* **8,** e1002764 (2012).
81. Kosakovsky Pond, S. L., Poon, A. F., Leigh Brown, A. J. & Frost, S. D. A maximum likelihood method for detecting directional evolution in protein sequences and its application to influenza A virus. *Mol. Biol. Evol.* **25,** 1809–1824 (2008).
82. Pond, S. L., Frost, S. D. & Muse, S. V. HyPhy: hypothesis testing using phylogenies. *Bioinformatics* **21,** 676–679 (2005).
83. Gao, F. *et al.* The heterosexual human immunodeficiency virus type 1 epidemic in Thailand is caused by an intersubtype (A/E) recombinant of African origin. *J. Virol.* **70,** 7013–7029 (1996).

©2014 Macmillan Publishers Limited. All rights reserved

a



b

Extended Data Figure 1 | Amino acid sequences of CAP256-VRC26 heavy and light chains. **a**, **b**, Sequences of the 12 B-cell culture derived antibodies, inferred germline *V* and *J* genes, and inferred intermediates are compared to the predicted UCA. **a**, Heavy chain. **b**, Lambda light chain.

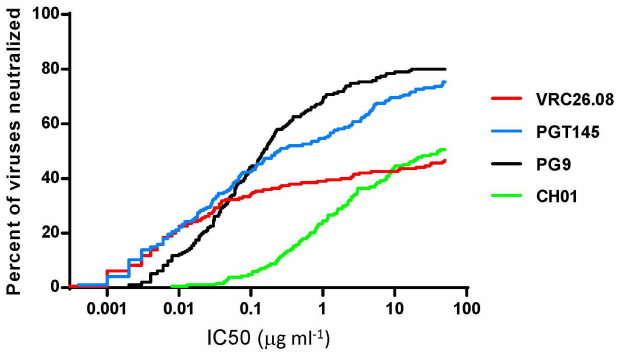
©2014 Macmillan Publishers Limited. All rights reserved

a

	IC50	CAP256-VRC26.01	CAP256-VRC26.02	CAP256-VRC26.03	CAP256-VRC26.04	CAP256-VRC26.05	CAP256-VRC26.06	CAP256-VRC26.07	CAP256-VRC26.08	CAP256-VRC26.09	CAP256-VRC26.10	CAP256-VRC26.11	CAP256-VRC26.12
Autologous	CAP256.PI	>50	>50	>50	>50	>50	0.030	>50	>50	>50	>50	>50	>50
	CAP256.SU	0.14	0.015	0.004	0.003	0.007	0.055	0.008	0.003	0.002	0.031	0.055	0.032

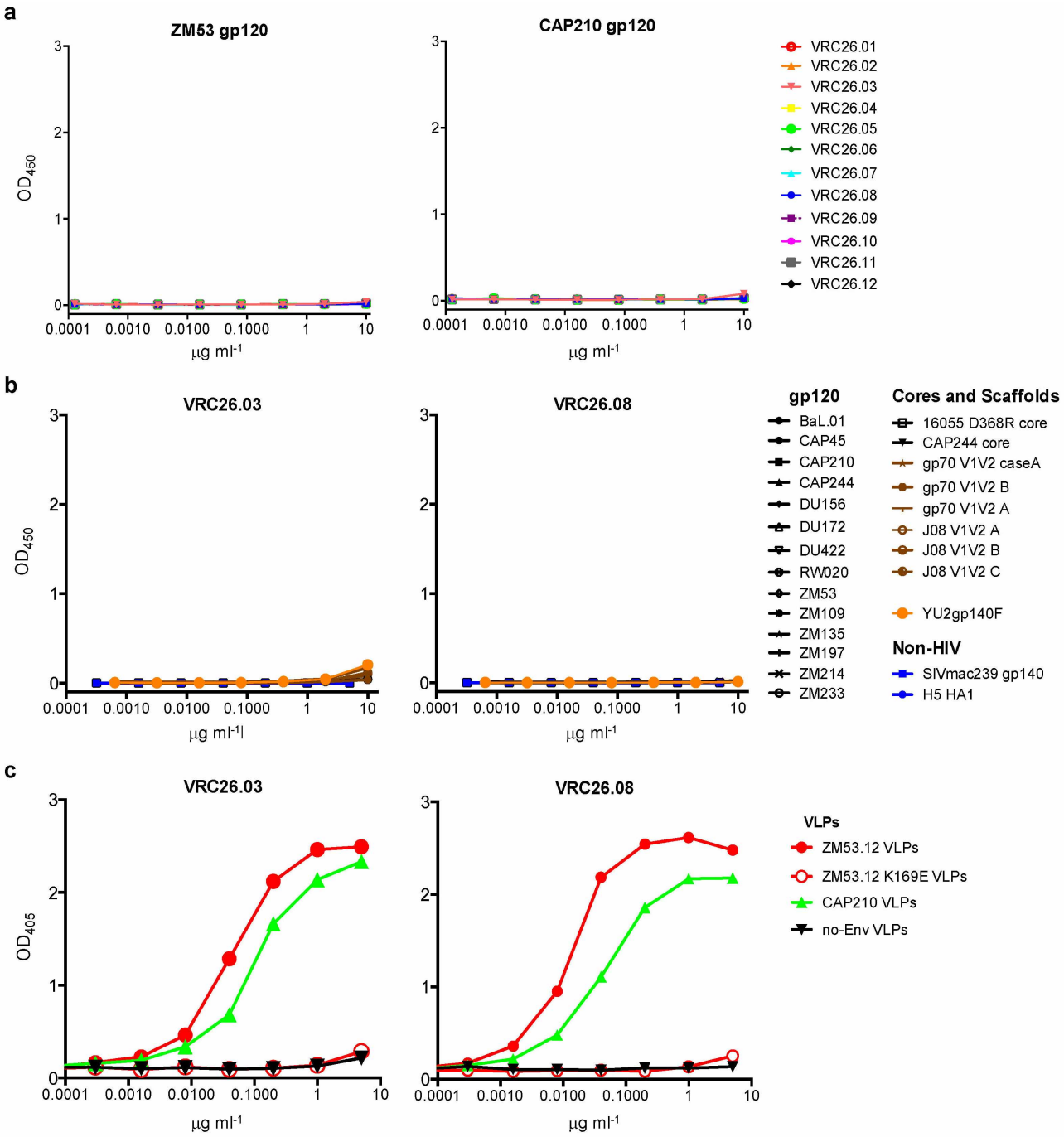
Heterologous by clade	IC50	CAP256-VRC26.01	CAP256-VRC26.02	CAP256-VRC26.03	CAP256-VRC26.04	CAP256-VRC26.05	CAP256-VRC26.06	CAP256-VRC26.07	CAP256-VRC26.08	CAP256-VRC26.09	CAP256-VRC26.10	CAP256-VRC26.11	CAP256-VRC26.12
C	96ZM651.02	>50	>50	>50	>50	>50	>50	>50	2.630	0.991	>50	>50	>50
	CAP210.E8	0.166	0.062	0.008	0.005	0.013	1.200	0.021	0.003	0.002	0.100	0.073	0.072
	CAP244.D3	>50	>50	>50	>50	>50	>50	>50	>50	>50	>50	>50	>50
	CAP45.G3	31.8	>50	16.0	>50	>50	>50	>50	4.00	16.0	>50	>50	>50
	DU156.12	>50	>50	0.090	10.4	>50	>50	>50	0.006	0.016	>50	>50	>50
	DU172.17	>50	>50	>50	>50	>50	>50	>50	>50	>50	>50	>50	>50
	DU422.01	>50	>50	0.224	4.17	>50	>50	>50	0.008	0.023	8.20	11.5	>50
	ZM109.4	>50	>50	>50	>50	26.5	>50	>50	>50	>50	>50	>50	>50
	ZM135.10a	>50	>50	>50	>50	>50	>50	>50	>50	>50	>50	>50	>50
	ZM197.7	22.1	1.97	0.302	0.254	0.113	>50	>50	0.022	0.011	0.346	0.055	>50
	ZM214.15	>50	>50	0.100	>50	>50	>50	>50	3.23	0.333	>50	>50	>50
	ZM233.6	0.701	0.701	0.032	0.060	0.003	22.600	>50	0.001	0.001	0.228	0.322	>50
	ZM249.1	>50	>50	0.004	11.4	>50	>50	44.1	0.076	0.010	>50	34.5	>50
	ZM53.12	0.036	0.043	0.008	0.004	0.012	0.082	0.014	0.004	0.002	0.072	0.081	0.211
A	0260.v5.c36	>50	>50	>50	>50	>50	>50	>50	>50	>50	>50	>50	>50
	BG505.w6m	>50	>50	4.760	8.430	>50	>50	>50	0.143	0.054	>50	4.200	>50
	KER2008.12	0.308	>50	>50	>50	>50	>50	>50	>50	>50	>50	>50	>50
	KER2018.11	5.95	0.18	0.014	0.008	0.012	>50	3.100	42.7	0.002	0.335	1.76	>50
	MB201	>50	>50	>50	>50	>50	>50	>50	>50	>50	>50	>50	>50
	MB539.2B7	>50	>50	>50	>50	>50	>50	>50	31.9	40.7	>50	>50	>50
	Q168.a2	>50	>50	>50	>50	>50	>50	>50	0.148	0.181	>50	>50	>50
	Q23.17	>50	>50	0.867	23.6	>50	>50	>50	0.911	9.50	2.59	>50	>50
	Q259.d2.17	>50	>50	0.002	0.025	0.023	>50	42.5	0.001	0.008	24.6	>50	>50
	Q461.e2	>50	>50	>50	>50	>50	>50	>50	0.502	0.705	>50	>50	>50
	Q769.d22	>50	>50	>50	>50	>50	>50	>50	>50	>50	>50	>50	>50
	Q842.d12	>50	>50	>50	>50	>50	>50	>50	>50	10.1	>50	>50	>50
	RW020.2	>50	>50	>50	>50	>50	>50	>50	>50	>50	>50	>50	>50
	UG037.8	>50	>50	>50	>50	>50	>50	>50	>50	>50	>50	>50	>50
B	6535.3	>50	>50	>50	>50	>50	>50	>50	>50	>50	>50	>50	>50
	AC10.29	>50	>50	>50	>50	>50	0.030	>50	>50	>50	>50	>50	>50
	CAAN.A2	>50	>50	>50	>50	>50	>50	>50	>50	>50	>50	>50	>50
	PVO.04	>50	7.98	>50	>50	44.400	0.947	>50	11.800	>50	2.48	10.8	>50
	QH0692.42	>50	>50	>50	>50	>50	>50	>50	>50	>50	>50	>50	>50
	REJO.67	>50	>50	>50	>50	>50	>50	>50	>50	>50	>50	>50	>50
	RHPA.7	>50	>50	>50	>50	>50	>50	>50	>50	>50	>50	>50	>50
	SC422.8	>50	>50	>50	>50	>50	0.439	>50	>50	>50	>50	>50	>50
	THRO.18	>50	>50	>50	>50	>50	3.30	>50	>50	>50	>50	>50	>50
	TRJO.58	>50	>50	>50	>50	>50	>50	>50	>50	>50	>50	>50	>50
	TRO.11	>50	>50	>50	>50	>50	>50	>50	>50	>50	>50	>50	>50
	WITO.33	>50	>50	>50	>50	>50	0.005	>50	>50	>50	>50	>50	>50
D	191821.E6.1	>50	>50	1.50	>50	>50	>50	>50	0.003	0.054	>50	>50	>50
	3016.V5.c36	16.4	0.057	0.450	0.283	0.011	>50	>50	0.005	0.004	0.017	0.300	7.93
	6405.v4.c34	>50	>50	>50	>50	>50	>50	>50	>50	>50	>50	>50	>50
AE	C1080.c3	>50	>50	0.006	0.212	>50	>50	>50	0.023	0.019	>50	0.018	>50
	CM244.ec1	3.32	2.030	0.007	0.361	0.517	>50	6.90	1.00	0.105	0.914	26.7	>50
	CNE3	>50	>50	>50	>50	>50	>50	>50	>50	>50	>50	>50	>50
	TH976.17	>50	>50	>50	>50	>50	>50	>50	>50	>50	>50	>50	>50
	% breadth	19%	17%	36%	30%	21%	17%	13%	47%	47%	23%	26%	6%
	geomean IC50	1.88	0.40	0.08	0.32	0.10	0.38	1.51	0.11	0.07	0.60	0.94	0.49

b



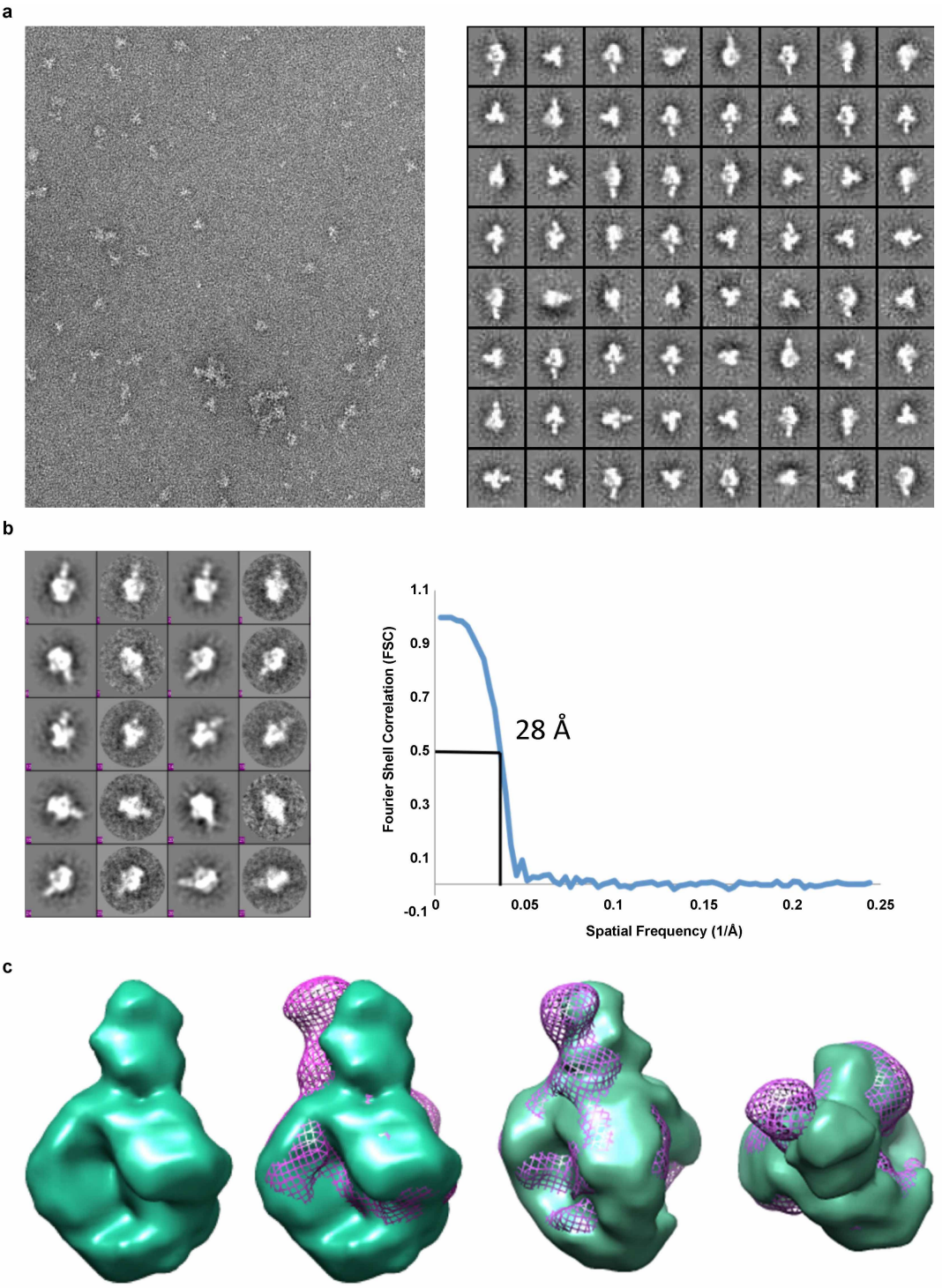
Extended Data Figure 2 | Neutralization breadth and potency of CAP256-VRC26 antibodies. a, Neutralization of autologous (CAP256 PI and SU) and 47 heterologous viruses by CAP256-VRC26 antibodies. Neutralization was measured using a TZM-bl assay with Env-pseudoviruses. Geometric mean was calculated for values $<50\ \mu g\ ml^{-1}$. **b**, Breadth-potency curves. Neutralization of a 194-virus panel was measured for VRC26.08, PG9, PGT145 and CH01. The curves show the percent of viruses neutralized at any given IC_{50}.

©2014 Macmillan Publishers Limited. All rights reserved



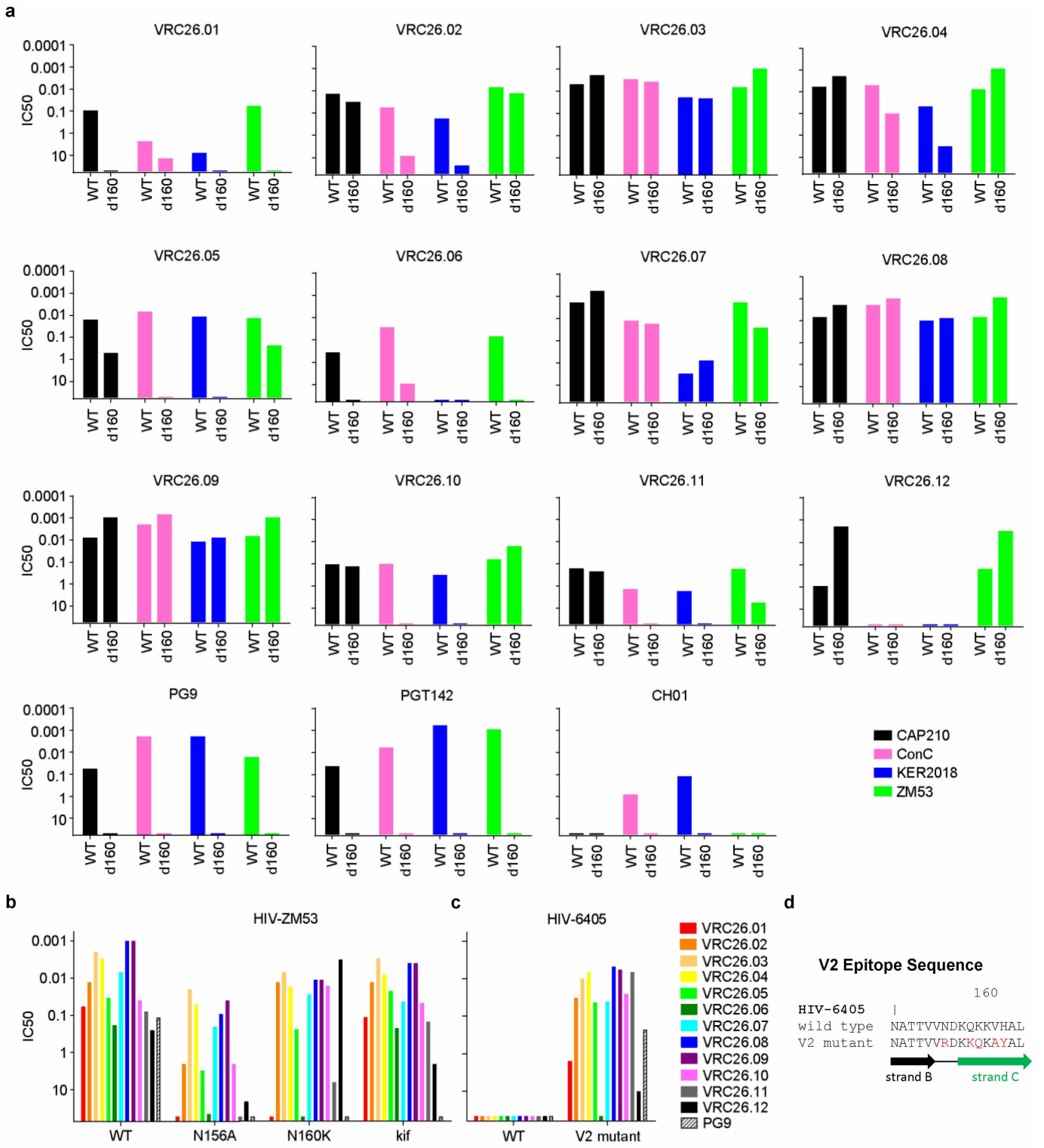
Extended Data Figure 3 | CAP256-VRC26 antibodies recognize a quaternary epitope. **a**, All 12 CAP256-VRC26 monoclonal antibodies were tested by ELISA against gp120 from ZM53 and CAP210. Positive control antibody PG9 bound to both gp120s (not shown). **b**, Twenty-three proteins and scaffolded V1V2 constructs were tested by ELISA for binding of CAP256-VRC26.03 and CAP256-VRC26.08. PG9 bound to several of these (not shown). Similar data were observed for CAP256-VRC26.06, .07 and .09. **c**, Binding of CAP256-VRC26.03 and CAP256-VRC26.08 to virus-like particles (VLP). VLP expressing ZM53, ZM53.K169E, CAP210 or no Env were concentrated by pelleting and used to coat ELISA plates; assays were performed without detergent to preserve the trimer spikes. Similar data were observed for CAP256-VRC26.06, .07 and .09.

©2014 Macmillan Publishers Limited. All rights reserved



Extended Data Figure 4 | Visualization of CAP256-VRC26.09 bound to Env trimers by negative-stain electron microscopy. **a**, Raw micrograph and corresponding reference free 2D class averages of VRC26.09 in complex with cleaved soluble BG505 SOSIP.664 gp140 trimers. **b**, Projection matching of 3D model refinement and FSC curve used to calculate resolution. Resolution, 28Å at FSC = 0.5. **c**, 3D reconstruction of VRC26.09:BG505 SOSIP.664 complex (green surface) alone and overlayed with PG9:SOSIP (purple mesh). The reconstructions are nearly identical in the trimer portion while displaying small differences in the Fab angles.

©2014 Macmillan Publishers Limited. All rights reserved



Extended Data Figure 5 | Effects of V2 mutations on neutralization activity of CAP256-VRC26 antibodies. **a**, Each panel shows neutralization of wild-type and N160 glycan mutant CAP210.E8, ConC, KER2018.11 and ZM53.12 viruses. CAP256-VRC26 monoclonal antibodies are partially and variably affected by loss of N160 glycan, in a virus-strain specific manner. In contrast, PG9-class antibodies PG9, PGT142, and CH01 are uniformly knocked out by N160 mutation. **b**, CAP256-VRC26 monoclonal antibodies are partially and variably affected by changes in V2 glycans. Neutralization by each antibody was measured against wild-type ZM32.12, mutants N156A and N160K, and ZM53.12 grown in the presence of kifunensine, an inhibitor of glycan processing. In contrast to CAP256-VRC26 antibodies, PG9 activity is knocked out by the mutations and by kifunensine. **c**, HIV-6405 wild type is resistant to PG9 and CAP256-VRC26 antibodies, and its PG9-sensitive mutant[34] is also sensitive to CAP256-VRC26 antibodies. **d**, Sequences of wild type and mutant HIV-6405.

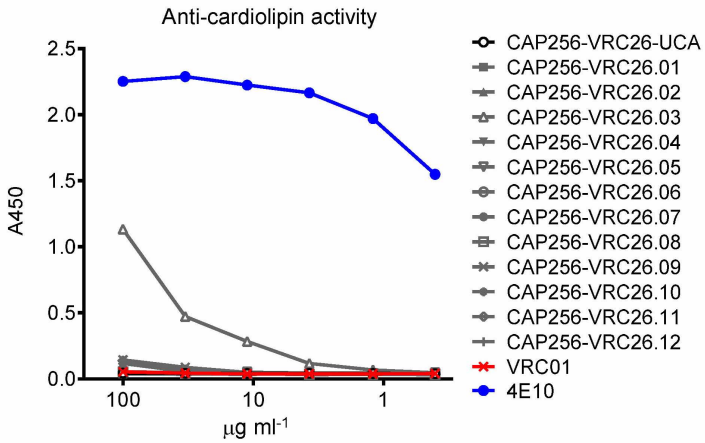
©2014 Macmillan Publishers Limited. All rights reserved

a

```
                                                    CDR H1                                  CDR H2
UCA              QVQLVESGGG VVQPGRSLRL SCAASGFTFS SYGMHWVRQA PGKGLEWVAV ISYDGSNKYY ADSVKGRFTI
038-190676 (1x)  .......... .......... .......... .......... .......... .......... ..........
038-195559 (1x)  .......... .....G.... .......S.. .......... .......... .......... ..........
038-006719 (35x) .......... .......... .......S.. .......... .......... .......... ..........
038-223402 (1x)  .......... .......... .......S.. .......... .......... .......... ..........
038-226205 (1x)  .......... .I........ .......S.. .......... .......... .......... ..........

                                                                CDR H3
UCA              SRDNSKNTLY LQMNSLRAED TAVYYCAKDL GESENEEWAT DYYDFSIGYP GQDPRGVVGA FDIWGQGTMV TVSS
038-190676       .......... .......... .......... .........S .....R.... .......... .......... ....
038-195559       .......... .......... ..L....... .........S .....GRD.. .........T .......... ....
038-223402       .......... .......... ..L....... .........S .....GRD.. .........T .......... ....
038-223402       .......... .......... ..L-...... .........S .....GRD.. .........T .......... ....
038-226205       .......... .......... ..L....... .........S .....GRD.. .........T .......... ....
```

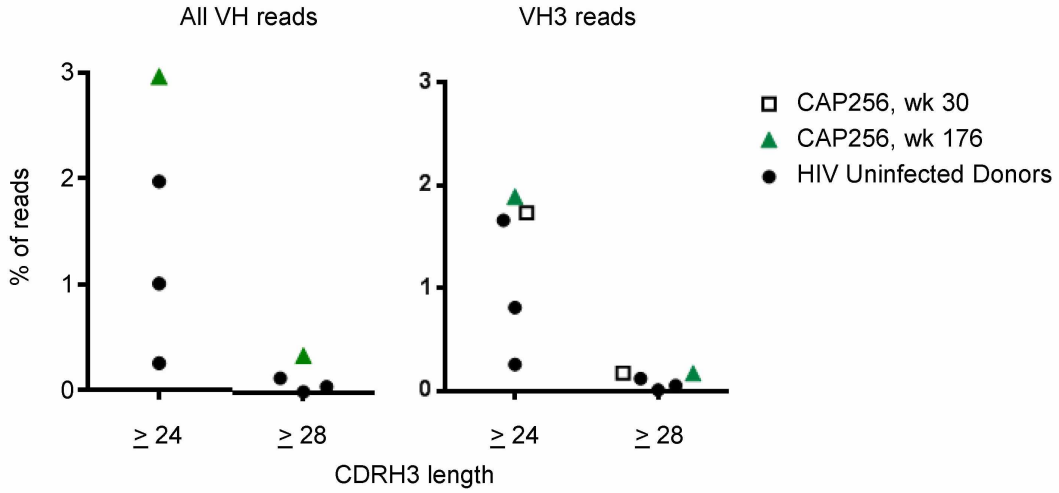
b



c

Antibody	Hep2 staining
CAP256-VRC26-UCA	-
CAP256-VRC26.01	-
CAP256-VRC26.02	-
CAP256-VRC26.03	-
CAP256-VRC26.04	-
CAP256-VRC26.05	-
CAP256-VRC26.06	-
CAP256-VRC26.07	-
CAP256-VRC26.08	-
CAP256-VRC26.09	-
CAP256-VRC26.10	-
CAP256-VRC26.11	-
CAP256-VRC26.12	-
VRC01	-
4E10	+

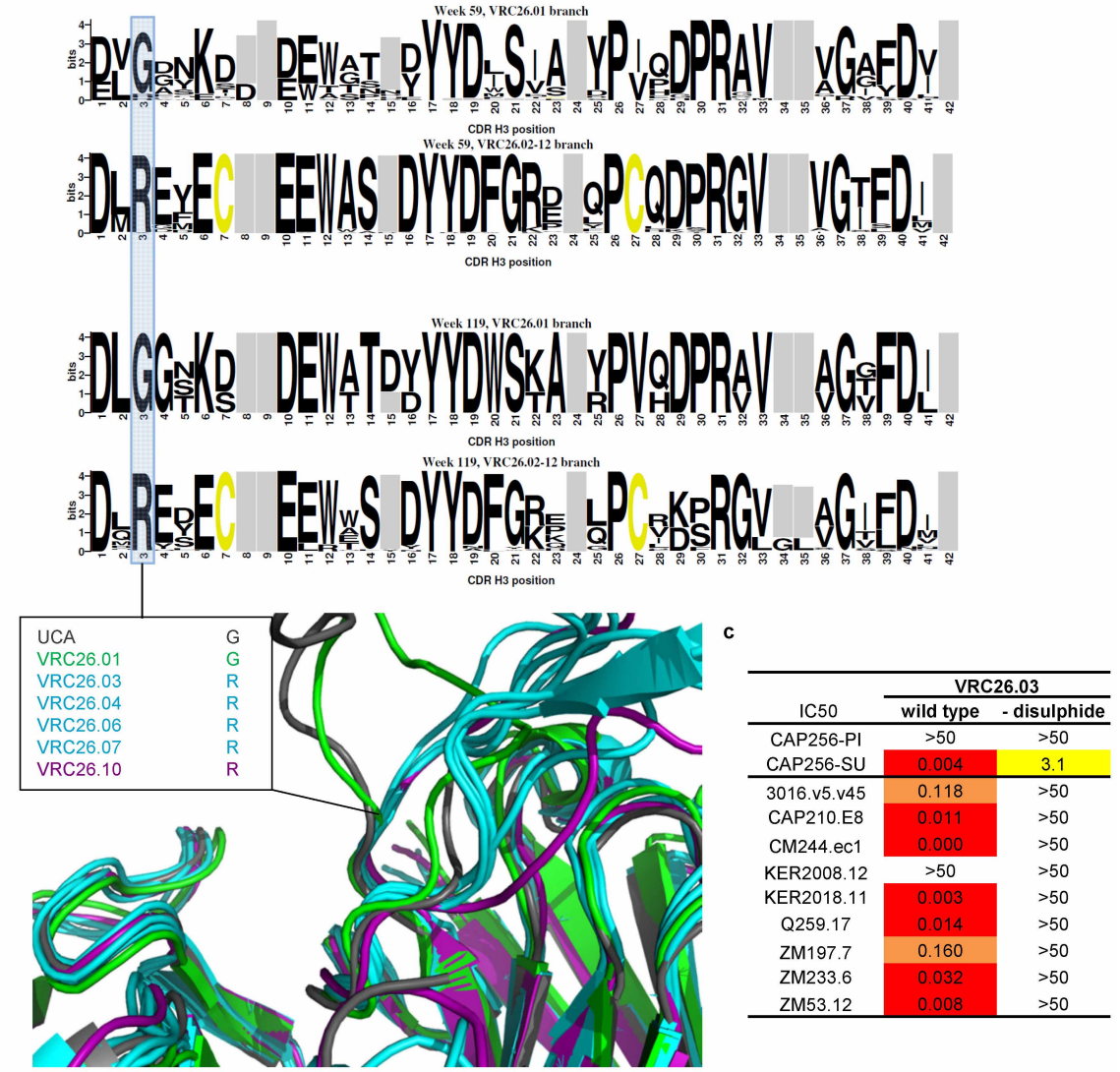
d



Extended Data Figure 6 | Origins of long CDR H3s in donor CAP256. **a**, Week 38 sequences from 454 that support the calculation of the UCA. Unique amino acid sequences with 2–5 residue changes in the CDR H3 are compared to the calculated UCA sequence. Each contained fewer than 3 combined nucleotide mutations in VH and JH. Parentheses, number of corresponding reads in the raw 454 data. **b**, **c**, Lack of autoreactivity. **b**, ELISA for binding to cardiolipin. 4E10 was strongly positive, CAP256-VRC26.03 was weakly positive, and the other 11 CAP256-VRC26 monoclonal antibodies and the UCA were negative along with control antibody VRC01. **c**, Staining on Hep2 cells was assessed at 50 and 25 µg ml^{-1}. Only the positive control, mAb 4E10, showed positive staining. **d**, Distribution of CDRH3 lengths among 454 sequencing reads of B cell transcripts. The percentage of high-quality NGS reads that have CDR H3 ≥ 24 or ≥ 28 are shown for three HIV-1 uninfected donors (solid circles on both right and left plots) and for donor CAP256 (week 176) amplified with all-VH primers donor, and CAP256 (week 30) amplified with VH3 primers. High-quality reads are defined as successful V and J assignments and a continuous open reading frame. CDRH3 lengths use the IMGT definitions.

©2014 Macmillan Publishers Limited. All rights reserved

a



b

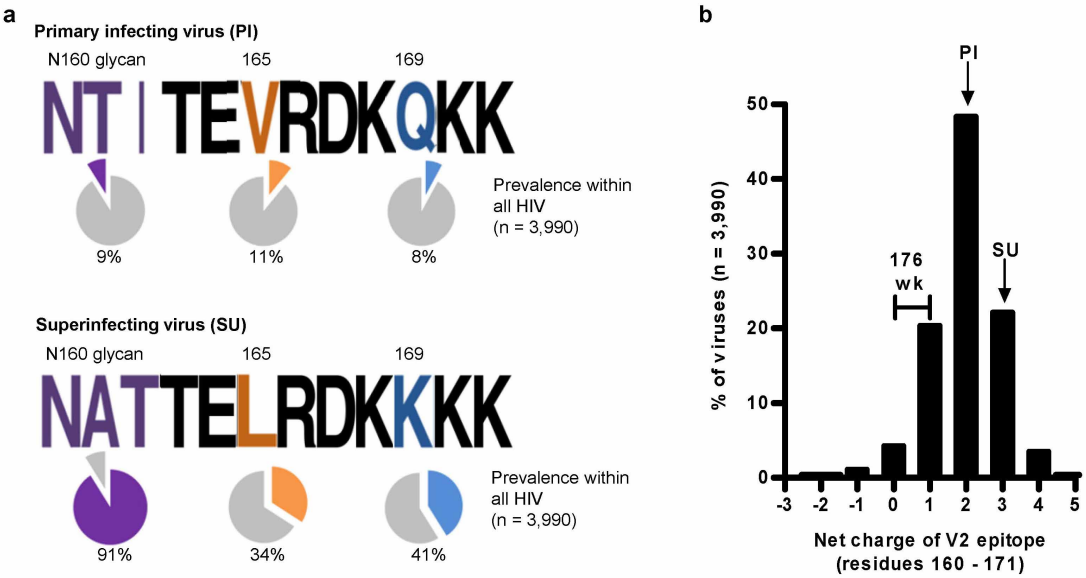
```
VRC26.01          CAKDVGDYKSDEWGTEYYDISISYPIQDPRAMVGAFDLW
VRC26.03          CAKDLREDECEEWWSDYYDFGKQLPCRKSRGVAGIFDGW
VRC26.03_mutant   CAKDLREDESEEWWSDYYDFGKQLPIRKSRGVAGIFDGW
```

c

IC50	VRC26.03 wild type	VRC26.03 - disulphide
CAP256-PI	>50	>50
CAP256-SU	0.004	3.1
3016.v5.v45	0.118	>50
CAP210.E8	0.011	>50
CM244.ec1	0.000	>50
KER2008.12	>50	>50
KER2018.11	0.003	>50
Q259.17	0.014	>50
ZM197.7	0.160	>50
ZM233.6	0.032	>50
ZM53.12	0.008	>50

Extended Data Figure 7 | Loss of flexibility at the base of the CDR H3. **a**, Top shows logograms of CDR H3 sequences extracted from the heavy chain phylogenetic tree from weeks 59 and 119. The height of each letter is proportional its frequency in the population. Sequences that lack a disulphide bond contain a highly conserved glycine at the third position of the CDR H3 (residue 97, Kabat definition). The appearance of the two cysteines that form the disulphide bond coincides with a glycine to arginine mutation at this site. Bottom shows overlay and close-up of crystal structures from Supplementary Fig. 6A. Loss of the glycine limits flexibility at the base of the CDR H3 and is shown in the crystal structures to be the initial site of divergence in the CDR H3 loops between the antibodies without the disulphide bond (UCA and CAP256-VRC26.01) and those with it (CAP256-VRC26.03, .04, .06, .07, .10). This mutation may contribute to the conserved trajectory of the CDR H3 protrusion towards the heavy chain that is seen in the more mature antibody structures. **b**, CDRH3 and flanking sequences for VRC26.01, VRC26.03, and a mutant VRC26.03 in which the conserved cysteines are changed to the corresponding amino acids found in VRC26.01. **c**, Neutralization activity of VRC26.03 and the mutant shown in panel **b**. The mutant shows reduced activity against CAP256 SU and complete loss of heterologous activity.

©2014 Macmillan Publishers Limited. All rights reserved



c Infecting viruses and effect of polymorphisms in V2 epitope

Env clone	Residues 160 - 171	Neutralization IC_{50} titers (μg ml^{-1})											
PI	NTITEVRDKQKK	>50	>50	>50	>50	>50	0.03	>50	>50	>50	>50	>50	>50
SU	NATTELRDKKKK	0.04	0.008	0.003	0.005	0.009	0.06	0.008	0.004	0.003	0.01	0.03	0.01
SU T162I	NAITELRDKKKK	0.02	0.05	0.002	0.003	1.7	0.04	0.01	0.005	0.004	0.4	0.1	0.1
SU L165V	NATTEVRDKKKK	0.05	0.01	0.003	0.004	0.007	0.05	0.04	0.006	0.008	0.02	0.04	0.05
SU K169Q	NATTELRDKQKK	>50	0.05	0.03	0.06	0.1	0.8	1.1	0.04	0.02	0.10	0.09	>50
		01	02	03	04	05	06	07	08	09	10	11	12

d Validation of escape mutations

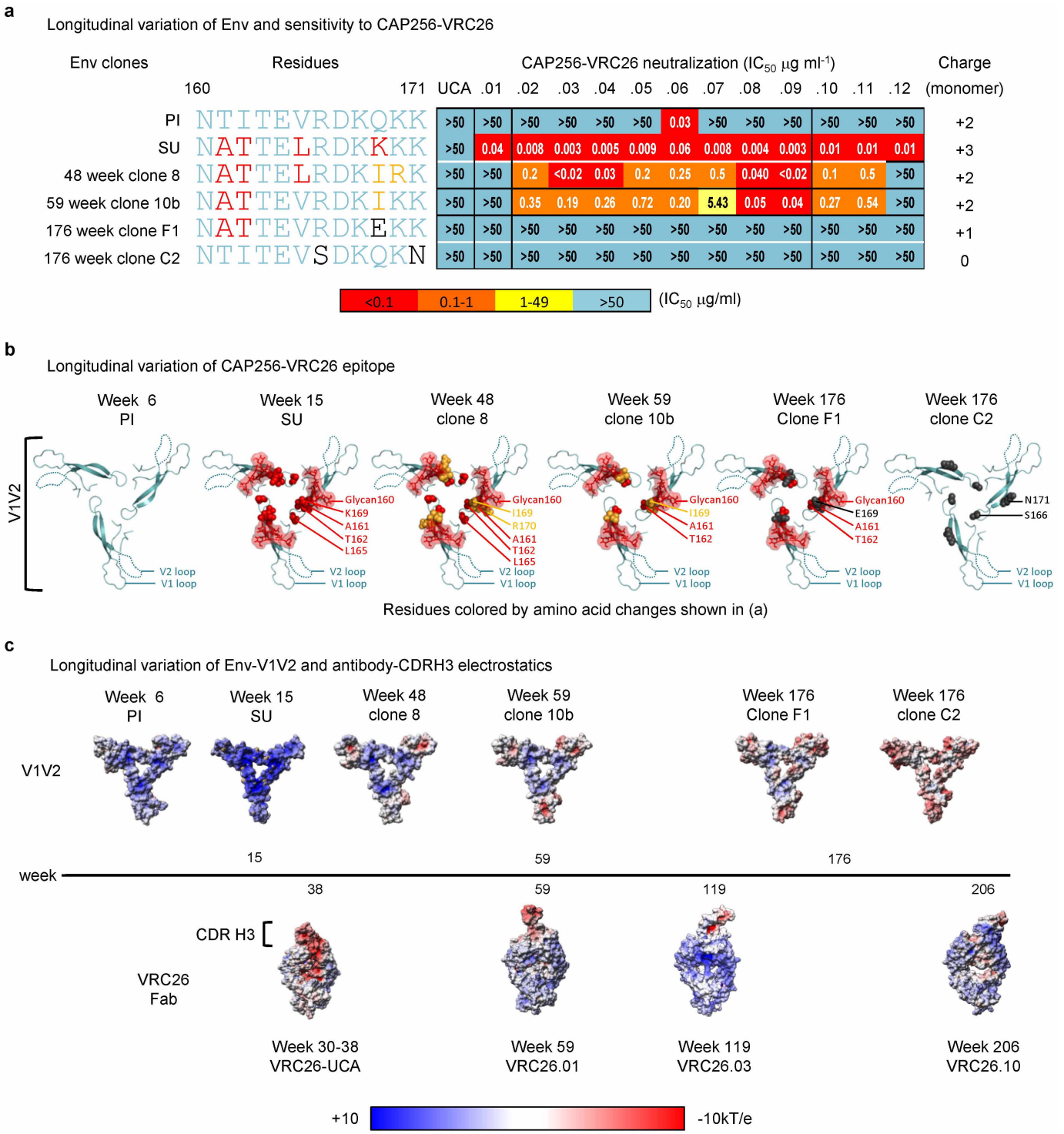
Env clone	Residues 160 - 171	Neutralization IC_{50} titers (μg ml^{-1})											Mutations first detected
SU K169I	NATTELRDKIKK	>50	0.1	0.02	0.05	0.20	0.05	1.4	0.04	0.02	0.08	0.1	>50	34 weeks
SU K171N	NATTELRDKKKN	0.1	0.03	0.004	0.01	0.03	0.16	0.02	0.005	0.004	0.03	0.02	>50	94 weeks
SU R166K	NATTELKDKKKK	>50	>50	4.8	16	>50	>50	>50	0.1	0.2	>50	>50	>50	
SU R166S	NATTELSDKKKK	>50	>50	>50	>50	>50	>50	>50	>50	>50	>50	>50	>50	176 weeks
SU K169E	NATTELRDKEKK	>50	>50	>50	>50	>50	>50	>50	>50	>50	>50	>50	>50	
		01	02	03	04	05	06	07	08	09	10	11	12	

e Reversion of I169 escape mutation in a 34 week clone

34 wk clones	Residues 160 - 171	Neutralization IC_{50} titers (μg ml^{-1})											
34 wk wt	NATTELRDKIKK	>50	0.05	0.02	0.7	0.1	0.2	1	0.05	0.03	0.08	0.04	>50
34 wk I169K	NATTELRDKKKK	0.05	<0.02	<0.02	<0.02	<0.02	<0.02	<0.02	<0.02	<0.02	<0.02	<0.02	<0.02
		CAP256-VRC26.01	CAP256-VRC26.02	CAP256-VRC26.03	CAP256-VRC26.04	CAP256-VRC26.05	CAP256-VRC26.06	CAP256-VRC26.07	CAP256-VRC26.08	CAP256-VRC26.09	CAP256-VRC26.10	CAP256-VRC26.11	CAP256-VRC26.12

Extended Data Figure 8 | Viral polymorphisms and escape mutations. **a**, Frequency of CAP256 PI and SU polymorphisms at positions 160–162 (glycosylation sequon), 165 and 169. Coloured slices on pie charts and percentages indicate prevalence of these polymorphisms within global circulating viruses in the Los Alamos Sequence Database ($n = 3,990$). **b**, Distribution of net charge of the V2 epitope, defined as residues 160–171, within global circulating viruses ($n = 3,990$). The charge of the PI, SU and 176 week clones are indicated. **c**, CAP256-VRC26 monoclonal antibody neutralization of the SU and PI viruses, and of the SU virus mutated to contain PI polymorphisms 162I, 165V or 169Q. **d**, CAP256-VRC26 monoclonal antibody neutralization of the SU virus mutated to contain known CAP256 escape mutations in the V2 epitope. **e**. CAP256-VRC26 monoclonal antibody neutralization of 34 week clone (designated wild type, wt) with an SU-like V1V2, compared to the I169K back mutant. **c–e,** The V2 epitope sequence, with mutated residues in red is shown on the left, IC_{50} values in the middle, and the time point when mutations were first detected in Env sequences on the right (weeks post-infection).

©2014 Macmillan Publishers Limited. All rights reserved



Extended Data Figure 9 | Longitudinal changes in CAP256 V1V2. **a**, Variation in the V1V2 sequence of six Env clones. Amino acid mutations from residues 160–171 are highlighted and corresponding changes in neutralization for the six Env clones by CAP256-VRC26.01-.12 and the UCA are shown. The charge of the displayed sequences that make up the central region of the trimer are shown on the right. **b**, Residue changes highlighted in **a** were mapped onto the V1V2 domain in the crystal structure of the HIV-1 BG505.664 SOSIP Env trimer. The structure is viewed looking towards the viral membrane along the trimer axis. Mutations are coloured as in panel **a** and represented as spheres (amino acids) or stick and surface (glycan). **c**, Electrostatic surface representations of the full V1V2 region for each Env clone(top row), Fabs (bottom row). Timeline of infection is shown in the middle. V1V2 sequences were modelled with SWISS-MODEL using the BG505.664 SOSIP as a template. Escape mutations R166S, K171N and K169E resulted in a net charge change in the V2 epitope from +3 (SU) to a rare 0. Antibody CDR H3s became less negatively charged over time, suggesting co-evolution of the viral epitope and the antibody paratope.

©2014 Macmillan Publishers Limited. All rights reserved

Extended Data Table 1 | Genetic characteristics of CAP256-VRC26 antibodies and V1V2-directed broadly neutralizing antibodies from other donors

a

Donor	Antibody	VH gene	VL gene	% Divergence, Nucleotide			
				from VH	from VL	from UCA-H	from UCA-H CDRH3
CAP256	*VRC26-I1*	IGHV3-30*18	IGLV1-51*02	2%	4%	3%	8%
	VRC26-I2			6%	7%	7%	13%
	VRC26.01			8%	4%	11%	18%
	VRC26.02			9%	5%	13%	27%
	VRC26.03			9%	7%	13%	28%
	VRC26.04			9%	8%	13%	28%
	VRC26.05			10%	5%	13%	24%
	VRC26.06			11%	7%	16%	30%
	VRC26.07			12%	8%	14%	26%
	VRC26.08			12%	10%	17%	33%
	VRC26.09			14%	10%	19%	34%
	VRC26.10			12%	4%	15%	26%
	VRC26.11			12%	14%	18%	32%
	VRC26.12			15%	8%	18%	27%
IAVI24	PG9	IGHV3-33*05	IGLV2-14*01	12%	8%		
	PG16			15%	12%		
CH0219	CH01	IGHV3-20*01	IGKV3-20*01	16%	11%		
	CH02			15%	14%		
	CH03			14%	11%		
	CH04			14%	11%		
IAVI84	PGT141	IGHV1-8*01	IGKV2-28*01	16%	13%		
	PGT142			16%	13%		
	PGT143			16%	13%		
	PGT144			17%	12%		
	PGT145			17%	17%		

b

Donor	Antibody	VH gene	VL gene	CDRH3 Length	% Divergence, Amino Acid			
					from VH	from VL	from UCA-H	from UCA-H CDRH3
CAP256	*VRC26-I1*	IGHV3-30*18	IGLV1-51*02	35	6%	5%	8%	20%
	VRC26-I2			35	11%	7%	13%	29%
	VRC26.01			35	16%	7%	18%	40%
	VRC26.02			35	16%	7%	27%	46%
	VRC26.03			35	14%	9%	28%	46%
	VRC26.04			35	14%	8%	28%	46%
	VRC26.05			35	20%	8%	24%	40%
	VRC26.06			36	18%	9%	30%	44%
	VRC26.07			35	18%	9%	26%	46%
	VRC26.08			37	16%	9%	33%	51%
	VRC26.09			37	21%	7%	34%	54%
	VRC26.10			35	17%	5%	26%	46%
	VRC26.11			35	23%	23%	32%	49%
	VRC26.12			35	22%	14%	27%	43%
IAVI24	PG9	IGHV3-33*05	IGLV2-14*01	28	20%	15%		
	PG16			28	21%	21%		
CH0219	CH01	IGHV3-20*01	IGKV3-20*01	24	29%	17%		
	CH02			24	22%	23%		
	CH03			24	22%	19%		
	CH04			24	23%	17%		
IAVI84	PGT141	IGHV1-8*01	IGKV2-28*01	32	28%	21%		
	PGT142			32	30%	21%		
	PGT143			32	28%	22%		
	PGT144			32	31%	23%		
	PGT145			31	30%	26%		

a, **b**, Data are from the present study and from references 19–21. CAP256-VRC26.01-12 are derived from B cell culture, while CAP256.VRC26-I1 and –I2 (in italics) are inferred intermediates. CDRH3 lengths use Kabat notation. **a**, Nucleotides. **b**, Amino acids.

©2014 Macmillan Publishers Limited. All rights reserved

Paper 1: Supplementary Information

doi:10.1038/nature13036

Supplementary Notes

Acknowledgements

We thank the participants in the CAPRISA 002 study for their commitment in attending the CAPRISA clinics in eThekwini and Vulindlela, South Africa each month for several years. Thanks also to Drs. Koleka Mlisana, Dr. Sengeziwe Sibeko, Dr. Nivashnee Naicker and the CAPRISA 002 clinical team and Ms. Natasha Samsunder and Ms. Shannie Herall in the CAPRISA laboratory. At NICD, we thank Drs. Bronwen Lambson, Mashudu Madzivhandila and Thandeka Khoza for technical help with SGA, viral sequencing and antibody production, and Cathrine Mitchell for germline VH allele identification. We thank Ellen Turk and Chien-Li Lin for technical assistance with large neutralization panels, Jonathan Stuckey and Brenda Hartman for assistance with figures, and members of the Structural Biology Section, Structural Bioinformatics Core Section, and Humoral Immunology Core and Section, Vaccine Research Center, National Institute of Allergy and Infectious Diseases (NIAID), National Institutes for Health (NIH), for comments and suggestions on the manuscript. We thank J. Baalwa, D. Ellenberger, F. Gao, B. Hahn, K. Hong, J. Kim, F. McCutchan, D. Montefiori, L. Morris, J. Overbaugh, E. Sanders-Buell, G. Shaw, R. Swanstrom, M. Thomson, S. Tovanabutra, C. Williamson, and L. Zhang for contributing the HIV-1 Envelope plasmids used in our neutralization panel. Thanks to Glaudina Loots of the Department of Science and Technology for the support that enabled the long-term follow-up on participant CAP256. We thank the WCMC HIVRAD Core for providing trimers and J.H. Lee for insights and technical assistance with EM data processing and analysis. We thank Gregory Ippolito for help and

advice, Bryan Briney for use of an unpublished hVL3 primer, and Scott Hunicke-Smith and Jessica Wheeler for MiSeq sequencing.

Support for this work was provided by the Intramural Research Program of the Vaccine Research Center, National Institute of Allergy and Infectious Diseases and the National Human Genome Research Institute, National Institutes of Health (NIH) and by the Neutralizing Antibody Consortium of the International AIDS Vaccine Initiative. JNB, PLM and LM were recipients of Columbia University-Southern African Fogarty AIDS International Training and Research Program (AITRP) administered through the Fogarty International Center, National Institutes of Health (NIH grant# 5 D43 TW000231). JNB received a University of the Witwatersrand Post-graduate Merit Award as well as a bursary from the Poliomyelitis Research Foundation. CKW received bursary funding from the National Research Foundation and the Poliomyelitis Research Foundation. PLM is a Wellcome Trust Intermediate Fellow in Public Health and Tropical Medicine (Grant 089933/Z/09/Z). Use of sector 22 (Southeast Region Collaborative Access team) at the Advanced Photon Source was supported by the US Department of Energy, Basic Energy Sciences, Office of Science, under contract number W-31-109-Eng-38. Studies on the CAPRISA cohort were supported by NIAID, NIH, and U.S. Department of Health and Human Services (Grant U19 AI51794) and the South African Department of Science and Technology. The EM work was supported by HIVRAD P01 AI82362 (J.P.M., I.A.W., and A.B.W.), IAVI and Scripps CHAV-ID and conducted at the National Resource for Automated Molecular Microscopy at The Scripps Research Institute, which is supported by the U. S. NIH NIGMS Biomedical Technology Research Center program (GM103310). Funding for the heavy-light chain paired sequencing was

provided by fellowships to B.J.D. from the Hertz Foundation, the University of Texas Donald D. Harrington Foundation and the National Science Foundation, and by the University of Texas Cockrell Family Regents Chair in Engineering (G.G.).

NISC Comparative Sequencing Program

Jesse Becker[1], Betty Benjamin[1], Robert Blakesley[1], Gerry Bouffard[1], Shelise Brooks[1], Holly Coleman[1], Mila Dekhtyar[1], Michael Gregory[1], Xiaobin Guan[1], Jyoti Gupta[1], Joel Han[1], April Hargrove[1], Shi-ling Ho[1], Taccara Johnson[1], Richelle Legaspi[1], Sean Lovett[1], Quino Maduro[1], Cathy Masiello[1], Baishali Maskeri[1], Jenny McDowell[1], Casandra Montemayor[1], James Mullikin[1], Morgan Park[1], Nancy Riebow[1], Karen Schandler[1], Brian Schmidt[1], Christina Sison[1], Mal Stantripop[1], James Thomas[1], Pam Thomas[1], Meg Vemulapalli[1] & Alice Young[1]

[1]NISC Comparative Sequencing Program, NIH, Bethesda, Maryland 20892, USA.

Virus ID	Clade	VRC26.01	VRC26.03	VRC26.06	VRC26.08
0260.v5.c36	A	>50	>50	>50	>50
0330.v4.c3	A	>50	>50	>50	>50
0439.v5.c1	A	>50	>50	>50	>50
3365.v2.c20	A	>50	20.8	>50	0.100
3415.v1.c1	A	>50	>50	>50	>50
3718.v3.c11	A	>50	0.377	>50	0.105
398-F1_F6_20	A		>50	>50	>50
BB201.B42	A	>50	0.001	1.38	0.001
BB539.2B13	A	>50	35.7	>50	0.194
BI369.9A	A	1.01	0.051	28.6	0.008
BS208.B1	A	16.7	0.009	>50	0.003
KER2008.12	A	0.308	>50	>50	>50
KER2018.11	A	5.95	0.014	42.7	0.003
KNH1209.18	A	>50	>50	>50	>50
MB201.A1	A	>50	>50	>50	>50
MB539.2B7	A	>50	>50	>50	31.9
MI369.A5	A	>50	7.88	>50	0.039
MS208.A1	A	>50	19.0	>50	0.115
Q23.17	A	>50	0.867	>50	0.010
Q259.17	A	>50	0.002	>50	0.001
Q769.d22	A	>50	>50	>50	>50
Q769.h5	A	>50	>50		
Q842.d12	A	>50	>50	>50	>50
QH209.14M.A2	A	>50	>50	>50	>50
RW020.2	A	>50	>50	>50	>50
UG037.8	A	>50	>50	>50	>50
3301.V1.C24	AC	2.78	0.047	2.92	0.013
3589.V1.C4	AC	>50	>50	>50	>50
6540.v4.c1	AC	>50	0.892	>50	0.077
6545.V4.C1	AC	>50	6.14	>50	0.026
0815.V3.C3	ACD	>50	>50	>50	>50
6095.V1.C10	ACD	2.32	0.434	>50	0.0007
3468.V1.C12	AD	>50	>50	>50	>50
Q168.a2	AD	>50	>50	>50	0.148
Q461.e2	AD	>50	>50	>50	0.502
620345.c1	AE	42.9	0.394	>50	0.001
BJOX009000.02.4	AE	>50	>50	>50	>50
BJOX010000.06.2	AE	>50	>50	>50	>50
BJOX025000.01.1	AE	>50	>50	>50	>50
BJOX028000.10.3	AE		>50	>50	>50
C1080.c3	AE	>50	0.006	>50	0.023
C2101.c1	AE	>50	>50	>50	>50
C3347.c11	AE		>50	>50	>50
C4118.09	AE	3.64	0.010	>50	0.002
CM244.ec1	AE		0.0007	6.90	0.002
CNE3	AE	>50	>50	>50	>50
CNE5	AE	2.21	0.004	>50	0.020
CNE55	AE	>50	0.019	>50	0.026
CNE56	AE	>50	>50	>50	>50
CNE59	AE	>50	>50	>50	>50

Virus ID	Clade	VRC26.01	VRC26.03	VRC26.06	VRC26.08
CNE8	AE		>50	>50	2.46
M02138	AE	>50	>50	>50	>50
R1166.c1	AE	>50	>50	>50	>50
R2184.c4	AE	>50	>50	>50	19.8
R3265.c6	AE		>50	>50	>50
TH023.6	AE		>50	>50	26.4
TH966.8	AE	>50	0.016	>50	0.036
TH976.17	AE	>50	2.95	>50	>50
235-47	AG	>50	>50	>50	0.265
242-14	AG	>50	0.062	>50	0.0003
263-8	AG	>50	>50	>50	0.031
269-12	AG	>50	>50	>50	>50
271-11	AG	>50	>50	>50	>50
928-28	AG	>50	3.60	>50	0.097
DJ263.8	AG	1.16	0.138	>50	0.031
T250-4	AG	0.018	0.0004	4.74	0.001
T251-18	AG	>50	>50	>50	>50
T253-11	AG	>50	>50	>50	49.5
T255-34	AG	>50	>50	>50	>50
T257-31	AG	11.0	0.004	>50	0.009
T266-60	AG	>50	0.943	>50	1.78
T278-50	AG	>50	>50	>50	>50
T280-5	AG	>50	>50	>50	>50
T33-7	AG	>50	>50	>50	>50
3988.25	B	>50	>50	>50	>50
5768.04	B	>50	>50	>50	>50
6101.10	B	>50	>50	>50	>50
6535.3	B	>50	>50	>50	>50
7165.18	B	>50	>50	>50	>50
45_01dG5	B		>50	0.877	>50
89.6.DG	B	>50	>50	>50	>50
AC10.29	B	>50	>50	0.030	>50
ADA.DG	B	>50	>50	12.5	>50
Bal.01	B	>50	>50	>50	>50
BaL.26	B	>50	>50	>50	>50
BG1168.01	B	>50	>50	>50	>50
BL01.DG	B	>50	>50	>50	>50
BR07.DG	B	>50	>50	>50	>50
BX08.16	B	>50	>50	12.6	>50
CAAN.A2	B	>50	>50	>50	>50
CNE10	B	>50	>50	>50	>50
CNE12	B	>50	>50	>50	>50
CNE14	B	>50	>50	>50	>50
CNE4	B	>50	>50	>50	>50
CNE57	B	>50	>50	>50	>50
HO86.8	B	>50	>50	>50	>50
HT593.1	B	>50	>50	>50	>50
HXB2.DG	B	>50	>50	>50	>50
JRCSF.JB	B	>50	>50	>50	>50
JRFL.JB	B	>50	>50	>50	>50

Supplementary Figure 1. Neutralization by CAP256-VRC26 antibodies of 194 Env-pseudoviruses.

Virus ID	Clade	VRC26.01	VRC26.03	VRC26.06	VRC26.08
MN.3	B	>50	>50	>50	>50
PVO.04	B	>50	>50	0.947	11.8
QH0515.01	B	>50	>50	>50	>50
QH0692.42	B	>50	>50	>50	>50
REJO.67	B	>50	>50	>50	>50
RHPA.7	B	>50	>50	>50	>50
SC422.8	B	>50	>50	0.439	>50
SF162.LS	B	>50	>50	>50	>50
SS1196.01	B	>50	>50	>50	>50
THRO.18	B	>50	>50	3.30	>50
TRJO.58	B	>50	>50	>50	>50
TRO.11	B	>50	>50	>50	>50
WITO.33	B	>50	>50	0.005	>50
YU2.DG	B	>50	>50	>50	>50
CH038.12	BC	9.82	0.020	1.44	0.009
CH070.1	BC	>50	0.553	>50	0.039
CH117.4	BC	15.8	0.002	0.741	0.003
CH181.12	BC	0.017	0.001	0.049	0.001
CNE15	BC	>50	>50	>50	>50
CNE19	BC			>50	11.1
CNE20	BC	>50	>50	>50	>50
CNE21	BC	>50	0.021	>50	0.001
CNE40	BC	>50	>50	>50	>50
CNE7	BC	10.2	0.829	>50	0.003
286.36	C	0.281	0.008	0.559	0.004
288.38	C	>50	>50	>50	>50
0013095-2.11	C	>50	>50	>50	0.021
001428-2.42	C	>50	0.010	>50	30.9
0077_V1.C16	C	10.8	0.032	>50	0.001
00836-2.5	C	>50	>50	>50	>50
0921.V2.C14	C	>50	0.048	>50	0.036
16055-2.3	C	0.016	0.004	0.504	0.004
16845-2.22	C	>50	>50	>50	>50
16936-2.21	C	>50	0.748	>50	0.250
25710-2.43	C	>50	0.017	>50	0.006
25711-2.4	C	>50	>50	>50	>50
25925-2.22	C	>50	0.021	>50	0.013
26191-2.48	C	13.3	0.004	>50	0.001
3168.V4.C10	C	>50	>50	>50	>50
3637.V5.C3	C	>50	>50	>50	>50
3873.V1.C24	C	0.677	0.017	>50	0.004
6322.V4.C1	C	16.5	0.007	>50	0.003
6471.V1.C16	C	>50	>50	>50	>50
6631.V3.C10	C	>50	>50	>50	>50
6644.V2.C33	C	>50	>50	>50	>50
6785.V5.C14	C	1.68	0.005	2.54	0.005
6838.V1.C35	C	>50	0.006	>50	0.001
96ZM651.02	C	>50	>50	>50	2.63
BR025.9	C	>50	>50	>50	>50
CAP210.E8	C	0.166	0.011	1.20	0.030

Virus ID	Clade	VRC26.01	VRC26.03	VRC26.06	VRC26.08
CAP244.D3	C	>50	>50	>50	46.0
CAP45.G3	C	31.8	10.7	>50	4.69
CNE30	C	>50	>50	>50	>50
CNE31	C	>50	>50	>50	>50
CNE53	C	>50	>50	>50	>50
CNE58	C	0.749	0.100	>50	0.006
DU123.06	C	>50	>50	>50	0.015
DU151.02	C	>50	0.361	>50	0.006
DU156.12	C	>50	0.090	>50	0.006
DU172.17	C	>50	>50	>50	>50
DU422.01	C	>50	0.224	>50	1.12
MW965.26	C	14.9	0.218	>50	0.003
SO18.18	C	0.046	0.004	0.046	0.002
TV1.29	C		>50	>50	>50
TZA125.17	C	>50	>50	>50	0.018
TZBD.02	C	>50	0.014	>50	0.036
ZA012.29	C	>50	>50	>50	>50
ZM106.9	C	>50	0.015	>50	0.010
ZM109.4	C	>50	>50	>50	>50
ZM135.10a	C	>50	>50	>50	>50
ZM176.66	C	>50	0.017	>50	0.029
ZM197.7	C	22.1	0.302	>50	0.002
ZM214.15	C	>50	0.100	>50	3.23
ZM215.8	C	>50	>50	>50	>50
ZM233.6	C	0.701	0.032	22.6	0.0003
ZM249.1	C	>50	0.004	>50	0.0009
ZM53.12	C	0.036	0.017	0.082	0.004
ZM55.28a	C	40.9	0.027	>50	0.005
3326.V4.C3	CD	0.029	0.011	0.226	0.007
3337.V2.C6	CD	>50	0.012	>50	0.044
3817.v2.c59	CD	>50	>50	>50	>50
191821.E6.1	D	>50	1.50	>50	0.003
231965.c1	D	>50	>50	>50	>50
247-23	D	>50	>50	>50	0.005
3016.v5.c45	D	16.4	0.450	>50	0.005
57128.vrc15	D	>50	>50	>50	>50
6405.v4.c34	D	>50	>50	>50	>50
A03349M1.vrc4a	D	>50	>50	>50	2.68
A07412M1.vrc12	D		33.7	>50	0.068
NKU3006.ec1	D	>50	>50	>50	>50
UG024.2	D	>50	>50	>50	0.843
P0402.c2.11	G		0.100	>50	0.006
P1981.C5.3	G	>50	0.045	>50	0.008
X1193.c1	G	>50	9.68	>50	0.343
X1254.c3	G	>50	>50	>50	>50
X1632.S2.B10	G	>50	0.034	>50	0.010
X2088.c9	G	>50	>50	>50	>50
% of viruses neutralized		18%	38%	12%	47%
median IC50 for neutralized viruses		2.55	0.032	1.20	0.013
geometric mean IC50 for neutralized viruses		1.74	0.065	1.06	0.029

Clade	Virus	Combined CAP256-VRC26 mAbs (IC50)	CAP256 plasma (ID50) wk 59	wk106	wk159	wk 220
	ZM53.12	0.002	979	14218	13474	15460
	ZM233.6	0.0003	238	4360	13476	5261
	CAP210.E8	0.002	7091	7830	13580	5250
	DU422.01	0.008	<45	346	1907	1968
	ZM197.7	0.008	<45	151	1062	1245
	DU156.12	0.016	<45	394	1363	1116
	CAP45.G3	4.7	287	7898	13402	1006
C	ZM214.15	0.33	<45	<45	920	538
	ZM109.4	26.5	<45	70	398	156
	ZM249.1	0.010	<45	<45	230	119
	CAP244.D3	>50	<45	<45	58	62
	DU172.17	>50	<45	<45	<45	<45
	ZM135.10a	>50	<45	68	69	<45
	Q842.d12	10.1	<45	47	658	602
A	Q23.17	9.5	<45	171	1107	448
	Q259.d2.17	0.008	<45	792	114	433
	Q168.a2	0.181	<45	70	2349	352
	Q461.e2	0.705	<45	<45	422	127
	Q769.d22	>50	<45	<45	<45	<45
	6535.3	>50	<45	214	788	284
	WITO.33	0.003	56	219	293	99
	TRO.11	>50	<45	<45	<45	69
	AC10.29	0.022	<45	64	48	66
	RHPA.7	>50	<45	<45	<45	49
	PVO.04	0.308	47	53	86	47
	CAAN.A2	>50	<45	<45	<45	<45
B	QH0692.42	>50	<45	<45	49	<45
	REJO.67	>50	<45	<45	<45	<45
	SC422.8	0.178	<45	<45	<45	<45
	THRO.18	4.250	<45	<45	<45	<45
	TRJO.58	>50	<45	<45	56	<45

Supplementary Figure 2. Neutralization of heterologous viruses by CAP256 plasma and mAbs. Neutralization of 31 viruses by CAP256-VRC26 antibodies and by plasma from CAP256 sampled at 4 timepoints. Plasma data are from ref. 25. Antibody values are shown as 50% inhibitory concentration (IC50) of a theoretical combination of all 12 antibodies (calculated as the lowest IC50 for each virus). Plasma is shown as 50% inhibitory dilution (ID50) with a starting dilution of 1:45.

a

Monoclonal antibodies

	PG16	PG9	PGT142	PGT145	10E8	4E10	2F5	m66.6	2G12	PGT121	PGT128	8ANC195	HJ16	CH103	VRC01	VRC02	NIH45-46	VRC-CH31	VRC-PG04	VRC-PG04b	VRC-PG20	12A12	3BNC117	8ANC131	b12	VRC03	VRC06	VRC06b
CAP256-VRC26.02	0.17	0.13	0.38	-0.07	-0.27	-0.17	-0.15	0.07	-0.03	-0.19	-0.30	-0.16	-0.28	-0.25	-0.23	-0.20	-0.28	-0.24	-0.27	-0.23	-0.14	-0.42	-0.38	-0.25	-0.29	0.05	0.01	0.05
CAP256-VRC26.03	0.35	0.35	0.26	-0.08	-0.22	-0.17	-0.22	0.00	-0.31	-0.20	-0.38	-0.43	-0.37	-0.30	-0.20	-0.32	-0.26	-0.53	-0.43	-0.38	0.00	-0.19	-0.33	-0.39	0.01	-0.07	0.00	-0.07
CAP256-VRC26.04	0.34	0.33	0.29	-0.10	-0.28	-0.07	-0.12	0.00	-0.31	-0.14	-0.28	-0.36	-0.37	-0.20	-0.09	-0.21	-0.17	-0.37	-0.31	-0.25	0.08	-0.21	-0.22	-0.25	-0.16	0.08	0.12	0.06
CAP256-VRC26.05	0.18	0.23	0.22	-0.05	-0.36	-0.24	-0.16	0.02	-0.12	-0.33	-0.44	-0.33	-0.20	-0.15	-0.05	0.02	-0.07	-0.20	-0.25	-0.25	0.00	-0.19	-0.18	-0.22	-0.38	0.10	0.12	0.12
CAP256-VRC26.06	0.16	0.08	0.50	0.25	0.02	0.04	0.07	0.31	0.32	0.15	-0.12	-0.01	-0.34	-0.17	-0.22	-0.12	-0.05	-0.17	-0.33	-0.35	-0.34	-0.22	-0.20	-0.20	0.07	-0.17	-0.10	-0.10
CAP256-VRC26.08	0.32	0.32	0.32	-0.12	-0.45	-0.30	-0.21	-0.11	-0.31	-0.24	-0.29	-0.36	-0.22	-0.24	-0.11	-0.14	-0.22	-0.30	-0.25	-0.17	0.16	-0.16	-0.22	-0.17	-0.20	-0.06	-0.04	-0.13
CAP256-VRC26.09	0.40	0.38	0.29	-0.10	-0.38	-0.25	-0.16	-0.10	-0.41	-0.21	-0.29	-0.40	-0.20	-0.17	-0.05	-0.14	-0.17	-0.27	-0.20	-0.13	0.21	-0.10	-0.15	-0.17	-0.18	-0.09	-0.05	-0.18
CAP256-VRC26.10	0.18	0.18	0.34	-0.12	-0.43	-0.14	-0.14	-0.01	-0.12	-0.14	-0.24	-0.26	-0.37	-0.22	-0.18	-0.16	-0.26	-0.27	-0.31	-0.26	-0.05	-0.34	-0.33	-0.20	-0.28	0.16	0.14	0.16
CAP256-VRC26.11	0.06	0.03	0.28	-0.17	-0.27	-0.14	-0.22	0.03	-0.06	-0.16	-0.27	-0.23	-0.31	-0.31	-0.33	-0.31	-0.37	-0.33	-0.35	-0.31	-0.23	-0.52	-0.49	-0.34	-0.18	-0.03	-0.06	-0.02

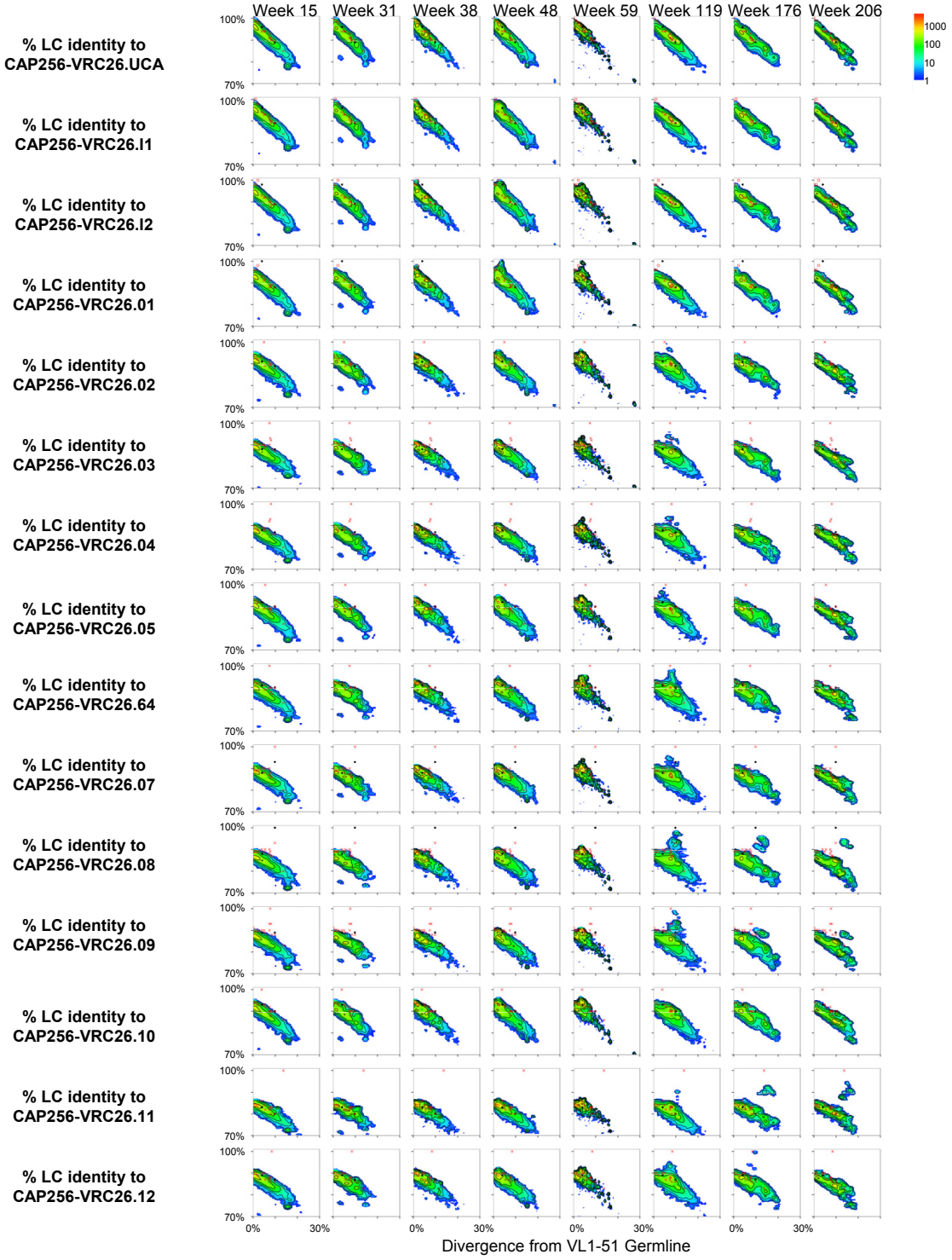
b

	10E8	12A12	2F5	2G12	3BNC117	4E10	8ANC131	b12	CH103	HJ16	m66.6	NIH45-46	PG16	PG9	PGT121	PGT128	PGT142	PGT145	VRC23	VRC-PG04	VRC01	VRC24	VRC-CH31	VRC-PG20
6535.3	0.17	0.5	4.9	2.57	0.26	0.46	0.36	0.87	4.67	>50	43.5	0.07	4.18	0.32	0	0.02	>50	>50	>50	1.001	1.88	0.01	>50	8.32
0260.v5.c36	7.94	0.32	>50	>50	0.2	3.17	1.18	>50	>50	>50	>50	0.4	2.1	1.65	0.04	0.06	>50	>50	6.97	0.58	0.53	>50	0.13	0.21
6405.v4.c34	0.39	1.12	7.51	12.1	0.17	3.92	43.6	>50	>50	>50	>50	0.73	>50	>50	0.02	6.86	>50	>50	37.9	2	2.53	>50	0.2	0.37
AC10.29	0.23	0.42	0.98	>50	6.05	0.41	>50	1.86	>50	>50	>50	0.36	0.01	0.06	0.03	0.01	0.01	0.006	>50	>50	1.19	0.88	46.1	>50
C1080.c3	0.1	0.05	0.06	>50	0.1	0.6	>50	>50	>50	>50	25.4	0.54	0	0	>50	0.12	0.04	0.001	32.4	1.857	1.07	>50	1.27	1.99
CAAN.A2	1.47	1.2	11.6	>50	0.67	8.49	1.72	>50	>50	11.8	>50	0.21	9.22	9.7	0.01	0.1	>50	5.53	12	1.883	1.17	0.29	>50	0.51
CAP210.E8	0.81	38.2	>50	>50	8.16	4	>50	>50	>50	>50	>50	>50	<0.023	0.13	>50	>50	0.15	>50	>50	>50	>50	>50	>50	>50
CAP244.D3	0.45	0.03	>50	>50	0.07	1.98	0.33	>50	>50	>50	>50	0.28	0.01	0.08	>50	>50	>50	12	>50	0.375	0.64	0.67	0.17	0.1
CAP45.G3	0.68	0.03	>50	>50	0.59	2.36	>50	0.11	>50	>50	>50	>50	0.001	0.003	2.08	>50	0.1	0.001	>50	>50	8.9	>50	>50	0.95
CNE3	1.51	0.11	6.79	>50	0.13	2.23	2.75	>50	>50	>50	24.9	1.99	0.12	0.07	>50	>50	0.02	0.252	>50	>50	3.18	>50	>50	0.11
DU156.12	0.03	0.03	>50	>50	0.04	<0.023	11.4	1.41	>50	>50	>50	0.03	0.003	0.04	0.01	0.02	0.004	0.001	>50	<0.023	0.09	9.28	3.18	0.02
DU172.17	0.05	0.04	>50	>50	0.29	<0.023	>50	0.55	>50	8.32	>50	>50	<0.023	0.23	0.1	0.04	>50	>50	>50	0.223	>50	>50	0.28	>50
DU422.01	0.78	>50	>50	>50	>50	1.65	>50	0.4	>50	>50	>50	>50	0.04	0.3	0.16	0.18	>50	>50	>50	>50	>50	>50	>50	>50
KER2008.12	24	0.27	6.98	6.8	0.25	1.28	>50	>50	>50	>50	>50	0.57	0.004	0.01	2.22	14.7	>50	8.33	3.78	0.301	0.58	>50	0.18	0.4
KER2018.11	3.79	0.53	2.01	>50	0.42	8.46	3.28	49.2	40	>50	23.8	0.83	0.001	0.004	>50	>50	0.000	0.003	>50	0.49	0.46	>50	0.51	0.23
MB201.A1	0.28	0.06	0.44	>50	0.46	2.21	27.4	>50	17.7	>50	22.1	0.17	0.01	0.06	0	0.02	0.46	2.49	1.68	0.061	0.17	0.28	0.04	0.07
MB539.2B7	15.1	0.22	2.49	>50	0.09	2.17	3.1	14	3.7	0.04	>50	0.4	0.02	0.06	>50	3.57	0.07	1.19	6.97	0.435	0.43	>50	0.26	0.25
PVO.04	3.08	0.35	>50	1.41	0.07	1.99	0.48	>50	>50	>50	>50	0.15	15	6.94	0.13	0.01	0.04	0.143	2.61	0.303	0.55	>50	0.19	2.23
Q168.a2	1.02	0.07	7.83	>50	0.05	18.7	0.3	>50	6.76	0.03	>50	0.14	0.02	0.08	>50	>50	0.49	0.86	5	0.057	0.15	>50	0.04	0.08
Q23.17	1.13	0.05	10.8	>50	0.02	0.13	0.27	>50	10.4	>50	>50	0.11	0	0.01	0	0.01	0	0.002	0.58	0.042	0.09	0.16	<0.023	0.04
Q259.17	4.77	0.02	16.1	>50	0.02	10.2	0.76	>50	10.6	>50	>50	0.05	0.03	0.05	>50	>50	3.95	45	>50	>50	0.06	>50	4.91	0.03
Q461.e2	1.72	0.16	13.4	>50	0.07	5.53	1.26	>50	>50	0.05	>50	0.21	4.62	2.53	>50	25.6	>50	16	7.93	0.334	0.38	>50	0.16	0.13
Q769.d22	0.89	0.01	0.61	>50	0.01	1.73	0.03	>50	1	>50	>50	0.01	0.07	0.01	>50	>50	>50	0.151	0.36	0.046	0.01	>50	0.04	0.01
Q842.d12	4.13	0.01	>50	>50	0	8.99	0.01	>50	1.46	>50	>50	0.02	0	0.02	0.02	0.03	0.02	0.067	0.11	0.011	0.01	>50	0.01	0.01
QH0692.42	0.69	1.04	2.22	4.99	0.28	1.6	2.63	0.79	25.2	7	>50	0.99	>50	>50	0.94	0.05	>50	>50	9.37	1.392	1.5	>50	0.94	45.3
REJO.67	0.16	0.08	0.3	>50	0.04	0.17	0.05	1.7	2.15	>50	>50	0.01	0.01	0.01	8.87	>50	0.21	0.0003	30	0.0003	0.05	0.13	0.05	0.02
RHPA.7	1.04	0.06	23.2	>50	0.02	13.3	5.1	0.13	8.53	0	>50	0.02	0.89	9.97	0.01	0.03	0.02	0.028	0.33	0.05	0.05	>50	0.13	22.1
RW020.2	1.93	0.03	7.55	>50	0.02	8.21	0.38	10.7	23.6	2.78	>50	0.14	0.16	0.11	0.002	0.01	>50	5.17	0.09	0.088	0.28	6.98	0.02	0.02
SC422.8	0.15	0.11	1.34	5.65	0.05	1.49	0.16	0.2	2.44	>50	17.1	0.03	2.19	0.54	0.1	2.41	1.45	0.027	1.46	0.073	0.12	>50	0.14	0.05
TH976.17	0.3	0.02	0.13	>50	0.03	0.21	11	>50	>50	0.06	28.3	0.12	>50	>50	>50	>50	>50	>50	1.23	0.021	0.13	>50	<0.023	0.03
THRO.18	0.21	1.6	>50	>50	2.8	1.77	19.7	0.96	>50	>50	>50	1.88	0.89	9.9	>50	>50	0	0.006	>50	>50	5.1	>50	37.9	17.6
TRJO.58	1.21	0.11	>50	>50	0.06	8.75	14.5	>50	>50	>50	>50	0.03	0.58	0.21	4.31	0.01	>50	>50	>50	0.088	0.07	>50	0.22	0.09
TRO.11	0.04	0.12	>50	0.36	0.03	0.6	9.97	>50	5.34	0.06	>50	1.04	4.06	41.5	0.01	0.02	1.86	0.029	17.8	0.2	0.3	0.55	0.04	15.5
UG037.8	0.13	0.04	0.2	>50	0.02	0.5	0.19	>50	1.76	>50	>50	0.06	0	0.02	0.07	0.02	1.63	2.33	0.78	0.045	0.09	>50	0.05	0.02
WITO.33	0.13	0.04	2.29	0.74	0.03	1.2	12.7	9.67	7.35	>50	18.3	0.04	0	0.01	0.79	>50	0	0	>50	0.631	0.11	>50	0.09	>50
ZM109.4	0.26	0.01	>50	>50	0.04	0.71	17.1	>50	21.2	8.15	>50	0.05	7.47	0.13	13.7	>50	>50	0.012	30.3	0	0.1	>50	0.03	0.24
ZM135.10a	0.1	0.48	>50	>50	0.07	0.03	24.5	>50	>50	>50	>50	0.28	>50	>50	1.5	30	>50	>50	12.2	>50	0.98	>50	0.36	>50
ZM197.7	0.07	0.53	35.7	>50	0.4	0.43	>50	>50	35.4	>50	>50	0.31	0.54	0.39	>50	>50	0.12	0.523	3.08	1.55	0.6	>50	0.61	0.18
ZM214.15	1.41	0.08	>50	>50	0.09	1.45	1.63	4.78	41.4	0.04	>50	0.13	>50	>50	0.68	1.44	>50	>50	11.5	0.701	0.7	>50	0.15	2.86
ZM249.1	0.72	0.04	>50	>50	0.04	2.75	10	2.73	7.23	>50	>50	0.04	0.04	0.04	>50	10.7	0.05	1.99	0.1	0.037	0.07	>50	0.04	0.03

Supplementary Figure 3. Correlations of neutralization fingerprints. a, Correlation of neutralization fingerprints between CAP256-VRC26 antibodies and a panel of HIV-1 broadly neutralizing antibodies**.** VRC26.01, .07, and .12 were excluded due to low breadth. **b**. The neutralization data used to generate correlations shown in panel A. Data from Extended Data Figure 2A was also used.



Supplementary Figure 4A. Longitudinal heavy chain identity-divergence plots for all 12 isolated antibodies, UCA, and inferred intermediates I1 and I2. CAP256-VRC26.01 and CAP256-VRC26.08 are shown as black dots; all other isolated antibodies are shown as red Xes; UCA, I1, and I2 are shown as open red squares.



Supplementary Figure 4B. Longitudinal light chain identity-divergence plots for all 12 isolated antibodies, UCA, and inferred intermediates I1 and I2. CAP256-VRC26.01 and CAP256-VRC26.08 are shown as black dots; all other isolated antibodies are shown as red Xes; UCA, I1, and I2 are shown as open red squares. Unlike the heavy chain plots, most of the light chain plots do not show distinct islands, likely because light chains do not have the added junctional diversity of a D gene and thus share greater overall sequence homology, even among unrelated sequences.

a

```
IGHV3-30*18     CAGGTGCAGCTGGTGGAGTCTGGGGGAGGCGTGGTCCAGCCTGGGAGGTCCCTGAGACTCTCCTGTGCAGCCTCTGGA
IGHD3-3*01      ~~~~~~~~~~~~~~~~~~~~~~~~~~~~~~~~~~~~~~~~~~~~~~~~~~~~~~~~~~~~~~~~~~~~~~~~~~~~
IGHJ3*02        ~~~~~~~~~~~~~~~~~~~~~~~~~~~~~~~~~~~~~~~~~~~~~~~~~~~~~~~~~~~~~~~~~~~~~~~~~~~~
UCA_heavy       ............................................................................

IGHV3-30*18     TTCACCTTCAGTAGCTATGGCATGCACTGGGTCCGCCAGGCTCCAGGCAAGGGGCTGGAGTGGGTGGCAGTTATATCA
IGHD3-3*01      ~~~~~~~~~~~~~~~~~~~~~~~~~~~~~~~~~~~~~~~~~~~~~~~~~~~~~~~~~~~~~~~~~~~~~~~~~~~~
IGHJ3*02        ~~~~~~~~~~~~~~~~~~~~~~~~~~~~~~~~~~~~~~~~~~~~~~~~~~~~~~~~~~~~~~~~~~~~~~~~~~~~
UCA_heavy       ............................................................................

IGHV3-30*18     TATGATGGAAGTAATAAATACTATGCAGACTCCGTGAAGGGCCGATTCACCATCTCCAGAGACAATTCCAAGAACACG
IGHD3-3*01      ~~~~~~~~~~~~~~~~~~~~~~~~~~~~~~~~~~~~~~~~~~~~~~~~~~~~~~~~~~~~~~~~~~~~~~~~~~~~
IGHJ3*02        ~~~~~~~~~~~~~~~~~~~~~~~~~~~~~~~~~~~~~~~~~~~~~~~~~~~~~~~~~~~~~~~~~~~~~~~~~~~~
UCA_heavy       ............................................................................

IGHV3-30*18     CTGTATCTGCAAATGAACAGCCTGAGAGCTGAGGACACGGCTGTGTATTACTGTGCGAAAGA~~~~~~~~~~~~~~~~
IGHD3-3*01      ~~~~~~~~~~~~~~~~~~~~~~~~~~~~~~~~~~~~~~~~~~~~~~~~~~~~~~~~~~~~~~~~~~~~~~~~~~~~
IGHJ3*02        ~~~~~~~~~~~~~~~~~~~~~~~~~~~~~~~~~~~~~~~~~~~~~~~~~~~~~~~~~~~~~~~~~~~~~~~~~~~~
UCA_heavy       ..........................................................TCTGGGAGAAAGCGAA

IGHV3-30*18     ~~~~~~~~~~~~~~~~~~~~~~~~~~~~~~~~~~~~~~~~~~~~~~~~~~~~~~~~~~~~~~~~~~~~~~~~~~~~
IGHD3-3*01      ~~~~~~~~~~~~~~~~~~~~~~~~G~~~~~~~~~~~~~~~~~~~~~~~~~~~~~~~~~~~~~~~~~~~~~~~~~~~
IGHJ3*02        ~~~~~~~~~~~~~~~~~~~~~~~~~~~~~~~~~~~~~~~~~~~~~~~~~~~~~~~~~~~~~~~~~~~~~~~~~~~~
UCA_heavy       AATGAAGAGTGGGCGACGGAT-.............C..T......-------CCCTGGCCAAGACCCACGGGGCGTGG

IGHV3-30*18     ~~~~~~~~~~~~~~~~~~~~~~~~~~~~~~~~~~~~~~~~~~~~~~~~~~~~~~~~~~~~~~~~~~~~~~~~~~~~
IGHD3-3*01      ~~~~~~~~~~~~~~~~~~~~~~~~~~~~~~~~~~~~~~~~~~~~~~~~~~~~~~~~~~~~~~~~~~~~~~~~~~~~
IGHJ3*02        ~~~~~TGATGCTTTTGATATCTGGGGCCAAGGGACAATGGTCACCGTCTCTTCA
UCA_heavy       TTGGA----.....................................................
```

b

```
IGLV1-51*02     CAGTCTGTGTTGACGCAGCCGCCCTCAGTGTCTGCGGCCCCAGGACAGAAGGTCACCATCTCCTGCTCTGGAAGCAGC
IGLJ1*01        ~~~~~~~~~~~~~~~~~~~~~~~~~~~~~~~~~~~~~~~~~~~~~~~~~~~~~~~~~~~~~~~~~~~~~~~~~~~~
UCA_light       ............................................................................

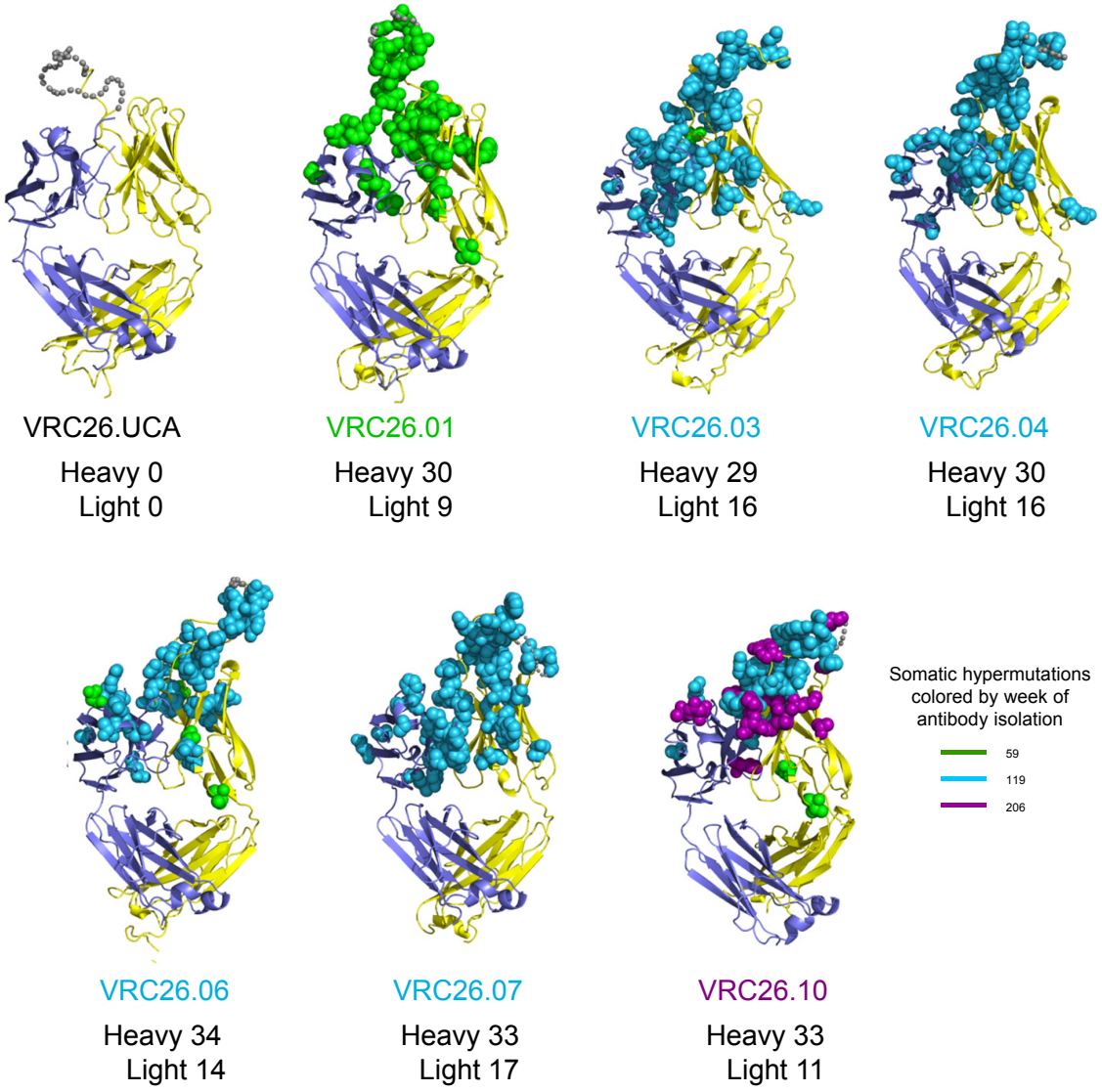
IGLV1-51*02     TCCAACATTGGGAATAATTATGTATCCTGGTACCAGCAGCTCCCAGGAACAGCCCCCAAACTCCTCATCTATGAAAAT
IGLJ1*01        ~~~~~~~~~~~~~~~~~~~~~~~~~~~~~~~~~~~~~~~~~~~~~~~~~~~~~~~~~~~~~~~~~~~~~~~~~~~~
UCA_light       ............................................................................

IGLV1-51*02     AATAAGCGACCCTCAGGGATTCCTGACCGATTCTCTGGCTCCAAGTCTGGCACGTCAGCCACCCTGGGCATCACCGGA
IGLJ1*01        ~~~~~~~~~~~~~~~~~~~~~~~~~~~~~~~~~~~~~~~~~~~~~~~~~~~~~~~~~~~~~~~~~~~~~~~~~~~~
UCA_light       ............................................................................

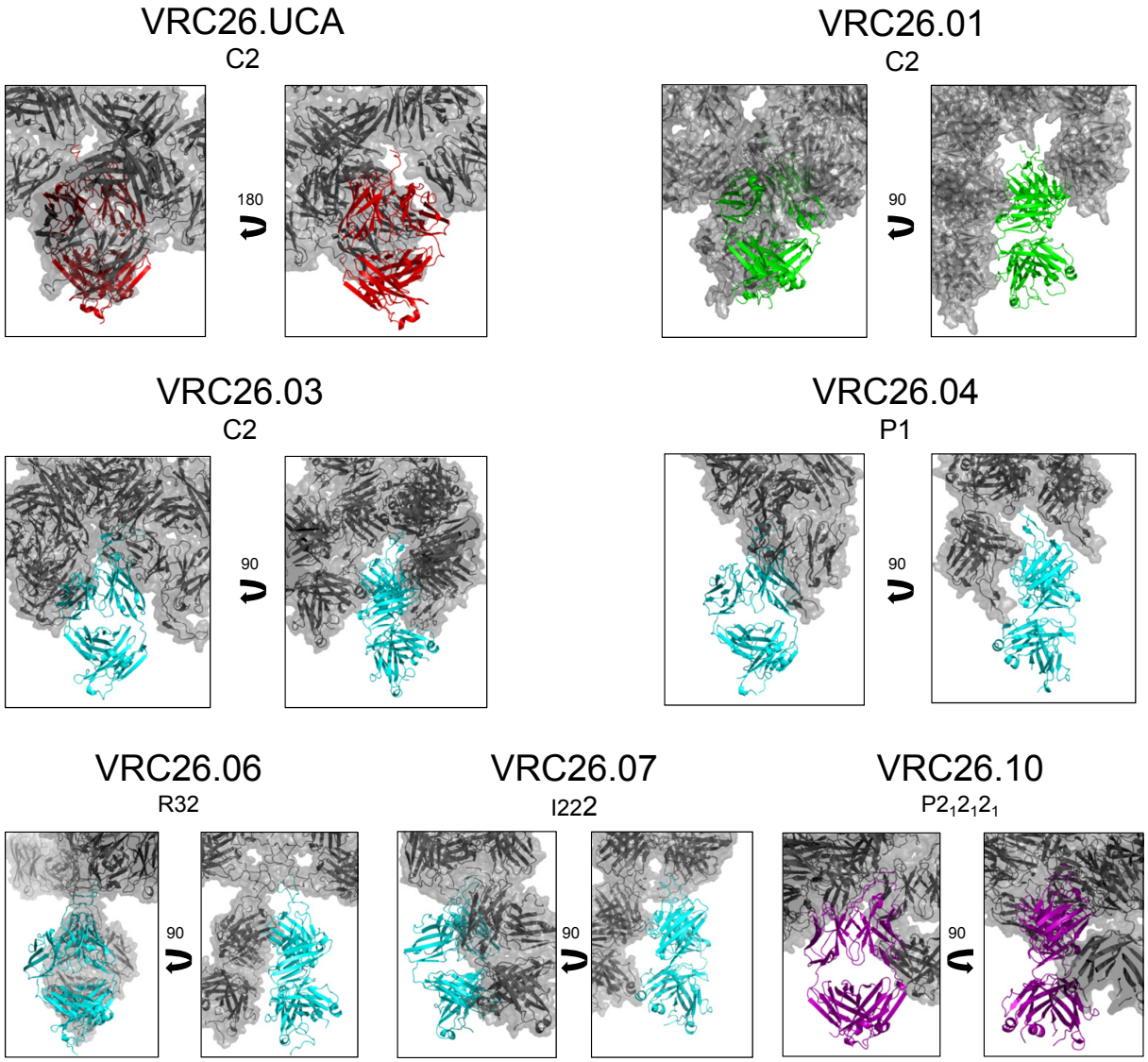
IGLV1-51*02     CTCCAGACTGGGGACGAGGCCGATTATTACTGCGGAACATGGGATAGCAGCCTGAGTGCTGG---~~~~~~~~~~~~~~~
IGLJ1*01        ~~~~~~~~~~~~~~~~~~~~~~~~~~~~~~~~~~~~~~~~~~~~~~~~~~~~~~~~~~~~~~~~TTATGTCTTCGGA
UCA_light       ..........................................................CGG---..........

IGLV1-51*02     ~~~~~~~~~~~~~~~~~~~~~~~~~
IGLJ1*01        ACTGGGACCAAGGTCACCGTCCTA
UCA_light       .........................
```

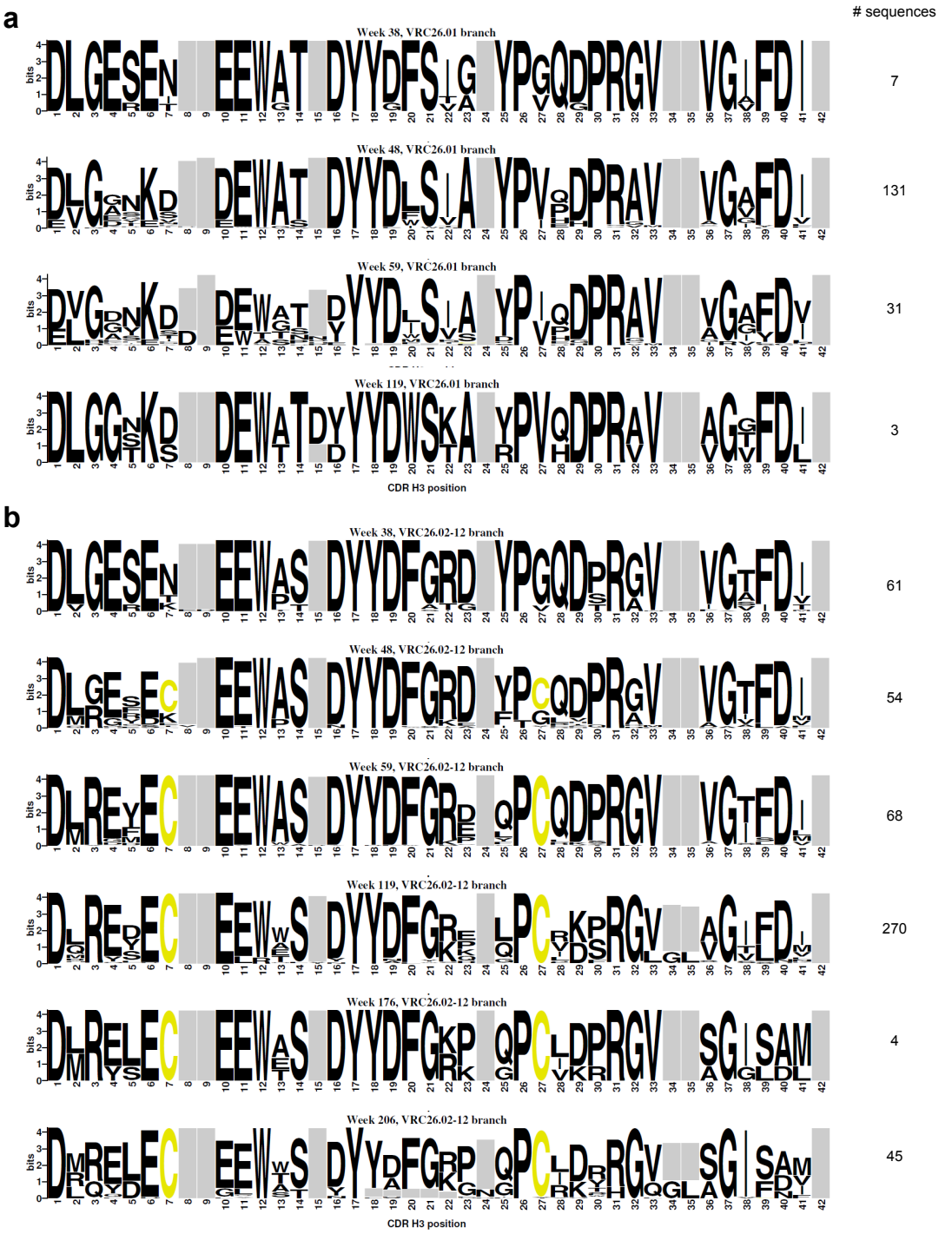
Supplementary Figure 5. VDJ recombination analysis for CAP256-VRC26 lineage. Nucleotide sequence and recombination analysis of the calculated unmutated common ancestor (UCA) of the CAP256-VRC26 lineage. **a**, heavy chain. **b**, light chain. Nucleotides that were excised from the germline genes by recombination are indicated by red italics. Predicted P-insertions are in bold font and N-insertions are underlined. The heavy chain UCA had a complete 35 amino acid CDR H3, formed from a single D gene and N-insertions of 34 and 31 nucleotides in length.



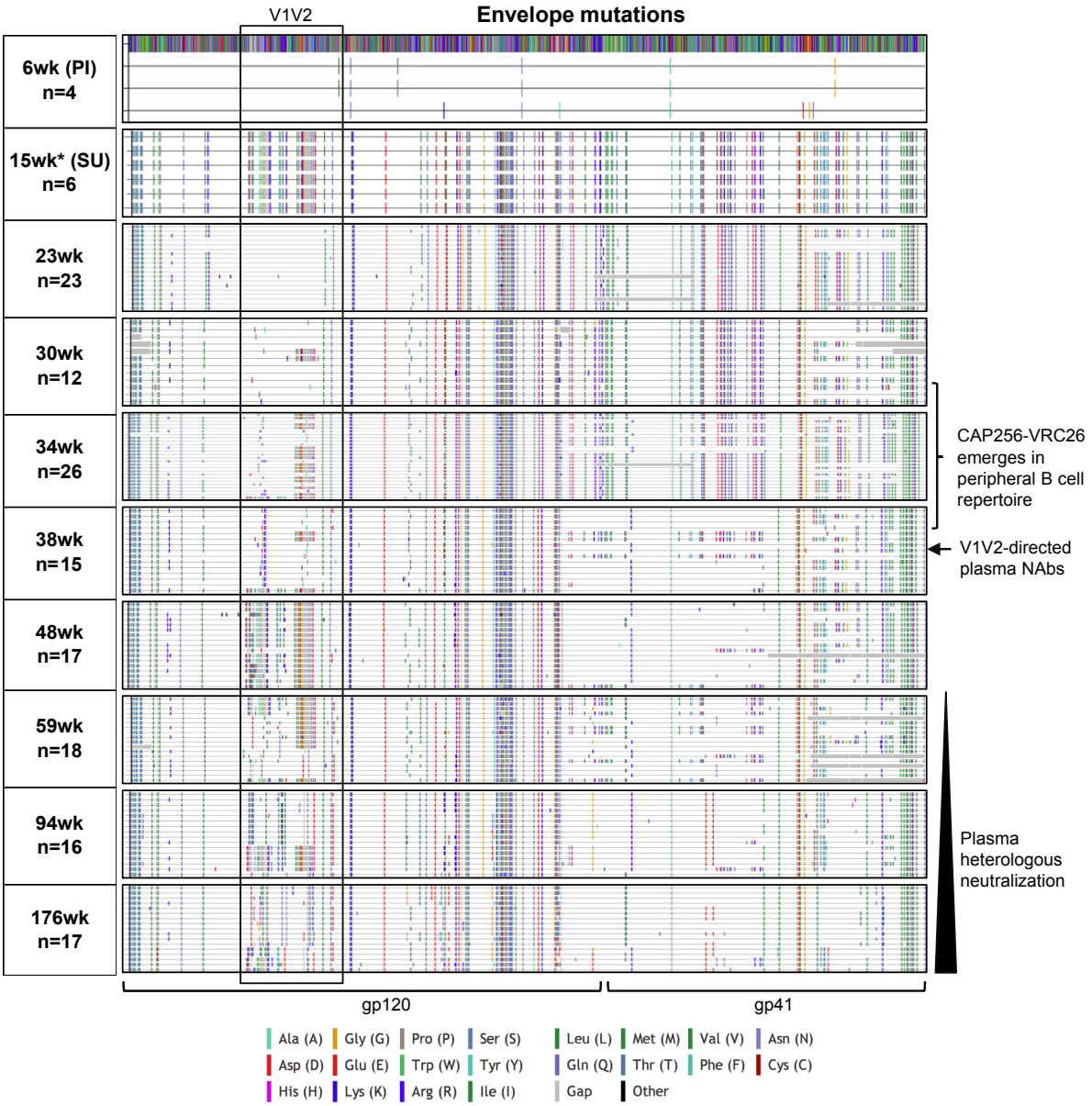
Supplementary Figure 6A. Full Fab structures of CAP256-VRC26 antibodies highlighting somatic hypermutation by week of appearance. The structures of antigen-binding fragments of CAP256-VRC26 antibodies are depicted in ribbon diagram representation with heavy chains in yellow and light chains in blue. Somatic hypermutations are shown in all atom representation, and colored according to the week post-infection from which they first appeared in isolated antibodies VRC26.01-12 (week 59, green; week 119, cyan; week 206, purple). Grey dashes indicate disordered regions of the CDR H3. The numbers of heavy and light chain mutations from the UCA are shown below the structures. See Fig. 4 for phylogenetic placement.



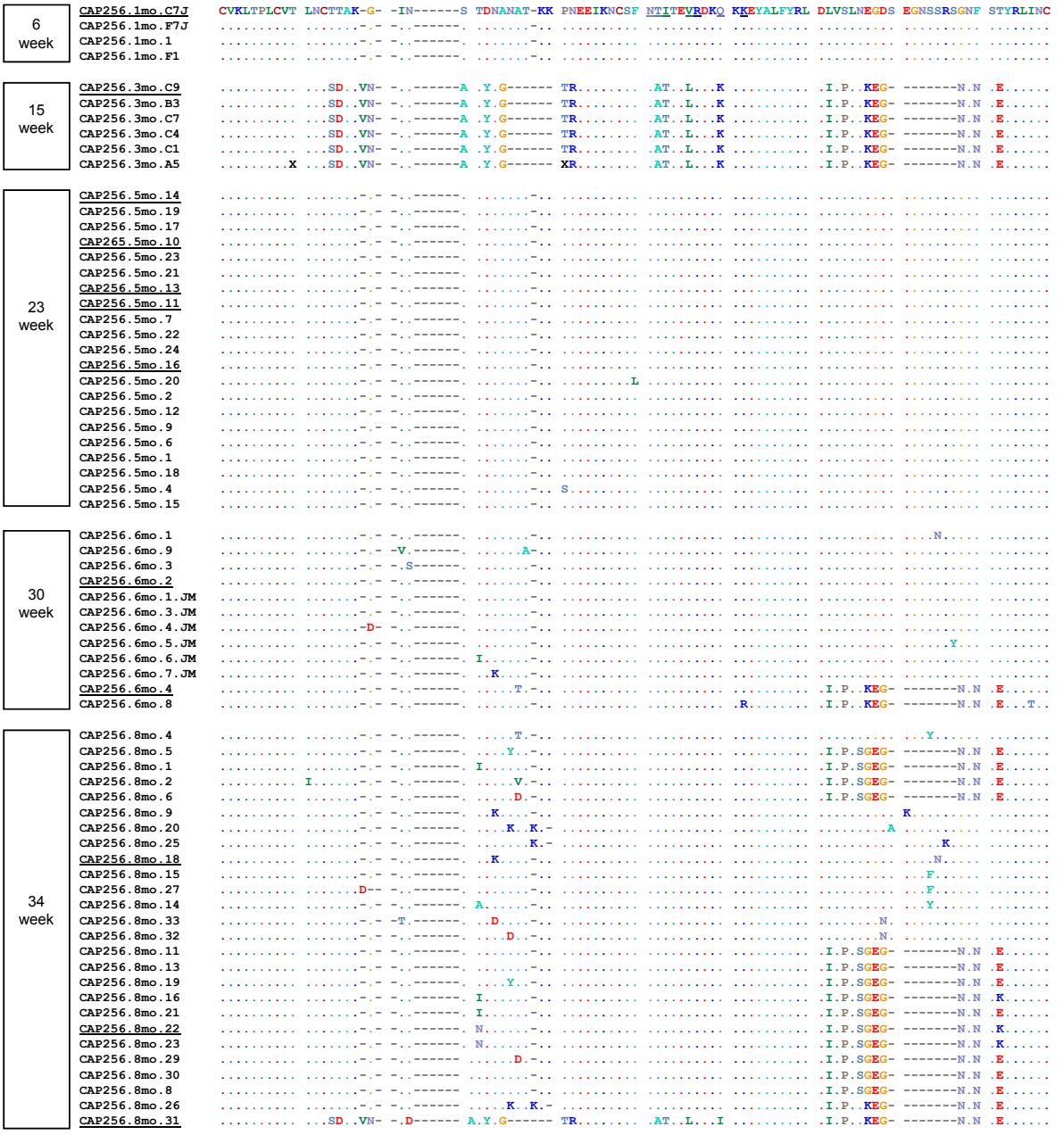
Supplementary Figure 6B. Crystal packing of CAP256-VRC26 structures. Each of the VRC26 Fab crystal structures are shown as ribbon diagrams. Neighboring molecules which pack close to the CDR H3 are displayed as grey ribbon diagrams with transparent surface representations. The space group for each structure is noted. Despite the variety of space groups and packing contacts, the five structures from later time points (cyan and purple) all display CDR H3 loops that protrude over the heavy chain.



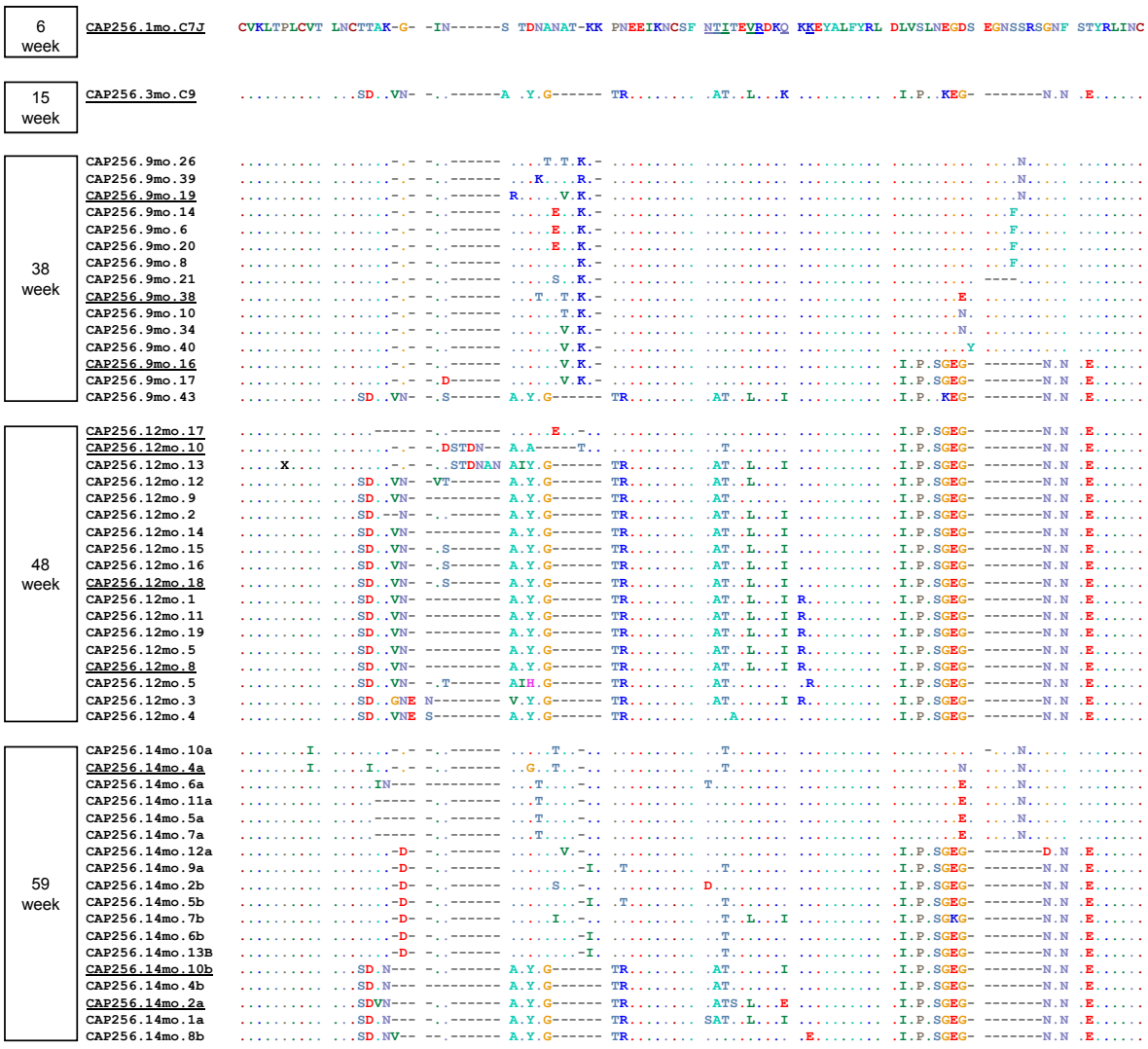
Supplementary Figure 7. Logograms of CDR H3 sequences extracted from the heavy chain phylogenetic tree in Fig. 3c, segregated by time point and subfamily. The letters in each stack represent the amino acids observed at that position, and the height of each letter is proportional to its frequency in the population. The cysteine residues that are part of a conserved disulfide bond are shown in yellow. Grey bars indicate gaps. **a,** CDR H3 sequences from the branch of the tree that includes CAP256-VRC26.01. **b,** CDR H3 sequences from the branch of the tree that includes all of the other isolated antibodies, CAP256-VRC26.02-12.



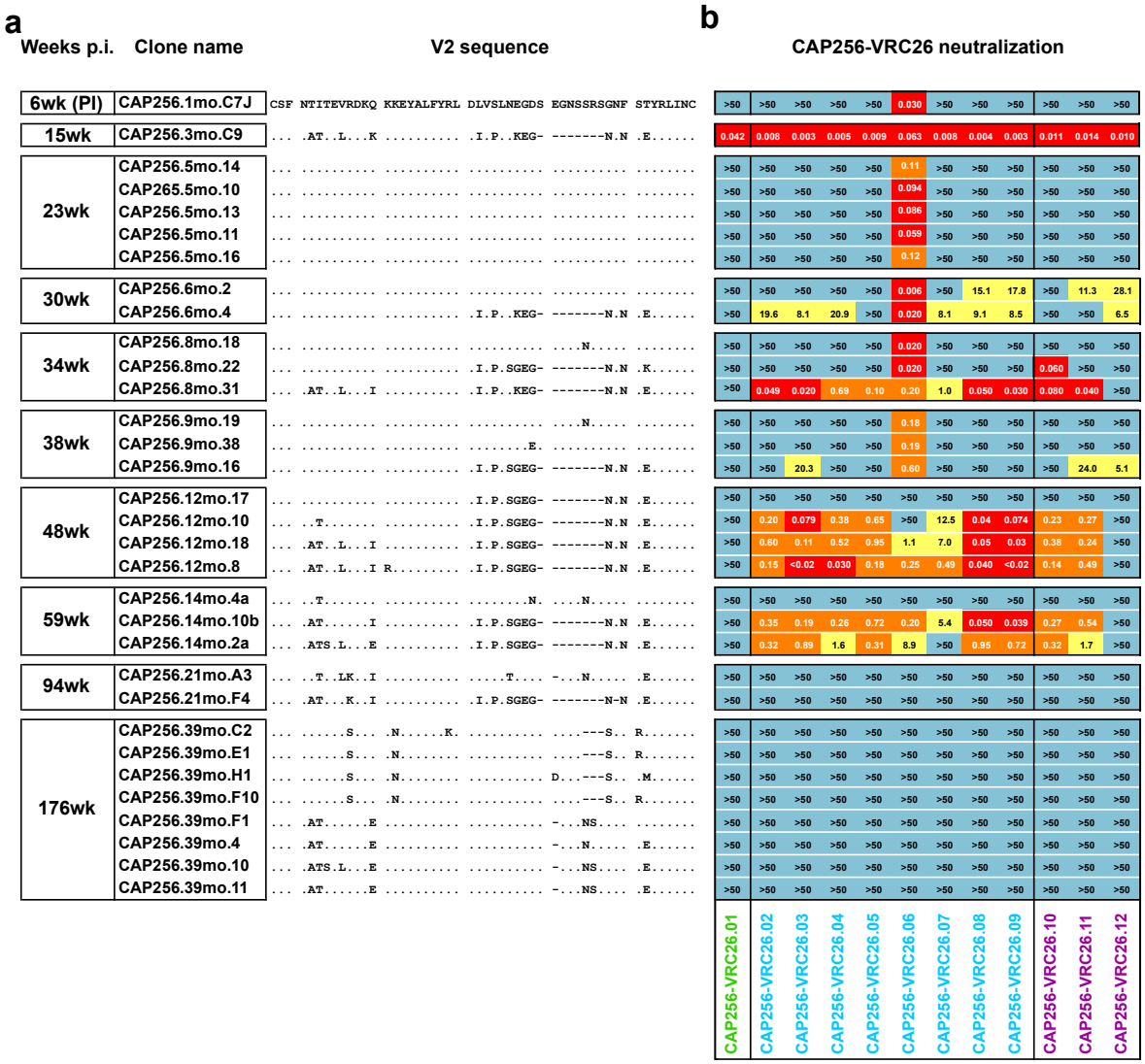
Supplementary Figure 8. HIV-1 envelope gp160 sequences amplified from CAP256 donor, shown in highlighter format. The primary infecting virus (PI) is designated as master (amino acid colors indicated in key) and the V1V2 region is boxed. The development of the CAP256-VRC26 antibody lineage, V1V2 plasma directed neutralizing antibodies, and plasma heterologous neutralization, are indicated on the right. Asterisk denotes sequences amplified with strain-specific primers matching the SU virus.



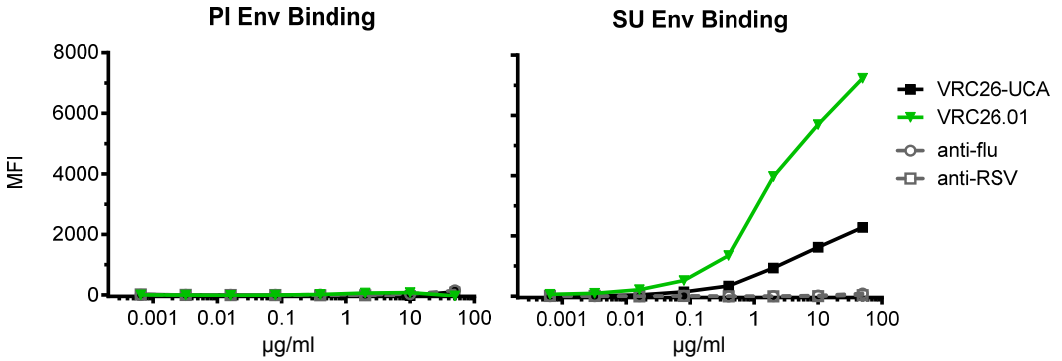
Supplementary Figure 9. HIV-1 envelope V1V2 sequences amplified from CAP256 donor, by week, with the primary infecting virus (PI) designated as master. Sequences cloned for neutralization assays are underlined. The location of key residues between 160 and 169 is highlighted.


6 week
15 week
38 week
48 week
59 week
CAP256.1mo.C7J
CAP256.3mo.C9
CAP256.9mo.26
CAP256.9mo.39
CAP256.9mo.19
CAP256.9mo.14
CAP256.9mo.6
CAP256.9mo.20
CAP256.9mo.8
CAP256.9mo.21
CAP256.9mo.38
CAP256.9mo.10
CAP256.9mo.34
CAP256.9mo.40
CAP256.9mo.16
CAP256.9mo.17
CAP256.9mo.43
CAP256.12mo.17
CAP256.12mo.10
CAP256.12mo.13
CAP256.12mo.12
CAP256.12mo.9
CAP256.12mo.2
CAP256.12mo.14
CAP256.12mo.15
CAP256.12mo.16
CAP256.12mo.18
CAP256.12mo.1
CAP256.12mo.11
CAP256.12mo.19
CAP256.12mo.5
CAP256.12mo.8
CAP256.12mo.5
CAP256.12mo.3
CAP256.12mo.4
CAP256.14mo.10a
CAP256.14mo.4a
CAP256.14mo.6a
CAP256.14mo.11a
CAP256.14mo.5a
CAP256.14mo.7a
CAP256.14mo.12a
CAP256.14mo.9a
CAP256.14mo.2b
CAP256.14mo.5b
CAP256.14mo.7b
CAP256.14mo.6b
CAP256.14mo.13B
CAP256.14mo.10b
CAP256.14mo.4b
CAP256.14mo.2a
CAP256.14mo.1a
CAP256.14mo.8b


6 week
15 week
94 week
176 week
CAP256.1mo.C7J
CAP256.3mo.C9
CAP256.21mo.D12
CAP256.21mo.A11b
CAP256.21mo.A3
CAP256.21mo.A6
CAP256.21mo.A1
CAP256.21mo.F1
CAP256.21mo.C4
CAP256.21mo.B2
CAP256.21mo.E12
CAP256.21mo.B10
CAP256.21mo.F4
CAP256.21mo.C1
CAP256.21mo.D6
CAP256.21mo.C2
CAP256.21mo.A1
CAP256.21mo.A11
CAP256.39mo.C2
CAP256.39mo.B1
CAP256.39mo.E1
CAP256.39mo.H1
CAP256.39mo.F10
CAP256.39mo.6
CAP256.39mo.8
CAP256.39mo.12
CAP256.39mo.13
CAP256.39mo.17
CAP256.39mo.18
CAP256.39mo.20
CAP256.39mo.F1
CAP256.39mo.4
CAP256.39mo.22
CAP256.39mo.10
CAP256.39mo.11



Supplementary Figure 10. Sequences of individual Env clones tested in Figure 5d. a, HIV-1 envelope clones by week, from 6 to 176 weeks post infection, with the amino acid sequence of the V1V2 region shown. **b,** Neutralization (IC_{50} values) by each of the 12 CAP256-VRC26 mAbs tested against Env clones. The CAP256 mAbs are colored to indicate the time point when the sequences were first detected by next generation sequencing (as in Fig 3).



Supplementary Figure 11. CAP256-VRC26 UCA does not bind to PI Env. CAP256-VRC26 UCA and the early antibody CAP256-VRC26.01 bind to cell-surface expressed Env from the superinfecting virus (SU) but not the primary infecting virus (PI). Assay performed as in Figure 6. Assay shown is representative of 3 independent experiments. MFI, median fluorescence intensity.

Supplementary Table 1. Statistics for heavy-light chain paired deep sequencing.

Time point	V-gene primers	PBMC recovered (viable/nonviable)	PBMC viability	Viable CD27+ B cells recovered*	Est. CD27+ B cells analyzed*	VRC-26 paired HC reads	250bp reads post-QF (R1+R2)
wk34	FR1**	12 m / 8 m	60%	30k	13 k	0	5,558,841
	LP**	*same as above*	*above*	*above*	13 k	0	6,174,263
wk48	FR1	2.9 m / 12.2 m	19%	9 k	8.1 k	17762	2,233,614
wk59	FR1	6.7 m / 5.9 m	53%	4.5 k	4 k	14	5,623,331
wk69	FR1	6.2 m / 5.0 m	55%	31 k	28 k	158	2,486,745
wk119	FR1	5.1 m / 0.5 m	89%	50 k	23 k	735	5,523,921
	LP	*same as above*	*above*	*above*	23 k	18	4,259,354

*CD27+ hemocytometer estimates
** Primers shown in Supplementary Table 5

Supplementary Table 2. Crystallographic data collection and refinement statistics
Values in parentheses are for highest-resolution shell

	VRC26.UCA	VRC26.01	VRC26.03	VRC26.04	VRC26.06	VRC26.07	VRC26.10
Data collection							
Space group	C2	C2	C2	P1	R32:H	I222	P212121
Cell constants							
a, b, c (Å)	85.5, 81.2, 69.2	104.4 71.2 82.9	99.2, 80.9, 87.6	68.0, 85.5, 103.3	253.5, 253.5, 70.1	70.1, 87.3, 224.4	43.4, 46.2, 232.5
a, b, g (°)	90.0, 124.0, 90.0	90.0, 93.3, 90	90.0, 116.7, 90.0	97.9, 107.7, 91.7	90.0, 90.0, 120.0	90.0, 90.0, 90.0	90,0, 90.0, 90.0
Wavelength (Å)	1.00	1.00	1.00	1.00	1.00	1.00	1.00
Resolution (Å)	50.0-2.90 (3.0-2.9)	50.0-1.90 (1.93-1.90)	50.0-2.70 (2.75-2.70)	50.0-3.15 (3.20-3.15)	50.0-3.0 (3.11-3.0)	40-2.6 (2.64-2.60)	50-1.91 (1.94-1.91)
R_{merge}	11 (37)	8 (54)	15(44)	14(39)	13(54)	13(51)	13(46)
I / sI	5.9 (1.8)	16.3 (2.1)	6.9(1.8)	5.8(1.8)	16.6(2.1)	12.5(1.7)	8.4(2.5)
Completeness (%)	85.7 (82.8)	100 (99.8)	88.4 (51.1)	95.9 (79.6)	98.8 (88.5)	93.9 (53.0)	65.2 (50)
Redundancy	2.3 (2.2)	3.7 (3.2)	2.9(1.7)	1.9(1.8)	10.0(5.0)	6.5(3.9)	4.1(3.9)
Molecules/ASU	1	1	1	4	1	1	1
Refinement							
Resolution (Å)	33.1-2.9 (3.0-2.9)	34.7-1.90 (1.96-1.90)	40.1-2.69 (2.79-2.69)	35.63-3.12 (3.2-3.12)	40.9-3.0 (3.1-3.0)	30.0-2.6 (2.71-2.62)	32.77-1.90 (1.97-1.91)
Unique reflections	7,500 (660)	48,060 (3,241)	13,071(641)	36,806(2,685)	16,997(1,487)	19,901(1,816)	24,684(2,029)
R_{work} / R_{free} (%)	21.1/24.6	18/19.9	20.3/24.5	25.6/28.5	19.3/23.3	22.1/24.5	21.0, 24.1
No. atoms							
Protein	3249	3324	3447	13,508	3477	3361	3323
Water	17	197	47	0	0	17	267
B-factors (Å^2)							
Protein	55.0	33.3	47.8	51.3	66.3	36.2	22.2
Water	27.5	43.7	39	na	na	33.2	25.1
R.m.s. deviations							
Bond lengths (Å)	0.004	0.008	0.003	0.009	0.003	0.005	0.005
Bond angles (°)	.885	1.22	0.82	1.15	0.79	1.01	.96
Ramachandran							
Most favored regions (%)	90.2	98.2	92.0	91.0	96.0	92.5	96.5
Additional allowed regions (%)	9.4	1.8	7.8	8.4	3.8	7.5	3.3
Disallowed regions (%)	0.6	0.0	0.2	0.6	0.2	0.0	0.2

Supplementary Table 3. Signals of selective pressure within in the V2 epitope (residues 160-171) of primary infecting (PI)-like and superinfecting (SU)-like viruses. Signals of selective pressure were detected at each site using MEME (to detect episodic diversifying selection, with p values >0.05 considered significant) and DEPS (directional selection; maximum Bayes Factor >20 considered significant, with the preferred amino acid selected for indicated in parentheses).

HXB2 position	Analysis* †	Output	PI	SU
160	Directional (DEPS)	Max BF	ns	ns
	Diversifying (MEME)	P value	ns	ns
161	Directional (DEPS)	Max BF	ns	ns
	Diversifying (MEME)	P value	ns	ns
162	Directional (DEPS)	Max BF	ns	ns
	Diversifying (MEME)	P value	ns	ns
163	Directional (DEPS)	Max BF	ns	ns
	Diversifying (MEME)	P value	ns	ns
164	Directional (DEPS)	Max BF	ns	ns
	Diversifying (MEME)	P value	ns	ns
165	Directional (DEPS)	Max BF (Preferred residues)	ns	**191 (V)**
	Diversifying (MEME)	P value	ns	ns
166	Directional (DEPS)	Max BF (Preferred residues)	**3403 (S)**	ns
	Diversifying (MEME)	P value	ns	ns
167	Directional (DEPS)	Max BF	ns	ns
	Diversifying (MEME)	P value	ns	ns
168	Directional (DEPS)	Max BF	ns	ns
	Diversifying (MEME)	P value	ns	ns
169	Directional (DEPS)	Max BF (Preferred residues)	ns	**77095 (IQ)**
	Diversifying (MEME)	P value	ns	**0.0001**
170	Directional (DEPS)	Max BF	ns	ns
	Diversifying (MEME)	P value	ns	ns
171	Directional (DEPS)	Max BF (Preferred residues)	**290 (K)**	ns
	Diversifying (MEME)	P value	ns	ns

*DEPS ns = <20; †MEME ns = >0.05; BF = Bayes Factor

Supplementary Table 4. PCR Primers used to prepare amplicon for 454 pyrosequencing.

For all timepoints except week 176

Heavy Chain: VH3 only	**5' pool**	
	XLR-A_VH3 LEADER-A	CCATCTCATCCCTGCGTGTCTCCGACTCAG TAAAAGGTGTCCAGTGT
	XLR-A_VH3 LEADER-B	CCATCTCATCCCTGCGTGTCTCCGACTCAG TAAGAGGTGTCCAGTGT
	XLR-A_VH3 LEADER-C	CCATCTCATCCCTGCGTGTCTCCGACTCAG TAGAAGGTGTCCAGTGT
	XLR-A_VH3 LEADER-D	CCATCTCATCCCTGCGTGTCTCCGACTCAG GCTATTTTTAAAGGTGTCCAGTGT
	XLR-A_VH3 LEADER-E	CCATCTCATCCCTGCGTGTCTCCGACTCAG TACAAGGTGTCCAGTGT
	XLR-A_VH3 LEADER-F	CCATCTCATCCCTGCGTGTCTCCGACTCAG TTAAAGCTGTCCAGTGT
	3' pool	
	XLR-B_3xwCgammaCH1-2	CCTATCCCCTGTGTGCCTTGGCAGTCTCAG GG GGA AGA CCG ATG GGC CCT TGG T
	XLR-B_3CmuCH1	CCTATCCCCTGTGTGCCTTGGCAGTCTCAG GGGAATTCTCACAGGAGACGA
Lambda Chain	**5' pool**	
	XLR-A_5L-VL1/2	CCATCTCATCCCTGCGTGTCTCCGACTCAG GCACAGGGTCCTGGGCCCAGTCTG
	XLR-A_5L-VL3	CCATCTCATCCCTGCGTGTCTCCGACTCAG GCTCTGTGACCTCCTATGAGCTG
	XLR-A_5L-VL4/5	CCATCTCATCCCTGCGTGTCTCCGACTCAG GGTCTCTCTCSCAGCYTGTGCTG
	XLR-A_5L-VL6	CCATCTCATCCCTGCGTGTCTCCGACTCAG GTTCTTGGGCCAATTTTATGCTG
	XLR-A_5L-VL7/8	CCATCTCATCCCTGCGTGTCTCCGACTCAG GAGTGGATTCTCAGACTGTGGTG
	XLR-A_5MP-VL1	CCATCTCATCCCTGCGTGTCTCCGACTCAG GCTCACTGCACAGGGTCCTGGGCC
	XLR-A_5MP-VL3-1	CCATCTCATCCCTGCGTGTCTCCGACTCAG GCTTACTGCACAGGATCCGTGGCC
	XLR-A_5MP-VL3-19	CCATCTCATCCCTGCGTGTCTCCGACTCAG ACTCTTTGCATAGGTTCTGTGGTT
	XLR-A_5MP-VL3-21	CCATCTCATCCCTGCGTGTCTCCGACTCAG TCTCACTGCACAGGCTCTGTGACC
	XLR-A_5MP-VL7-43	CCATCTCATCCCTGCGTGTCTCCGACTCAG ACTTGCTGCCCAGGGTCCAATTC
	3' primer	
	XLR-B_3CL	CCTATCCCCTGTGTGCCTTGGCAGTCTCAG CACCAGTGTGGCCTTGTTGGCTTG

Used for week 176 sample only

Heavy Chain: Vh_all	**5' pool**	
	XLR-A_5L-VH1	CCATCTCATCCCTGCGTGTCTCCGACTCAG ACAGGTGCCCACTCCCAGGTGCAG
	XLR-A_5L-VH3	CCATCTCATCCCTGCGTGTCTCCGACTCAG AAGGTGTCCAGTGTGARGTGCAG
	XLR-A_5L-VH4/6	CCATCTCATCCCTGCGTGTCTCCGACTCAG CCCAGATGGGTCCTGTCCCAGGTGCAG
	XLR-A_5L-VH5	CCATCTCATCCCTGCGTGTCTCCGACTCAG CAAGGAGTCTGTTCCGAGGTGCAG
	XLR-A_5xwL-VH1	CCATCTCATCCCTGCGTGTCTCCGACTCAG GCAGCCACAGGTGCCCACTCC
	XLR-A_5xwL-VH1-24	CCATCTCATCCCTGCGTGTCTCCGACTCAG CAGCAGCTACAGGCACCCACGC
	XLR-A_5xwL-VH1-69	CCATCTCATCCCTGCGTGTCTCCGACTCAG GGCAGCAGCTACAGGTGTCCAGTCC
	XLR-A_VH3-L1-MP	CCATCTCATCCCTGCGTGTCTCCGACTCAG GCTATTTTAAAAGGTGTCCAATGT
	XLR-A_VH3/4-L1-MP	CCATCTCATCCCTGCGTGTCTCCGACTCAG GTGGCAGCTCCCAGATGGGTCCTGTC
	XLR-A_VH3/4-L3-MP	CCATCTCATCCCTGCGTGTCTCCGACTCAG GTTGCAGTTTTAAAAGGTGTCCAGTG
	XLR-A_VH5-L1-MP	CCATCTCATCCCTGCGTGTCTCCGACTCAG GCTGTTCTCCAAGGAGTCTGTTCC
	3' pool	
	XLR-B_3xwCgammaCH1	CCTATCCCCTGTGTGCCTTGGCAGTCTCAG GGGGAAGACCGATGGGCCCTTGGTGG
	XLR-B_3CmuCH1	CCTATCCCCTGTGTGCCTTGGCAGTCTCAG GGGAATTCTCACAGGAGACGA
Light Chains (kappa+lambda)	**5' pool**	
	XLR-A_5xwL-VK1/2	CCATCTCATCCCTGCGTGTCTCCGACTCAG ATGAGGSTCCCYGCTCAGCTCCTGGG
	XLR-A_5L-VK3	CCATCTCATCCCTGCGTGTCTCCGACTCAG CTCTTCCTCCTGCTACTCTGGCTCCCAG
	XLR-A_5L-VK4	CCATCTCATCCCTGCGTGTCTCCGACTCAG ATTTCTCTGTTGCTCTGGATCTCTG
	XLR-A_5L-VL1/2	CCATCTCATCCCTGCGTGTCTCCGACTCAG GCACAGGGTCCTGGGCCCAGTCTG
	XLR-A_5L-VL3	CCATCTCATCCCTGCGTGTCTCCGACTCAG GCTCTGTGACCTCCTATGAGCTG
	XLR-A_5L-VL4/5	CCATCTCATCCCTGCGTGTCTCCGACTCAG GGTCTCTCTCSCAGCYTGTGCTG
	XLR-A_5L-VL6	CCATCTCATCCCTGCGTGTCTCCGACTCAG GTTCTTGGGCCAATTTTATGCTG
	XLR-A_5L-VL7/8	CCATCTCATCCCTGCGTGTCTCCGACTCAG GAGTGGATTCTCAGACTGTGGTG
	XLR-A_5MP-VL1	CCATCTCATCCCTGCGTGTCTCCGACTCAG GCTCACTGCACAGGGTCCTGGGCC
	XLR-A_5MP-VL3-1	CCATCTCATCCCTGCGTGTCTCCGACTCAG GCTTACTGCACAGGATCCGTGGCC
	XLR-A_5MP-VL3-19	CCATCTCATCCCTGCGTGTCTCCGACTCAG ACTCTTTGCATAGGTTCTGTGGTT
	XLR-A_5MP-VL3-21	CCATCTCATCCCTGCGTGTCTCCGACTCAG TCTCACTGCACAGGCTCTGTGACC
	XLR-A_5MP-VL7-43	CCATCTCATCCCTGCGTGTCTCCGACTCAG ACTTGCTGCCCAGGGTCCAATTC
	3' pool	
	XLR-B_3xwCK1	CCTATCCCCTGTGTGCCTTGGCAGTCTCAG CAGCAGGCACACAACAGAGGCAGTTCC
	XLR-B_3CL	CCTATCCCCTGTGTGCCTTGGCAGTCTCAG CACCAGTGTGGCCTTGTTGGCTTG

Supplementary Table 5. Additional primers used in Heavy-light chain paired deep sequencing.

Conc (nM)	Primer ID	Primer Sequence
40	VH1_LP	tattcccatcgcggcgcACAGGTGCCCACTCCCAGGTGCAG
40	VH3_LP	tattcccatcgcggcgcAAGGTGTCCAGTGTGARGTGCAG
40	VH4/6_LP	tattcccatcgcggcgcCCCAGATGGGTCCTGTCCCAGGTGCAG
40	VH5_LP	tattcccatcgcggcgcCAAGGAGTCTGTTCCGAGGTGCAG
40	hVλ1for_LP	gcgccgcgatgggaataNNNNNNNNNNNNNNNNTCTGCTCGAGTTCGGTCAGGTCCTGGGCCCAGTCTGTGCTG
40	hVλ2for_LP	gcgccgcgatgggaataNNNNNNNNNNNNNNNNTCTGCTCGAGTTCGGTCAGGTCCTGGGCCCAGTCTGCCCTG
40	hVλ3for-2_LP	gcgccgcgatgggaataNNNNNNNNNNNNNNNNTCTGCTCGAGTTCGGTCAYWCTGCACAGGCTCTGTGACCTCCTAT
40	hVλ4/5for_LP	gcgccgcgatgggaataNNNNNNNNNNNNNNNNTCTGCTCGAGTTCGGTCAGGTCTCTCTCSCAGCYTGTGCTG
40	hVλ6for_LP	gcgccgcgatgggaataNNNNNNNNNNNNNNNNTCTGCTCGAGTTCGGTCAGTTCTTGGGCCAATTTTATGCTG
40	hVλ7for_LP	gcgccgcgatgggaataNNNNNNNNNNNNNNNNTCTGCTCGAGTTCGGTCAGGTCCAATTCYCAGGCTGTGGTG
40	hVλ8for_LP	gcgccgcgatgggaataNNNNNNNNNNNNNNNNTCTGCTCGAGTTCGGTCAGAGTGGATTCTCAGACTGTGGTG
40	hVκ1/2for_LP	gcgccgcgatgggaataNNNNNNNNNNNNNNNNTCTGCTCGAGTTCGGTCAATGAGGSTCCCYGCTCAGCTGCTGG
40	hVκ3for_LP	gcgccgcgatgggaataNNNNNNNNNNNNNNNNTCTGCTCGAGTTCGGTCACTCTTCCTCCTGCTACTCTGGCTCCCAG
40	hVκ4for_LP	gcgccgcgatgggaataNNNNNNNNNNNNNNNNTCTGCTCGAGTTCGGTCAATTTCTCTGTTGCTCTGGATCTCTG

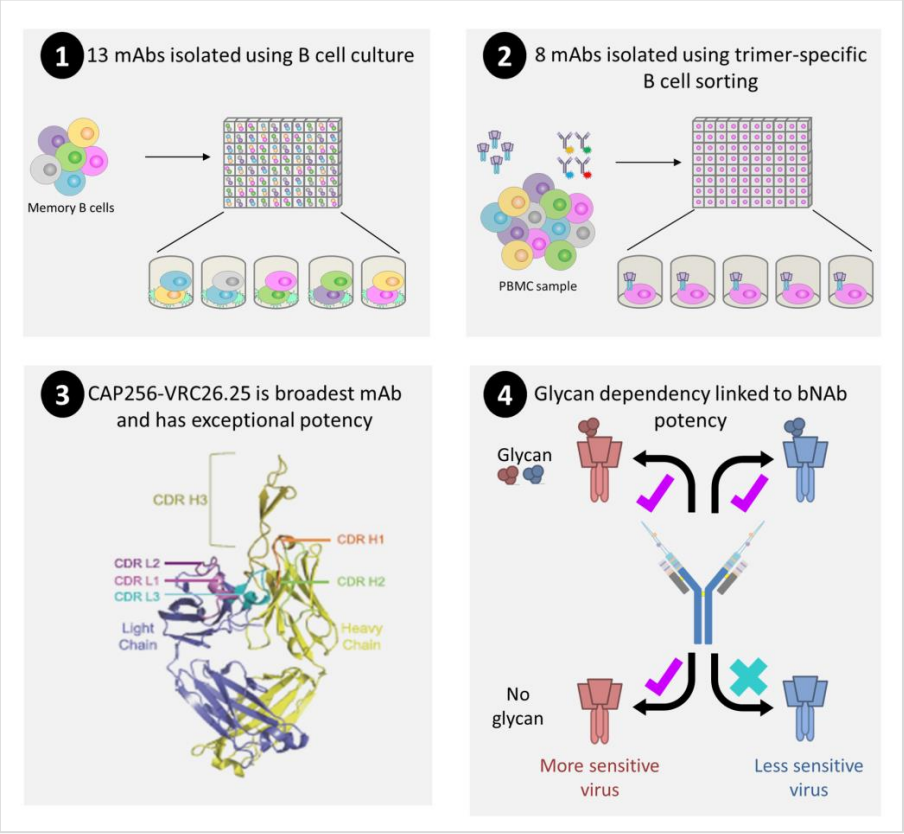
2. New member of the V1V2-directed CAP256-VRC26 lineage that shows increased breadth and exceptional potency

Doria-Rose NA, **Bhiman JN**, Roark RS, Schramm CA, Gorman J, Chuang G-Y, Pancera M, Cale EM, Ernandes MJ, Louder MK, Asokan M, Bailer RT, Druz A, Fraschilla IR, Garrett NJ, Jarosinski M, Lynch RM, McKee K, O'Dell S, Pegu A, Schmidt SD, Staupe RP, Sutton MS, Wang K, Wibmer CK, Haynes BF, Abdool-Karim S, Shapiro L, Kwong PD, Moore PL, Morris L, Mascola JR.

Journal of Virology. 2016: 90: 76–91. doi:10.1128/JVI.01791-15. PMID: 26468542

This publication described the isolation of 21 additional CAP256-VCR26 mAbs, characterized the broadest member of the lineage and showed that the glycan dependency of these mAbs is linked to their potency.

Graphical Abstract



AMERICAN SOCIETY FOR MICROBIOLOGY | Journal of Virology

New Member of the V1V2-Directed CAP256-VRC26 Lineage That Shows Increased Breadth and Exceptional Potency

Nicole A. Doria-Rose,[a] Jinal N. Bhiman,[b,c] Ryan S. Roark,[a] Chaim A. Schramm,[d] Jason Gorman,[a] Gwo-Yu Chuang,[a] Marie Pancera,[a] Evan M. Cale,[a] Michael J. Ernandes,[a] Mark K. Louder,[a] Mangaiarkarasi Asokan,[a] Robert T. Bailer,[a] Aliaksandr Druz,[a] Isabella R. Fraschilla,[a] Nigel J. Garrett,[e] Marissa Jarosinski,[a] Rebecca M. Lynch,[a] Krisha McKee,[a] Sijy O'Dell,[a] Amarendra Pegu,[a] Stephen D. Schmidt,[a] Ryan P. Staupe,[a] Matthew S. Sutton,[a] Keyun Wang,[a] Constantinos Kurt Wibmer,[b,c] Barton F. Haynes,[f] Salim Abdool-Karim,[e,g] Lawrence Shapiro,[d] Peter D. Kwong,[a] Penny L. Moore,[b,c,e] Lynn Morris,[b,c,e] John R. Mascola[a]

Vaccine Research Center, National Institute of Allergy and Infectious Diseases, National Institutes of Health, Bethesda, Maryland, USA[a]; Centre for HIV and STIs, National Institute for Communicable Diseases of the National Health Laboratory Services, Johannesburg, South Africa[b]; University of the Witwatersrand, Johannesburg, South Africa[c]; Department of Biochemistry and Systems Biology, Columbia University, New York, New York, USA[d]; Centre for the AIDS Programme of Research in South Africa (CAPRISA), University of KwaZulu Natal, Durban, South Africa[e]; Duke University School of Medicine and Center for HIV/AIDS Vaccine Immunology-Immunogen Discovery at Duke University, Durham, North Carolina, USA[f]; Department of Epidemiology, Columbia University, New York, New York, USA[g]

ABSTRACT

The epitopes defined by HIV-1 broadly neutralizing antibodies (bNAbs) are valuable templates for vaccine design, and studies of the immunological development of these antibodies are providing insights for vaccination strategies. In addition, the most potent and broadly reactive of these bNAbs have potential for clinical use. We previously described a family of 12 V1V2-directed neutralizing antibodies, CAP256-VRC26, isolated from an HIV-1 clade C-infected donor at years 1, 2, and 4 of infection (N. A. Doria-Rose et al., Nature 509:55–62, 2014, http://dx.doi.org/10.1038/nature13036). Here, we report on the isolation and characterization of new members of the family mostly obtained at time points of peak serum neutralization breadth and potency. Thirteen antibodies were isolated from B cell culture, and eight were isolated using trimeric envelope probes for differential single B cell sorting. One of the new antibodies displayed a 10-fold greater neutralization potency than previously published lineage members. This antibody, CAP256-VRC26.25, neutralized 57% of diverse clade viral isolates and 70% of clade C isolates with remarkable potency. Among the viruses neutralized, the median 50% inhibitory concentration was 0.001 μg/ml. All 33 lineage members targeted a quaternary epitope focused on V2. While all known bNAbs targeting the V1V2 region interact with the N160 glycan, the CAP256-VRC26 antibodies showed an inverse correlation of neutralization potency with dependence on this glycan. Overall, our results highlight the ongoing evolution within a single antibody lineage and describe more potent and broadly neutralizing members with potential clinical utility, particularly in areas where clade C is prevalent.

IMPORTANCE

Studies of HIV-1 broadly neutralizing antibodies (bNAbs) provide valuable information for vaccine design, and the most potent and broadly reactive of these bNAbs have potential for clinical use. We previously described a family of V1V2-directed neutralizing antibodies from an HIV-1 clade C-infected donor. Here, we report on the isolation and characterization of new members of the family mostly obtained at time points of peak serum neutralization breadth and potency. One of the new antibodies, CAP256-VRC26.25, displayed a 10-fold greater neutralization potency than previously described lineage members. It neutralized 57% of diverse clade viral isolates and 70% of clade C isolates with remarkable potency: the median 50% inhibitory concentration was 0.001 μg/ml. Our results highlight the ongoing evolution within a single antibody lineage and describe more potent and broadly neutralizing members with potential clinical utility, particularly in areas where clade C is prevalent.

Neutralizing antibodies (NAbs) against HIV-1 are likely to be a major component of an effective vaccine-induced immune response. Cross-reactive NAbs commonly arise during HIV-1 infection, though only a small subset of infected patients produces NAbs with a high neutralization breadth and potency (1–4). In contrast, the HIV-1 envelope glycoprotein (Env) vaccine immunogens tested to date have failed to elicit cross-reactive neutralizing antibodies (5, 6). Thus, studying the development of broadly neutralizing antibodies (bNAbs) in infected individuals may provide important lessons for vaccine design (5, 7–10). In addition, the isolation of bNAbs from selected donors has greatly aided our understanding of the HIV-1 Env structure (11–13) and vulnerability to neutralizing antibodies (14–16), and such antibodies have the potential to be used for the prevention or treatment of HIV-1 infection (8, 17).

NAbs directed to the V1V2 region of HIV-1 Env are of particular interest for vaccine design, as this site is antigenic and commonly targeted in HIV infection (18, 19). To date, families of V1V2-directed bNAbs have been isolated from only four different donors (20–23). These antibodies typically have a long, anionic heavy chain complementarity-determining region 3 (CDRH3), which penetrates the glycan shield, and heavy chain variable (VH) gene mutation levels of 10 to 20%. They bind to the apex region of the intact trimer and bind poorly or not at all to most monomeric forms of the protein. Negative-stain electron microscopy studies show that such antibodies bind with a stoichiometry of one per trimer and likely interact with more than one protomer (21, 24), consistent with the location of V1V2 at the apex of the trimer (11, 12). This category of antibodies typically relies on glycan residues, specifically, N156 and N160 in V2 (23). Glycan dependence some-

Downloaded from http://jvi.asm.org/ on December 21, 2015 by Penny Moore

times results in incomplete neutralization, referred to as the plateau effect (23, 25, 26), due in part to the microheterogeneity of glycoforms at these residues, resulting in a resistant subpopulation within a virus preparation (27).

Our group has extensively studied the antibodies from donor CAP256, who developed high-titer plasma neutralizing antibodies to the V1V2 region that first appeared at 1 year and peaked at 3 years of HIV-1 infection (21, 28, 29). This donor was infected with a clade C virus and 15 weeks later was superinfected with a different clade C virus. We isolated 12 V1V2-directed antibodies at multiple time points over 4 years of infection; all were somatically related and termed the CAP256-VRC26 lineage, where CAP256 denotes the donor and VRC26 denotes the antibody lineage. Members of this antibody lineage have a very long CDRH3 of 35 to 37 amino acids and modest levels of V-gene mutation (8 to 15% sequence divergence compared with that of the germ line). 454 pyrosequencing of virus from early time points showed that the long CDRH3 was present at the origin of the lineage and allowed accurate inference of an unmutated common ancestor (UCA) that was able to bind and neutralize the superinfecting virus (21).

Here, we report on the isolation and characterization of 21 new members of the CAP256-VRC26 family. These antibodies were isolated either by B cell culture or by single-cell sorting with trimeric Env probes. One of the antibodies, CAP256-VRC26.25 (where the antibody name indicates donor-lineage.clone), neutralizes 57% of HIV-1 isolates, including 70% of clade C isolates, with an overall 10-fold greater potency than the previously described family members. Structure, epitope mapping, and phylogenetic analyses provide a deeper understanding of the origin and evolution of this important lineage.

MATERIALS AND METHODS

Study subject. Centre for the AIDS Programme of Research in South Africa (CAPRISA) participant CAP256 was enrolled into the CAPRISA Acute Infection Study (30) that was established in 2004 in KwaZulu-Natal, South Africa, for follow-up and subsequent identification of HIV seroconversion. CAP256 was one of the seven women in this cohort who developed neutralization breadth (31). The CAPRISA 002 Acute Infection Study was reviewed and approved by the research ethics committees of the University of KwaZulu-Natal (E013/04), the University of Cape Town (025/2004), and the University of the Witwatersrand (MM040202). CAP256 provided written informed consent for study participation. Samples were drawn between 2005 and 2009.

B cell cultures. Peripheral blood mononuclear cells (PBMCs) isolated from CAP256 blood draws at week 193 were stained with LIVE/DEAD Fixable Aqua (Invitrogen), CD19-Cy7-phycoerythrin (PE), IgM-Cy5-PE, IgD-PE, CD16-Pacific Blue, and CD3-Cy7-allophycocyanin (APC) (BD Pharmingen). The IgD-negative (IgD^-) IgM-negative (IgM^-) B cells were bulk sorted on a BD FACSAria II flow cytometer as described previously (19). Cells were plated at 2 B cells per well in 384-well plates and cultured for 14 days in the presence of CD40L-expressing irradiated feeder cells, interleukin-2 (IL-2) (Roche), and interleukin-21 (IL-21) (Gibco), as described previously (32, 33). Culture supernatants were screened by microneutralization against HIV-1 ZM53.12 and CAP210.E8 Env pseudoviruses as described in reference 34.

Expression and purification of trimeric HIV-1 Env BG505 SOSIP.664 probes. An Avi tag (GLNDIFEAQKIEWHE) was inserted at the C terminus of the previously described construct BG505 SOSIP.664.T332N gp140, referred to here as BG505 SOSIP (35). For BG505 SOSIP.K169E-Avi, lysine (K) 169 was mutated to a glutamic acid (E) by site-directed mutagenesis. Both constructs were transfected and purified as described previously (12). Briefly, HEK 293 cells were cotransfected with BG505 SOSIP and furin plasmid DNAs at a 4:1 ratio. Transfection supernatants were harvested and purified through either a VRC01 or a 2G12 antibody affinity column. Proteins were eluted with 3 M $MgCl_2$, 10 mM Tris, pH 8.0. The eluate was concentrated and applied to a Superdex 200 column equilibrated in 5 mM HEPES, pH 7.5, 150 mM NaCl, 0.02% azide or phosphate-buffered saline. The fractions corresponding to the trimeric proteins were pooled, concentrated, flash-frozen in liquid nitrogen, and stored at −80°C. The proteins were biotinylated at the Avi tag sequence using BirA ligase and then conjugated to streptavidin-APC or streptavidin-PE (Invitrogen) as described previously (36).

The probes were assessed for the correct antigenicity by binding to antibody-coated beads. Anti-mouse kappa light chain beads (Becton Dickinson, San Jose, CA) were incubated with anti-human IgG (Becton Dickinson), washed, incubated with 2 μg/ml antibody CAP256-VRC26.09, PGT128, or F105, and washed again. BG505 SOSIP-streptavidin-APC or BG505 SOSIP.K169E-streptavidin-PE (1.5 μg) was then incubated with the beads, and the beads were washed and analyzed on an LSR II flow cytometer (Becton Dickinson).

Cell sorting. PBMCs from week 159 were stained for IgG-positive (IgG^+) B cells using LIVE/DEAD Fixable Aqua (Invitrogen), IgG-fluorescein isothiocyanate, CD19-Cy7-PE, IgM-Cy5-PE, CD14-PE-Texas Red (ECD), CD4-ECD, CD3-Cy7-APC, and CD8-Brilliant Violet 711 (BD Pharmingen). At the same time, they were stained with BG505 SOSIP-streptavidin-APC and BG505 SOSIP.K169E-streptavidin-PE. Cells that were BG505 SOSIP-streptavidin-APC positive (APC^+) IgG^+ $CD19^+$ were sorted using a BD FACSAria II flow cytometer into single wells of a 96-well plate containing RNase inhibitor (New England Biolabs), SuperScript reverse transcriptase buffer (Invitrogen), dithiothreitol, and Igepal as described previously (36).

Isolation and expression of CAP256-VRC26 family genes. Kappa and lambda light chain gene and IgG heavy chain gene variable regions were amplified from neutralization-positive B cell culture wells as described in reference 33 or from 96-well sort plates as described in reference 36. Briefly, cells were lysed and subjected to reverse transcription-PCR (RT-PCR) as described in reference 37 using a modified primer set (see Table S1 in the supplemental material). These primers were developed by our group or were described previously (see Table S1 in the supplemental material) (37–39). Briefly, cells were lysed and subjected to RT-PCR as described previously (37) using a modified primer and a round of nested PCR with 3 different multiplex primer pools, which were used to amplify either the heavy chains or the light chains. The amplicons were subcloned, expressed, and purified as described in reference 19. For antibodies CAP256-VRC26.13 to CAP256-VRC26.21, wells that previously yielded VRC26-lineage lambda chains but no heavy chains were subjected to RT-PCR using IgA-specific 3′ primers. All heavy chains were subcloned and expressed as IgG1 regardless of the class of the original amplicon.

Neutralization assays. Single-round-of-replication Env pseudoviruses were prepared, titers were determined, and the pseudoviruses were

Received 31 July 2015 Accepted 21 September 2015
Accepted manuscript posted online 14 October 2015
Citation Doria-Rose NA, Bhiman JN, Roark RS, Schramm CA, Gorman J, Chuang G-Y, Pancera M, Cale EM, Ernandes MJ, Louder MK, Asokan M, Bailer RT, Druz A, Fraschilla IR, Garrett NJ, Jarosinski M, Lynch RM, McKee K, O'Dell S, Pegu A, Schmidt SD, Staupe RP, Sutton MS, Wang K, Wibmer CK, Haynes BF, Abdool-Karim S, Shapiro L, Kwong PD, Moore PL, Morris L, Mascola JR. 2016. New member of the V1V2-directed CAP256-VRC26 lineage that shows increased breadth and exceptional potency. J Virol 90:76–91. doi:10.1128/JVI.01791-15.
Editor: G. Silvestri
Address correspondence to John R. Mascola, jmascola@nih.gov.
Supplemental material for this article may be found at http://dx.doi.org/10.1128/JVI.01791-15.
Copyright © 2015, American Society for Microbiology. All Rights Reserved.

Downloaded from http://jvi.asm.org/ on December 21, 2015 by Penny Moore

used to infect TZM-bl target cells as described previously (40, 41). The neutralization breadth of CAP256-VRC26.25, CAP256-VRC26.26, and CAP256-VRC26.27, as well as that of previously described antibodies, was determined using a previously described panel (19, 36) of up to 200 geographically and genetically diverse Env pseudoviruses representing the major subtypes and circulating recombinant forms. The remaining CAP256-VRC26 antibodies were assayed on a 46-virus subset of this panel, along with the autologous virus strains CAP256.2.00.C7J (a primary infecting [PI] strain) and CAP256.206.c9 (a superinfecting [SU] strain). The data were calculated as a reduction in the number of luminescence units compared with the number for the control wells and are reported as the 50% inhibitory concentration (IC_{50}; in micrograms per microliter) for monoclonal antibodies (MAbs).

N160 glycan mutant Env pseudoviruses were generated by site-directed mutagenesis as described previously (28, 42). All N160 glycan mutants had the N160K mutation, except for ConC, which had the N160A mutation. The N156 mutants (this study) were generated as N156A mutants by site-directed mutagenesis (GeneImmune, New York, NY). The BG505 pseudovirus had the wild-type sequence (threonine) at position 332, unlike the BG505 SOSIP probe, which bears a T332N mutation (35).

Neutralization and autoreactivity data for CAP256-VRC26.25 were generated with a variant that had the amino acid change K126Q in the light chain, which was inserted during subcloning. We confirmed that this single amino acid change did not alter the neutralization data.

Autoreactivity. CAP256-VRC26.01 to CAP256-VRC26.32 and UCA antibodies were assayed at 25 and 50 $\mu g\ ml^{-1}$ for autoreactivity to HEp-2 cells (Inverness Medical Professional Diagnostics) by indirect immunofluorescence and for binding to cardiolipin as described previously using a Quanta Lite ACA IgG III assay (INOVA Diagnostics Inc., San Diego, CA) (43). The UCA and seven of the antibodies with the broadest activity were further evaluated on a panel of autoantigens using an AtheNA Multi-Lyte ANA-II Plus test system (Alere, Orlando, FL) to detect semiquantitatively IgG antibodies to 9 separate analytes, SSA, SSB, Sm, RNP, Scl-70, Jo-1, centromere B, double-stranded DNA (dsDNA), and histone, as reported previously (43); values of >120 at 25 $\mu g\ ml^{-1}$ were considered positive (43).

Next-generation sequencing analysis. 454 pyrosequencing was performed on PBMCs from week 34, the results for which are reported here, as well as PBMCs from weeks 38, 49, 59, 119, 176, and 206, the results for which were described previously (21). mRNA was prepared from 10 million to 15 million PBMCs as follows: cells were lysed in 600 μl buffer RLT (Qiagen) per 10 million PBMCs and run over a QIAshredder (Qiagen). The flowthrough was applied to the DNA column from an Allprep kit (Qiagen), and that flowthrough was used for subsequent purification using an Oligotex kit (Qiagen). cDNA was synthesized using SuperScript II reverse transcriptase (Invitrogen) and oligo$(dT)_{12–18}$ primers with incubation at 70°C for 1 min, chilling on ice, and then synthesis at 42°C for 2 h. Individual PCRs were performed with Phusion polymerase (Thermo) for 30 cycles. Primers (21) consisted of pools of 5 to 7 oligonucleotides specific for all lambda chain gene families or for VH3 family genes and had adapters for 454 next-generation sequencing. For PBMCs from week 176 only, heavy chain PCR was performed with primers for all VH families and mixed lambda chain and kappa chain primers were used for the light chain (21). PCR products were gel purified (Qiagen). Pyrosequencing of the PCR products was performed on a GSFLX sequencing instrument (Roche-454 Life Sciences, Bradford, CT, USA) on a half chip per reaction (full chips were used for PBMCs from week 176). On average, ~250,000 raw reads were produced.

Next-generation sequencing data from each time point were processed through an Antibodyomics pipeline (https://github.com/scharch/SONAR) as previously described (21, 44). Briefly, a series of Python scripts was used to check transcripts for appropriate length (300 to 600 nucleotides), provide calls for germ line V and J gene assignments by BLAST analysis, and check for in-frame junctions and open reading frames. Reads for which the V and J genes were successfully assigned and that had an in-frame junction and no stop codons were clustered using the CDHit program (45) at 97.25% identity, and singletons were discarded. In order to better account for possible errors introduced during sequencing, we restricted our analysis to sequences appearing at least twice in any one data set. This resulted in approximately 50% fewer final heavy chain sequences than we previously reported, but the phylogenetic structure of the lineage remained the same. In addition, we used a CDRH3 signature contained in all previously reported sequences as a less computationally intensive way of finding related heavy chain sequences. Thus, heavy chain sequences that matched the CAP256-VRC26 VH and JH assignments and that had CDRH3s that were at least 30 amino acids long and that had a YY motif were selected and combined across all time points. Light chains that matched the CAP256-VRC26 VL and JL assignments and that had a light chain complementarity-determining region 3 (CDRL3) with at least 92% sequence identity to a known CAP256-VRC26 family member were manually inspected, and those with a recombination pattern matching that of the known antibodies were combined across all time points. Selected heavy and light chains from all time points were reclustered so that sequences observed at multiple time points are represented only once in the final data set. A final manual inspection was used to remove sequences with apparent PCR crossover or homopolymer indel errors.

Heavy and light chain trees were built using the FASTML program (46), and the light chain tree was manually edited to match the heavy chain arrangement as previously described (21). Ancestral sequences were inferred from these trees using the DNAML program (47) as previously described (21).

CAP256-VRC26.25 Fab crystallization and structure determination. Fab was prepared by inserting an HRV3C recognition site (GLEVL FQGP) after Lys 235. Purified IgG was incubated with HRV3C protease overnight at 4°C, and the digested protein was passed over protein A agarose to remove the Fc fragment and subsequently purified over a Superdex 200 gel filtration column. The Fab preparation was then screened against 576 crystallization conditions using a Mosquito crystallization robot. Initial crystals were grown by the vapor diffusion method in sitting drops at 20°C by mixing 0.1 μl of protein with 0.1 μl of reservoir solution. Crystals were manually reproduced in hanging drops by mixing 1.0 μl protein complex with 1.0 μl reservoir solution. Crystals grown in a reservoir solution of 23% polyethylene glycol (PEG) 8000 and 0.1 M HEPES, pH 7.5, were flash frozen in liquid nitrogen with 20% PEG 400 as a cryoprotectant. Diffraction data were collected at a wavelength of 1.00 Å at the SER-CAT beamline ID-22 (Advanced Photon Source, Argonne National Laboratory). All diffraction data were processed with the HKL2000 suite (48), and model building and refinement were performed in the COOT (49) and PHENIX (50) programs, respectively. Ribbon diagram representations of protein crystal structures were made with the PyMOL program (51), and electrostatics were calculated and rendered with the UCSF Chimera program (52). Data collection and refinement statistics are shown in Table S2 in the supplemental material.

Amino acid frequency analysis. The resistance score for a given amino acid (or a gap) was defined as the ratio of its number of occurrences in sequences from resistant strains to its overall number of occurrences for the given residue position (53). A higher score indicates that the amino acid was preferentially found among sequences from resistant strains, with a score of 1 indicating that the amino acid was found only among sequences from resistant strains. Associations were analyzed using Fisher's exact test with the Bonferroni correction for multiple comparisons. Alignments were generated using the MUSCLE algorithm implemented in Geneious software, version 8.1.7 (54). Logo plots were generated with the Weblogo application (http://weblogo.berkeley.edu/) (55) and manually colored by the use of Inkscape software (https://inkscape.org).

Accession numbers. Sequences from this study are available in GenBank under the following accession numbers: for the heavy and light chain sequences for CAP256-VRC26.13 to CAP256-VRC26.33, GenBank accession numbers KT371076 to KT371117; for 454 pyrosequencing data

Downloaded from http://jvi.asm.org/ on December 21, 2015 by Penny Moore

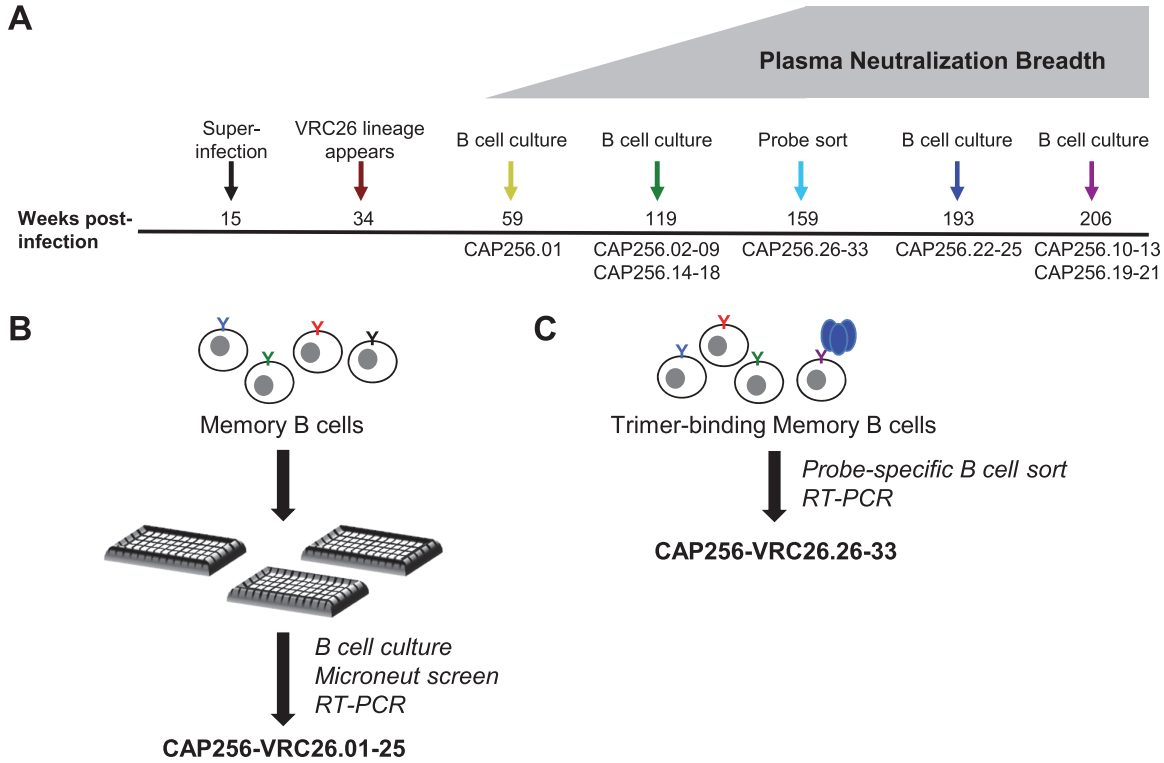


FIG 1 Schematics of CAP256-VRC26 antibody isolation. (A) Timeline of antibody isolation. Numbers above the line indicate the week postinfection. The names of the antibodies isolated at each time point are shown below the line. (B) Schematic of high-throughput B cell culture method. Sorted IgD^- IgM^- B cells were plated at a density of ~2 cells per well into 384-well plates, followed by assessment by a microneutralization assay (Microneut) on day 14. (C) Schematic of probe sorting method. IgG^+ B cells bound to APC-labeled BG505 SOSIP were sorted into 96-well plates, followed by reverse transcription-PCR to recover the IgG genes.

sets from CAP256 at week 34, Sequence Read Archive accession numbers SRR2126754 and SRR2126755; and for pyrosequencing data sets of bioinformatically identified lineage members from week 34, GenBank accession numbers KT371118 to KT371320. Coordinates and structure factors for CAP256-VRC26.25 have been deposited with the Protein Data Bank (PDB) under accession number 5DT1.

RESULTS

Isolation of new antibodies. To further understand the CAP256-VRC26 lineage and in an attempt to find broader and more potent members, we isolated antibodies from time points of peak serum neutralization potency and breadth (Fig. 1A). We used several methods to isolate an additional 21 antibodies. These included repeated PCR amplifications with cDNA from wells from the original B cell cultures, using the new primers described below; a B cell culture of PBMCs from week 193 (Fig. 1B); and single-cell sorting with antigen-specific probes (Fig. 1C), using a PBMC sample from week 159 (at the peak of neutralization breadth in plasma [28, 29]). The recovered antibodies are named as follows: donor-lineage.clone, for example, CAP256-VRC26.25. For brevity, in some figures we refer to them as donor.clone, for example, CAP256.25.

(i) B cell cultures. The B cell culture method used here involves sorting of IgM^- IgD^- B cells, followed by culture for 2 weeks and then microneutralization assays of culture supernatants (32, 34) (Fig. 1B). Previous B cell cultures from donor CAP256 (21) yielded multiple wells from which VRC26-lineage lambda chains, but not IgG heavy chains, were recovered. We used IgA-specific 3′ primers (39) with new sets of multiplex 5′ primers (see Materials and Methods and Table S1 in the supplemental material) and recovered nine VRC26-lineage heavy chains from these wells. Some of these may have derived from IgA^+ B cells, as IgA^+ B cells were not excluded in the sorting. Unexpectedly, two wells yielded both IgG and IgA amplicons with identical variable regions but distinct constant regions (Fig. 2A). We concluded that class switching had occurred in the well during the 2-week culture. The combination of CD40L and IL-21 was previously shown to support IgG-to-IgA class switching in human B cells (56–58). We therefore made the assumption that all such wells originally contained IgG^+ B cells. All antibody sequences were subcloned and expressed as IgG1. This strategy yielded 9 antibodies (CAP256-VRC26.13 to CAP256-VRC26.21) derived from the PBMCs from weeks 119 and 206. We subsequently performed a B cell culture with B cells derived from week 193 and, using the new primer sets described in the Materials and Methods and Table S1 in the supplemental material, recovered four additional antibodies (CAP256-VRC26.22 to CAP256-VRC26.25).

(ii) Single-cell sort with trimer probes. The recent development of the trimer mimic BG505 SOSIP (35) provides a probe that can be used to sort B cells expressing antibodies to quaternary epitopes (59). The broader antibodies of the CAP256-VRC26 lineage neutralize BG505, and thus, we chose to use this probe with the goal of isolating lineage members with broader neutralization capacities (Fig. 1C). To increase the specificity of the probe for the CAP256-VRC26 lineage, we assessed potential mutations that

Downloaded from http://jvi.asm.org/ on December 21, 2015 by Penny Moore

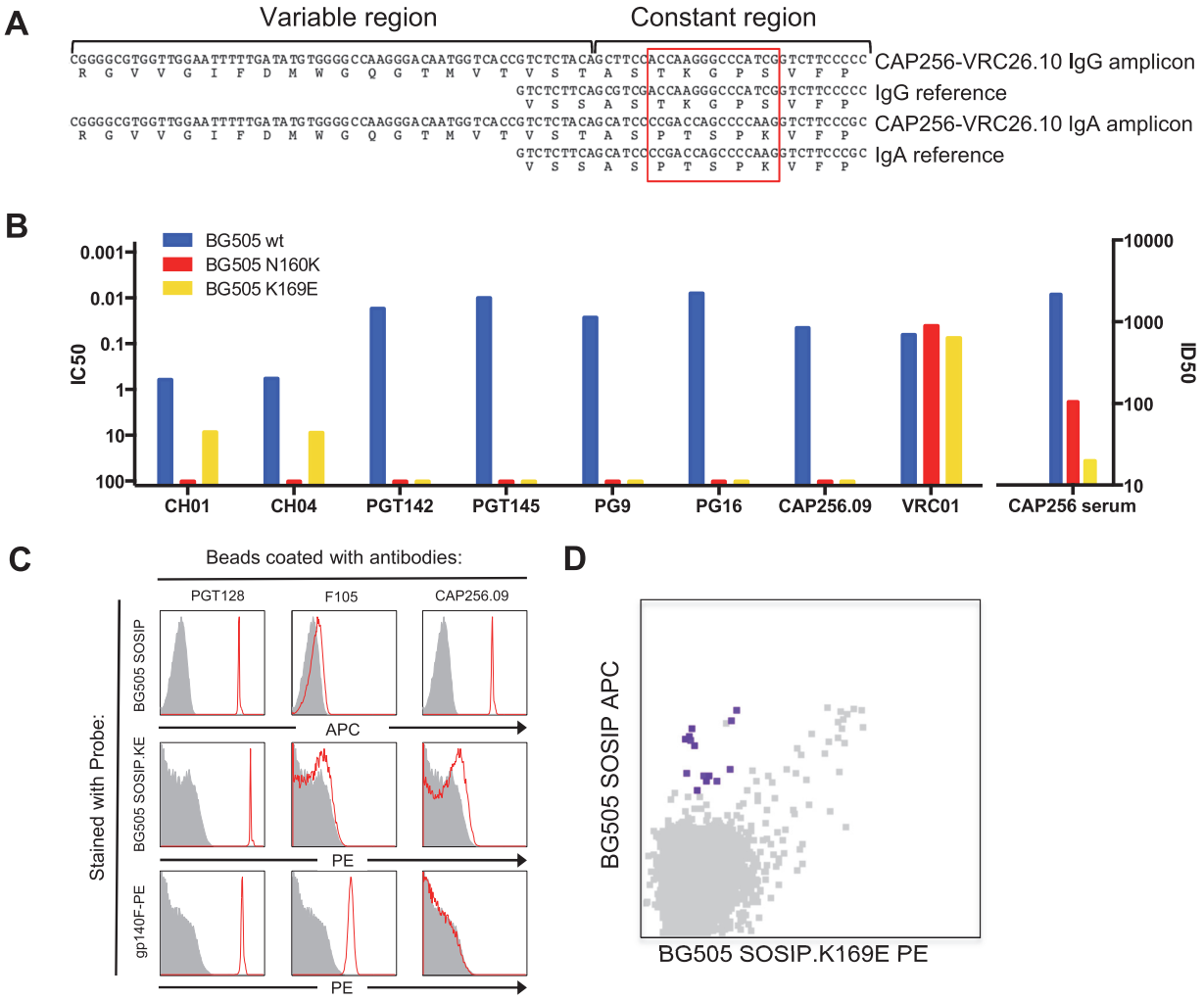


FIG 2 Isolation of CAP256-VRC26 antibodies. (A) Class switch occurs under B cell culture conditions. Identical VDJ regions appear in both IgA and IgG forms in the same well. The red box highlights sequences that differ between IgG and IgA. (B to D) The BG505 trimer with a mutation in V2 selects for CAP256-VRC26-lineage B cells. (B) Effect of N160K and K169E mutations on neutralization of HIV BG505 by V1V2-directed antibodies and CAP256 plasma. wt, wild type; ID50, 50% inhibitory dilution. (C) Quality and specificity of probes. BG505 SOSIP-APC, BG505 SOSIP.K169E-PE, or gp140F-PE probes were used to stain beads coated with the PGT128, F105, or CAP256-VRC26.09 (CAP256.09) antibody. Histograms of anti-HIV antibodies (red) are overlaid on those for the anti-influenza virus control (gray). (D) Probe-specific B cell sorting. CAP256 PBMCs were stained with B cell markers and probes. Sorted IgG^+ BG505 SOSIP-APC^+ BG505-SOSIP-K169E-PE^- B cells (purple) are shown overlaid on all live, IgG^+ B cells (gray).

would knock out V1V2 antibody binding and neutralization: using an Env pseudovirus of BG505, we made a variant with a deletion of the N160 glycan (the N160K mutant) and a variant with a mutation in V2 strand C (the K169E mutant). While the N160K mutation rendered BG505 resistant to PG9-, CH01-, and PGT145-lineage antibodies, neutralization by CAP256 plasma and CAP256-VRC26.09 was more affected by the K169E mutation than by the N160K mutation (Fig. 2B). We therefore made a K169E mutation in the BG505 SOSIP trimer. Wild-type and mutant molecules were fluorescently labeled, and their antigenicity was assessed by binding them to beads coated with known antibodies (Fig. 2C). The BG505 SOSIP wild-type probe bound strongly to PGT128 and CAP256-VRC26.09 and did not bind to the weakly neutralizing antibody F105. The K169E mutant had similar binding, but as expected, it did not bind to CAP256-VRC26.09. As a control, YU2-gp140-foldon, which does not present quaternary epitopes (60, 61), was observed to bind PGT128 and F105 but not CAP256-VRC26.09 (Fig. 2C). Using the BG505 SOSIP probe pair, we sorted single IgG^+ B cells from week 159 (Fig. 2D), a time point at which the donor's plasma showed peak neutralization breadth and potency (28, 29). We amplified and subcloned Ig genes from cells that were positive for the wild-type probe but did not bind the K169E probe. Fourteen wells yielded heavy chain amplicons, light chain amplicons, or both. In 11 of the 14 wells, the amplicon(s) matched the VRC26 lineage, and 8 such wells yielded heavy chain-light chain pairs. All eight pairs were expressed and had neutralizing activity, thus producing lineage members CAP256-VRC26.26 to CAP256-VRC26.33.

Characteristics of the new CAP256-VRC26 antibodies. The 21 new CAP256-VRC26 antibodies showed a range in the levels of nucleotide mutations from the sequences of the germ line genes: mutations in 4.2 to 18% of the nucleotides compared with the sequences of the VH3-30*18 alleles and 2.5 to 15% of the nucleotides compared with the sequences of the VL1-51*02 alleles

Downloaded from http://jvi.asm.org/ on December 21, 2015 by Penny Moore

TABLE 1 Genetic and neutralization characteristics of CAP256-VRC26 antibodies[a]

Source (wk, isolation method)	Antibody name	% mutation from the sequence of the following allele:		CDRH3 length (no. of amino acids)	Neutralization of 46 strains	
		VH3-30*18	VL1-51*02		% neutralization breadth	Median IC_{50} (μg/ml)
Wk 59, culture	*CAP256-VRC26.01*	*8.3*	*3.9*	*35*	*20*	*3.32*
Wk 119, culture	*CAP256-VRC26.02*	*8.7*	*4.9*	*35*	*17*	*0.44*
	CAP256-VRC26.03	*8.7*	*7.4*	*35*	*35*	*0.06*
	CAP256-VRC26.04	*9.0*	*8.1*	*35*	*30*	*0.27*
	CAP256-VRC26.05	*10*	*5.6*	*35*	*22*	*0.02*
	CAP256-VRC26.06	*11*	*7.4*	*36*	*17*	*0.69*
	CAP256-VRC26.07	*12*	*7.7*	*35*	*13*	*5.00*
	CAP256-VRC26.08	*12*	*9.8*	*37*	*46*	*0.08*
	CAP256-VRC26.09	*14*	*9.8*	*37*	*46*	*0.02*
Wk 206, culture	*CAP256-VRC26.10*	*12*	*3.9*	*35*	*24*	*0.35*
	CAP256-VRC26.11	*13*	*14*	*35*	*26*	*1.04*
	CAP256-VRC26.12	*15*	*8.4*	*35*	*7*	*0.21*
	CAP256-VRC26.13	**15**	**9.5**	**35**	**7**	**0.09**
Wk 119, culture	**CAP256-VRC26.14**	**10**	**7.7**	**35**	**24**	**0.75**
	CAP256-VRC26.15	**10**	**6.7**	**35**	**33**	**0.34**
	CAP256-VRC26.16	**10**	**7.7**	**35**	**28**	**0.67**
	CAP256-VRC26.17	**12**	**8.1**	**35**	**28**	**0.14**
	CAP256-VRC26.18	**12**	**7.4**	**35**	**26**	**1.66**
Wk 206, culture	**CAP256-VRC26.19**	**13**	**10**	**35**	**46**	**0.16**
	CAP256-VRC26.20	**16**	**13**	**37**	**2**	**1.87**
	CAP256-VRC26.21	**18**	**14**	**37**	**13**	**0.58**
Wk 193, culture	**CAP256-VRC26.22**	**16**	**13**	**37**	**46**	**0.04**
	CAP256-VRC26.23	**9.7**	**6.3**	**35**	**7**	**0.03**
	CAP256-VRC26.24	**4.2**	**2.5**	**35**	**7**	**0.46**
	CAP256-VRC26.25	**12**	**9.8**	**36**	**63**	**0.003**
Wk 159, sorting with new probes	**CAP256-VRC26.26**	**17**	**9.8**	**37**	**59**	**0.05**
	CAP256-VRC26.27	**16**	**9.5**	**37**	**59**	**0.05**
	CAP256-VRC26.28	**15**	**12**	**37**	**41**	**0.08**
	CAP256-VRC26.29	**15**	**13**	**37**	**46**	**0.09**
	CAP256-VRC26.30	**16**	**13**	**37**	**28**	**0.76**
	CAP256-VRC26.31	**15**	**10**	**37**	**20**	**1.66**
	CAP256-VRC26.32	**11**	**15**	**35**	**20**	**0.10**
	CAP256-VRC26.33	**9.4**	**6.5**	**35**	**22**	**0.27**

[a] Italics indicate results for antibodies published previously (21); bold font indicates the results for antibodies that are newly reported here.

(Table 1). Similarly, they varied in the rates of mutations from the inferred sequence of the UCA: 7 to 23% of the nucleotides compared with the sequence of the UCA heavy chain and 3.6 to 17% of the nucleotides compared with the sequence of the UCA lambda chain (see Table S3 in the supplemental material). All had the long CDRH3s that are characteristic of this lineage (Table 1; see Table S3 in the supplemental material): 35 or 37 amino acids, as seen previously (21), or 36 amino acids in the case of CAP256-VRC26.25. As was observed with the initial set of MAbs, the new MAbs showed no or marginal autoreactivity when tested in multiple assays (see Fig. S1 in the supplemental material).

Like the original 12 lineage members, the new CAP256-VRC26 antibodies showed a range of neutralization breadth and potency. With a 46-virus multiclade panel, their neutralization breadth varied from 2% to 63% (Table 1; see also Table S4 in the supplemental material). The member of the lineage with the broadest neutralization breadth and the most potency was CAP256-VRC26.25, which had a median IC_{50} of 0.003 μg/ml for this panel, which makes it 10-fold more potent than the most potent family members described previously (21). Two others, CAP256-VRC26.26 and CAP256-VRC26.27, also had broader neutralization than previous relatives but were not as potent as CAP256-VRC26.25. The antibodies CAP256-VRC26.19, CAP256-VRC26.22, and CAP256-VRC26.29 were similar to CAP256-VRC26.08 in neutralization breadth, neutralizing 46% of this panel (Table 1).

We also isolated antibodies that showed less neutralization breadth and potency than previously isolated family members. The sequence of the antibody with the lowest level of somatic mutation, CAP256-VRC26.24, showed only 4.2% divergence from the sequence of the heavy chain germ line and 2.5% from the

Downloaded from http://jvi.asm.org/ on December 21, 2015 by Penny Moore

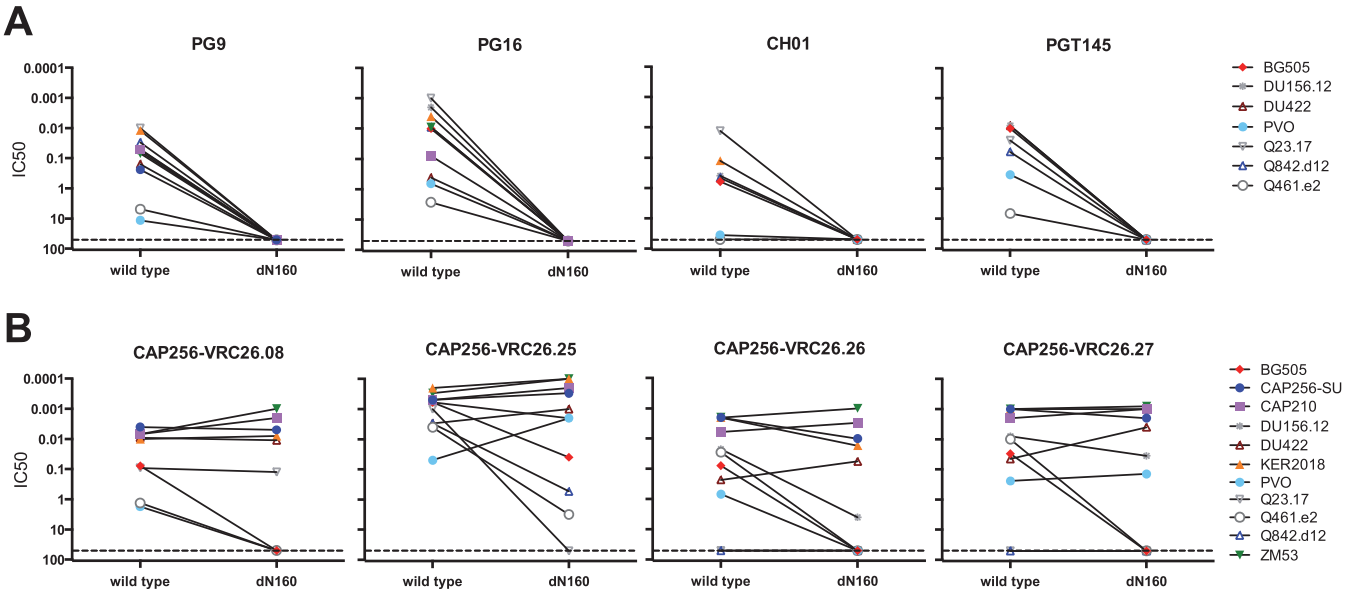


FIG 3 CAP256-VRC26 antibodies interact with N160 glycan in a potency-dependent manner. Wild-type Env pseudoviruses and mutants lacking the N160 glycan (dN160) were tested in a TZM-bl neutralization assay. Each pair of dots shows the IC_{50}s for one virus pair, with the results for the wild type being shown on the left and those for the mutant lacking the N160 glycan being shown on the right. Each graph shows data for one antibody. (A) Results for four representative PG9-like antibodies; (B) results for the four most potent CAP256-VRC26 antibodies.

sequence of the light chain. Its neutralization capacity was less broad than that of other early lineage members and it was less potent than other early lineage members, such as CAP256-VRC26.01 (Table 1). Other poor neutralizers included CAP256-VRC26.13; notably, it differed from CAP256-VRC26.12 by only 2 nucleotides or a single amino acid, even though they originated from different culture wells. An independent well yielded sequences that were 100% identical to the sequence of CAP256-VRC26.13. While these closely related lineage members were not broadly neutralizing, they did potently neutralize the autologous CAP256 superinfecting (SU) strain (see Table S4 in the supplemental material).

Like the previously identified members of the lineage (21), the new CAP256-VRC26 antibodies are highly dependent on a quaternary epitope and target V1V2. We assayed for binding to gp120 derived from HIV-1 strain CAP210, which is potently neutralized by all lineage members except CAP256-VRC26.20. None of the antibodies bound to this gp120 (see Fig. S2 in the supplemental material). CAP256-VRC26.25 was further tested on 10 additional clade C gp120s, with no binding being observed; however, it bound strongly to the BG505 SOSIP molecule, confirming the trimer preference of these antibodies. In addition, none of the 33 antibodies were able to neutralize R166A and K169E mutants in HIV-1 strain ConC (see Fig. S3A in the supplemental material), BG505.w2, or ZM53.12, and the 33 antibodies showed modest effects on ConC with mutations at amino acids 167 and 168, similar to the donor CAP256 plasma (28). Thus, the epitope recognized by the new CAP256-VRC26 antibodies is similar to that recognized by the previously described relatives.

Glycan independence of CAP256-VRC26 antibodies. The PG9-like broadly neutralizing antibodies (PG9/PG16, CH01-04, and the PGT145/PGDM1400-family antibodies) target a V1V2 epitope with quaternary epitope specificity (20, 22, 23, 59). These antibodies have been shown to require both glycan and protein contacts on Env (62, 63), with a strict dependence on the glycan at N160 (20, 22, 23, 42) and with contacts to other glycans, typically at N156 (62). We therefore investigated the glycan requirements of the CAP256-VRC26 antibodies. Removing the glycan at N156 did not abrogate neutralization; it conferred a slight decrease in potency against HIV-1 strains BG505 and ZM53 and variable effects against Q461.e2, similar to the effect that we observed with PG9 (see Fig. S3B in the supplemental material). However, removing the glycan at N160 had more dramatic effects. As expected, V1V2-directed antibodies PG9, PG16, CH01, and PGT145 were unable to neutralize glycan N160 mutants (Fig. 3A). In contrast, CAP256-VRC26 antibodies were affected in a potency-dependent manner. The N160 mutations had little effect on the susceptibility of viruses that were potently neutralized by CAP256-VRC26 antibodies but did reduce or abrogate the sensitivity of viruses that were less potently neutralized (Fig. 3B). When the data for all antibodies were combined, wild-type viruses with an IC_{50} of >0.1 μg/ml were more likely to show a neutralization reduction of at least 10-fold than the more potently neutralized viruses ($P = 0.029$, Fisher's exact test). Thus, the CAP256-VRC26 antibodies can maintain potent neutralization of viruses, despite the lack of the N160 glycan.

Phylogenetic analysis of the lineage. To deepen our understanding of the CAP256-VRC26 lineage, we placed the 12 previously cloned antibodies, together with the 21 new lineage members, within the context of total B cell transcripts. A revised algorithm (see Materials and Methods) was used to analyze 454 pyrosequencing-derived sequences from week 34 (64) and reanalyze all sequences from weeks 38 to 206 (21). Phylogenetic trees derived from maximum likelihood analysis of the transcripts of all members of the lineage, along with the 33 cloned antibody sequences, are displayed in Fig. 4. As noted previously (21), the tree for heavy chain sequences bifurcates into an upper branch and a lower branch. Sequences that map to the upper branch are plen-

Downloaded from http://jvi.asm.org/ on December 21, 2015 by Penny Moore

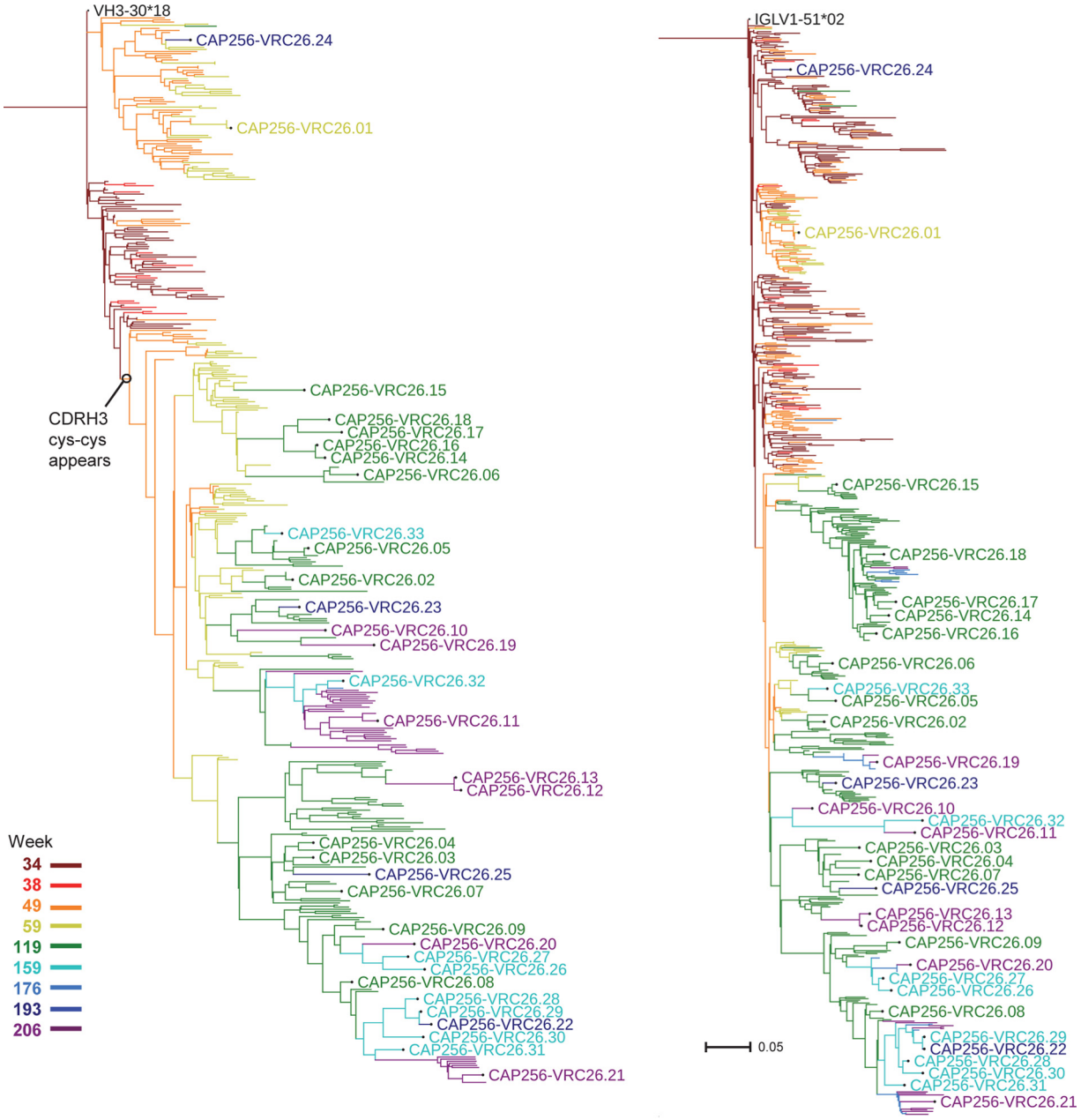


FIG 4 Development of the CAP256-VRC26 lineage. Maximum likelihood trees of heavy chain (left) and lambda chain (right) sequences. Labeled branches show heavy chains of antibodies from B cell cultures or probe sorts; unlabeled branches represent sequences from 454 pyrosequencing. The color coding indicates the time of sampling. The circle indicates the first node in which the signature Cys-Cys motif appears in the CDRH3. Scale, rate of nucleotide change (per site) between nodes.

tiful among B cell transcripts from weeks 34 to 59 but are rare among B cell transcripts obtained at week 119 or later. In contrast, the lower branch contains sequences from all time points. One notable feature of the sequences in the lower branch is a Cys-Cys which may stabilize the CDRH3 structure (21); it appears at week 49 and sequences from all subsequent times of the lower branch. Week 34 sequences do not contain Cys-Cys and appear in both the upper and lower branches of the tree.

The placement of the cloned antibodies on these trees led to several observations. The CAP256-VRC26.24 sequence is 4% mutated from the germ line sequence, clustered with week 59 sequences, and is located in the top (CAP256-VRC26.01) branch, yet it was isolated from week 193 PBMCs; we speculate that it is derived from a long-lived memory cell. CAP256-VRC26.25, the antibody with the broadest neutralization and greatest potency, has a 1-amino-acid insertion in the CDRH3 sequence compared to the UCA sequence (see Table S3 in the supplemental material) and lacks close relatives in the pyrosequencing data set, and its closest relatives are weakly neutralizing. Six of the eight antibodies that were derived from the probe sort, including the CAP256-VRC26.26 and CAP256-VRC26.27 antibodies with very broad neutralization capacities, cluster with other broad

Downloaded from http://jvi.asm.org/ on December 21, 2015 by Penny Moore

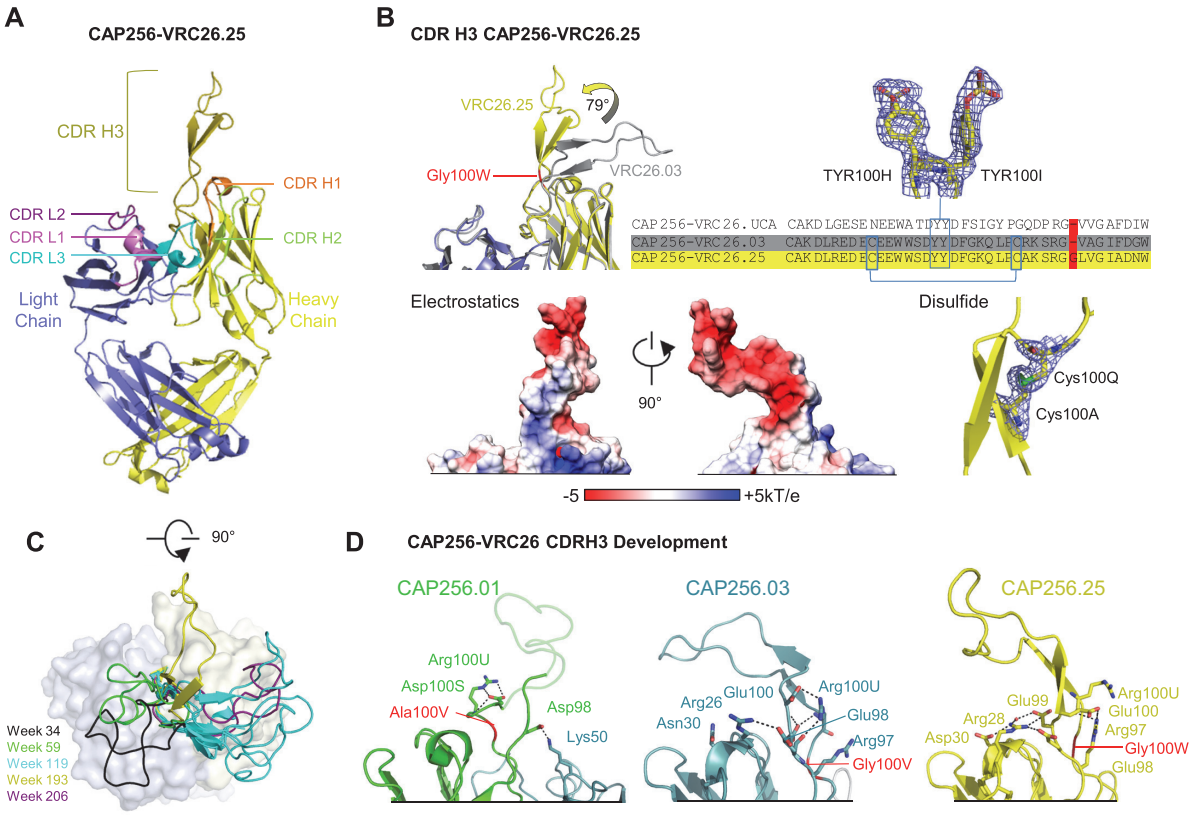


FIG 5 Structural characteristics of CAP256-VRC26.25. (A) Crystal structure of the antigen-binding fragment (Fab) of CAP256-VRC26.25 shown in ribbon diagram representation. CDRs are highlighted. (B) The CDRH3 of CAP256-VRC26.25 contains an inserted Gly and is rotated 79 degrees compared to the orientation of the other lineage members without the insertion. Gray, CAP256-VRC26.03; red, the location of the insertion in the structure and the sequence alignment. (Bottom left) The electrostatics of the highly anionic CDRH3 (charge, −7) in the same orientation in the image above. The CDRH3 contains two sulfated tyrosines and a disulfide bond (blue mesh, $2F_o$-F_c at 1 sigma). (Bottom right) Electron density of the disulfide bond acquired through affinity maturation. (C) The CDRH3s bend in different directions. All CAP256-VRC26 structures are shown, with CDRH3s projecting up from the top of the antibody. Loops are colored by the week of isolation: black, week 34, CAP256-VRC26.UCA; green, week 59, CAP256-VRC26.01; cyan, week 119, CAP256-VRC26.03, CAP256-VRC26.04, CAP256-VRC26.06, and CAP256-VRC26.07; yellow, week 193, CAP256-VRC26.25; purple, week 206, CAP256-VRC26.10. Disordered residues in the crystal structures were modeled using the Loopy program. These consist of 19, 14, 3, 11, and 10 residues for CAP256-VRC26.UCA, CAP256-VRC26.01, CAP256-VRC26.06, CAP256-VRC26.07, and CAP256-VRC26.10, respectively. All CDRH3 residues are well defined for CAP256-VRC26.03, CAP256-VRC26.04, and CAP256-VRC26.25. (D) The orientation at the base of the protruding CDRH3 loop is partially stabilized through interactions with residues in the CDRH1. Shown are interactions for CAP256-VRC26.01, CAP256-VRC26.03, and CAP256-VRC26.25. Modeled residues of CAP256-VRC26.01 are transparent.

neutralizers, CAP256-VRC26.08, CAP256-VRC26.09, and CAP256-VRC26.22; all of these bear a 2-amino-acid insertion in the CDRH3 sequence compared to the UCA sequence. However, weak neutralizers CAP256-VRC26.20, CAP256-VRC26.30, and CAP256-VRC26.31 also appear in this cluster and have this insertion. Thus, the antibodies that are the most closely genetically related do not always display the same level of neutralizing activity.

CAP256-VRC26.25 structure. To investigate the differences in neutralization potency and breadth among these antibodies, we solved the crystal structure of the CAP256-VRC26.25 antigen-binding fragment (Fab) to 2 Å. The structure was well defined, including the electron density for the entire CDRH3. Like the other lineage members, this antibody has a long CDRH3 projecting away from the body of the Fab (Fig. 5A). A disulfide bond was observed near the base of the CDRH3, as expected, and density confirming the two computationally predicted sulfated tyrosines was also visible (Fig. 5B). We compared this structure to the structures solved previously for seven other lineage members; of these, CAP256-VRC26.03 had a complete CDRH3 structure, while several others contained disordered regions of various lengths in the CDRH3 (21). Notably, the CDRH3 of CAP256-VRC26.25 bends in a considerably different direction than the others. The angle of rotation between the CDRH3s of Fabs CAP256-VRC26.03 and CAP256-VRC26.25, aligned by framework regions, is 79 degrees (Fig. 5B). When all structures are overlaid (Fig. 5C), we observe that the UCA and the early antibody CAP256-VRC26.01 bend in a similar direction, CAP256-VRC26.03, CAP256-VRC26.04, CAP256-VRC26.06, CAP256-VRC26.07, and CAP256-VRC26.10 bend in nearly the opposite direction, and CAP256-VRC26.25 bends in a direction different from the direction of all of these. The angle likely depends on the identity of amino acid at position 100V or 100W. The Gly of CAP256-VRC26.25 inserted at the base of the CDRH3 allows additional flexibility in the initial projection of the CDRH3, providing a different range of angles for the antibody to initially engage the viral spike (Fig. 5D). Thus, stabilization of the overall CDRH3 structure combined with a local flexibility at the base may contribute to the improved neutralization breadth and

Downloaded from http://jvi.asm.org/ on December 21, 2015 by Penny Moore

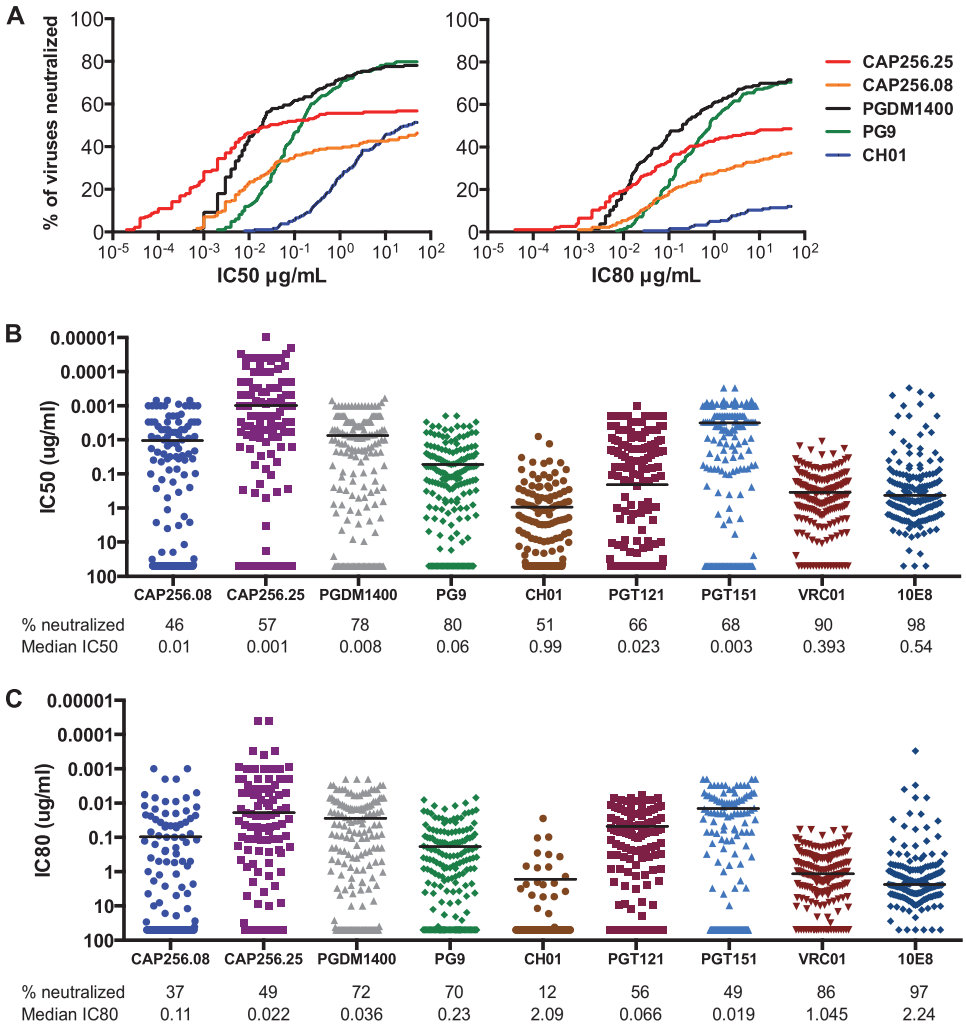


FIG 6 Neutralization breadth and potency of CAP256-VRC26.08, CAP256-VRC26.25, and selected broadly neutralizing antibodies. The neutralization of a multiclade virus panel ($n = 183$) was assessed by a TZM-bl pseudovirus assay. (A) Neutralization breadth-potency curves for V1V2-directed bNAbs. Curves show the percentage of virus neutralized at any given IC_{50} or IC_{80}. (B, C) Neutralization by bNAbs directed to diverse epitopes. Each dot shows the value for a single virus. Bars, median value of viruses that are neutralized. (B) IC_{50}s; (C) IC_{80}s.

potency of CAP256-VRC26.25 compared to those of the other lineage members.

CAP256-VRC26.25 has broad neutralization and is highly potent. CAP256-VRC26.25 is the most potent member of the lineage. On a multiclade panel of 183 Env pseudoviruses, it neutralized 57% of isolates with a median IC_{50} of 0.001 µg/ml (Fig. 6; see also Table S5 in the supplemental material), which makes it 10-fold more potent than the previously published CAP256-VRC26.08 variant. We also compared CAP256-VRC26.08 and CAP256-VRC26.25 to the V1V2-directed antibodies PGDM1400, PG9, and CH01 (Fig. 6A) and additional antibodies to other neutralization epitopes (Fig. 6B and C; see also Table S5 in the supplemental material). A remarkable characteristic of CAP256-VRC26.25 is the highly potent neutralization of some viruses. This can be seen as the leftward shift of the potency-breadth plots compared to the locations of the results for the other antibodies (Fig. 6A) and as dots close to an IC_{50} of 0.0001 µg/ml on the scatter plot (Fig. 6B).

We also examined the completeness of neutralization. Like other V1V2-directed broadly neutralizing antibodies (23, 65), the CAP256-VRC26 antibodies neutralize some viruses to a maximum of less than 90%. About 30% of sensitive viruses were neutralized with this plateau effect. This fraction is very similar to that for the V1V2-directed bNAb PGDM1400 (see Fig. S4 in the supplemental material).

To further characterize and compare the new CAP256-VRC26-lineage antibodies, we tested variants CAP256-VRC26.08, CAP256-VRC26.25, CAP256-VRC26.26, and CAP256-VRC26.27 on a multiclade panel of Env pseudoviruses (see Table S5 in the supplemental material). CAP256-VRC26.26 and CAP256-VRC26.27 have neutralization capacities nearly as broad as the neutralization capacity of CAP256-VRC26.25 at a cutoff of 50 µg/ml but less so at an IC_{50} of <0.01 µg/ml (Fig. 7A), confirming the superior potency of CAP256-VRC26.25. We also analyzed the neutralization breadth within different HIV-1 clades (Fig. 7B). Against clade C, CAP256-VRC26.25 had a neutralization breadth of 70% at the IC_{50} level (Fig. 7B; see also Fig. S5 in the supplemental material), with even greater coverage of strains from clade G

Downloaded from http://jvi.asm.org/ on December 21, 2015 by Penny Moore

A

% Neutralized (IC50)	CAP256-VRC26.08	CAP256-VRC26.25	CAP256-VRC26.26	CAP256-VRC26.27
<50ug/ml	47	58	59	55
<10ug/ml	43	58	55	53
<1.0ug/ml	40	57	51	48
<0.1ug/ml	35	53	40	42
<0.01ug/ml	22	46	34	35

% Neutralized (IC80)	CAP256-VRC26.08	CAP256-VRC26.25	CAP256-VRC26.26	CAP256-VRC26.27
<50ug/ml	37	49	49	43
<10ug/ml	34	48	42	42
<1.0ug/ml	28	42	33	35
<0.1ug/ml	20	33	28	28
<0.01ug/ml	14	18	21	22

B

		% of viruses neutralized (IC50<50)			
Clade	N	CAP256-VRC26.08	CAP256-VRC26.25	CAP256-VRC26.26	CAP256-VRC26.27
A	26	46	69	58	58
AE	21	43	48	57	57
AG	16	56	81	69	69
B	40	3	15	13	10
BC	10	70	100	80	80
C	57	67	70	72	67
D	8	50	63	75	63
G	7	57	71	71	71
other	13	69	69	69	62
All	198	47	58	59	55
non-B	158	58	70	68	65

		% of viruses neutralized (IC80<50)			
Clade	N	CAP256-VRC26.08	CAP256-VRC26.25	CAP256-VRC26.26	CAP256-VRC26.27
A	26	27	54	38	35
AE	21	33	48	52	48
AG	16	50	69	63	56
B	40	0	10	8	3
BC	10	60	80	60	60
C	57	53	60	63	60
D	8	38	63	50	50
G	7	57	71	71	57
other	13	62	62	46	46
All	198	37	49	49	43
non-B	158	46	60	56	52

other: AC, ACD, AD, CD

FIG 7 Neutralization breadth, potency, and clade dependency of CAP256-VRC26 antibodies. The neutralization of large virus panels was assessed by a TZM-bl pseudovirus assay. (Left) IC_{50}s; (right) IC_{80}s. (A) Values indicate the percentage of viruses ($n = 198$) neutralized at the given cutoff; (B) values indicate the percentage of viruses neutralized within each virus clade.

and circulating recombinant forms AG and BC. While CAP256-VRC26.25 neutralized 70% of non-clade B strains overall, it neutralized only 15% of clade B strains. To understand the basis of this preference, we performed an amino acid frequency analysis (53) for positions 154 to 184 in V2. Specifically, based on sequence alignments, we searched for amino acids that were preferentially found among CAP256-VRC26.25-resistant strains versus CAP256-VRC26.25-sensitive strains for each residue position in V2 (Fig. 8A). Amino acids that were associated with resistance were found in at least one position among positions 166, 167, and 169 in 59% of resistant strains. These amino acids were observed in 71% of clade B strains and in 80% of resistant clade B strains. Conversely, the amino acid K or R at position 169 occurred in 86% of sensitive strains but in only 5% of clade B strains, with similar proportions occurring for D or E at position 164 (Fig. 8B). The occurrence of resistance-associated amino acids at one or more of these positions was statistically significant ($P < 0.001$ for each comparison, Fisher's exact test), as was the occurrence of the sensitivity-associated amino acids at positions 164 and 169. Thus, the characteristics of clade B sequences at V2 positions 164, 166, 167, and 169 may explain much of the resistance found in clade B strains.

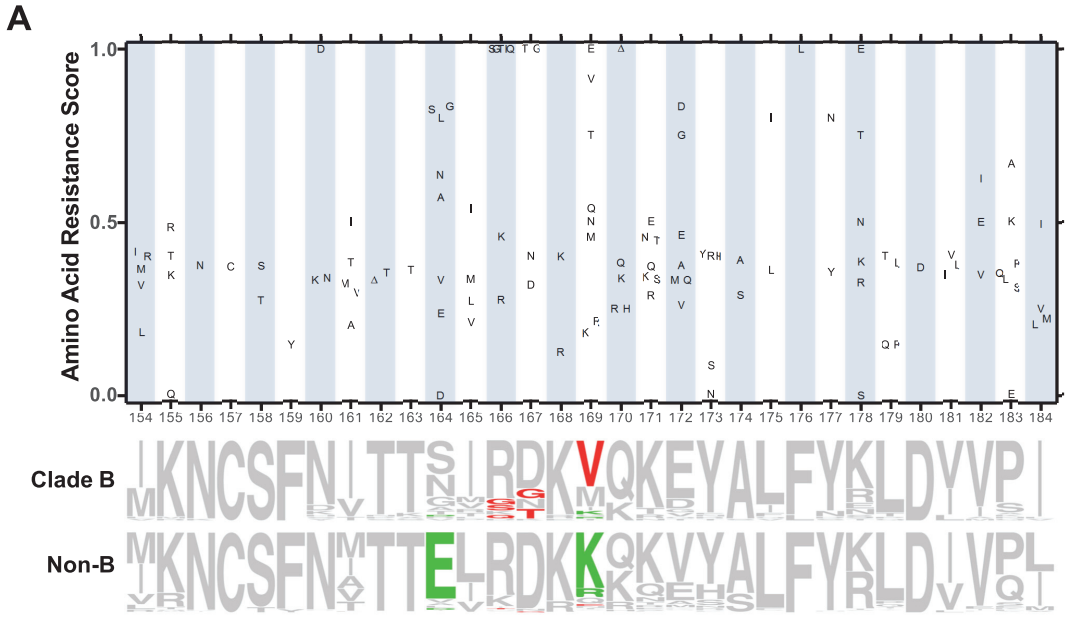
DISCUSSION

The data in this study provide a more comprehensive picture of the CAP256-VRC26 bNAb lineage. Using modified PCR primers, B cell culture, and trimeric Env-based probes, we isolated 21 new members of the CAP256-VRC26 family. Several of these new antibodies showed an increased neutralization breadth and potency compared to those of previously published antibodies of this lineage, particularly against HIV-1 clade C strains and other subtypes prevalent in sub-Saharan Africa. CAP256-VRC26.25 in particular showed exceptional potency, with a median IC_{50} against neutralized viruses of 0.001 μg/ml.

We isolated new clonal relatives of the CAP256-VRC26 lineage by two methods: B cell culture and antigen-specific B cell sorting. The differential BG505 SOSIP and BG505 SOSIP.K169E protein sorting approach proved to be a highly efficient and specific method for isolating new members of the CAP256-VRC26 lineage. Here, 11/14 sorted cells yielded CAP256-VRC26-lineage members, and two of the three most broadly neutralizing lineage members were isolated from the probe sort. The availability of nearly native trimers has potential for use in sorting for V1V2-directed and other quaternary epitope-specific antibodies in other donors (59), while the K169E mutant described here may have utility for additional donors with serum neutralization dependence on this V2 residue. However, this method has some limitations. Not all Env epitopes are displayed on the BG505 SOSIP molecule: the MPER region of gp41 is not contained in this construct, and some antibodies may not recognize the BG505 sequence. With regard to differential sorting with a knockout mutant, not all donors have neutralization activity that can be matched to that of a wild-type probe–mutant probe pair. Thus, the advantage of B cell culture is that it does not require a probe or, indeed, any *a priori* knowledge of the antibody specificity. Additionally, since the wells are screened by neutralization, there may be selection for the detection of highly potent antibodies. However, B cell culture is more labor-intensive and time-consuming than single-cell sorting and is most successful when the donor has high plasma neutralization titers (N. A. Doria-Rose and N. Longo, unpublished observations). In addition, culture conditions can induce *in vitro* class switching, which complicates the recovery

Downloaded from http://jvi.asm.org/ on December 21, 2015 by Penny Moore

A



B

Association	Position	Amino Acid	% of sequences with the indicated amino acid			
			Sensitive	Resistant	Non-Clade B	Clade B
Sensitivity	164	D or E	84%	42%	85%	3%
	169	R or K	86%	33%	81%	5%
Resistance	166	G,I,Q,S, or T	0%	23%	6%	20%
	167	T or G	0%	18%	2%	25%
	169	E or V	2%	34%	3%	55%
	one or more of the above		2%	59%	10%	73%

FIG 8 CAP256-VRC26.25 resistance analysis of amino acids in Env V2. (A) (Top) Amino acid frequency analysis. A total of 198 sequences were analyzed (see Fig. S6 in the supplemental material). The resistance score for each possible amino acid at a given residue position was defined as the ratio of its number of occurrences in sequences from CAP256-VRC26.25-resistant viruses to its overall number of occurrences. A higher score indicates that the amino acid was preferentially found among sequences from resistant viruses, with a score of 1 indicating that the amino was found only among sequences from resistant viruses. Amino acids that occurred at least 3 times at the given position are shown. (Bottom) Logo plot showing the frequency of all amino acids at each position for clade B ($n = 40$) and non-clade B ($n = 158$) sequences. Red, amino acids associated with resistance; green, amino acids associated with sensitivity. (B) Frequency of amino acids at positions associated with resistance or sensitivity. Values indicate the percentage of sequences in a given category that bear the indicated amino acids. For example, 84% of Env sequences from sensitive strains have D or E at position 164. A total of 125 sensitive strains and 73 resistant strains were analyzed. *P* was <0.001 for each comparison (Fisher's exact test with the Bonferroni correction).

of sequences by PCR, though this can be overcome by using IgA constant region primers. Of note, the most potent member of the lineage (CAP256-VRC26.25) was isolated from a B cell culture, attesting to the advantages of high-throughput functional screening.

Phylogenetic analysis of the complete CAP256-VRC26 lineage shows two main branches. The first branch, which included CAP256-VRC26.01 and CAP256-VRC26.24, may be an evolutionary dead end, in that members of the branch could not be detected in the B cell transcripts from time points after week 119. We recently showed that the antibodies in this branch were unable to tolerate viral escape mutations and were no longer selected for (64). The Cys-Cys disulfide bond in CDRH3 emerged in the second branch, and that sublineage continued to evolve, with sequences being observed at all time points. Within this sublineage, however, antibodies with broad or narrow heterologous neutralization are intermingled. This suggests that individual amino acid changes, rather than overall sequence relatedness, have greater effects on the neutralization capacity. Similarly, the levels of mutation compared with the sequence of the germ line V gene or that of the UCA did not correlate with neutralization. A similar pattern has been noted for other bNAb lineages (22, 59, 66). These observations suggest that somatic variant antibodies with a variety of antiviral capacities frequently evolve side-by-side during chronic HIV infection. The concurrent diversification of the viral quasispecies may drive this evolution: while some antibody mutations may improve the binding to specific autologous viral variants encountered in the germinal center, they may not be the same mutations that improve the neutralization breadth against heterologous viruses.

The CAP256-VRC26 antibodies share many characteristics with the three other published lineages of V1V2 directed broadly neutralizing antibodies: the PG9, PGT145, and CH01 lineages (20, 22, 23, 59). These antibodies have long, anionic CDRH3s, exhibit incomplete neutralization of some viruses (65), and share epitope requirements: they are highly quaternary epitope specific and pre-

Downloaded from http://jvi.asm.org/ on December 21, 2015 by Penny Moore

fer positive charges in strand C of V2 (53), and their activity is knocked out by a K169E mutation. However, in contrast to the three other lineages, which show a strong dependence on the N160 glycan (Fig. 3) (42), the CAP256-VRC26 antibodies showed variable and limited dependence on this glycan. The more potent that the antibody-mediated neutralization was, the less dependent it was on the presence of the N160 glycan. We speculate that potent neutralization is mediated mainly by protein-protein contacts but that more weakly recognized strains are bound via contacts with both protein and glycan. It is also possible that alternative glycans are bound when the N160 glycan is missing. Future structural studies may provide a better understanding of the mechanism. Notably, a mutant form of PG9 with increased potency was shown to neutralize some viruses lacking the N160 glycan (67); this observation is consistent with the notion that the very high potency of CAP256-VRC26.25 may relate to the lack of N160 glycan dependency.

CAP256-VRC26.25 neutralized 15% of clade B HIV-1 strains and 70% of non-clade B HIV-1 strains. Amino acids associated with sensitivity or resistance were noted at positions 164, 166, 167, and 169. The residues associated with sensitivity—D or E at position 164 and R or K at position 169—were rare in clade B; conversely, resistance-associated amino acids were more common in clade B strains than non-clade B strains. Of note, several of these preferences mirror the neutralization activity of the donor's plasma (28); furthermore, escape mutations that arose in the CAP256 donor virus near the time point of CAP256-VRC26.25 isolation include S at position 166 and E at position 169 (21, 64), both of which were associated with resistance in this virus panel.

In summary, we isolated 21 new members of the CAP256-VRC26 lineage, including 3 variants that have a broader neutralization capacity than the previously isolated family members. The best variant, CAP256-VRC26.25, was 10-fold more potent than the previously published members of this lineage, and its overall potency (IC_{50} = 0.001 μg/ml) was comparable to or better than that of existing bNAbs. In addition, the neutralization capacity of CAP256-VRC26.25 was quite broad, neutralizing ~60% of all viruses and ~ 70% of non-clade B viruses, including clade C viruses. The mechanism of its outstanding potency may relate to the reduced dependence on N160 glycan, the unique CDRH3 conformation, or other structural features that have yet to be elucidated. The high potency of this antibody may make it an attractive candidate for clinical development for prevention of infection or as part of antiretroviral regimens to treat HIV-1 infection.

ACKNOWLEDGMENTS

We thank the participants in the CAPRISA 002 study for their commitment. For technical assistance and advice, we thank the CAPRISA 002 clinical team, Natasha Samsunder, Shannie Heeralall, Ellen Turk, Chien-Li Lin, and Robert Banks. We thank Nancy S. Longo, Johannes Scheid, and Xueling Wu for advice on the development of PCR protocols and Brenda Hartman and Andrea Shiakolas for assistance with manuscript preparation. We thank J. Baalwa, D. Ellenberger, F. Gao, B. Hahn, K. Hong, J. Kim, F. McCutchan, D. Montefiori, L. Morris, J. Overbaugh, E. Sanders-Buell, G. Shaw, R. Swanstrom, M. Thomson, S. Tovanabutra, C. Williamson, and L. Zhang for contributing the HIV-1 envelope plasmids used in our neutralization panel.

FUNDING INFORMATION

National Institutes of Health provided funding to Penny L. Moore, Lynn Morris, Peter D. Kwong, and John R. Mascola under grant number AI116086-01. South African Medical Research Council provided funding to Penny L. Moore under grant number D1407250-01. Wellcome Trust provided funding to Penny L. Moore under grant number 089933/Z/09/Z.

CAPRISA is funded by the South African HIV/AIDS Research and Innovation Platform of the South African Department of Science and Technology and was initially supported by National Institute of Allergy and Infectious Diseases, National Institutes of Health, U.S. Department of Health and Human Services, grant U19 AI51794 (to Salim Abdool-Karim). The Columbia University-Southern African Fogarty AIDS International Training and Research Program, through the Fogarty International Center, National Institutes of Health, provided funding to Jinal N. Bhiman, Penny L. Moore, and Lynn Morris under grant number 5 D43 TW000231. Jinal N. Bhiman received a University of the Witwatersrand Postgraduate Merit Award as well as bursaries from the Poliomyelitis Research Foundation and the National Research Foundation of South Africa. Funding was provided by the intramural research programs of the Vaccine Research Center, Division of Intramural Research, National Institute of Allergy and Infectious Diseases, National Institutes of Health, USA. Use of sector 22 (Southeast Region Collaborative Access Team) at the Advanced Photon Source was supported by the US Department of Energy, Basic Energy Sciences, Office of Science, under contract number W-31-109-Eng-38. The funders had no role in study design, data collection and interpretation, or the decision to submit the work for publication.

REFERENCES

1. **Doria-Rose NA, Klein RM, Daniels MG, O'Dell S, Nason M, Lapedes A, Bhattacharya T, Migueles SA, Wyatt RT, Korber BT, Mascola JR, Connors M.** 2010. Breadth of human immunodeficiency virus-specific neutralizing activity in sera: clustering analysis and association with clinical variables. J Virol **84:**1631–1636. http://dx.doi.org/10.1128/JVI.01482-09.
2. **Hraber P, Seaman MS, Bailer RT, Mascola JR, Montefiori DC, Korber BT.** 2014. Prevalence of broadly neutralizing antibody responses during chronic HIV-1 infection. AIDS **28:**163–169. http://dx.doi.org/10.1097/QAD.0000000000000106.
3. **Simek MD, Rida W, Priddy FH, Pung P, Carrow E, Laufer DS, Lehrman JK, Boaz M, Tarragona-Fiol T, Miiro G, Birungi J, Pozniak A, McPhee DA, Manigart O, Karita E, Inwoley A, Jaoko W, Dehovitz J, Bekker LG, Pitisuttithum P, Paris R, Walker LM, Poignard P, Wrin T, Fast PE, Burton DR, Koff WC.** 2009. Human immunodeficiency virus type 1 elite neutralizers: individuals with broad and potent neutralizing activity identified by using a high-throughput neutralization assay together with an analytical selection algorithm. J Virol **83:**7337–7348. http://dx.doi.org/10.1128/JVI.00110-09.
4. **Sather DN, Armann J, Ching LK, Mavrantoni A, Sellhorn G, Caldwell Z, Yu X, Wood B, Self S, Kalams S, Stamatatos L.** 2009. Factors associated with the development of cross-reactive neutralizing antibodies during human immunodeficiency virus type 1 infection. J Virol **83:**757–769. http://dx.doi.org/10.1128/JVI.02036-08.
5. **Mascola JR, Haynes BF.** 2013. HIV-1 neutralizing antibodies: understanding nature's pathways. Immunol Rev **254:**225–244. http://dx.doi.org/10.1111/imr.12075.
6. **Excler JL, Robb ML, Kim JH.** 2015. Prospects for a globally effective HIV-1 vaccine. Vaccine http://dx.doi.org/10.1016/j.vaccine.2015.03.059.
7. **Overbaugh J, Morris L.** 2012. The antibody response against HIV-1. Cold Spring Harb Perspect Med **2:**a007039. http://dx.doi.org/10.1101/cshperspect.a007039.
8. **Klein F, Mouquet H, Dosenovic P, Scheid JF, Scharf L, Nussenzweig MC.** 2013. Antibodies in HIV-1 vaccine development and therapy. Science **341:**1199–1204. http://dx.doi.org/10.1126/science.1241144.
9. **Doria-Rose NA, Joyce MG.** 2015. Strategies to guide the antibody affinity maturation process. Curr Opin Virol **11:**137–147. http://dx.doi.org/10.1016/j.coviro.2015.04.002.
10. **Haynes BF, Kelsoe G, Harrison SC, Kepler TB.** 2012. B-cell-lineage

Downloaded from http://jvi.asm.org/ on December 21, 2015 by Penny Moore

immunogen design in vaccine development with HIV-1 as a case study. Nat Biotechnol **30:**423–433. http://dx.doi.org/10.1038/nbt.2197.

11. **Julien JP, Cupo A, Sok D, Stanfield RL, Lyumkis D, Deller MC, Klasse PJ, Burton DR, Sanders RW, Moore JP, Ward AB, Wilson IA.** 2013. Crystal structure of a soluble cleaved HIV-1 envelope trimer. Science **342:** 1477–1483. http://dx.doi.org/10.1126/science.1245625.
12. **Pancera M, Zhou T, Druz A, Georgiev IS, Soto C, Gorman J, Huang J, Acharya P, Chuang GY, Ofek G, Stewart-Jones GB, Stuckey J, Bailer RT, Joyce MG, Louder MK, Tumba N, Yang Y, Zhang B, Cohen MS, Haynes BF, Mascola JR, Morris L, Munro JB, Blanchard SC, Mothes W, Connors M, Kwong PD.** 2014. Structure and immune recognition of trimeric pre-fusion HIV-1 Env. Nature **514:**455–461. http://dx.doi.org/10.1038/nature13808.
13. **Lyumkis D, Julien JP, de Val N, Cupo A, Potter CS, Klasse PJ, Burton DR, Sanders RW, Moore JP, Carragher B, Wilson IA, Ward AB.** 2013. Cryo-EM structure of a fully glycosylated soluble cleaved HIV-1 envelope trimer. Science **342:**1484–1490. http://dx.doi.org/10.1126/science.1245627.
14. **Kwong PD, Mascola JR.** 2012. Human antibodies that neutralize HIV-1: identification, structures, and B cell ontogenies. Immunity **37:**412–425. http://dx.doi.org/10.1016/j.immuni.2012.08.012.
15. **Wibmer CK, Moore PL, Morris L.** 2015. HIV broadly neutralizing antibody targets. Curr Opin HIV AIDS **10:**135–143. http://dx.doi.org/10.1097/COH.0000000000000153.
16. **Burton DR, Mascola JR.** 2015. Antibody responses to envelope glycoproteins in HIV-1 infection. Nat Immunol **16:**571–576. http://dx.doi.org/10.1038/ni.3158.
17. **Kwong PD, Mascola JR, Nabel GJ.** 2013. Broadly neutralizing antibodies and the search for an HIV-1 vaccine: the end of the beginning. Nat Rev Immunol **13:**693–701. http://dx.doi.org/10.1038/nri3516.
18. **Walker LM, Simek MD, Priddy F, Gach JS, Wagner D, Zwick MB, Phogat SK, Poignard P, Burton DR.** 2010. A limited number of antibody specificities mediate broad and potent serum neutralization in selected HIV-1 infected individuals. PLoS Pathog **6:**e1001028. http://dx.doi.org/10.1371/journal.ppat.1001028.
19. **Georgiev IS, Doria-Rose NA, Zhou T, Kwon YD, Staupe RP, Moquin S, Chuang GY, Louder MK, Schmidt SD, Altae-Tran HR, Bailer RT, McKee K, Nason M, O'Dell S, Ofek G, Pancera M, Srivatsan S, Shapiro L, Connors M, Migueles SA, Morris L, Nishimura Y, Martin MA, Mascola JR, Kwong PD.** 2013. Delineating antibody recognition in polyclonal sera from patterns of HIV-1 isolate neutralization. Science **340:** 751–756. http://dx.doi.org/10.1126/science.1233989.
20. **Bonsignori M, Hwang KK, Chen X, Tsao CY, Morris L, Gray E, Marshall DJ, Crump JA, Kapiga SH, Sam NE, Sinangil F, Pancera M, Yongping Y, Zhang B, Zhu J, Kwong PD, O'Dell S, Mascola JR, Wu L, Nabel GJ, Phogat S, Seaman MS, Whitesides JF, Moody MA, Kelsoe G, Yang X, Sodroski J, Shaw GM, Montefiori DC, Kepler TB, Tomaras GD, Alam SM, Liao HX, Haynes BF.** 2011. Analysis of a clonal lineage of HIV-1 envelope V2/V3 conformational epitope-specific broadly neutralizing antibodies and their inferred unmutated common ancestors. J Virol **85:**9998–10009. http://dx.doi.org/10.1128/JVI.05045-11.
21. **Doria-Rose NA, Schramm CA, Gorman J, Moore PL, Bhiman JN, DeKosky BJ, Ernandes MJ, Georgiev IS, Kim HJ, Pancera M, Staupe RP, Altae-Tran HR, Bailer RT, Crooks ET, Cupo A, Druz A, Garrett NJ, Hoi KH, Kong R, Louder MK, Longo NS, McKee K, Nonyane M, O'Dell S, Roark RS, Rudicell RS, Schmidt SD, Sheward DJ, Soto C, Wibmer CK, Yang Y, Zhang Z, Mullikin JC, Binley JM, Sanders RW, Wilson IA, Moore JP, Ward AB, Georgiou G, Williamson C, Abdool Karim SS, Morris L, Kwong PD, Shapiro L, Mascola JR.** 2014. Developmental pathway for potent V1V2-directed HIV-neutralizing antibodies. Nature **509:**55–62. http://dx.doi.org/10.1038/nature13036.
22. **Walker LM, Huber M, Doores KJ, Falkowska E, Pejchal R, Julien JP, Wang SK, Ramos A, Chan-Hui PY, Moyle M, Mitcham JL, Hammond PW, Olsen OA, Phung P, Fling S, Wong CH, Phogat S, Wrin T, Simek MD, Koff WC, Wilson IA, Burton DR, Poignard P.** 2011. Broad neutralization coverage of HIV by multiple highly potent antibodies. Nature **477:**466–470. http://dx.doi.org/10.1038/nature10373.
23. **Walker LM, Phogat SK, Chan-Hui PY, Wagner D, Phung P, Goss JL, Wrin T, Simek MD, Fling S, Mitcham JL, Lehrman JK, Priddy FH, Olsen OA, Frey SM, Hammond PW, Kaminsky S, Zamb T, Moyle M, Koff WC, Poignard P, Burton DR.** 2009. Broad and potent neutralizing antibodies from an African donor reveal a new HIV-1 vaccine target. Science **326:**285–289. http://dx.doi.org/10.1126/science.1178746.
24. **Julien JP, Lee JH, Cupo A, Murin CD, Derking R, Hoffenberg S, Caulfield MJ, King CR, Marozsan AJ, Klasse PJ, Sanders RW, Moore JP, Wilson IA, Ward AB.** 2013. Asymmetric recognition of the HIV-1 trimer by broadly neutralizing antibody PG9. Proc Natl Acad Sci U S A **110:**4351–4356. http://dx.doi.org/10.1073/pnas.1217537110.
25. **Huang J, Kang BH, Pancera M, Lee JH, Tong T, Feng Y, Imamichi H, Georgiev IS, Chuang GY, Druz A, Doria-Rose NA, Laub L, Sliepen K, van Gils MJ, de la Pena AT, Derking R, Klasse PJ, Migueles SA, Bailer RT, Alam M, Pugach P, Haynes BF, Wyatt RT, Sanders RW, Binley JM, Ward AB, Mascola JR, Kwong PD, Connors M.** 2014. Broad and potent HIV-1 neutralization by a human antibody that binds the gp41-gp120 interface. Nature **515:**138–142. http://dx.doi.org/10.1038/nature13601.
26. **Pinter A, Honnen WJ, He Y, Gorny MK, Zolla-Pazner S, Kayman SC.** 2004. The V1/V2 domain of gp120 is a global regulator of the sensitivity of primary human immunodeficiency virus type 1 isolates to neutralization by antibodies commonly induced upon infection. J Virol **78:**5205–5215. http://dx.doi.org/10.1128/JVI.78.10.5205-5215.2004.
27. **Doores KJ, Burton DR.** 2010. Variable loop glycan dependency of the broad and potent HIV-1-neutralizing antibodies PG9 and PG16. J Virol **84:**10510–10521. http://dx.doi.org/10.1128/JVI.00552-10.
28. **Moore PL, Gray ES, Sheward D, Madiga M, Ranchobe N, Lai Z, Honnen WJ, Nonyane M, Tumba N, Hermanus T, Sibeko S, Mlisana K, Abdool Karim SS, Williamson C, Pinter A, Morris L.** 2011. Potent and broad neutralization of HIV-1 subtype C by plasma antibodies targeting a quaternary epitope including residues in the V2 loop. J Virol **85:**3128–3141. http://dx.doi.org/10.1128/JVI.02658-10.
29. **Moore PL, Sheward D, Nonyane M, Ranchobe N, Hermanus T, Gray ES, Abdool Karim SS, Williamson C, Morris L.** 2013. Multiple pathways of escape from HIV broadly cross-neutralizing V2-dependent antibodies. J Virol **87:**4882–4894. http://dx.doi.org/10.1128/JVI.03424-12.
30. **van Loggerenberg F, Mlisana K, Williamson C, Auld SC, Morris L, Gray CM, Abdool Karim Q, Grobler A, Barnabas N, Iriogbe I, Abdool Karim SS, CAPRISA 002 Acute Infection Study Team.** 2008. Establishing a cohort at high risk of HIV infection in South Africa: challenges and experiences of the CAPRISA 002 acute infection study. PLoS One **3:**e1954. http://dx.doi.org/10.1371/journal.pone.0001954.
31. **Gray ES, Madiga MC, Hermanus T, Moore PL, Wibmer CK, Tumba NL, Werner L, Mlisana K, Sibeko S, Williamson C, Abdool Karim SS, Morris L.** 2011. The neutralization breadth of HIV-1 develops incrementally over four years and is associated with $CD4^+$ T cell decline and high viral load during acute infection. J Virol **85:**4828–4840. http://dx.doi.org/10.1128/JVI.00198-11.
32. **Huang J, Doria-Rose NA, Longo NS, Laub L, Lin CL, Turk E, Kang BH, Migueles SA, Bailer RT, Mascola JR, Connors M.** 2013. Isolation of human monoclonal antibodies from peripheral blood B cells. Nat Protoc **8:**1907–1915. http://dx.doi.org/10.1038/nprot.2013.117.
33. **Huang J, Ofek G, Laub L, Louder MK, Doria-Rose NA, Longo NS, Imamichi H, Bailer RT, Chakrabarti B, Sharma SK, Alam SM, Wang T, Yang Y, Zhang B, Migueles SA, Wyatt R, Haynes BF, Kwong PD, Mascola JR, Connors M.** 2012. Broad and potent neutralization of HIV-1 by a gp41-specific human antibody. Nature **491:**406–412. http://dx.doi.org/10.1038/nature11544.
34. **Doria-Rose N, Bailer R, Louder M, Lin C-L, Turk E, Laub L, Longo N, Connors M, Mascola J.** 13 September 2013. High throughput HIV-1 microneutralization assay. Protocol Exchange. http://dx.doi.org/10.1038/protex.2013.069.
35. **Sanders RW, Derking R, Cupo A, Julien JP, Yasmeen A, de Val N, Kim HJ, Blattner C, de la Pena AT, Korzun J, Golabek M, de Los Reyes K, Ketas TJ, van Gils MJ, King CR, Wilson IA, Ward AB, Klasse PJ, Moore JP.** 2013. A next-generation cleaved, soluble HIV-1 Env trimer, BG505 SOSIP.664 gp140, expresses multiple epitopes for broadly neutralizing but not non-neutralizing antibodies. PLoS Pathog **9:**e1003618. http://dx.doi.org/10.1371/journal.ppat.1003618.
36. **Wu X, Yang ZY, Li Y, Hogerkorp CM, Schief WR, Seaman MS, Zhou T, Schmidt SD, Wu L, Xu L, Longo NS, McKee K, O'Dell S, Louder MK, Wycuff DL, Feng Y, Nason M, Doria-Rose N, Connors M, Kwong PD, Roederer M, Wyatt RT, Nabel GJ, Mascola JR.** 2010. Rational design of envelope identifies broadly neutralizing human monoclonal antibodies to HIV-1. Science **329:**856–861. http://dx.doi.org/10.1126/science.1187659.
37. **Tiller T, Meffre E, Yurasov S, Tsuiji M, Nussenzweig MC, Wardemann H.** 2008. Efficient generation of monoclonal antibodies from

Downloaded from http://jvi.asm.org/ on December 21, 2015 by Penny Moore

single human B cells by single cell RT-PCR and expression vector cloning. J Immunol Methods **329:**112–124. http://dx.doi.org/10.1016/j.jim.2007.09.017.

38. **Scheid JF, Mouquet H, Ueberheide B, Diskin R, Klein F, Oliveira TY, Pietzsch J, Fenyo D, Abadir A, Velinzon K, Hurley A, Myung S, Boulad F, Poignard P, Burton DR, Pereyra F, Ho DD, Walker BD, Seaman MS, Bjorkman PJ, Chait BT, Nussenzweig MC.** 2011. Sequence and structural convergence of broad and potent HIV antibodies that mimic CD4 binding. Science **333:**1633–1637. http://dx.doi.org/10.1126/science.1207227.
39. **Liao HX, Levesque MC, Nagel A, Dixon A, Zhang R, Walter E, Parks R, Whitesides J, Marshall DJ, Hwang KK, Yang Y, Chen X, Gao F, Munshaw S, Kepler TB, Denny T, Moody MA, Haynes BF.** 2009. High-throughput isolation of immunoglobulin genes from single human B cells and expression as monoclonal antibodies. J Virol Methods **158:**171–179. http://dx.doi.org/10.1016/j.jviromet.2009.02.014.
40. **Shu Y, Winfrey S, Yang ZY, Xu L, Rao SS, Srivastava I, Barnett SW, Nabel GJ, Mascola JR.** 2007. Efficient protein boosting after plasmid DNA or recombinant adenovirus immunization with HIV-1 vaccine constructs. Vaccine **25:**1398–1408. http://dx.doi.org/10.1016/j.vaccine.2006.10.046.
41. **Montefiori DC.** 2009. Measuring HIV neutralization in a luciferase reporter gene assay. Methods Mol Biol **485:**395–405. http://dx.doi.org/10.1007/978-1-59745-170-3_26.
42. **Wu X, Changela A, O'Dell S, Schmidt SD, Pancera M, Yang Y, Zhang B, Gorny MK, Phogat S, Robinson JE, Stamatatos L, Zolla-Pazner S, Kwong PD, Mascola JR.** 2011. Immunotypes of a quaternary site of HIV-1 vulnerability and their recognition by antibodies. J Virol **85:**4578–4585. http://dx.doi.org/10.1128/JVI.02585-10.
43. **Haynes BF, Fleming J, St Clair EW, Katinger H, Stiegler G, Kunert R, Robinson J, Scearce RM, Plonk K, Staats HF, Ortel TL, Liao HX, Alam SM.** 2005. Cardiolipin polyspecific autoreactivity in two broadly neutralizing HIV-1 antibodies. Science **308:**1906–1908. http://dx.doi.org/10.1126/science.1111781.
44. **Wu X, Zhang Z, Schramm CA, Joyce MG, Do Kwon Y, Zhou T, Sheng Z, Zhang B, O'Dell S, McKee K, Georgiev IS, Chuang GY, Longo NS, Lynch RM, Saunders KO, Soto C, Srivatsan S, Yang Y, Bailer RT, Louder MK, NISC Comparative Sequencing Program, Mullikin JC, Connors M, Kwong PD, Mascola JR, Shapiro L.** 2015. Maturation and diversity of the VRC01-antibody lineage over 15 years of chronic HIV-1 infection. Cell **161:**470–485. http://dx.doi.org/10.1016/j.cell.2015.03.004.
45. **Li W, Jaroszewski L, Godzik A.** 2001. Clustering of highly homologous sequences to reduce the size of large protein databases. Bioinformatics **17:**282–283. http://dx.doi.org/10.1093/bioinformatics/17.3.282.
46. **Ashkenazy H, Penn O, Doron-Faigenboim A, Cohen O, Cannarozzi G, Zomer O, Pupko T.** 2012. FastML: a web server for probabilistic reconstruction of ancestral sequences. Nucleic Acids Res **40:**W580–W584. http://dx.doi.org/10.1093/nar/gks498.
47. **Felsenstein J.** 2005. PHYLIP (phylogeny inference package) version 3.6. http://cmgm.stanford.edu/phylip/dnaml.html.
48. **Otwinowski Z, Minor W.** 1997. Processing of X-ray diffraction data collected in oscillation mode. Methods Enzymol **276:**307–326. http://dx.doi.org/10.1016/S0076-6879(97)76066-X.
49. **Emsley P, Cowtan K.** 2004. Coot: model-building tools for molecular graphics. Acta Crystallogr D Biol Crystallogr **60:**2126–2132. http://dx.doi.org/10.1107/S0907444904019158.
50. **Adams PD, Gopal K, Grosse-Kunstleve RW, Hung LW, Ioerger TR, McCoy AJ, Moriarty NW, Pai RK, Read RJ, Romo TD, Sacchettini JC, Sauter NK, Storoni LC, Terwilliger TC.** 2004. Recent developments in the PHENIX software for automated crystallographic structure determination. J Synchrotron Radiat **11:**53–55. http://dx.doi.org/10.1107/S0909049503024130.
51. **DeLano WL.** 2002. The PyMOL molecular graphics system, DeLano Scientific, San Carlos, CA.
52. **Pettersen EF, Goddard TD, Huang CC, Couch GS, Greenblatt DM, Meng EC, Ferrin TE.** 2004. UCSF Chimera—a visualization system for exploratory research and analysis. J Comput Chem **25:**1605–1612. http://dx.doi.org/10.1002/jcc.20084.
53. **Doria-Rose NA, Georgiev I, O'Dell S, Chuang GY, Staupe RP, McLellan JS, Gorman J, Pancera M, Bonsignori M, Haynes BF, Burton DR, Koff WC, Kwong PD, Mascola JR.** 2012. A short segment of the HIV-1 gp120 V1/V2 region is a major determinant of resistance to V1/V2 neutralizing antibodies. J Virol **86:**8319–8323. http://dx.doi.org/10.1128/JVI.00696-12.
54. **Kearse M, Moir R, Wilson A, Stones-Havas S, Cheung M, Sturrock S, Buxton S, Cooper A, Markowitz S, Duran C, Thierer T, Ashton B, Meintjes P, Drummond A.** 2012. Geneious Basic: an integrated and extendable desktop software platform for the organization and analysis of sequence data. Bioinformatics **28:**1647–1649. http://dx.doi.org/10.1093/bioinformatics/bts199.
55. **Crooks GE, Hon G, Chandonia JM, Brenner SE.** 2004. WebLogo: a sequence logo generator. Genome Res **14:**1188–1190. http://dx.doi.org/10.1101/gr.849004.
56. **Avery DT, Bryant VL, Ma CS, de Waal Malefyt R, Tangye SG.** 2008. IL-21-induced isotype switching to IgG and IgA by human naive B cells is differentially regulated by IL-4. J Immunol **181:**1767–1779. http://dx.doi.org/10.4049/jimmunol.181.3.1767.
57. **Zan H, Cerutti A, Dramitinos P, Schaffer A, Casali P.** 1998. CD40 engagement triggers switching to IgA1 and IgA2 in human B cells through induction of endogenous TGF-beta: evidence for TGF-beta but not IL-10-dependent direct S mu→S alpha and sequential S mu→S gamma, S gamma→S alpha DNA recombination. J Immunol **161:**5217–5225.
58. **Cerutti A, Zan H, Schaffer A, Bergsagel L, Harindranath N, Max EE, Casali P.** 1998. CD40 ligand and appropriate cytokines induce switching to IgG, IgA, and IgE and coordinated germinal center and plasmacytoid phenotypic differentiation in a human monoclonal IgM^+IgD^+ B cell line. J Immunol **160:**2145–2157.
59. **Sok D, van Gils MJ, Pauthner M, Julien JP, Saye-Francisco KL, Hsueh J, Briney B, Lee JH, Le KM, Lee PS, Hua Y, Seaman MS, Moore JP, Ward AB, Wilson IA, Sanders RW, Burton DR.** 2014. Recombinant HIV envelope trimer selects for quaternary-dependent antibodies targeting the trimer apex. Proc Natl Acad Sci U S A **111:**17624–17629. http://dx.doi.org/10.1073/pnas.1415789111.
60. **Pancera M, Lebowitz J, Schon A, Zhu P, Freire E, Kwong PD, Roux KH, Sodroski J, Wyatt R.** 2005. Soluble mimetics of human immunodeficiency virus type 1 viral spikes produced by replacement of the native trimerization domain with a heterologous trimerization motif: characterization and ligand binding analysis. J Virol **79:**9954–9969. http://dx.doi.org/10.1128/JVI.79.15.9954-9969.2005.
61. **Sharma SK, de Val N, Bale S, Guenaga J, Tran K, Feng Y, Dubrovskaya V, Ward AB, Wyatt RT.** 2015. Cleavage-independent HIV-1 Env trimers engineered as soluble native spike mimetics for vaccine design. Cell Rep **11:**539–550. http://dx.doi.org/10.1016/j.celrep.2015.03.047.
62. **McLellan JS, Pancera M, Carrico C, Gorman J, Julien JP, Khayat R, Louder R, Pejchal R, Sastry M, Dai K, O'Dell S, Patel N, Shahzad-ul-Hussan S, Yang Y, Zhang B, Zhou T, Zhu J, Boyington JC, Chuang GY, Diwanji D, Georgiev I, Kwon YD, Lee D, Louder MK, Moquin S, Schmidt SD, Yang ZY, Bonsignori M, Crump JA, Kapiga SH, Sam NE, Haynes BF, Burton DR, Koff WC, Walker LM, Phogat S, Wyatt R, Orwenyo J, Wang LX, Arthos J, Bewley CA, Mascola JR, Nabel GJ, Schief WR, Ward AB, Wilson IA, Kwong PD.** 2011. Structure of HIV-1 gp120 V1/V2 domain with broadly neutralizing antibody PG9. Nature **480:**336–343. http://dx.doi.org/10.1038/nature10696.
63. **Pancera M, Shahzad-Ul-Hussan S, Doria-Rose NA, McLellan JS, Bailer RT, Dai K, Loesgen S, Louder MK, Staupe RP, Yang Y, Zhang B, Parks R, Eudailey J, Lloyd KE, Blinn J, Alam SM, Haynes BF, Amin MN, Wang LX, Burton DR, Koff WC, Nabel GJ, Mascola JR, Bewley CA, Kwong PD.** 2013. Structural basis for diverse N-glycan recognition by HIV-1-neutralizing V1-V2-directed antibody PG16. Nat Struct Mol Biol **20:**804–813. http://dx.doi.org/10.1038/nsmb.2600.
64. **Bhiman JN, Anthony C, Doria-Rose NA, Karimanzira O, Schramm CA, Khoza T, Kitchin D, Botha G, Gorman J, Garrett NJ, Abdool-Karim SS, Shapiro L, Williamson C, Kwong PD, Mascola JR, Morris L, Moore PL.** 12 October 2015. Viral variants that initiate and drive maturation of V1V2-directed HIV-1 broadly neutralizing antibodies. Nat Med http://dx.doi.org/10.1038/nm.3963.
65. **McCoy LE, Falkowska E, Doores KJ, Le K, Sok D, van Gils MJ, Euler Z, Burger JA, Seaman MS, Sanders RW, Schuitemaker H, Poignard P, Wrin T, Burton DR.** 2015. Incomplete neutralization and deviation from sigmoidal neutralization curves for HIV broadly neutralizing monoclonal antibodies. PLoS Pathog **11:**e1005110. http://dx.doi.org/10.1371/journal.ppat.1005110.
66. **Liao HX, Lynch R, Zhou T, Gao F, Alam SM, Boyd SD, Fire AZ,**

Downloaded from http://jvi.asm.org/ on December 21, 2015 by Penny Moore

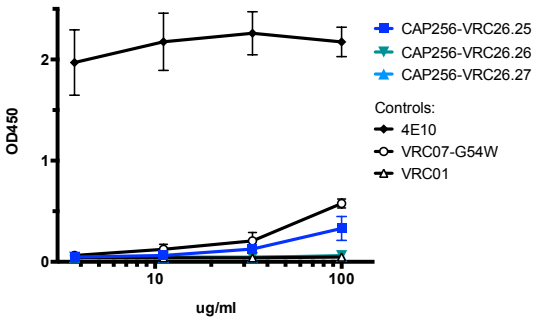
Roskin KM, Schramm CA, Zhang Z, Zhu J, Shapiro L, NISC Comparative Sequencing Program, Mullikin JC, Gnanakaran S, Hraber P, Wiehe K, Kelsoe G, Yang G, Xia SM, Montefiori DC, Parks R, Lloyd KE, Scearce RM, Soderberg KA, Cohen M, Kamanga G, Louder MK, Tran LM, Chen Y, Cai F, Chen S, Moquin S, Du X, Joyce MG, Srivatsan S, Zhang B, Zheng A, Shaw GM, Hahn BH, Kepler TB, Korber BT, Kwong PD, Mascola JR, Haynes BF. 2013. Co-evolution of a broadly neutralizing HIV-1 antibody and founder virus. Nature **496:**469–476. http://dx.doi.org/10.1038/nature12053.

67. **Willis JR, Sapparapu G, Murrell S, Julien JP, Singh V, King HG, Xia Y, Pickens JA, LaBranche CC, Slaughter JC, Montefiori DC, Wilson IA, Meiler J, Crowe JE, Jr.** 2015. Redesigned HIV antibodies exhibit enhanced neutralizing potency and breadth. J Clin Invest **125:**2523–2531. http://dx.doi.org/10.1172/JCI80693.

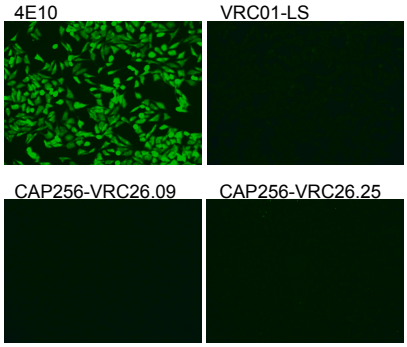
Downloaded from http://jvi.asm.org/ on December 21, 2015 by Penny Moore

Paper 2: Supplementary Info

A



B



C

	Cardiolipin Binding	Hep2 staining
CAP256-VRC26.UCA	-	-
CAP256-VRC26.01	-	-
CAP256-VRC26.02	-	-
CAP256-VRC26.03	+/-	+/-
CAP256-VRC26.04	-	-
CAP256-VRC26.05	-	-
CAP256-VRC26.06	-	-
CAP256-VRC26.07	-	-
CAP256-VRC26.08	-	-
CAP256-VRC26.09	-	-
CAP256-VRC26.10	-	-
CAP256-VRC26.11	-	-
CAP256-VRC26.12	-	-
CAP256-VRC26.13	-	-
CAP256-VRC26.14	-	-
CAP256-VRC26.15	-	-
CAP256-VRC26.16	-	-
CAP256-VRC26.17	-	-
CAP256-VRC26.18	-	-
CAP256-VRC26.19	-	-
CAP256-VRC26.20	-	-
CAP256-VRC26.21	-	-
CAP256-VRC26.22	-	-
CAP256-VRC26.23	-	-
CAP256-VRC26.24	-	-
CAP256-VRC26.25	+/-	-
CAP256-VRC26.26	-	-
CAP256-VRC26.27	-	-
CAP256-VRC26.28	-	-
CAP256-VRC26.29	-	-
CAP256-VRC26.30	-	-
CAP256-VRC26.31	-	-
CAP256-VRC26.32	-	-

VRC01-LS	-	-
VRC07-523	+/-	+
VRC07-G54W	+	+++
4E10	++	+

D

		Autoantigen								
Antibody	µg/ml	SSA	SSB	Sm	RNP	Scl 70	Jo 1	dsDNA	Cent B	Histone
Synagis	50	3	6	5	1	1	5	6	1	3
	25	5	5	4	2	0	7	3	1	3
4E10	50	**162**	**242**	19	26	6	**206**	9	14	31
	25	113	**176**	9	14	5	**161**	6	8	17
CAP256-VRC26.UCA	50	2	3	10	2	7	2	8	4	3
	25	2	4	6	2	4	2	5	1	3
	12.5	2	6	2	1	3	2	5	2	3
	6.25	3	5	3	0	2	5	0	2	2
CAP256-VRC26.03	50	3	3	3	3	3	3	10	5	5
	25	3	5	3	2	2	2	9	2	3
	12.5	3	9	4	1	1	3	4	2	1
	6.25	3	3	4	2	2	2	0	2	1
CAP256-VRC26.08	50	3	7	5	3	3	2	17	5	2
	25	1	5	4	2	3	1	9	3	3
	12.5	4	5	1	2	1	2	3	2	2
	6.25	4	8	2	2	1	2	2	2	2
CAP256-VRC26.09	50	4	6	4	1	2	3	7	3	3
	25	4	2	4	2	2	2	6	2	2
	12.5	2	4	3	2	1	3	5	3	2
	6.25	3	3	3	1	1	2	2	2	1
CAP256 VRC26.22	50	6	6	29	7	30	6	90	25	17
	25	4	5	14	4	15	4	44	9	10
	12.5	6	5	8	2	7	3	28	4	6
	6.25	1	7	8	3	6	4	22	3	6
CAP256 VRC26.25	50	3	3	7	2	6	3	4	2	2
	25	4	7	6	4	3	3	0	2	2
	12.5	3	5	2	2	3	2	4	1	1
	6.25	3	6	5	3	2	1	4	2	3
CAP256-VRC26.26	50	4	9	6	3	3	4	2	1	2
	25	4	5	4	1	3	2	4	1	1
	12.5	2	6	3	0	3	5	1	2	2
	6.25	2	1	1	1	2	4	1	1	1
CAP256-VRC26.27	50	1	3	2	3	2	2	4	2	2
	25	4	6	2	2	1	2	1	2	2
	12.5	4	5	4	1	2	4	7	2	3
	6.25	4	3	2	3	1	4	3	1	2

Figure S1. Autoreactivity assays. **A-C.** Thirty-two CAP256-VRC26 antibodies as well as control antibodies were assessed for binding to cardiolipin by ELISA, and to Hep2 cells by indirect immunofluorescence. 4E10 and VRC07-523-LS, positive controls; VRC01-LS, negative control. **A**, Representative cardiolipin ELISA. **B,** Representative images from Hep2 staining. **C**, Summary of cardiolipin and Hep2 assays. Scale for cardiolipin: -, <0.12 at 33 ug/ml; +/-, 0.12-0.2; +, 0.2-1.0; ++, 1.0-2.0 ; +++, >2.0. Hep2 staining was assessed semi-quantitatively as in ref. 44. **D**, CAP256-VRC26 UCA and seven of the broadest antibodies were further tested an autoantigen panel by ATHENA. Values >120 at 25 µg/ml, highlighted in yellow, are considered positive (ref. 43).

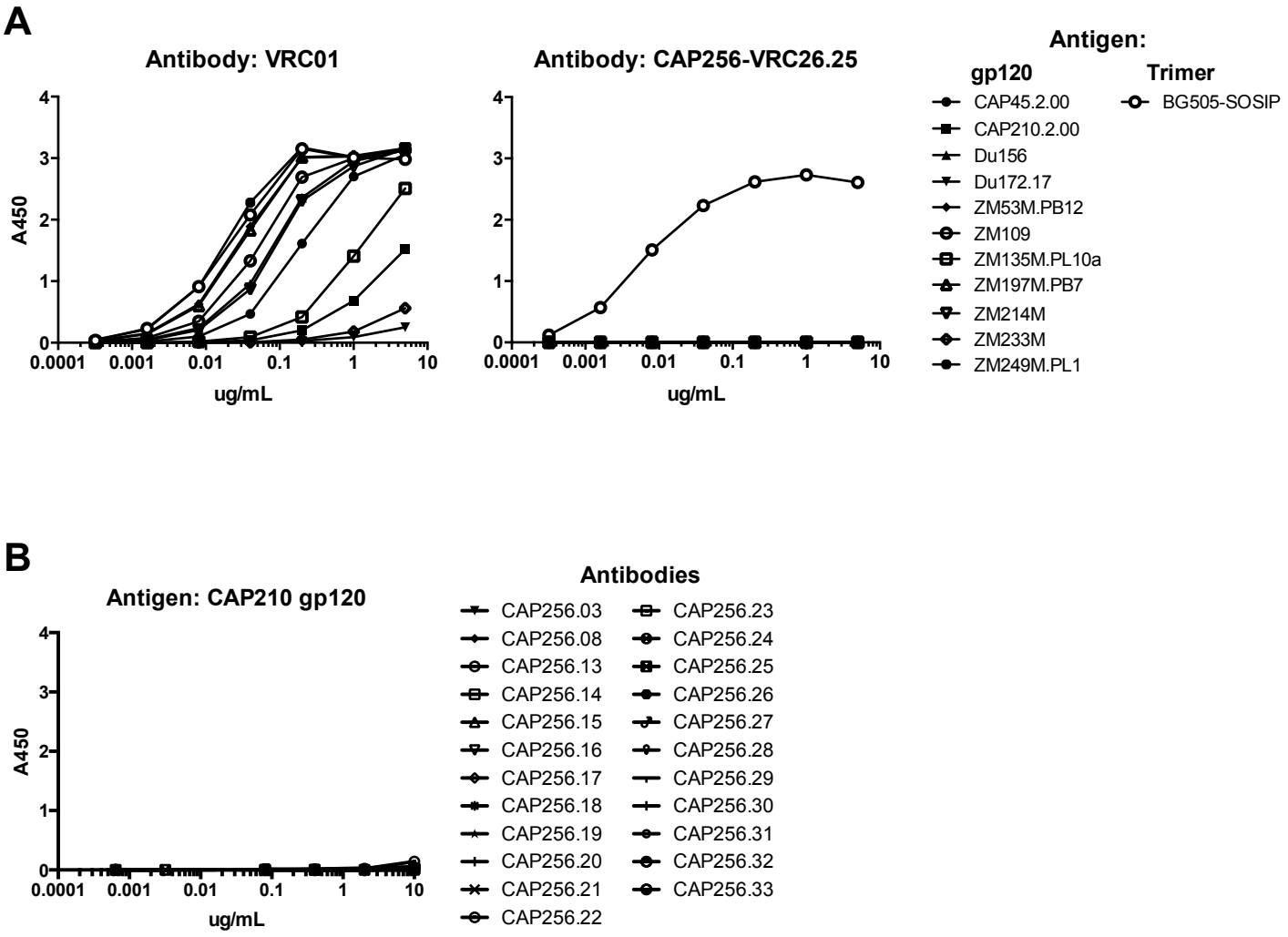


Figure S2. CAP256-VRC26 antibodies only bind to trimeric HIV-1 Env proteins. Binding was assessed by ELISA. **A**, VRC01 and CAP256-VRC26.25 were assayed for binding to gp120 proteins derived from 11 clade C isolates or to BG505-SOSIP trimer. **B,** CAP256-VRC26 antibodies were assayed for binding to gp120 from clade C isolate CAP210.2.00.

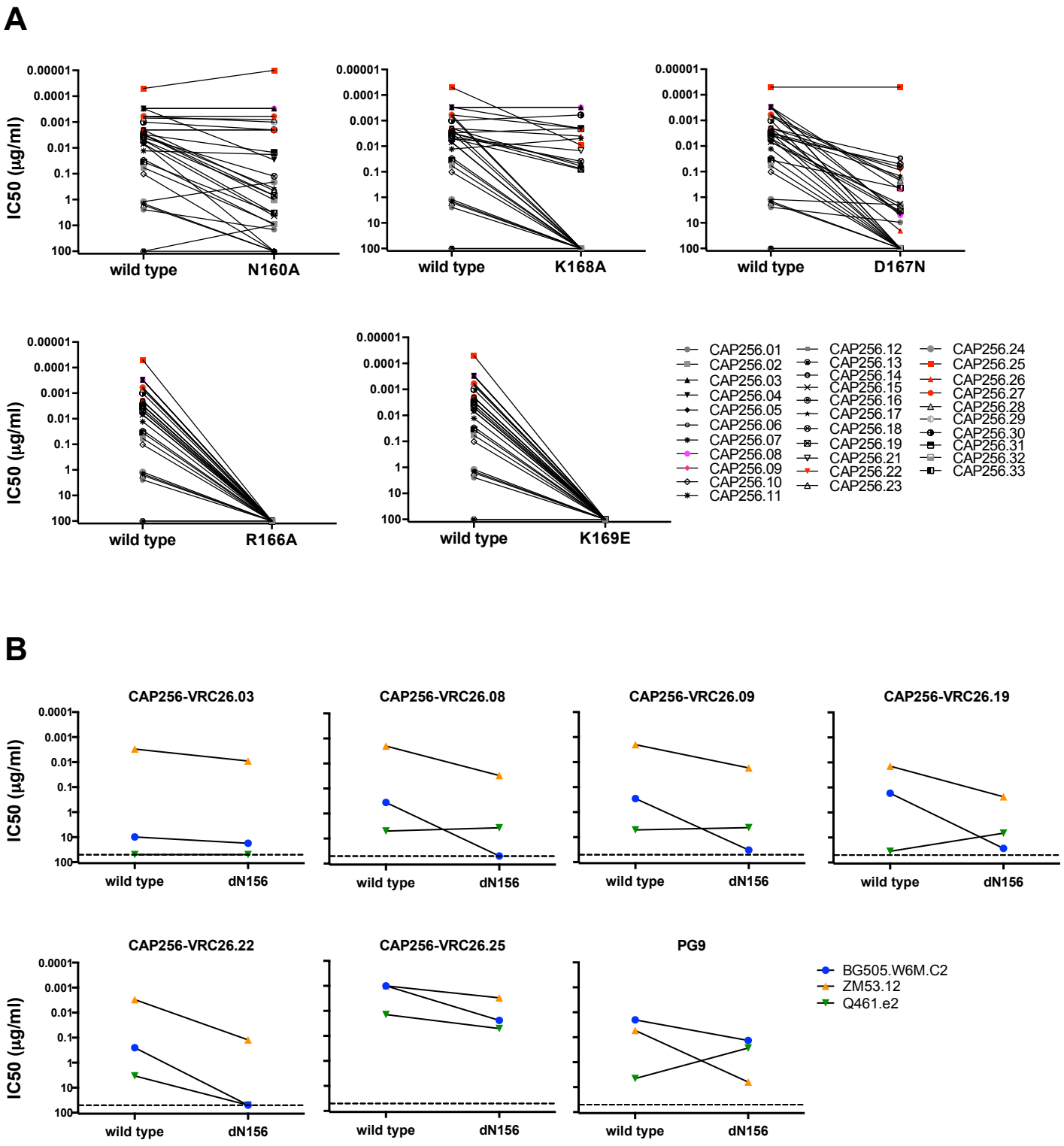


Figure S3. Epitope mapping of CAP256-VRC26 antibodies. A, Neutralization of HIV-1 ConC virus (wild type) and its V2 mutants by CAP256-VRC26 antibodies. Each pair of dots shows the IC50s for one virus pair. Each graph shows data for one virus pair. **B**, Neutralization of wild type and mutants lacking the N156 glycan (dN156). Each pair of dots shows the IC50s for one virus pair. Each graph shows data for antibody. 7 representative antibodies are shown.

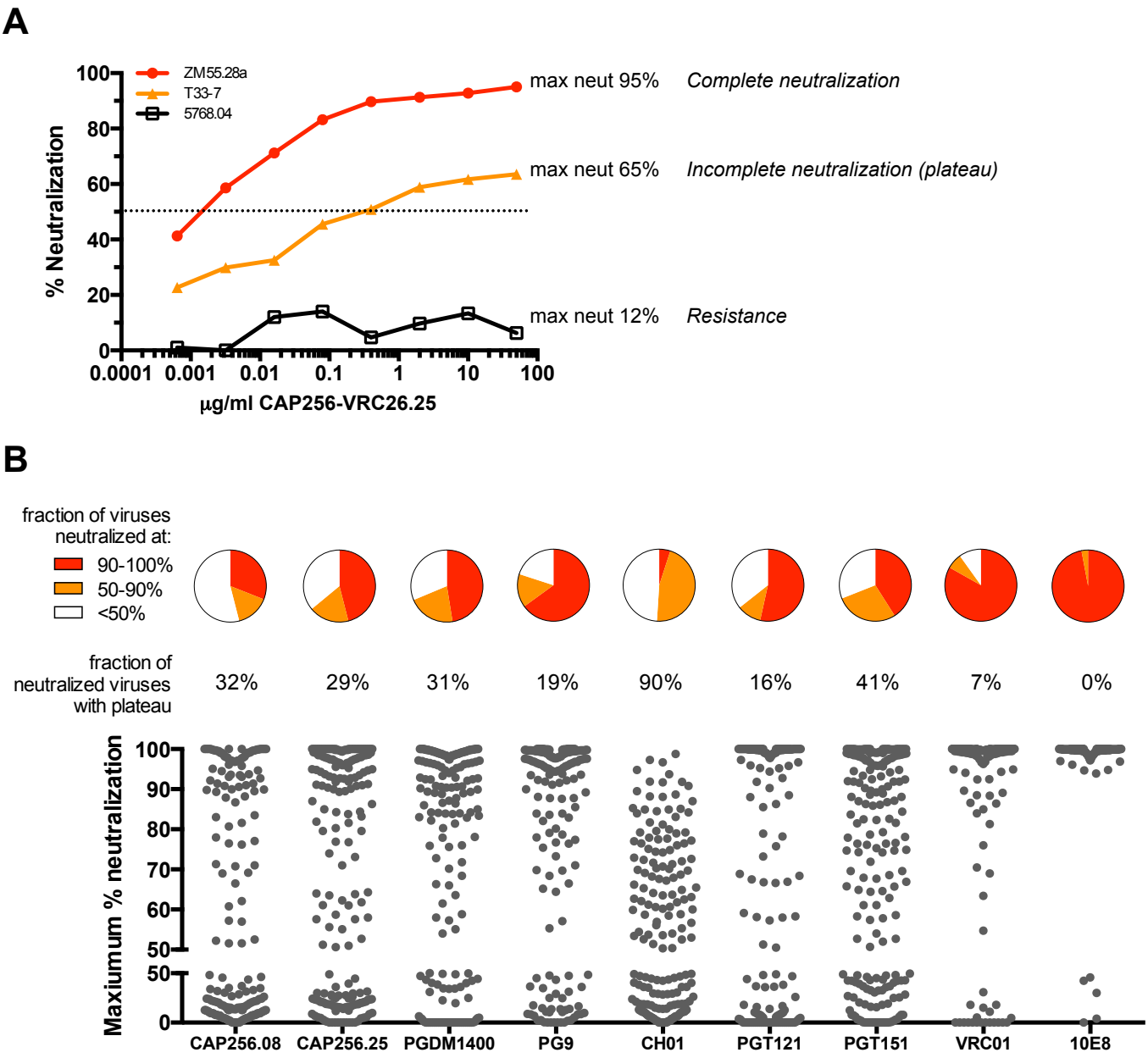


Figure S4. Plateau effect and completeness of neutralization. A, Representative curves for neutralization by CAP256-VRC26.25, demonstrating complete, plateau, or lack of neutralization. **B**, Maximum neutralization. Selected antibodies were assayed against a multiclade panel (n=183). Top, pie charts show the proportion of viruses that are neutralized to a maximum of >90% (red), 50-90% (orange) or <50% (white). Viruses that do not reach 50% neutralization at the input concentration of 50 µg/ml are considered resistant. Values are the fraction of neutralized viruses with maximum neutralization 50-90% (plateau). Bottom, each point shows the maximum % neutralization of one virus.

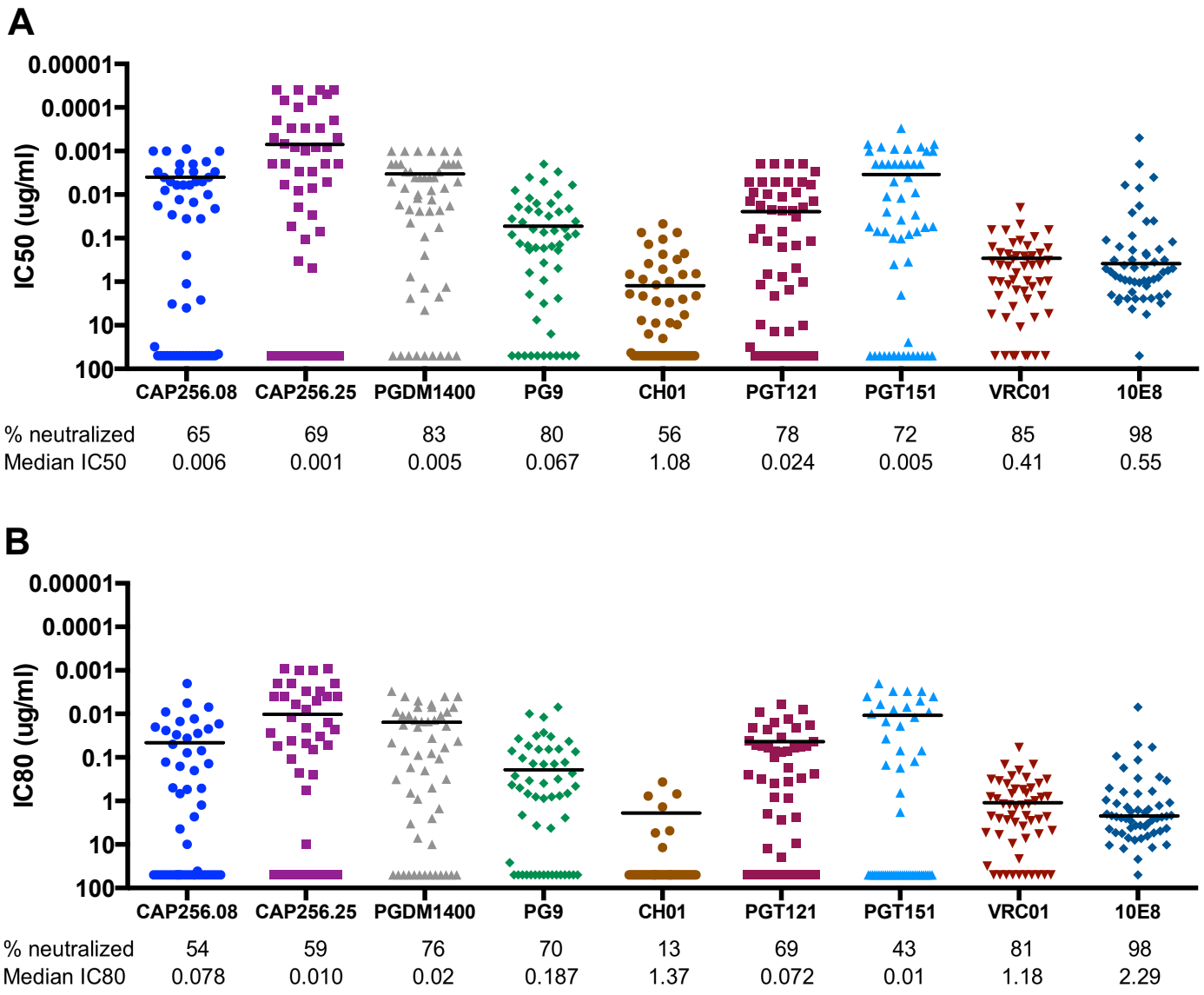


Figure S5. Breadth and potency of CAP256-VRC26 and selected broadly neutralizing antibodies against clade C viruses. Neutralization of a clade C panel (n=54) was assessed by TZM-bl pseudovirus assay. **A**, IC50s. **B**, IC80s.

Table S1. Primers used for cloning heavy, kappa, and lambda variable genes.

Heavy Chain First Round

Heavy Chain Primer mix G1: anneal at 54			Reference
pool	VH1 LEADER-A	ATGGACTGGACCTGGAGGAT	Scheid2011
	VH1 LEADER-B	ATGGACTGGACCTGGAGCAT	Scheid2011
	VH1 LEADER-C	ATGGACTGGACCTGGAGAAT	Scheid2011
	VH1 LEADER-D	GGTTCCTCTTTGTGGTGGC	Scheid2011
	VH1 LEADER-E	ATGGACTGGACCTGGAGGGT	Scheid2011
	VH1-LEADER-F	ATGGACTGGATTTGGAGGAT	Scheid2011
	VH1-LEADER-G	AGGTTCCTCTTTGTGGTGGCAG	Scheid2011
pool	3'Cg CH1	GGA AGG TGT GCA CGC CGC TGG TC	Tiller2008
	IgA-ext	CGA YGA CCA CGT TCC CAT CT	Liao2009

Heavy Chain Primer mix G2: anneal at 48			
pool	VH3 LEADER-A	TAAAAGGTGTCCAGTGT	Scheid2011
	VH3 LEADER-B	TAAGAGGTGTCCAGTGT	Scheid2011
	VH3 LEADER-C	TAGAAGGTGTCCAGTGT	Scheid2011
	VH3 LEADER-E	TACAAGGTGTCCAGTGT	Scheid2011
	VH3 LEADER-F	TTAAAGCTGTCCAGTGT	Scheid2011
	VH4 LEADER-D	ATGAAACATCTGTGGTTCTT	Scheid2011
	VH5 LEADER-A	TTCTCCAAGGAGTCTGT	Scheid2011
pool	3'Cg CH1	GGA AGG TGT GCA CGC CGC TGG TC	Tiller2008
	IgA-ext	CGA YGA CCA CGT TCC CAT CT	Liao2009

Heavy Chain Primer mix G3: anneal at 52			
pool	VH3 LEADER-D	GCTATTTTTAAAGGTGTCCAGTGT	Scheid2011
	VH4 LEADER-A	ATGAAACACCTGTGGTTCTTCC	Scheid2011
	VH4 LEADER-B	ATGAAACACCTGTGGTTCTT	Scheid2011
	VH4 LEADER-C	ATGAAGCACCTGTGGTTCTT	Scheid2011
	VH5 LEADER-B	CCTCCACAGTGAGAGTCTG	Scheid2011
	VH6 LEADER-A	ATGTCTGTCTCCTTCCTCATC	Scheid2011
	VH7 LEADER-A	GGCAGCAGCAACAGGTGCCCA	Scheid2011
pool	3'Cg CH1	GGA AGG TGT GCA CGC CGC TGG TC	Tiller2008
	IgA-ext	CGA YGA CCA CGT TCC CAT CT	Liao2009

Heavy Chain Second Round

Second Round Heavy chain primers anneal at 58.
use for G1,G2,G3 first round amplicons

pool	5'L-VH 1	ACA GGT GCC CAC TCC CAG GTG CAG	Tiller2008
	5'L-VH 3	AAG GTG TCC AGT GTG ARG TGC AG	Tiller2008
	5'L-VH 4/6	CCC AGA TGG GTC CTG TCC CAG GTG CAG	Tiller2008
	5'L-VH 5	CAA GGA GTC TGT TCC GAG GTG CAG	Tiller2008
pool	5xwL-VH1	GCA GCC ACA GGT GCC CAC TCC	this study
	5xwL-VH1-24	CAG CAG CTA CAG GCA CCC ACG C	this study
	5xwL-VH1-69	GGC AGC AGC TAC AGG TGT CCA GTC C	this study
	VH3-L1-MP	GCT ATT TTA AAA GGT GTC CAA TGT	this study
	VH3/4-L1-MP	GTG GCA GCT CCC AGA TGG GTC CTG TC	this study
	VH3/4-L3-MP	GTT GCA GTT TTA AAA GGT GTC CAG TG	this study
	VH5-L1-MP	GCT GTT CTC CAA GGA GTC TGT TCC	this study
pool	3'IgGint	GTT CGG GGA AGT AGT CCT TGA C	Tiller2008
	IgA1-int	GCT GGT GCT GCA GAG GCT CAG	Liao2009
	IgA2-int	GCT GGT GCT GTC GAG GCT CAG	Liao2009

Kappa

First round: 58 deg

pool	5'L-VK 1/2	ATG AGG STC CCY GCT CAG CTG CTG G	Tiller2008
	5'L-VK 3	CTC TTC CTC CTG CTA CTC TGG CTC CCA G	Tiller2008
	5'L-VK 4	ATT TCT CTG TTG CTC TGG ATC TCT G	Tiller2008
single	3'CK 543	GTT TCT CGT AGT CTG CTT TGC TCA	Tiller2008

Second round: 52 deg

pool	5' L-Vk1.1-MS	TGC TGC TCT GGY TCC CA	this study
	5' L-Vk1.2-MS	TCT GKY TCY CAG GTG CCA	this study
	5' L-Vk1.3-MS	CTR CTR CTC TGG STC C	this study
	5' L-Vk2-MS	TGG GGC TGC TAA TGC TCT	this study
	5' L-Vk3-MS	CTG GCT CMC AGA TAC CAC	this study
	5'L Vk4 Tiller	ATT TCT CTG TTG CTC TGG ATC TCT G	Tiller2008
	5' L-Vk5-MS	CCT CCT TTG GAT CTC TGA TAC CA	this study
	5'L-Vk6-MS	TTC TGC TSC TCT GGG TTC C	this study
single	3'CK 494	GTG CTG TCC TTG CTG TCC TGC T	Tiller2008

Lambda

First round, 58 deg

pool	5'L-VL1/10-RL	CCTCCTCACTCACTSTGCAG	this study
	5'L-VL5/6-RL	CTCCTCKCTCACTGCACAG	this study
	5'L-VL2-RL	CCTCCTCACTCAGGGCACAG	this study
	5'L-VL9-RL	CCTCCTCAGTCTCCTCACAG	this study
	5'L-VL4-RL	CTGCCCTTCATTTTCTCCACAG	this study
	5'L-VL3-RL	GCGTCCTTGCTTACTGCACAG	this study
	5'L-VL8-RL	GACTCCTTGCTTATGGATCAG	this study
	5'L-VL7-RL	CCTCCTCACTTGCTGCCCAG	this study
single	3'Cl	CAC CAG TGT GGC CTT GTT GGC TTG	Tiller2008

Second round, 60 deg

pool	5'L Vl 1	GGT CCT GGG CCC AGT CTG TGC TG	Tiller2008
	5'L Vl 2	GGT CCT GGG CCC AGT CTG CCC TG	Tiller2008
	5'L Vl 3	GCT CTG TGA CCT CCT ATG AGC TG	Tiller2008
	5'L Vl 4/5	GGT CTC TCT CSC AGC YTG TGC TG	Tiller2008
	5'L Vl 6	GTT CTT GGG CCA ATT TTA TGC TG	Tiller2008
	5'L Vl 7	GGT CCA ATT CYC AGG CTG TGG TG	Tiller2008
	5'L Vl 8	GAG TGG ATT CTC AGA CTG TGG TG	Tiller2008
single	3'XhoI Cl	CTC CTC ACT CGA GGG YGG GAA CAG AGT G	Tiller2008

Table S2 Data collection and refinement statistics for crystallography.
Values in parentheses are for highest-resolution shell.
One crystal was used to measure the data.

	CAP256-VRC26.25
PDB ID	5DT1
Data collection	
Space group	$P\,2_1 2 2_1$
Cell dimensions	
a , *b* , *c* (Å)	77.0, 77.0, 85.2
a, b, g (°)	90.0, 90.0, 90.0
Wavelength (Å)	1
Resolution (Å)	50.00-1.96 (2.04-1.96)
R_{merge}	11.4 (32.9)
I / sI	12.0 (2.0)
Completeness (%)	90.8 (50.4)
Redundancy	5.3 (1.6)
Refinement	
Resolution (Å)	42.6-1.96 (2.03-1.96)
No. reflections	33621 (1632)
R_{work} / R_{free}	16.9/21.5
No. atoms (total)	3856
Protein	3484
Ligand (glycan)	39
Water	333
B-factors	
Protein	33.2
Ligand (glycan)	92.8
Water	37.3
R.m.s. deviations	
Bond lengths (Å)	0.007
Bond angles (°)	0.89
Ramachandran	
Favored (%)	97
Outliers (%)	0.1

Table S3. V-D-J junction sequence (inclusive of CDRH3) and mutation away from UCA.

Antibody	Junction (CDRH3)	Heavy Chain		Light Chain	
		nt	aa	nt	aa
CAP256-VRC26.UCA	CAKDLGESENEEWA-TDYYDFSIGYPGQDPR--GVVGAFDIW	--	--	--	--
CAP256-VRC26.01	CAKDVGDYKSDEWG-TEYYDISISYPIQDPR--AMVGAFDLW	10.2	20.8	3.9	8.1
CAP256-VRC26.02	CAKDIREYECEYWT-SDYYDFGRPQPCIDSR--GVVGTFDVW	12.3	20.1	9.0	14.4
CAP256-VRC26.03	CAKDLREDECEEWW-SDYYDFGKQLPCRKSR--GVAGIFDGW	12.5	20.8	10.2	14.4
CAP256-VRC26.04	CAKDLREDECEEWW-SDYYDFGKQLPCRKSR--GVAGIFDKW	13.0	23.6	9.0	11.7
CAP256-VRC26.05	CARDQRYYECEEWA-SDYYDFGREQPCLDPR--GVVGIFDLW	12.7	23.4	11.7	13.5
CAP256-VRC26.06	CARDLRELECEEWTLYNYYDFGSRGPCVDPR--GVAGSFDVW	15.4	22.9	9.3	15.3
CAP256-VRC26.07	CAKDLREDECEEWW-SDYYDFGKKLPCRKSR--GVAGVFDKW	14.1	25.3	10.5	16.2
CAP256-VRC26.08	CVRDQREDECEEWW-SDYYDFGRELPCRKFRGLGLAGIFDIW	16.9	28.8	10.2	14.4
CAP256-VRC26.09	CVKDQREDECEEWW-SDYYDFGRELPCRKSRGLGLAGIFDMW	18.5	22.9	5.4	9.9
CAP256-VRC26.10	CAKDMREYECEYWT-SDYYDFGRPQPCIDRR--GVVGIFDMW	12.7	27.8	17.4	27.9
CAP256-VRC26.11	CVKDMRELECEEWA-SDYYDFGKPQPCLDRR--GVSGISAWW	12.7	26.4	12.3	20.7
CAP256-VRC26.12	CARDLRESECEEWE-SDYYDFGKKGPCVKPR--GVAGGLDLW	12.7	25.7	13.2	21.6
CAP256-VRC26.13	CARDLRESECEEWE-SDYYDFGKKGPCVKPR--GVAGGLDLW	14.1	22.2	10.2	16.2
CAP256-VRC26.14	CARDVREMECEEWA-SDYYDFGRGGPCRDFR--GVVGILDIW	14.6	17.4	9.0	12.6
CAP256-VRC26.15	CARDLREYECELWA-SDYYDFGKPQPCEDPR--GVVGTSDIW	17.6	22.2	8.7	13.5
CAP256-VRC26.16	CARDVREMECEEWA-SDYYDFGRGGPCRDFR--GVVGILDIW	17.4	22.9	10.8	18.0
CAP256-VRC26.17	CARDMREMECEEWA-SDYYDFGRPGPCRDLR--GVVGTFDIW	16.9	22.9	9.6	15.3
CAP256-VRC26.18	CARDMREMECEEWA-SDYYDFGRSGPCRDFR--GVVGVFDIW	13.4	25.7	10.8	19.8
CAP256-VRC26.19	CARDSREYECELWT-SDYYDFGKPQPCIDTR--DVGGLFDMW	18.1	30.8	13.5	23.4
CAP256-VRC26.20	CVRDQREDECEERW-SDYYHFGRVLPCRKYRGLGLAGVFDIW	20.3	34.2	14.1	20.7
CAP256-VRC26.21	CVRDRQEDECEEWW-SDYYAFGRGGPCRKYHGQGLAGIFDIW	22.8	32.2	13.8	21.6
CAP256-VRC26.22	CVRDRQEDECVEWW-SDYYNFGRELPCSKFRGLGLAGIFDIW	21.2	22.2	7.8	9.9
CAP256-VRC26.23	CAKDLREYECEEWR-SDYYDFGRDQPCIDSQ--GVVGILDIW	12.3	16.7	3.6	6.3
CAP256-VRC26.24	CAKDLGGIKNDEWG-TDYYDISVSYPVQDPR--AVAGIFDVW	7.2	21.5	8.7	15.3
CAP256-VRC26.25	CAKDLREDECEEWW-SDYYDFGKQLPCAKSRG-GLVGIADNW	16.9	22.8	10.5	16.2
CAP256-VRC26.26	CVRDQREDECEEWW-SDYYDFGKELPCRKFRGLGLAGIFDVW	20.8	30.1	10.8	19.8
CAP256-VRC26.27	CVRDQREDECEEWW-SDYYDFGKELPCRKFRGLGLAGIFDIW	19.4	28.8	10.5	19.8
CAP256-VRC26.28	CVRDRQEDECVEWW-SDYYNFGRELPCSKFRGLGLAGIFDIW	21.0	30.8	12.9	18.9
CAP256-VRC26.29	CVRDRQEDECVEWW-SDYYNFGRELPCSKFRGLGLAGIFDIW	20.3	30.8	13.8	21.6
CAP256-VRC26.30	CVRDRQEDECEEWW-SDYYNFGRELPCRKFRGQGLAGIFDIW	21.2	30.1	13.5	20.7
CAP256-VRC26.31	CVRDRQEDECEEWW-SDYYNFGRELPCRKFRGPGLAGIFDIW	20.1	29.5	10.8	18.9
CAP256-VRC26.32	CVKDLRELECEEWT-SDYYDFGRPQPCIDPR--GVSGISAMW	14.6	25.0	18.3	27.0
CAP256-VRC26.33	CARDQRYYECEEWA-SDYYDFGREQPCQDPR--GVVGIFDIW	11.6	20.8	9.3	13.5

Table S4. Neutralization (IC50 values) for all 33 CAP256-VRC26 antibodies against autologous (PI and SU) and 46 heterologous HIV-1 Env-pseudoviruses.

Virus		CAP256-VRC26.01	CAP256-VRC26.02	CAP256-VRC26.03	CAP256-VRC26.04	CAP256-VRC26.05	CAP256-VRC26.06	CAP256-VRC26.07	CAP256-VRC26.08	CAP256-VRC26.09	CAP256-VRC26.10	CAP256-VRC26.11	CAP256-VRC26.12	CAP256-VRC26.13	CAP256-VRC26.14	CAP256-VRC26.15	CAP256-VRC26.16	CAP256-VRC26.17	CAP256-VRC26.18	CAP256-VRC26.19	CAP256-VRC26.20	CAP256-VRC26.21	CAP256-VRC26.22	CAP256-VRC26.23	CAP256-VRC26.24	CAP256-VRC26.25	CAP256-VRC26.26	CAP256-VRC26.27	CAP256-VRC26.28	CAP256-VRC26.29	CAP256-VRC26.30	CAP256-VRC26.31	CAP256-VRC26.32	CAP256-VRC26.33
Autologous	CAP256.PI	>50	>50	>50	>50	>50	0.030	>50	>50	>50	>50	>50	>50	>50	>50	>50	>50	>50	>50	>50	>50	>50	>50	>50	>50	1.33	>50	>50	>50	>50	>50	>50	>50	>50
	CAP256.SU	0.14	0.015	0.004	0.003	0.007	0.055	0.008	0.003	0.002	0.031	0.055	0.032	0.019	0.004	0.008	0.004	0.003	0.008	0.015	>50	0.002	0.002	0.019	0.040	0.0005	0.003	<0.0006	<0.0006	<0.0006	<0.0006	<0.0006	0.004	0.007
Clade C	962M651.02	>50	>50	>50	>50	>50	>50	>50	2.63	0.991	>50	>50	>50	>50	>50	>50	>50	>50	>50	>50	>50	>50	>50	>50	>50	0.173	0.111	0.047	>50	>50	37.800	>50	>50	>50
	CAP210.E8	0.166	0.062	0.008	0.005	0.013	1.20	0.021	0.003	0.002	0.100	0.073	0.072	0.094	0.012	0.019	0.009	0.006	0.019	0.025	>50	0.005	0.003	0.019	0.460	0.0005	0.007	0.002	<0.0006	<0.0006	<0.0006	<0.0006	0.003	0.008	0.017
	CAP244.D3	>50	>50	>50	>50	>50	>50	>50	>50	>50	>50	>50	>50	>50	>50	>50	>50	>50	>50	>50	>50	>50	>50	>50	>50	>50	36.600	>50	>50	>50	>50	>50	>50	>50	>50
	CAP45.G3	31.8	>50	16.0	>50	>50	>50	>50	4.00	16.0	>50	>50	>50	>50	>50	>50	>50	>50	>50	>50	>50	>50	1.400	>50	>50	0.00006	0.080	0.025	0.016	0.076	0.317	>50	>50	0.622
	DU156.12	>50	>50	0.090	10.4	>50	>50	>50	0.006	0.016	>50	>50	>50	>50	>50	10.4	48.7	18.7	>50	1.34	>50	>50	0.150	>50	>50	0.002	0.013	0.006	0.171	0.136	0.848	4.460	>50	>50
	DU172.17	>50	>50	>50	>50	>50	>50	>50	>50	>50	>50	>50	>50	>50	>50	>50	>50	>50	>50	>50	>50	>50	>50	>50	>50	>50	0.500	4.360	>50	>50	>50	>50	>50	>50	>50
	DU422.01	>50	>50	0.224	4.17	>50	>50	>50	0.008	0.023	8.20	11.5	>50	>50	49.0	0.153	3.90	0.510	5.40	0.057	>50	1.10	0.012	>50	>50	0.003	0.080	0.015	0.075	0.072	0.400	1.660	>50	29.500
	ZM109.4	>50	>50	>50	>50	26.5	>50	>50	>50	>50	>50	>50	>50	>50	>50	>50	>50	>50	>50	2.82	>50	>50	>50	>50	>50	0.001	0.025	0.027	>50	>50	>50	>50	>50	>50
	ZM135.10a	>50	>50	>50	>50	>50	>50	>50	>50	>50	>50	>50	>50	>50	>50	>50	>50	>50	>50	>50	>50	>50	>50	>50	>50	>50	>50	>50	>50	>50	>50	>50	>50	>50	>50
	ZM197.7	22.1	1.97	0.302	0.254	0.113	>50	>50	0.022	0.011	0.346	0.055	>50	>50	4.96	14.6	2.21	2.20	1.89	0.135	>50	>50	0.090	>50	>50	0.002	0.011	0.004	0.193	0.136	1.000	3.220	0.097	1.730
	ZM214.15	>50	>50	0.100	>50	>50	>50	>50	3.230	0.333	>50	>50	>50	>50	>50	>50	>50	>50	>50	>50	>50	>50	>50	>50	>50	0.006	14.100	3.860	6.850	13.600	>50	>50	>50	>50
	ZM233.6	0.701	0.701	0.032	0.060	0.003	22.6	>50	0.001	0.001	0.228	0.322	>50	>50	0.028	0.192	0.031	0.008	0.037	0.009	>50	26.5	0.001	>50	29.800	0.00003	0.001	<0.0006	0.002	0.003	0.188	0.740	0.015	0.004
	ZM249.1	>50	>50	0.004	11.4	>50	>50	44.1	0.076	0.010	>50	34.5	>50	>50	>50	>50	45.0	1.230	>50	0.076	>50	>50	0.130	>50	>50	0.001	0.023	0.004	0.082	0.093	0.762	>50	16.800	22.500
	ZM53.12	0.036	0.043	0.008	0.004	0.012	0.082	0.014	0.004	0.002	0.072	0.081	0.211	0.039	0.006	0.014	0.006	0.005	0.010	0.020	1.87	0.003	0.002	0.028	0.047	0.0003	0.001	<0.0006	<0.0006	0.001	<0.0006	<0.0006	0.011	0.015
Clade A	0260.v5.c36	>50	>50	>50	>50	>50	>50	>50	>50	>50	>50	>50	>50	>50	>50	>50	>50	>50	>50	>50	>50	>50	>50	>50	>50	6.540	0.780	2.100	>50	>50	>50	>50	>50	>50
	BG505.w6m	>50	>50	4.76	8.43	>50	>50	>50	0.143	0.054	>50	4.20	>50	>50	0.750	11.7	0.360	0.400	1.900	0.130	>50	>50	0.035	>50	>50	0.001	0.066	0.102	0.044	0.046	9.040	>50	>50	>50
	KER2008.12	0.308	>50	>50	>50	>50	>50	>50	>50	>50	>50	>50	>50	>50	>50	>50	>50	>50	>50	>50	>50	>50	1.230	>50	>50	0.005	>50	11.300	0.760	0.684	>50	>50	>50	>50
	KER2018.11	5.95	0.180	0.014	0.008	0.012	>50	3.10	0.005	0.002	0.335	1.76	>50	>50	0.030	0.040	0.062	0.064	0.030	0.005	>50	0.060	0.002	10.000	>50	0.0002	0.001	0.0007	<0.0006	<0.0006	<0.0006	0.002	0.032	0.037
	MB201	>50	>50	>50	>50	>50	>50	>50	>50	>50	>50	>50	>50	>50	>50	>50	>50	>50	>50	>50	>50	>50	>50	>50	>50	>50	>50	>50	>50	>50	>50	>50	>50	>50	>50
	MB539.2B7	>50	>50	>50	>50	>50	>50	>50	31.9	40.7	>50	>50	>50	>50	>50	>50	>50	>50	>50	0.431	>50	>50	17.900	>50	>50	0.186	0.634	1.150	29.400	13.300	>50	>50	>50	>50
	Q168.a2	>50	>50	>50	>50	>50	>50	>50	0.148	0.181	>50	>50	>50	>50	>50	>50	>50	>50	>50	7.04	>50	>50	0.007	>50	>50	0.001	0.005	0.003	0.003	0.007	0.199	4.160	>50	>50
	Q23.17	>50	>50	0.867	23.6	>50	>50	>50	0.911	9.50	2.59	>50	>50	>50	>50	0.338	>50	6.42	35.0	0.233	>50	>50	0.006	>50	>50	0.001	>50	>50	0.005	0.023	>50	>50	>50	>50
	Q259.d2.17	>50	>50	0.002	0.025	0.023	>50	42.5	0.001	0.008	24.6	>50	>50	>50	2.13	0.657	5.78	0.076	5.31	2.16	>50	25.4	0.005	>50	>50	0.002	0.011	0.005	0.012	0.019	0.107	0.262	>50	>50
	Q461.e2	>50	>50	>50	>50	>50	>50	>50	0.502	0.705	>50	>50	>50	>50	>50	19.9	>50	>50	>50	15.60	>50	>50	4.100	>50	>50	0.007	0.024	0.014	1.590	2.000	>50	>50	>50	>50
	Q769.d22	>50	>50	>50	>50	>50	>50	>50	>50	>50	>50	>50	>50	>50	>50	>50	>50	>50	>50	>50	>50	>50	>50	>50	>50	>50	>50	>50	>50	>50	>50	>50	>50	>50	>50
	Q842.d12	>50	>50	>50	>50	>50	>50	>50	>50	10.1	>50	>50	>50	>50	>50	9.35	>50	>50	>50	0.160	>50	>50	0.630	>50	>50	0.005	17.100	10.600	0.779	1.690	>50	>50	>50	>50
	RW020.2	>50	>50	>50	>50	>50	>50	>50	>50	>50	>50	>50	>50	>50	>50	>50	>50	>50	>50	>50	>50	>50	>50	>50	>50	>50	>50	>50	>50	>50	>50	>50	>50	>50	>50
	UG037.8	>50	>50	>50	>50	>50	>50	>50	>50	>50	>50	>50	>50	>50	>50	>50	>50	>50	>50	>50	>50	>50	>50	>50	>50	>50	>50	>50	>50	>50	>50	>50	>50	>50	>50
Clade B	6535.3	>50	>50	>50	>50	>50	>50	>50	>50	>50	>50	>50	>50	>50	>50	>50	>50	>50	>50	>50	>50	>50	>50	>50	>50	>50	>50	>50	>50	>50	>50	>50	>50	>50	>50
	AC10.29	>50	>50	>50	>50	>50	0.030	>50	>50	>50	>50	>50	>50	>50	>50	>50	>50	>50	>50	2.98	>50	>50	>50	>50	>50	0.077	>50	>50	>50	20.400	>50	>50	>50	>50
	CAAN.A2	>50	>50	>50	>50	>50	>50	>50	>50	>50	>50	>50	>50	>50	>50	>50	>50	>50	>50	>50	>50	>50	>50	>50	>50	>50	>50	>50	>50	>50	>50	>50	>50	>50	>50
	PVO.04	>50	7.98	>50	>50	44.4	0.947	>50	11.8	>50	2.48	10.8	>50	>50	>50	30.0	>50	>50	>50	1.10	>50	>50	9.03	>50	>50	0.072	0.562	0.371	6.000	4.000	12.600	>50	17.800	>50
	QH0692.42	>50	>50	>50	>50	>50	>50	>50	>50	>50	>50	>50	>50	>50	>50	>50	>50	>50	>50	>50	>50	>50	>50	>50	>50	>50	>50	>50	>50	>50	>50	>50	>50	>50	>50
	REJO.67	>50	>50	>50	>50	>50	>50	>50	>50	>50	>50	>50	>50	>50	>50	>50	>50	>50	>50	>50	>50	>50	>50	>50	>50	>50	>50	>50	>50	>50	>50	>50	>50	>50	>50
	RHPA.7	>50	>50	>50	>50	>50	>50	>50	>50	>50	>50	>50	>50	>50	>50	>50	>50	>50	>50	>50	>50	>50	>50	>50	>50	>50	>50	>50	>50	>50	>50	>50	>50	>50	>50
	SC422.8	>50	>50	>50	>50	>50	0.439	>50	>50	>50	>50	>50	>50	>50	>50	>50	>50	>50	>50	>50	>50	>50	>50	>50	>50	47.200	1.740	4.860	>50	>50	>50	>50	>50	>50
	THRO.18	>50	>50	>50	>50	>50	3.30	>50	>50	>50	>50	>50	>50	>50	>50	>50	>50	>50	>50	>50	>50	>50	>50	>50	>50	19.800	0.667	1.230	>50	>50	>50	>50	>50	>50
	TRJO.58	>50	>50	>50	>50	>50	>50	>50	>50	>50	>50	>50	>50	>50	>50	>50	>50	>50	>50	>50	>50	>50	>50	>50	>50	>50	>50	>50	>50	>50	>50	>50	>50	>50	>50
	TRO.11	>50	>50	>50	>50	>50	>50	>50	>50	>50	>50	>50	>50	>50	>50	>50	>50	>50	>50	>50	>50	>50	>50	>50	>50	>50	>50	>50	>50	>50	>50	>50	>50	>50	>50
	WITO.33	>50	>50	>50	>50	>50	0.005	>50	>50	>50	>50	>50	>50	>50	>50	>50	>50	>50	>50	>50	>50	>50	>50	>50	>50	>50	>50	>50	>50	>50	>50	>50	>50	>50	>50
Clade D	3016.V5.c36	16.4	0.057	0.450	0.283	0.011	>50	>50	0.005	0.004	0.017	0.300	7.930	3.740	0.012	0.160	0.012	0.011	0.028	0.039	>50	>50	0.022	>50	>50	0.0002	0.022	0.006	0.008	0.012	1.050	>50	0.284	0.506
	6405.v4.c34	>50	>50	>50	>50	>50	>50	>50	>50	>50	>50	>50	>50	>50	>50	>50	>50	>50	>50	>50	>50	>50	>50	>50	>50	>50	>50	>50	>50	>50	>50	>50	>50	>50	>50
Clade AE	C1080.c3	>50	>50	0.036	0.212	>50	>50	>50	0.023	0.019	>50	0.018	>50	>50	0.779	>50	5.90	>50	2.15	14.5	>50	>50	0.013	>50	>50	0.004	0.016	0.149	0.012	0.009	0.073	1.670	>50	>50
	CM244.ec1	3.32	2.03	0.007	0.361	0.517	>50	6.90	1.00	0.105	0.914	26.7	>50	>50	6.16	0.112	0.670	0.140	1.42	0.024	>50	>50	4.540	>50	>50	0.092	0.047	0.056	0.640	1.130	>50	>50	0.561	0.036
	CNE3	>50	>50	>50	>50	>50	>50	>50	>50	>50	>50	>50	>50	>50	>50	>50	>50	>50	>50	>50	>50	>50	>50	>50	>50	>50	>50	>50	>50	>50	>50	>50	>50	>50	>50
	TH976.17	>50	>50	>50	>50	>50	>50	>50	>50	>50	>50	>50	>50	>50	>50	>50	>50	>50	>50	>50	>50	>50	>50	>50	>50	0.106	>50	>50	>50	>50	>50	>50	>50	>50	>50
nonHIV	SIVmac251.30	>50					>50		>50	>50															>50	>50								
	% breadth	20%	17%	35%	30%	22%	17%	13%	46%	46%	24%	26%	7%	7%	24%	33%	28%	28%	26%	46%	2%	13%	46%	7%	7%	63%	59%	59%	41%	46%	28%	20%	20%	22%
	Median IC50 (ug/ml)	3.32	0.441	0.061	0.269	0.018	0.693	5.00	0.076	0.023	0.346	1.04	0.211	0.094	0.750	0.338	0.670	0.140	1.66	0.160	1.87	0.580	0.035	0.028	0.460	0.003	0.047	0.047	0.082	0.093	0.762	1.66	0.097	0.272

Supplemental Table 5A. Neutralization data. Analysis of this data set is shown in Figure 6.

IC50

Virus ID	Clade	CAP256-VRC26.08	CAP256-VRC26.25	PGDM1400	PGT145	PG9	CH01	PGT121	PGT151	VRC01	10E8
0260.v5.c36	A	>50	3.28	0.003	>50	1.12	>50	0.039	0.020	0.718	17.7
0330.v4.c3	A	>50	0.003	0.007	0.697	0.013	0.468	0.041	0.002	0.072	1.27
0439.v5.c1	A	>50	>50	25.7	3.78	>50	>50	>50	0.003	0.282	1.44
3365.v2.c20	A	0.100	0.009	0.006	0.339	0.060	1.00	0.059	0.001	0.096	2.30
3415.v1.c1	A	>50	0.351	0.031	>50	0.096	5.46	>50	0.001	0.131	5.29
3718.v3.c11	A	0.105	0.016	0.004	0.046	0.038	0.272	1.40	0.009	0.486	2.36
BB201.B42	A	0.001	0.00003	0.001	0.030	0.007	0.126	0.003	0.006	0.366	0.798
BG505.W6M.C2	A	0.173	0.0004	0.001	0.016	0.053	0.633	0.041	0.0003	0.056	0.310
BI369.9A	A	0.008	0.0005	0.008	0.018	0.017	0.387	0.008	0.008	0.310	0.231
BS208.B1	A	0.003	0.00004	0.003	0.001	0.008	0.045	>50	0.002	0.011	0.358
KER2008.12	A	>50	0.008	0.003	8.33	0.007	0.802	2.22	0.001	0.844	22.0
KER2018.11	A	0.003	0.00008	0.004	0.003	0.008	0.159	>50	0.002	0.881	2.01
KNH1209.18	A	>50	0.005	5.13	>50	0.180	38.9	0.002	0.002	0.142	1.44
MB201.A1	A	>50	>50	0.278	2.49	0.103	0.243	0.005	0.005	0.286	0.225
MB539.2B7	A	31.9	0.202	0.002	1.19	0.060	>50	>50	0.001	0.685	7.10
MI369.A5	A	0.039	0.001	0.012	0.010	0.050	0.849	0.022	0.004	0.434	0.691
MS208.A1	A	0.0007	0.002	0.002	0.231	0.079	3.05	>50	0.0007	0.335	0.604
Q23.17	A	0.010	0.002	0.0007	0.002	0.003	0.008	0.004	0.003	0.092	0.783
Q259.17	A	0.001	0.00003	0.020	45.0	0.050	>50	>50	>50	0.074	4.52
Q769.d22	A	>50	>50	0.002	0.151	0.011	>50	>50	>50	0.038	1.57
Q842.d12	A	>50	0.001	0.003	0.067	0.024	0.223	0.016	0.001	0.036	2.31
QH209.14M.A2	A	>50	>50	0.031	0.004	>50	>50	>50	0.0009	0.043	1.74
RW020.2	A	>50	>50	0.005	5.17	0.124	>50	0.002	0.002	0.393	1.36
UG037.8	A	>50	>50	0.056	2.33	0.014	0.287	0.065	>50	0.126	0.095
3301.V1.C24	AC	0.013	0.002	0.009	0.193	0.230	>50	0.009	0.003	0.163	3.96
3589.V1.C4	AC	>50	>50	>50	>50	0.027	7.29	>50	0.001	0.162	1.43
6540.v4.c1	AC	0.077	0.003	0.008	0.003	0.030	0.465	>50	0.003	>50	3.01
6545.V4.C1	AC	0.026	0.005	0.009	0.003	0.036	0.171	>50	0.002	>50	2.03
0815.V3.C3	ACD	>50	>50	>50	>50	>50	>50	0.020	0.400	0.028	0.461
6095.V1.C10	ACD	0.0007	0.0003	0.024	0.002	0.151	>50	37.3	>50	1.37	0.602
3468.V1.C12	AD	>50	>50	>50	>50	1.62	31.5	0.042	0.070	0.055	0.553
Q168.a2	AD	0.148	0.0009	0.005	0.860	0.060	2.26	>50	0.003	0.126	1.93
Q461.e2	AD	0.502	0.001	0.080	16.0	2.05	>50	>50	1.01	0.569	1.53
620345.c1	AE	0.001	0.005	0.300	0.056	1.01	>50	>50	>50	>50	1.50
BJOX009000.02.4	AE	>50	>50	0.097	0.099	1.94	10.1	14.7	>50	2.15	0.558
BJOX010000.06.2	AE	>50	>50	2.88	>50	0.303	1.57	>50	>50	9.00	0.074
BJOX025000.01.1	AE	>50	>50	0.010	1.44	0.096	>50	>50	>50	0.238	0.221
BJOX028000.10.3	AE	>50	>50	0.023	4.00	0.690	>50	>50	>50	3.08	0.045
C1080.c3	AE	0.023	0.006	0.0008	0.010	0.002	0.033	>50	>50	0.212	0.099
C2101.c1	AE	>50	>50	0.016	0.005	0.031	1.62	>50	>50	0.111	1.17
C3347.c11	AE	>50	>50	0.003	0.004	0.030	6.07	>50	>50	0.217	0.006
C4118.09	AE	0.002	0.00004	0.003	0.002	0.038	0.254	>50	0.071	0.100	0.068
CNE3	AE	>50	>50	0.020	0.252	0.064	>50	>50	>50	0.358	1.85
CNE5	AE	0.018	0.0003	0.002	0.002	0.008	0.104	>50	>50	0.394	1.31
CNE55	AE	0.026	0.0002	0.008	0.002	0.197	>50	>50	>50	0.564	0.102
CNE56	AE	>50	>50	8.16	1.63	>50	>50	>50	>50	1.12	0.070
CNE59	AE	>50	>50	0.005	0.018	0.060	2.61	>50	>50	0.422	0.001
R1166.c1	AE	>50	>50	0.791	4.44	1.10	13.1	>50	>50	0.172	0.503
R2184.c4	AE	19.8	0.002	0.002	0.050	0.384	>50	>50	>50	0.269	0.686
TH966.8	AE	0.036	0.004	0.006	0.002	0.015	0.049	>50	>50	0.446	0.024
TH976.17	AE	>50	0.006	>50	>50	>50	>50	>50	>50	0.456	0.216
235-47.SG3	AG	0.265	0.045	0.013	3.38	0.124	1.14	0.110	1.50	0.015	0.200
242-14	AG	0.0007	0.0001	0.007	0.033	0.048	>50	>50	0.001	>50	0.912
263-8	AG	0.031	0.011	0.020	13.2	0.211	>50	1.23	>50	0.251	0.243
269-12	AG	>50	0.005	1.92	4.36	1.42	7.68	0.164	0.001	0.330	0.106
271-11	AG	>50	>50	0.021	35.7	0.059	1.44	11.7	>50	0.055	0.587
928-28	AG	0.097	0.002	0.003	>50	0.038	4.51	31.0	>50	0.639	0.128
DJ263.8	AG	0.031	0.001	0.002	0.018	0.091	2.99	0.064	0.001	0.213	0.015
T250-4	AG	0.001	0.0005	0.0006	0.0004	0.004	0.042	0.001	0.0008	>50	0.480
T251-18	AG	>50	>50	9.43	0.318	>50	2.23	10.8	0.065	5.38	0.419
T253-11	AG	49.5	0.008	0.003	>50	0.142	3.06	>50	0.003	0.601	0.919
T255-34	AG	>50	>50	0.236	>50	0.020	21.1	>50	0.001	0.699	0.289
T257-31	AG	0.009	0.0002	0.005	3.49	0.019	0.768	>50	0.0009	2.14	0.592
T266-60	AG	1.78	0.004	0.510	0.071	0.321	2.49	0.160	0.003	3.69	>50
T33-7	AG	>50	0.266	0.001	4.97	0.019	0.323	>50	3.00	0.026	0.806
3988.25	B	>50	0.001	0.010	0.007	0.045	>50	0.002	0.003	0.747	0.143
5768.04	B	>50	>50	0.003	0.020	0.270	0.825	0.039	0.008	0.639	3.63
6101.10	B	>50	>50	>50	>50	>50	>50	0.002	0.013	0.063	0.002
6535.3	B	>50	>50	>50	>50	0.166	0.428	0.003	0.002	2.73	0.365
7165.18	B	>50	>50	0.918	0.056	>50	2.30	0.019	>50	25.1	0.602
89.6.DG	B	>50	>50	>50	>50	>50	>50	0.016	>50	1.25	0.290

89.6.DG	B	>50	>50	>50	>50	>50	>50	0.016	>50	1.25	0.290
AC10.29	B	>50	0.002	0.010	0.006	0.031	16.3	0.028	0.004	1.60	0.171
ADA.DG	B	>50	>50	0.028	0.005	0.216	>50	0.002	>50	0.801	0.011
Bal.01	B	>50	>50	0.122	>50	0.569	>50	0.011	0.004	0.156	0.638
BaL.26	B	>50	>50	0.017	1.41	0.030	>50	0.010	0.004	0.047	0.538
BG1168.01	B	>50	>50	>50	>50	>50	>50	>50	0.006	1.07	0.405
BL01.DG	B	>50	>50	>50	>50	>50	>50	>50	0.003	>50	0.146
BR07.DG	B	>50	>50	>50	>50	>50	>50	0.064	0.013	2.80	0.025
BX08.16	B	>50	0.0006	0.020	0.007	0.017	0.590	0.002	0.003	0.456	0.205
CAAN.A2	B	>50	>50	>50	5.53	6.31	>50	0.005	0.001	1.09	1.14
CNE10	B	>50	>50	>50	>50	0.222	>50	0.005	>50	0.939	0.0009
CNE12	B	>50	>50	>50	>50	>50	>50	0.002	0.004	1.15	0.121
CNE14	B	>50	>50	>50	>50	>50	>50	0.002	0.0009	0.507	0.068
CNE4	B	>50	>50	>50	>50	>50	>50	11.5	>50	0.971	0.055
CNE57	B	>50	>50	>50	>50	>50	>50	0.008	0.003	0.755	0.058
HO86.8	B	>50	>50	0.021	0.002	0.051	0.186	>50	5.77	>50	0.549
HT593.1	B	>50	>50	0.426	0.058	0.345	>50	>50	0.004	1.07	0.038
HXB2.DG	B	>50	>50	>50	>50	1.00	>50	>50	0.005	0.071	0.002
JRCSF.JB	B	>50	>50	0.009	0.001	0.004	0.782	0.061	0.003	0.483	0.523
JRFL.JB	B	>50	>50	>50	4.90	>50	>50	0.017	0.003	0.034	0.155
MN.3	B	>50	>50	>50	>50	17.1	>50	>50	>50	0.018	*0.0003*
PVO.04	B	11.8	0.016	1.14	0.143	7.63	24.2	0.132	0.015	0.567	2.81
QH0515.01	B	>50	>50	>50	>50	>50	>50	8.70	0.002	1.31	1.82
QH0692.42	B	>50	>50	>50	>50	>50	>50	0.940	0.085	1.96	0.581
REJO.67	B	>50	>50	0.001	0.0004	0.006	0.620	8.87	0.032	0.116	0.234
RHPA.7	B	>50	>50	0.345	0.028	9.97	8.33	0.014	0.003	0.066	1.27
SC422.8	B	>50	>50	0.777	0.027	0.542	>50	0.098	0.002	0.205	0.232
SF162.LS	B	>50	>50	>50	>50	>50	>50	0.004	0.005	0.282	0.105
SS1196.01	B	>50	>50	0.246	19.4	0.147	>50	0.002	>50	0.359	0.361
THRO.18	B	>50	17.7	0.087	0.006	4.87	9.32	>50	>50	7.76	0.100
TRJO.58	B	>50	>50	>50	>50	0.173	>50	4.31	0.242	0.177	0.980
TRO.11	B	>50	>50	0.632	0.029	>50	>50	0.006	>50	0.730	0.023
WITO.33	B	>50	>50	0.001	0.001	0.007	0.013	0.787	0.003	0.157	0.120
YU2.DG	B	>50	>50	0.304	0.035	2.08	>50	0.068	>50	0.140	2.23
CH038.12	BC	0.072	0.001	>50	46.5	5.53	>50	0.004	>50	0.542	0.583
CH070.1	BC	0.039	0.026	0.002	0.003	0.006	>50	0.003	>50	9.90	4.67
CH117.4	BC	0.003	0.000005	0.002	0.012	0.006	1.16	>50	2.18	0.153	0.203
CH181.12	BC	0.001	0.0000	0.001	0.0003	0.004	0.494	0.007	>50	1.04	0.456
CNE15	BC	>50	0.301	0.005	2.60	0.005	0.356	19.0	0.003	0.181	0.703
CNE19	BC	19.7	0.0000	0.003	0.068	0.015	1.90	0.007	0.002	0.269	0.090
CNE20	BC	>50	0.0005	0.006	0.042	0.047	1.18	0.002	>50	8.77	0.108
CNE21	BC	0.001	0.0001	0.002	0.002	0.063	>50	0.004	0.0009	0.566	1.14
CNE40	BC	>50	0.016	0.483	0.214	0.812	>50	0.224	0.005	0.602	0.0004
CNE7	BC	0.003	0.003	0.007	0.259	1.02	>50	0.032	0.020	0.327	0.184
286.36	C	0.005	0.0003	0.024	0.003	0.185	8.92	0.002	0.005	0.406	0.946
288.38	C	>50	>50	1.32	2.61	2.42	8.83	0.006	>50	3.73	0.322
0013095-2.11	C	0.021	0.029	0.007	16.6	0.012	0.981	>50	>50	0.169	0.002
001428-2.42	C	30.9	0.070	0.004	0.0006	0.002	0.074	0.023	0.011	0.020	1.73
0077_V1.C16	C	0.001	0.006	0.002	0.194	0.083	42.9	>50	0.0007	2.09	2.45
00836-2.5	C	>50	>50	0.004	0.887	>50	>50	31.8	0.009	0.255	0.797
0921.V2.C14	C	0.036	0.0001	0.005	0.011	0.004	0.382	>50	>50	0.260	1.25
16055-2.3	C	0.004	0.0005	0.002	0.008	0.016	>50	1.02	0.070	0.093	0.605
16845-2.22	C	>50	>50	>50	46.7	1.96	5.74	9.41	>50	6.62	0.006
16936-2.21	C	0.250	0.002	1.38	5.14	>50	>50	0.003	0.103	0.301	0.221
25710-2.43	C	0.008	0.0000	0.008	0.002	0.031	2.50	0.014	2.00	0.973	0.040
25711-2.4	C	>50	>50	0.763	7.46	0.932	2.78	0.010	0.002	1.18	1.01
25925-2.22	C	0.013	0.0000	0.004	0.003	0.025	2.10	0.024	0.002	0.907	0.491
26191-2.48	C	0.001	0.0001	0.018	0.053	0.132	3.00	0.150	>50	0.325	2.40
3168.V4.C10	C	>50	0.109	0.056	0.028	0.092	1.18	0.485	>50	0.215	2.47
3637.V5.C3	C	>50	>50	>50	>50	>50	>50	>50	0.055	5.46	2.02
6322.V4.C1	C	0.003	0.0008	0.012	0.073	>50	>50	>50	>50	>50	4.23
6471.V1.C16	C	>50	>50	>50	>50	>50	>50	>50	24.4	>50	5.61
6631.V3.C10	C	>50	>50	>50	>50	>50	>50	>50	0.002	>50	1.06
6644.V2.C33	C	>50	>50	>50	>50	0.025	>50	0.018	>50	0.233	0.007
6785.V5.C14	C	0.005	0.0003	0.010	0.105	0.008	0.879	0.019	>50	0.416	0.550
6838.V1.C35	C	0.001	0.0007	0.001	0.215	0.006	0.137	0.119	0.025	0.338	0.457
96ZM651.02	C	2.63	0.494	0.092	7.33	>50	>50	0.009	0.001	1.01	0.018
BR025.9	C	>50	>50	0.004	8.67	0.019	0.224	0.002	0.081	0.437	0.315
CAP210.E8	C	0.003	0.0002	0.001	>50	0.165	15.7	>50	0.002	>50	0.815
CAP244.D3	C	46.0	>50	4.48	12.0	0.067	0.655	>50	0.069	1.01	0.316
CAP256.206.C9	C	0.002	0.0002	0.005	2.20	0.060	2.13	0.009	>50	0.628	0.950
CAP45.G3	C	4.00	0.0000	0.002	0.0008	0.003	0.105	2.08	0.001	5.63	0.919
CNE30	C	>50	>50	>50	>50	>50	>50	0.061	0.100	0.954	0.873
CNE31	C	>50	>50	0.246	0.068	15.8	>50	0.789	0.002	1.30	0.942
CNE53	C	>50	>50	0.017	0.019	0.080	0.236	0.022	>50	0.113	0.425
CNE58	C	0.006	0.0000	0.004	0.062	0.022	0.047	>50	0.0007	0.221	0.501
DU123.06	C	0.015	0.008	0.001	0.024	0.062	0.515	0.033	>50	6.73	0.122
DU151.02	C	0.006	0.0003	0.001	0.006	0.016	0.671	0.005	0.070	11.0	0.588
DU156.12	C	0.006	0.002	0.001	0.008	0.041	0.305	0.005	0.002	0.159	0.004
DU172.17	C	>50	>50	2.37	>50	0.190	7.70	0.104	0.0009	>50	0.026
DU422.01	C	1.12	0.053	>50	>50	>50	>50	0.164	0.400	>50	0.189
MW965.26	C	0.003	0.019	0.023	0.147	0.619	>50	0.011	0.038	0.048	0.0005
SO18.18	C	0.002	0.0008	0.003	0.002	0.021	9.73	0.002	0.002	0.066	2.37

TV1.29	C	>50	0.339	0.002	3.34	0.005	0.680	0.118	0.0003	>50	0.156
TZA125.17	C	0.018	0.002	0.044	0.115	0.140	>50	9.96	0.056	>50	0.484
TZBD.02	C	0.036	0.003	0.013	0.035	0.170	20.0	0.005	0.001	0.065	1.94
ZA012.29	C	>50	>50	2.21	1.26	7.47	>50	0.005	0.054	0.300	3.09
ZM106.9	C	0.010	0.007	0.002	0.016	0.492	>50	0.005	>50	0.256	>50
ZM109.4	C	>50	0.003	0.003	0.012	0.154	>50	13.7	0.348	0.150	0.353
ZM135.10a	C	>50	>50	>50	>50	>50	>50	1.50	>50	1.66	0.180
ZM176.66	C	0.029	0.0001	0.003	0.032	0.010	1.89	13.8	0.0008	0.065	0.246
ZM197.7	C	0.002	0.005	0.024	0.523	0.369	>50	>50	0.002	0.966	0.088
ZM214.15	C	3.23	0.002	>50	>50	>50	>50	0.682	0.012	2.09	2.46
ZM215.8	C	>50	>50	0.002	>50	0.073	>50	0.014	0.029	0.442	0.041
ZM233.6	C	0.003	0.0005	0.002	0.008	0.148	0.074	1.14	0.004	2.51	0.110
ZM249.1	C	0.0009	0.0008	0.001	1.99	0.043	>50	>50	0.0009	0.128	0.735
ZM53.12	C	0.003	0.0001	0.007	0.154	0.036	>50	0.002	>50	1.57	2.19
ZM55.28a	C	0.005	0.001	0.022	0.687	3.15	>50	0.070	0.0008	0.411	2.85
3326.V4.C3	CD	0.007	0.0000	0.006	0.009	0.030	>50	>50	0.224	0.088	1.25
3337.V2.C6	CD	0.044	0.0002	>50	>50	>50	>50	21.1	0.001	0.100	1.53
3817.v2.c59	CD	>50	>50	>50	>50	0.004	0.092	>50	>50	>50	0.354
231965.c1	D	>50	>50	0.001	0.122	0.682	>50	>50	0.002	0.278	6.32
247-23	D	0.005	0.0001	0.008	0.017	0.092	>50	>50	>50	3.57	0.659
3016.v5.c45	D	0.005	0.0002	>50	25.4	0.283	>50	>50	0.078	0.172	0.240
57128.vrc15	D	>50	0.004	0.003	0.118	0.122	>50	2.16	>50	>50	0.611
6405.v4.c34	D	>50	>50	>50	>50	>50	>50	0.019	0.020	2.40	0.674
A03349M1.vrc4a	D	2.68	0.004	0.013	4.60	>50	>50	0.013	>50	5.59	0.436
NKU3006.ec1	D	>50	>50	>50	>50	>50	>50	>50	>50	0.766	1.06
P1981.C5.3	G	0.008	0.002	0.160	1.08	0.201	>50	0.004	0.001	0.414	0.0005
X1193.c1	G	0.343	0.001	0.162	0.015	0.120	>50	0.028	0.010	0.194	0.724
X1254.c3	G	>50	>50	>50	1.27	0.035	18.5	0.024	0.032	0.051	5.85
X1632.S2.B10	G	0.009	0.0004	0.001	0.006	0.087	5.25	>50	0.070	0.133	0.579
X2088.c9	G	>50	>50	>50	>50	>50	>50	0.003	>50	>50	>50

	CAP256-VRC26.08	CAP256-VRC26.25	PGDM1400	PGT145	PG9	CH01	PGT121	PGT151	VRC01	10E8
# Viruses	183	183	183	183	183	183	183	183	183	183
# Viruses Neutralized										
IC50 <50ug/ml	85	104	143	138	146	94	120	124	165	180
IC50 <10ug/ml	78	103	142	128	144	83	109	123	163	178
IC50 <1.0ug/ml	72	102	131	98	125	47	96	117	124	126
IC50 <0.1ug/ml	64	95	113	76	85	10	81	110	28	34
IC50 <0.01ug/ml	41	85	78	38	22	1	42	83	0	13
% VS Neutralized										
IC50 <50ug/ml	46	57	78	75	80	51	66	68	90	98
IC50 <10ug/ml	43	56	78	70	79	45	60	67	89	97
IC50 <1.0ug/ml	39	56	72	54	68	26	52	64	68	69
IC50 <0.1ug/ml	35	52	62	42	46	5	44	60	15	19
IC50 <0.01ug/ml	22	46	43	21	12	1	23	45	0	7
Median IC50	0.010	0.001	0.008	0.060	0.064	0.991	0.023	0.003	0.393	0.544
Geometric Mean	0.026	0.002	0.016	0.095	0.085	1.06	0.053	0.007	0.396	0.336

Supplemental Table 5B. Neutralization data. Analysis of this data set is shown in Figure 6.

IC80

Virus ID	Clade	CAP256-VRC26.08	CAP256-VRC26.25	PGDM1400	PGT145	PG9	CH01	PGT121	PGT151	VRC01	10E8
0260.v5.c36	A	>50	>50	0.014	>50	8.41	>50	0.143	>50	1.50	27.7
0330.v4.c3	A	>50	1.04	0.015	18.5	0.038	>50	0.194	0.009	0.188	3.72
0439.v5.c1	A	>50	>50	>50	16.1	>50	>50	>50	>50	0.628	4.81
3365.v2.c20	A	>50	>50	0.040	34.7	0.233	>50	1.34	0.002	0.181	5.74
3415.v1.c1	A	>50	>50	0.395	>50	0.540	>50	>50	0.003	0.297	9.14
3718.v3.c11	A	>50	>50	0.014	0.971	0.136	5.33	8.64	0.055	12.1	7.47
BB201.B42	A	0.500	0.001	0.004	2.00	0.026	2.35	0.011	0.115	0.932	2.78
BG505.W6M.C2	A	>50	0.012	0.003	0.160	0.141	>50	0.337	0.003	0.153	1.41
BI369.9A	A	0.099	0.004	0.023	0.348	0.067	2.16	0.043	0.519	0.925	1.24
BS208.B1	A	0.012	0.0004	0.009	0.008	0.027	0.313	>50	0.070	0.059	2.93
KER2008.12	A	>50	0.183	0.012	>50	0.028	>50	>50	0.060	1.76	>50
KER2018.11	A	0.001	0.002	0.012	0.037	0.029	2.02	>50	0.006	1.84	6.38
KNH1209.18	A	>50	8.85	>50	>50	>50	>50	0.007	0.007	0.370	5.09
MB201.A1	A	>50	>50	0.938	38.1	0.305	>50	0.026	0.211	0.633	1.57
MB539.2B7	A	>50	4.00	0.005	>50	0.256	>50	>50	0.010	1.29	>50
MI369.A5	A	2.86	0.019	0.042	0.132	0.226	>50	0.087	0.125	1.15	3.01
MS208.A1	A	1.00	0.232	0.500	30.3	0.609	>50	>50	0.002	1.04	2.54
Q23.17	A	>50	1.30	0.004	6.73	0.012	0.028	0.019	0.013	0.252	3.02
Q259.17	A	0.259	0.0003	10.0	>50	0.340	>50	>50	>50	0.251	10.7
Q769.d22	A	>50	>50	0.005	4.71	0.038	>50	>50	>50	0.103	4.08
Q842.d12	A	>50	0.123	0.007	0.837	0.068	3.75	0.047	0.010	0.089	6.53
QH209.14M.A2	A	>50	>50	0.106	0.018	>50	>50	>50	0.003	0.116	4.70
RW020.2	A	>50	>50	0.020	>50	0.771	>50	0.009	0.005	0.859	4.10
UG037.8	A	>50	>50	0.203	>50	0.080	>50	0.237	>50	0.301	0.661
3301.V1.C24	AC	0.002	0.020	0.075	2.30	1.40	>50	0.030	0.070	0.431	10.2
3589.V1.C4	AC	>50	>50	>50	>50	0.098	>50	>50	0.006	0.385	4.32
6540.v4.c1	AC	29.2	0.051	0.022	0.046	0.105	>50	>50	0.020	>50	7.86
6545.V4.C1	AC	27.6	0.096	0.026	0.070	0.144	>50	>50	0.010	>50	6.06
0815.V3.C3	ACD	>50	>50	>50	>50	>50	>50	0.072	>50	0.093	1.76
6095.V1.C10	ACD	0.100	0.005	0.062	0.050	1.13	>50	>50	>50	3.81	0.004
3468.V1.C12	AD	>50	>50	>50	>50	>50	>50	1.05	>50	0.171	2.75
Q168.a2	AD	>50	>50	0.013	25.4	0.179	>50	>50	0.014	0.284	5.23
Q461.e2	AD	19.3	0.080	0.579	>50	15.6	>50	>50	>50	1.54	4.45
620345.c1	AE	0.090	0.051	>50	1.99	>50	>50	>50	>50	>50	4.16
BJOX009000.02.4	AE	>50	>50	0.437	0.468	7.73	>50	>50	>50	6.38	3.25
BJOX010000.06.2	AE	>50	>50	42.2	>50	1.55	16.7	>50	>50	21.2	0.844
BJOX025000.01.1	AE	>50	>50	0.090	10.3	0.826	>50	>50	>50	0.979	1.94
BJOX028000.10.3	AE	>50	>50	0.243	>50	3.68	>50	>50	>50	10.3	0.610
C1080.c3	AE	0.046	0.718	0.003	0.247	0.008	>50	>50	>50	0.587	0.683
C2101.c1	AE	>50	>50	0.041	0.049	0.139	>50	>50	>50	0.279	4.72
C3347.c11	AE	>50	>50	0.015	0.023	0.103	>50	>50	>50	0.706	0.047
C4118.09	AE	0.020	0.001	0.009	0.009	0.093	2.41	>50	>50	0.342	1.03
CNE3	AE	>50	>50	>50	21.4	0.598	>50	>50	>50	0.962	4.82
CNE5	AE	0.241	0.024	0.006	0.013	0.027	>50	>50	>50	1.14	3.92
CNE55	AE	5.00	0.006	0.030	0.015	2.08	>50	>50	>50	1.53	1.26
CNE56	AE	>50	>50	26.0	5.91	>50	>50	>50	>50	2.93	0.490
CNE59	AE	>50	>50	0.019	0.664	0.443	>50	>50	>50	1.13	0.030
R1166.c1	AE	>50	>50	2.50	43.6	3.90	>50	>50	>50	0.407	1.75
R2184.c4	AE	>50	5.00	0.006	0.482	2.23	>50	>50	>50	1.76	2.23
TH966.8	AE	0.052	0.089	0.016	0.023	0.061	0.098	>50	>50	1.44	0.315
TH976.17	AE	>50	8.00	>50	>50	>50	>50	>50	>50	1.23	1.50
235-47.SG3	AG	16.4	2.55	0.043	20.2	0.803	>50	0.842	>50	0.160	0.889
242-14	AG	0.300	0.005	0.033	1.36	0.151	>50	>50	0.020	>50	3.10
263-8	AG	1.88	0.270	0.088	>50	1.27	>50	7.73	>50	0.631	0.996
269-12	AG	>50	0.182	4.33	39.4	5.17	>50	1.26	0.005	1.05	0.654
271-11	AG	>50	>50	0.081	>50	0.948	>50	>50	>50	0.279	4.21
928-28	AG	4.31	0.041	0.200	>50	0.225	41.3	>50	>50	1.17	0.878
DJ263.8	AG	0.099	0.014	0.009	0.170	0.551	>50	0.202	0.005	3.53	0.176
T250-4	AG	0.007	0.002	0.002	0.030	0.017	0.284	0.012	0.003	>50	2.23
T251-18	AG	>50	>50	>50	1.13	>50	>50	>50	>50	10.9	2.09
T253-11	AG	>50	32.5	0.016	>50	0.819	>50	>50	0.016	1.29	3.27
T255-34	AG	>50	>50	>50	>50	0.126	>50	>50	0.005	1.97	1.83
T257-31	AG	0.118	0.002	0.017	>50	0.059	>50	>50	0.003	6.65	1.94
T266-60	AG	12.0	0.110	1.24	0.276	1.42	>50	0.620	0.023	8.63	>50
T33-7	AG	>50	>50	0.008	>50	0.162	3.13	>50	>50	0.060	3.23
3988.25	B	>50	0.110	0.100	0.021	0.200	>50	0.008	0.009	1.46	0.651
5768.04	B	>50	>50	0.200	0.725	2.54	>50	0.897	0.076	1.54	9.18
6101.10	B	>50	>50	>50	>50	>50	>50	0.018	0.366	0.198	0.021
6535.3	B	>50	>50	>50	>50	1.22	>50	0.011	0.006	7.90	2.88
7165.18	B	>50	>50	4.88	0.217	>50	>50	0.074	>50	>50	2.54
89.6.DG	B	>50	>50	>50	>50	>50	>50	0.077	>50	3.64	1.14
AC10.29	B	>50	1.00	0.090	0.024	0.191	>50	0.118	0.018	3.36	0.947
ADA.DG	B	>50	>50	0.252	0.047	>50	>50	0.015	>50	1.84	0.127
Bal.01	B	>50	>50	>50	>50	>50	>50	0.044	0.029	0.556	2.49
BaL.26	B	>50	>50	39.4	>50	0.356	>50	0.050	0.020	0.200	2.24
BG1168.01	B	>50	>50	>50	>50	>50	>50	>50	0.046	3.99	1.52
BL01.DG	B	>50	>50	>50	>50	>50	>50	>50	0.019	>50	1.34
BR07.DG	B	>50	>50	>50	>50	>50	>50	0.338	>50	7.74	0.304
BX08.16	B	>50	>50	0.199	0.100	0.101	>50	0.007	0.060	1.09	1.33
CAAN.A2	B	>50	>50	>50	16.5	>50	>50	0.027	0.008	2.85	5.97

CNE10	B	>50	>50	>50	>50	1.68	>50	0.027	>50	2.12	0.033
CNE12	B	>50	>50	>50	>50	>50	>50	0.014	3.00	2.61	0.875
CNE14	B	>50	>50	>50	>50	>50	>50	0.007	0.020	1.25	0.706
CNE4	B	>50	>50	>50	>50	>50	>50	>50	>50	2.80	0.707
CNE57	B	>50	>50	>50	>50	>50	>50	0.035	0.019	1.62	0.423
HO86.8	B	>50	>50	0.104	0.026	0.345	>50	>50	>50	>50	2.59
HT593.1	B	>50	>50	1.02	0.154	4.05	>50	>50	0.019	2.58	0.304
HXB2.DG	B	>50	>50	>50	>50	40.0	>50	>50	0.070	0.178	0.007
JRCSF.JB	B	>50	>50	0.071	0.007	0.016	>50	0.219	0.030	1.21	2.38
JRFL.JB	B	>50	>50	>50	48.4	>50	>50	0.071	0.020	0.103	0.824
MN.3	B	>50	>50	>50	>50	>50	>50	>50	>50	0.064	*0.0003*
PVO.04	B	>50	0.289	3.17	0.448	20.7	>50	0.436	>50	1.39	8.54
QH0515.01	B	>50	>50	>50	>50	>50	>50	>50	0.007	3.56	5.46
QH0692.42	B	>50	>50	>50	>50	>50	>50	9.70	>50	5.16	2.84
REJO.67	B	>50	>50	0.003	0.002	0.056	>50	>50	0.307	0.291	1.20
RHPA.7	B	>50	>50	0.877	0.076	>50	>50	0.046	0.020	0.162	5.05
SC422.8	B	>50	>50	3.37	0.076	18.1	>50	0.362	0.010	0.471	1.06
SF162.LS	B	>50	>50	>50	>50	>50	>50	0.017	0.034	0.770	0.766
SS1196.01	B	>50	>50	2.06	>50	1.15	>50	0.011	>50	0.905	1.91
THRO.18	B	>50	>50	0.250	0.017	>50	>50	>50	>50	>50	0.715
TRJO.58	B	>50	>50	>50	>50	1.81	>50	>50	2.95	0.340	4.33
TRO.11	B	>50	>50	1.97	0.092	>50	>50	0.032	>50	1.70	0.398
WITO.33	B	>50	>50	0.002	0.004	0.020	0.103	3.25	0.025	0.458	0.943
YU2.DG	B	>50	>50	0.742	0.091	>50	>50	0.178	>50	0.324	9.46
CH038.12	BC	0.400	0.015	>50	>50	>50	>50	0.020	>50	1.29	2.63
CH070.1	BC	0.500	>50	0.004	0.259	0.018	>50	0.015	>50	>50	14.1
CH117.4	BC	0.042	0.00004	0.004	0.275	0.020	>50	>50	>50	0.352	0.883
CH181.12	BC	0.009	0.00004	0.002	0.0003	0.019	>50	0.039	>50	2.01	2.75
CNE15	BC	>50	>50	0.029	>50	0.018	>50	>50	0.088	0.452	2.72
CNE19	BC	>50	0.008	0.007	1.32	0.068	>50	0.063	1.00	0.718	0.813
CNE20	BC	>50	0.109	0.013	0.917	0.163	>50	0.008	>50	>50	0.650
CNE21	BC	0.023	0.002	0.005	0.014	0.397	>50	0.018	0.003	1.65	4.55
CNE40	BC	>50	0.449	1.53	1.41	7.71	>50	1.85	>50	4.43	0.003
CNE7	BC	0.046	0.024	0.032	1.99	4.28	>50	0.096	0.600	1.02	0.958
286.36	C	0.024	0.004	0.046	0.012	0.668	>50	0.009	0.122	1.22	4.41
288.38	C	>50	>50	9.87	47.1	>50	>50	0.035	>50	5.95	2.29
0013095-2.11	C	>50	>50	0.015	>50	0.074	>50	>50	>50	0.266	0.058
001428-2.42	C	>50	>50	0.018	0.020	0.007	>50	0.076	>50	0.059	4.95
0077_V1.C16	C	0.020	0.023	0.007	1.31	0.342	>50	>50	0.002	4.78	12.4
00836-2.5	C	>50	>50	0.200	>50	>50	>50	>50	>50	0.799	1.39
0921.V2.C14	C	1.00	0.002	0.014	0.171	0.012	>50	>50	>50	0.794	3.68
16055-2.3	C	0.015	0.005	0.007	0.073	0.037	>50	12.2	>50	0.287	2.84
16845-2.22	C	>50	>50	>50	>50	>50	>50	>50	>50	21.5	0.094
16936-2.21	C	>50	0.065	>50	>50	>50	>50	0.013	>50	0.825	0.958
25710-2.43	C	0.540	0.004	0.015	0.011	0.139	>50	0.055	>50	2.25	0.282
25711-2.4	C	>50	>50	3.31	>50	3.69	>50	0.041	0.019	2.30	2.33
25925-2.22	C	0.078	0.0009	0.011	0.046	0.071	>50	0.072	0.070	2.11	2.01
26191-2.48	C	0.050	0.003	>50	3.17	0.809	>50	0.393	>50	0.900	5.44
3168.V4.C10	C	>50	>50	0.502	0.101	0.393	>50	1.94	>50	0.553	7.32
3637.V5.C3	C	>50	>50	>50	>50	>50	>50	>50	>50	9.49	7.93
6322.V4.C1	C	0.002	0.012	0.036	1.61	>50	>50	>50	>50	>50	10.2
6471.V1.C16	C	>50	>50	>50	>50	>50	>50	>50	>50	>50	21.9
6631.V3.C10	C	>50	>50	>50	>50	>50	>50	>50	0.009	>50	3.69
6644.V2.C33	C	>50	>50	>50	>50	0.103	>50	0.171	>50	0.659	0.115
6785.V5.C14	C	0.036	0.006	0.059	9.61	0.043	>50	0.072	>50	1.17	2.55
6838.V1.C35	C	0.200	0.042	0.080	14.0	0.032	>50	0.840	>50	0.995	1.55
96ZM651.02	C	>50	>50	0.652	>50	>50	>50	0.044	0.070	3.09	0.175
BR025.9	C	>50	>50	0.009	>50	0.065	1.37	0.008	>50	2.67	1.27
CAP210.E8	C	0.009	0.004	1.50	>50	0.876	>50	>50	0.037	>50	3.84
CAP244.D3	C	>50	>50	>50	>50	0.231	11.8	>50	>50	2.83	1.85
CAP256.206.C9	C	0.006	0.002	0.014	>50	0.142	>50	0.059	>50	1.37	4.28
CAP45.G3	C	0.070	0.001	0.006	0.016	0.010	0.693	19.6	0.012	31.6	3.38
CNE30	C	>50	>50	>50	>50	>50	>50	0.249	>50	2.56	4.16
CNE31	C	>50	>50	0.898	0.328	>50	>50	2.68	0.006	2.73	2.72
CNE53	C	>50	>50	0.089	0.094	0.430	>50	0.054	>50	0.320	1.73
CNE58	C	0.028	0.003	0.011	0.864	0.064	0.776	>50	0.003	0.506	2.52
DU123.06	C	2.29	10.0	0.020	0.355	0.315	4.87	0.101	>50	>50	0.597
DU151.02	C	1.24	0.008	0.004	0.050	0.054	>50	0.021	>50	>50	2.24
DU156.12	C	0.515	0.051	0.003	0.198	0.143	5.46	0.023	0.008	0.403	0.051
DU172.17	C	>50	>50	7.10	>50	0.758	>50	0.846	0.010	>50	0.300
DU422.01	C	40.9	0.109	>50	>50	>50	>50	0.365	>50	>50	1.10
MW965.26	C	0.677	0.572	0.317	6.69	26.0	>50	0.051	0.650	0.146	0.007
SO18.18	C	0.013	0.004	0.009	0.200	0.065	>50	0.006	0.007	0.145	5.60
TV1.29	C	>50	>50	0.004	>50	0.027	>50	0.318	0.004	>50	0.681
TZA125.17	C	4.40	0.028	0.316	2.50	0.808	>50	>50	1.82	>50	2.17
TZBD.02	C	0.140	0.016	0.042	0.685	0.676	>50	0.060	0.005	0.197	5.39

ZA012.29	C	>50	>50	>50	>50	>50	>50	0.021	>50	0.680	6.43
ZM106.9	C	0.500	0.055	0.005	0.203	4.19	>50	0.018	>50	0.535	>50
ZM109.4	C	>50	0.253	0.070	0.149	2.44	>50	>50	>50	0.392	2.45
ZM135.10a	C	>50	>50	>50	>50	>50	>50	9.25	>50	5.72	1.14
ZM176.66	C	10.0	0.001	0.007	1.46	0.033	>50	>50	0.003	0.319	2.16
ZM197.7	C	0.030	0.033	0.170	6.17	2.13	>50	>50	0.015	2.18	0.629
ZM214.15	C	>50	0.231	>50	>50	>50	>50	2.37	0.175	5.33	7.10
ZM215.8	C	>50	>50	0.011	>50	0.497	>50	0.057	0.149	1.26	0.342
ZM233.6	C	0.022	0.002	0.004	0.396	0.457	0.366	0.296	>50	7.27	0.509
ZM249.1	C	0.128	0.021	2.50	>50	0.267	>50	>50	0.004	0.348	1.62
ZM53.12	C	0.007	0.0009	0.019	6.89	0.129	>50	0.016	>50	3.81	10.4
ZM55.28a	C	0.159	0.048	0.106	5.35	>50	>50	0.233	0.003	1.18	11.8
3326.V4.C3	CD	0.044	0.0003	0.012	0.170	0.103	>50	>50	>50	>50	4.51
3337.V2.C6	CD	0.100	0.001	>50	>50	>50	>50	>50	0.002	0.193	5.51
3817.v2.c59	CD	>50	>50	>50	>50	0.015	0.734	>50	>50	>50	2.30
231965.c1	D	>50	>50	3.00	2.90	>50	>50	>50	0.008	1.26	12.9
247-23	D	1.18	0.005	0.020	0.633	0.422	>50	>50	>50	0.396	1.77
3016.v5.c45	D	2.67	0.005	>50	>50	12.6	>50	>50	9.71	>50	1.42
57128.vrc15	D	>50	2.00	0.400	1.48	0.465	>50	>50	>50	5.83	2.46
6405.v4.c34	D	>50	>50	>50	>50	>50	>50	0.080	3.00	9.94	3.45
A03349M1.vrc4a	D	>50	0.120	0.272	>50	>50	>50	0.155	>50	14.8	1.20
NKU3006.ec1	D	>50	>50	>50	>50	>50	>50	>50	>50	1.99	3.33
P1981.C5.3	G	0.039	0.022	>50	39.4	2.68	>50	0.013	4.44	1.04	0.020
X1193.c1	G	8.04	0.600	0.517	0.052	0.378	>50	0.091	0.300	0.426	2.47
X1254.c3	G	>50	>50	>50	10.1	0.125	>50	0.069	>50	0.147	>50
X1632.S2.B10	G	0.037	0.010	0.005	0.091	0.849	>50	>50	>50	0.597	2.35
X2088.c9	G	>50	>50	>50	>50	>50	>50	0.009	>50	>50	>50

	CAP256-VRC26.08	CAP256-VRC26.25	PGDM1400	PGT145	PG9	CH01	PGT121	PGT151	VRC01	10E8
# Viruses	183	183	183	183	183	183	183	183	183	183
# Viruses Neutralized										
IC80 <50ug/ml	68	89	131	109	129	22	102	90	158	177
IC80 <10ug/ml	61	87	127	92	123	19	100	90	151	167
IC80 <1.0ug/ml	49	78	111	69	98	9	88	83	76	52
IC80 <0.1ug/ml	32	61	83	37	40	2	63	71	6	13
IC80 <0.01ug/ml	8	35	33	6	2	0	10	33	0	5
% VS Neutralized										
IC80 <50ug/ml	37	49	72	60	70	12	56	49	86	97
IC80 <10ug/ml	33	48	69	50	67	10	55	49	83	91
IC80 <1.0ug/ml	27	43	61	38	54	5	48	45	42	28
IC80 <0.1ug/ml	17	33	45	20	22	1	34	39	3	7
IC80 <0.01ug/ml	4	19	18	3	1	0	5	18	0	3
Median IC80	0.109	0.022	0.036	0.328	0.233	2.09	0.066	0.019	1.05	2.24
Geometric Mean	0.184	0.026	0.064	0.405	0.280	1.40	0.096	0.027	0.985	1.50

Supplemental Table 5C. Neutralization data. Analysis of this data set is shown in Figures 7-8

IC50

Virus ID	Clade	CAP256-VRC26.08	CAP256-VRC26.25	CAP256-VRC26.26	CAP256-VRC26.27
0260.v5.c36	A	>50	3.28	1.12	0.957
0330.v4.c3	A	>50	0.003	>50	>50
0439.v5.c1	A	>50	>50	1.09	0.381
3365.v2.c20	A	0.100	0.009	0.616	0.116
3415.v1.c1	A	>50	0.351	>50	>50
3718.v3.c11	A	0.105	0.016	4.10	6.44
398-F1_F6_20	A	>50	>50	>50	>50
BB201.B42	A	0.001	0.00003	0.189	0.017
BG505.W6M.C2	A	0.173	0.0004	0.015	0.009
BI369.9A	A	0.008	0.0005	0.002	0.001
BS208.B1	A	0.003	0.00004	0.005	0.001
KER2008.12	A	>50	0.008	10.1	1.02
KER2018.11	A	0.003	0.00008	0.003	0.002
KNH1209.18	A	>50	0.005	>50	>50
MB201.A1	A	>50	>50	>50	>50
MB539.2B7	A	31.9	0.202	0.651	1.13
MI369.A5	A	0.039	0.001	0.212	0.006
MS208.A1	A	0.0007	0.002	0.540	0.021
Q23.17	A	0.010	0.002	>50	>50
Q259.17	A	0.001	0.00003	0.031	0.008
Q769.d22	A	>50	>50	>50	>50
Q769.h5	A	>50	>50	>50	>50
Q842.d12	A	>50	0.001	22.8	3.08
QH209.14M.A2	A	>50	>50	>50	>50
RW020.2	A	>50	>50	>50	>50
UG037.8	A	>50	>50	>50	>50
246-F3.C10.2	AC	0.002	0.014	15.4	>50
3301.V1.C24	AC	0.013	0.002	0.012	0.007
3589.V1.C4	AC	>50	>50	>50	>50
6540.v4.c1	AC	0.077	0.003	0.057	0.031
6545.V4.C1	AC	0.026	0.005	0.310	0.075
0815.V3.C3	ACD	>50	>50	>50	>50
6095.V1.C10	ACD	0.0007	0.0003	0.005	0.001
3468.V1.C12	AD	>50	>50	>50	>50
Q168.a2	AD	0.148	0.0009	0.017	0.003
Q461.e2	AD	0.502	0.001	0.003	0.006
620345.c1	AE	0.001	0.005	0.006	0.004
BJOX009000.02.4	AE	>50	>50	0.264	0.290
BJOX010000.06.2	AE	>50	>50	>50	>50
BJOX025000.01.1	AE	>50	>50	>50	>50
BJOX028000.10.3	AE	>50	>50	>50	>50
C1080.c3	AE	0.023	0.006	0.310	0.030
C2101.c1	AE	>50	>50	0.683	1.92
C3347.c11	AE	>50	>50	0.047	0.041
C4118.09	AE	0.002	0.00004	0.002	0.0004
CM244.ec1	AE	0.556	0.061	0.002	0.007

CNE3	AE	>50	>50	>50	>50
CNE5	AE	0.018	0.0003	0.007	0.003
CNE55	AE	0.026	0.0002	0.002	0.0005
CNE56	AE	>50	>50	>50	>50
CNE59	AE	>50	>50	>50	>50
CNE8	AE	2.46	0.001	0.011	0.003
R1166.c1	AE	>50	>50	>50	>50
R2184.c4	AE	>50	0.002	0.005	0.003
R3265.c6	AE	19.8	>50	>50	>50
TH966.8	AE	>50	0.004	0.001	0.006
TH976.17	AE	0.036	0.006	>50	>50
235-47.SG3	AG	>50	0.045	6.08	1.02
242-14	AG	0.265	0.0001	0.015	0.002
263-8	AG	0.0007	0.011	0.012	0.003
269-12	AG	0.031	0.005	0.592	0.379
271-11	AG	>50	>50	>50	>50
928-28	AG	>50	0.002	0.856	0.073
DJ263.8	AG	0.097	0.001	0.011	0.008
T250-4	AG	0.031	0.0005	0.002	0.0009
T251-18	AG	0.001	>50	>50	>50
T253-11	AG	>50	0.008	0.004	0.024
T255-34	AG	49.5	>50	>50	>50
T257-31	AG	>50	0.0002	0.003	0.001
T266-60	AG	0.009	0.004	0.817	0.263
T278-50	AG	1.78	3.67	>50	>50
T280-5	AG	>50	0.002	0.265	0.312
T33-7	AG	>50	0.266	>50	>50
3988.25	B	>50	0.001	0.265	0.277
5768.04	B	>50	>50	>50	>50
6101.10	B	>50	>50	>50	>50
6535.3	B	>50	>50	>50	>50
7165.18	B	>50	>50	>50	>50
45_01dG5	B	>50	0.004	3.34	4.77
89.6.DG	B	>50	>50	>50	>50
AC10.29	B	>50	0.002	>50	>50
ADA.DG	B	>50	>50	>50	>50
Bal.01	B	>50	>50	>50	>50
BaL.26	B	>50	>50	>50	>50
BG1168.01	B	>50	>50	>50	>50
BL01.DG	B	>50	>50	>50	>50
BR07.DG	B	>50	>50	>50	>50
BX08.16	B	>50	0.0006	>50	>50
CAAN.A2	B	>50	>50	>50	>50
CNE10	B	>50	>50	>50	>50
CNE12	B	>50	>50	>50	>50
CNE14	B	>50	>50	>50	>50
CNE4	B	>50	>50	>50	>50
CNE57	B	>50	>50	>50	>50
HO86.8	B	>50	>50	>50	>50
HT593.1	B	>50	>50	>50	>50
HXB2.DG	B	>50	>50	>50	>50
JRCSF.JB	B	>50	>50	>50	>50
JRFL.JB	B	>50	>50	>50	>50
MN.3	B	>50	>50	>50	>50

PVO.04	B	11.8	0.016	0.473	0.164
QH0515.01	B	>50	>50	>50	>50
QH0692.42	B	>50	>50	>50	>50
REJO.67	B	>50	>50	>50	>50
RHPA.7	B	>50	>50	>50	>50
SC422.8	B	>50	>50	5.45	>50
SF162.LS	B	>50	>50	>50	>50
SS1196.01	B	>50	>50	>50	>50
THRO.18	B	>50	17.7	0.726	0.645
TRJO.58	B	>50	>50	>50	>50
TRO.11	B	>50	>50	>50	>50
WITO.33	B	>50	>50	>50	>50
YU2.DG	B	>50	>50	>50	>50
CH038.12	BC	0.072	0.001	0.259	0.016
CH070.1	BC	0.039	0.026	0.001	0.001
CH117.4	BC	0.003	0.000	0.0006	0.00001
CH181.12	BC	0.001	0.0000	0.001	0.0000
CNE15	BC	>50	0.301	>50	>50
CNE19	BC	19.7	0.0000	1.78	1.17
CNE20	BC	>50	0.0005	>50	>50
CNE21	BC	0.001	0.0001	0.007	0.003
CNE40	BC	>50	0.016	4.07	2.98
CNE7	BC	0.003	0.003	0.002	0.002
286.36	C	0.004	0.0003	0.004	0.0007
288.38	C	>50	>50	>50	>50
0013095-2.11	C	0.021	0.029	0.003	0.001
001428-2.42	C	30.9	0.070	29.7	>50
0077_V1.C16	C	0.001	0.006	0.010	0.002
00836-2.5	C	>50	>50	>50	>50
0921.V2.C14	C	0.036	0.0001	0.001	0.0002
16055-2.3	C	0.004	0.0005	0.008	0.002
16845-2.22	C	>50	>50	>50	>50
16936-2.21	C	0.250	0.002	3.46	0.347
25710-2.43	C	0.006	0.0000	0.005	0.001
25711-2.4	C	>50	>50	>50	>50
25925-2.22	C	0.013	0.0000	0.001	0.001
26191-2.48	C	0.001	0.0001	0.001	0.005
3168.V4.C10	C	>50	0.109	>50	>50
3637.V5.C3	C	>50	>50	>50	>50
3873.V1.C24	C	0.004	0.004	0.006	0.003
6322.V4.C1	C	0.001	0.0008	0.012	0.003
6471.V1.C16	C	>50	>50	>50	>50
6631.V3.C10	C	>50	>50	>50	>50
6644.V2.C33	C	>50	>50	>50	>50
6785.V5.C14	C	0.005	0.0003	0.005	0.001
6838.V1.C35	C	0.001	0.0007	0.020	0.004
96ZM651.02	C	2.63	0.494	0.037	0.024
BR025.9	C	>50	>25	>50	>50
CAP210.E8	C	0.003	0.0002	0.002	0.001
CAP244.D3	C	46.0	>50	36.6	>50
CAP256.206.C9	C	0.002	0.0002	0.003	0.001
CAP45.G3	C	4.00	0.0000	0.004	0.002
Ce1176.A3	C	0.793	0.020	3.78	0.657
CE703010217.B6	C	14.9	0.002	0.062	0.034

CNE30	C	>50	>50	>50	>50
CNE31	C	>50	>50	>50	>50
CNE53	C	>50	>50	>50	>50
CNE58	C	0.006	0.0000	0.001	0.002
DU123.06	C	0.015	0.008	0.004	0.005
DU151.02	C	0.006	0.0003	0.001	0.001
DU156.12	C	0.006	0.002	0.011	0.004
DU172.17	C	>50	>50	0.788	1.78
DU422.01	C	1.12	0.053	0.080	0.015
MW965.26	C	0.003	0.019	0.016	0.020
SO18.18	C	0.002	0.0008	0.005	0.002
TV1.29	C	>50	0.339	0.189	1.26
TZA125.17	C	0.018	0.002	0.008	0.001
TZBD.02	C	0.036	0.003	0.003	0.004
ZA012.29	C	>50	>50	>50	>50
ZM106.9	C	0.010	0.007	0.012	0.005
ZM109.4	C	>50	0.003	0.003	0.003
ZM135.10a	C	>50	>50	>50	>50
ZM176.66	C	0.029	0.0001	0.001	0.0008
ZM197.7	C	0.002	0.005	0.027	0.001
ZM214.15	C	3.23	0.002	45.7	>50
ZM215.8	C	>50	>50	>50	>50
ZM233.6	C	0.003	0.0005	0.004	0.001
ZM249.1	C	0.0009	0.0008	0.007	0.002
ZM53.12	C	0.004	0.0001	0.003	0.001
ZM55.28a	C	0.005	0.001	0.010	0.001
3326.V4.C3	CD	0.007	0.0000	0.001	0.0002
3337.V2.C6	CD	0.044	0.0002	0.175	0.012
3817.v2.c59	CD	>50	>50	>50	>50
231965.c1	D	>50	>50	0.578	>50
247-23	D	0.005	0.0001	0.006	0.002
3016.v5.c45	D	0.005	0.0002	0.022	0.006
57128.vrc15	D	>50	0.004	0.003	0.011
6405.v4.c34	D	>50	>50	>50	>50
A03349M1.vrc4a	D	2.68	0.004	0.006	0.013
A07412M1.vrc12	D	0.068	0.002	0.0008	0.002
NKU3006.ec1	D	>50	>50	>50	>50
P0402.c2.11	G	0.006	0.001	0.003	0.003
P1981.C5.3	G	0.008	0.002	0.005	0.002
X1193.c1	G	0.343	0.001	0.302	0.145
X1254.c3	G	>50	>50	>50	>50
X1632.S2.B10	G	0.010	0.0004	0.007	0.002
X2088.c9	G	>50	>50	>50	>50
X2131.C1.B5	G	>50	0.005	0.880	1.03

	CAP256-VRC26.08	CAP256-VRC26.25	CAP256-VRC26.26	CAP256-VRC26.27
# Viruses	198	198	198	198
Total VS Neutralized				
IC50 <50ug/ml	93	116	112	106
IC50 <10ug/ml	85	115	106	106
IC50 <1.0ug/ml	78	113	96	94
IC50 <0.1ug/ml	68	106	73	81
IC50 <0.01ug/ml	43	93	51	65
% VS Neutralized				
IC50 <50ug/ml	47	59	57	54
IC50 <10ug/ml	43	58	54	54
IC50 <1.0ug/ml	39	57	48	47
IC50 <0.1ug/ml	34	54	37	41
IC50 <0.01ug/ml	22	47	26	33
Median IC50	0.013	0.002	0.012	0.005
Geometric Mean	0.029	0.002	0.035	0.011

Supplemental Table 5D. Neutralization data. Analysis of this data set is shown in Figures 7-8

IC80

Virus ID	Clade	CAP256-VRC26.08	CAP256-VRC26.25	CAP256-VRC26.26	CAP256-VRC26.27
0260.v5.c36	A	>50	>50	18.6	>50
0330.v4.c3	A	>50	1.04	>50	>50
0439.v5.c1	A	>50	>50	5.12	3.56
3365.v2.c20	A	>50	>50	>50	>50
3415.v1.c1	A	>50	>50	>50	>50
3718.v3.c11	A	>50	>50	>50	>50
398-F1_F6_20	A	>50	>50	>50	>50
BB201.B42	A	0.500	0.001	7.11	0.816
BG505.W6M.C2	A	>50	0.012	0.999	0.050
BI369.9A	A	0.001	0.004	0.060	0.011
BS208.B1	A	0.0003	0.0004	0.021	0.008
KER2008.12	A	>50	0.183	>50	>50
KER2018.11	A	0.001	0.002	0.022	0.007
KNH1209.18	A	>50	8.85	>50	>50
MB201.A1	A	>50	>50	>50	>50
MB539.2B7	A	>50	4.00	>50	>50
MI369.A5	A	2.86	0.019	4.53	0.572
MS208.A1	A	1.00	0.232	26.8	4.59
Q23.17	A	>50	1.30	>50	>50
Q259.17	A	0.259	0.0003	2.65	1.10
Q769.d22	A	>50	>50	>50	>50
Q769.h5	A	>50	>50	>50	>50
Q842.d12	A	>50	0.123	>50	>50
QH209.14M.A2	A	>50	>50	>50	>50
RW020.2	A	>50	>50	>50	>50
UG037.8	A	>50	>50	>50	>50
246-F3.C10.2	AC	0.119	1.77	>50	>50
3301.V1.C24	AC	0.002	0.020	0.038	0.020
3589.V1.C4	AC	>50	>50	>50	>50
6540.v4.c1	AC	29.2	0.051	32.3	>50
6545.V4.C1	AC	27.6	0.096	>50	>50
0815.V3.C3	ACD	>50	>50	>50	>50
6095.V1.C10	ACD	0.100	0.005	0.023	0.011
3468.V1.C12	AD	>50	>50	>50	>50
Q168.a2	AD	>50	>25	0.626	5.00
Q461.e2	AD	19.3	0.080	0.048	0.039
620345.c1	AE	0.090	0.051	0.248	0.056
BJOX009000.02.4	AE	>50	>50	11.0	>50
BJOX010000.06.2	AE	>50	>50	>50	>50
BJOX025000.01.1	AE	>50	>50	>50	>50
BJOX028000.10.3	AE	>50	>50	>50	>50
C1080.c3	AE	0.046	0.718	5.03	0.403
C2101.c1	AE	>50	>50	>50	>50
C3347.c11	AE	>50	>50	0.773	0.646
C4118.09	AE	0.0003	0.001	0.004	0.002
CM244.ec1	AE	11.1	2.75	0.053	0.236
CNE3	AE	>50	>50	>50	>50
CNE5	AE	0.241	0.024	0.068	0.023
CNE55	AE	5.00	0.006	0.008	0.002
CNE56	AE	>50	>50	>50	>50
CNE59	AE	>50	>50	>50	>50
CNE8	AE	>50	1.00	0.086	0.035
R1166.c1	AE	>50	>50	>50	>50
R2184.c4	AE	>50	5.00	0.047	0.060

R3265.c6	AE	>50	>50	>50	>50
TH966.8	AE	>50	0.089	0.042	0.064
TH976.17	AE	0.052	8.00	>50	>50
235-47.SG3	AG	>50	2.55	>50	>50
242-14	AG	16.4	0.005	0.731	0.054
263-8	AG	0.300	0.270	0.071	0.018
269-12	AG	1.88	0.182	15.9	>50
271-11	AG	>50	>50	>50	>50
928-28	AG	>50	0.041	13.3	2.31
DJ263.8	AG	4.31	0.014	0.048	0.024
T250-4	AG	0.005	0.002	0.008	0.003
T251-18	AG	0.0003	>50	>50	>50
T253-11	AG	>50	32.5	0.124	0.601
T255-34	AG	>50	>50	>50	>50
T257-31	AG	>50	0.002	0.010	0.004
T266-60	AG	0.004	0.110	4.71	2.15
T278-50	AG	12.0	>50	>50	>50
T280-5	AG	>50	0.008	5.64	17.1
T33-7	AG	>50	>50	>50	>50
3988.25	B	>50	0.110	19.4	>50
5768.04	B	>50	>50	>50	>50
6101.10	B	>50	>50	>50	>50
6535.3	B	>50	>50	>50	>50
7165.18	B	>50	>50	>50	>50
45_01dG5	B	>50	0.272	>50	>50
89.6.DG	B	>50	>50	>50	>50
AC10.29	B	>50	1.00	>50	>50
ADA.DG	B	>50	>50	>50	>50
Bal.01	B	>50	>50	>50	>50
BaL.26	B	>50	>50	>50	>50
BG1168.01	B	>50	>50	>50	>50
BL01.DG	B	>50	>50	>50	>50
BR07.DG	B	>50	>50	>50	>50
BX08.16	B	>50	>50	>50	>50
CAAN.A2	B	>50	>50	>50	>50
CNE10	B	>50	>50	>50	>50
CNE12	B	>50	>50	>50	>50
CNE14	B	>50	>50	>50	>50
CNE4	B	>50	>50	>50	>50
CNE57	B	>50	>50	>50	>50
HO86.8	B	>50	>50	>50	>50
HT593.1	B	>50	>50	>50	>50
HXB2.DG	B	>50	>50	>50	>50
JRCSF.JB	B	>50	>50	>50	>50
JRFL.JB	B	>50	>50	>50	>50
MN.3	B	>50	>50	>50	>50
PVO.04	B	>50	0.289	2.33	0.842
QH0515.01	B	>50	>50	>50	>50
QH0692.42	B	>50	>50	>50	>50
REJO.67	B	>50	>50	>50	>50
RHPA.7	B	>50	>50	>50	>50
SC422.8	B	>50	>50	>50	>50
SF162.LS	B	>50	>50	>50	>50
SS1196.01	B	>50	>50	>50	>50
THRO.18	B	>50	>50	48.8	>50
TRJO.58	B	>50	>50	>50	>50
TRO.11	B	>50	>50	>50	>50
WITO.33	B	>50	>50	>50	>50

YU2.DG	B	>50	>50	>50	>50
CH038.12	BC	0.400	0.015	23.6	0.436
CH070.1	BC	0.500	>50	0.177	0.165
CH117.4	BC	0.0008	0.00004	0.004	0.0008
CH181.12	BC	0.0003	0.00004	0.006	0.001
CNE15	BC	>50	>50	>50	>50
CNE19	BC	>50	0.008	>50	>50
CNE20	BC	>50	0.109	>50	>50
CNE21	BC	0.023	0.002	0.057	0.023
CNE40	BC	>50	0.449	>50	>50
CNE7	BC	0.046	0.024	0.012	0.010
286.36	C	0.001	0.004	0.016	0.009
288.38	C	>50	>50	>50	>50
0013095-2.11	C	>50	>50	0.011	0.007
001428-2.42	C	>50	>50	>50	>50
0077_V1.C16	C	0.020	0.023	0.026	0.005
00836-2.5	C	>50	>50	>50	>50
0921.V2.C14	C	1.00	0.002	0.004	0.001
16055-2.3	C	0.015	0.005	0.021	0.007
16845-2.22	C	>50	>50	>50	>50
16936-2.21	C	>50	0.065	>50	>50
25710-2.43	C	0.005	0.004	0.039	0.013
25711-2.4	C	>50	>50	>50	>50
25925-2.22	C	0.007	0.0009	0.053	0.012
26191-2.48	C	0.050	0.003	0.069	0.045
3168.V4.C10	C	>50	>50	>50	>50
3637.V5.C3	C	>50	>50	>50	>50
3873.V1.C24	C	0.072	0.020	0.017	0.013
6322.V4.C1	C	0.002	0.012	0.053	0.009
6471.V1.C16	C	>50	>50	>50	>50
6631.V3.C10	C	>50	>50	>50	>50
6644.V2.C33	C	>50	>50	>50	>50
6785.V5.C14	C	0.036	0.006	0.026	0.008
6838.V1.C35	C	0.200	0.042	4.82	0.273
96ZM651.02	C	>50	>50	0.408	0.152
BR025.9	C	>50	>50	>50	>50
CAP210.E8	C	0.009	0.004	0.008	0.005
CAP244.D3	C	>50	>50	>50	>50
CAP256.206.C9	C	0.006	0.002	0.009	0.006
CAP45.G3	C	0.070	0.001	0.111	0.034
Ce1176.A3	C	>50	>50	>50	>50
CE703010217.B6	C	>50	5.00	4.40	2.19
CNE30	C	>50	>50	>50	>50
CNE31	C	>50	>50	>50	>50
CNE53	C	>50	>50	>50	>50
CNE58	C	0.0009	0.003	0.012	0.010
DU123.06	C	2.29	10.0	0.035	0.024
DU151.02	C	1.24	0.008	0.070	0.022
DU156.12	C	0.515	0.051	0.136	0.045
DU172.17	C	>50	>50	9.60	>50
DU422.01	C	40.9	0.109	3.37	0.224
MW965.26	C	0.677	0.572	0.661	0.268
SO18.18	C	0.0003	0.004	0.013	0.006
TV1.29	C	>50	>50	17.5	>50
TZA125.17	C	4.40	0.028	0.020	0.005
TZBD.02	C	0.140	0.016	0.013	0.017
ZA012.29	C	>50	>50	>50	>50
ZM106.9	C	0.500	0.055	0.245	0.081
ZM109.4	C	>50	0.253	0.203	0.600
ZM135.10a	C	>50	>50	>50	>50
ZM176.66	C	0.002	0.001	0.009	0.007
ZM197.7	C	0.030	0.033	0.074	0.008
ZM214.15	C	>50	0.231	>50	>50
ZM215.8	C	>50	>50	>50	>50

ZM215.8	C	>50	>50	>50	>50
ZM233.6	C	0.022	0.002	0.018	0.011
ZM249.1	C	0.128	0.021	0.524	0.036
ZM53.12	C	0.007	0.0009	0.009	0.005
ZM55.28a	C	0.159	0.048	0.033	0.005
3326.V4.C3	CD	0.0008	0.0003	0.005	0.002
3337.V2.C6	CD	0.034	0.001	>50	3.87
3817.v2.c59	CD	>50	>50	>50	>50
231965.c1	D	>50	>50	>50	>50
247-23	D	1.18	0.005	0.022	0.016
3016.v5.c45	D	2.67	0.005	>50	>50
57128.vrc15	D	>50	2.00	0.100	0.324
6405.v4.c34	D	>50	>50	>50	>50
A03349M1.vrc4a	D	>50	0.120	0.182	0.119
A07412M1.vrc12	D	2.63	0.034	0.004	0.009
NKU3006.ec1	D	>50	>50	>50	>50
P0402.c2.11	G	0.032	0.009	0.009	0.008
P1981.C5.3	G	0.039	0.022	0.013	0.007
X1193.c1	G	8.04	0.600	4.03	4.61
X1254.c3	G	>50	>50	>50	>50
X1632.S2.B10	G	0.037	0.010	0.029	0.011
X2088.c9	G	>50	>50	>50	>50
X2131.C1.B5	G	>50	0.113	39.4	>50

	CAP256-VRC26.08	CAP256-VRC26.25	CAP256-VRC26.26	CAP256-VRC26.27
# Viruses	198	198	198	198
Total VS Neutralized				
IC80 <50ug/ml	73	99	91	83
IC80 <10ug/ml	66	97	80	82
IC80 <1.0ug/ml	53	84	67	73
IC80 <0.1ug/ml	38	65	51	57
IC80 <0.01ug/ml	21	37	13	27
% VS Neutralized				
IC80 <50ug/ml	37	50	46	42
IC80 <10ug/ml	33	49	40	41
IC80 <1.0ug/ml	27	42	34	37
IC80 <0.1ug/ml	19	33	26	29
IC80 <0.01ug/ml	11	19	7	14
Median IC80	0.072	0.024	0.068	0.023
Geometric Mean	0.085	0.032	0.164	0.043

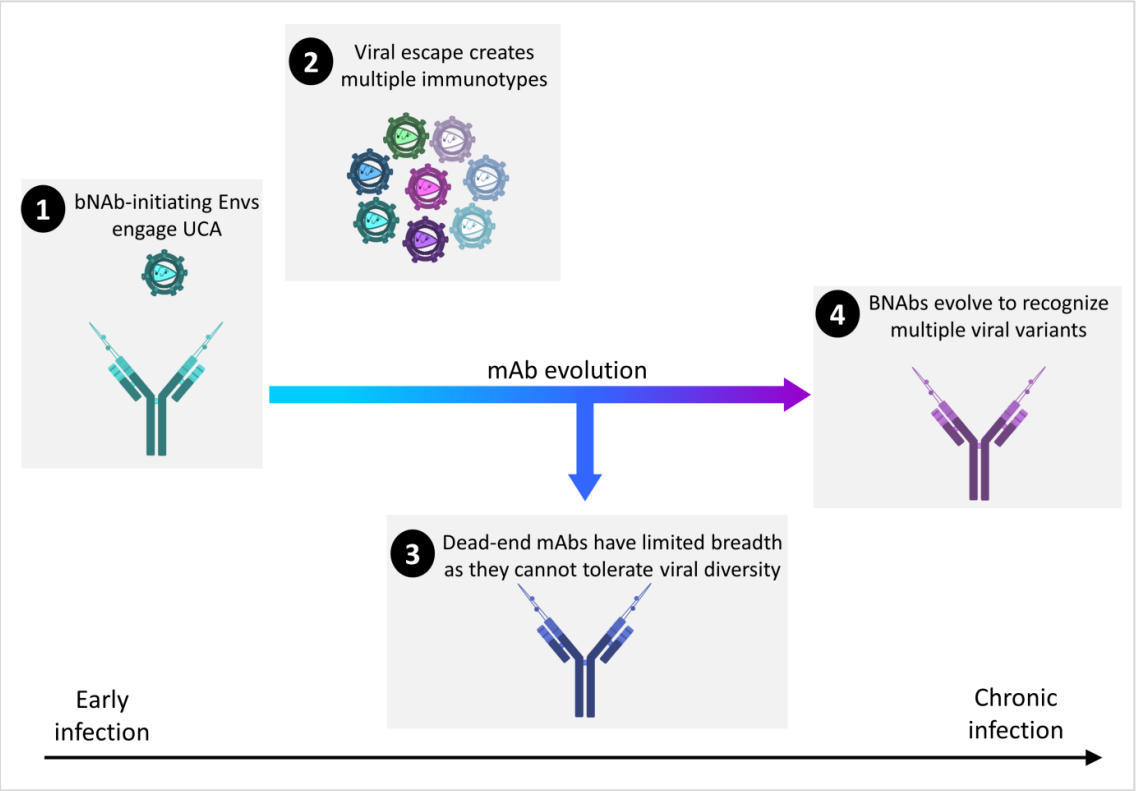
3. Viral variants that initiate and drive maturation of V1V2-directed HIV-1 broadly neutralizing antibodies

Bhiman JN, Anthony C, Doria-Rose NA, Karimanzira O, Schramm CA, Khoza T, Kitchin D, Botha G, Gorman J, Garrett NJ, Abdool Karim SS, Shapiro L, Williamson C, Kwong PD, Mascola JR, Morris L, Moore PL.

Nature Medicine. 2015: 21(11): 1332-6. PMID: 26457756; PMCID: PMC4637988

This publication identified the viral variants that initially engaged the rare CAP256-VRC25-UCA and showed how creation of multiple viral immunotypes drove maturation of this mAb lineage towards neutralization breadth.

Graphical Abstract



Viral variants that initiate and drive maturation of V1V2-directed HIV-1 broadly neutralizing antibodies

Jinal N Bhiman[1,2], Colin Anthony[3], Nicole A Doria-Rose[4], Owen Karimanzira[1], Chaim A Schramm[5], Thandeka Khoza[1], Dale Kitchin[1], Gordon Botha[3], Jason Gorman[4], Nigel J Garrett[6], Salim S Abdool Karim[6], Lawrence Shapiro[4,5], Carolyn Williamson[3,6,7], Peter D Kwong[4], John R Mascola[4], Lynn Morris[1,2,6] & Penny L Moore[1,2,6]

© 2015 Nature America, Inc. All rights reserved.

The elicitation of broadly neutralizing antibodies (bNAbs) is likely to be essential for a preventative HIV-1 vaccine, but this has not yet been achieved by immunization. In contrast, some HIV-1-infected individuals naturally mount bNAb responses during chronic infection, suggesting that years of maturation may be required for neutralization breadth[1–6]. Recent studies have shown that viral diversification precedes the emergence of bNAbs, but the significance of this observation is unknown[7,8]. Here we delineate the key viral events that drove neutralization breadth within the CAP256-VRC26 family of 33 monoclonal antibodies (mAbs) isolated from a superinfected individual. First, we identified minority viral variants, termed bNAb-initiating envelopes, that were distinct from both of the transmitted/founder (T/F) viruses and that efficiently engaged the bNAb precursor. Second, deep sequencing revealed a pool of diverse epitope variants (immunotypes) that were preferentially neutralized by broader members of the antibody lineage. In contrast, a 'dead-end' antibody sublineage unable to neutralize these immunotypes showed limited evolution and failed to develop breadth. Thus, early viral escape at key antibody-virus contact sites selects for antibody sublineages that can tolerate these changes, thereby providing a mechanism for the generation of neutralization breadth within a developing antibody lineage.

The identification of bNAbs against genetically diverse viruses such as HIV-1 (ref. 9), together with in-depth longitudinal evolutionary studies are providing key insights for vaccine design[7,8,10–12]. BNAbs to the variable regions 1 and 2 (V1V2) of the HIV-1 envelope (Env) are among the most prevalent and potent cross-reactive antibodies, but the virological events that allow for their elicitation and maturation remain unclear. We have previously described the CAP256-VRC26 mAb lineage, isolated from an HIV-1 subtype C–superinfected individual, which targets the V1V2 C-strand at the apex of the viral envelope glycoprotein (**Fig. 1a**)[7]. This lineage developed from a bNAb precursor or unmutated common ancestor (UCA) with a 35–amino acid heavy chain complementarity determining region 3 (CDRH3), and it acquired breadth through moderate levels of somatic hypermutation (SHM)[7]. To better define the complex viral populations responsible for eliciting these antibodies and driving their maturation, we performed next-generation sequencing (NGS) at 28 different time points over 4 years (with an average of 85,000 reads and 788 consensus sequences per time point). From 6–13 weeks, all sequences were closely related to the primary infecting virus (PI) (**Fig. 1b** and **Supplementary Fig. 1**), but at 15 weeks, when superinfection (SU) occurred, there was a dramatic shift in viral populations, with SU-like viruses accounting for 99.8% of 3,228 consensus sequences (**Supplementary Fig. 2**). From 17 weeks, V1V2 sequences from the PI and SU viruses persisted, rapidly forming a PI-SU recombinant population, although PI-like viruses dominated briefly at 23 weeks, perhaps as a result of immune escape from earlier non-V1V2-directed neutralizing antibodies that preferentially neutralized SU-like viruses[13]. Notably, diversification in all three viral populations (PI, SU and recombinants) increased after the CAP256-VRC26 lineage was first detected in blood by NGS at 34 weeks (**Fig. 1b** and **Supplementary Fig. 3**).

As residues 169 and 166 in the V1V2 C-strand form a crucial part of the CAP256-VRC26 bNAb epitope and are likely to be important in virus-mAb co-evolution, we focused on defining escape mutations at these positions. Residue 169 differed between the PI (169Q) and SU viruses (169K), with the majority of viral variants circulating after 23 weeks possessing a PI-derived 169Q mutation (**Fig. 1c** and **Supplementary Fig. 2**). From 27 weeks onwards, the virus sampled 11 different amino acids at position 169, and variation was most pronounced at 42 weeks (**Fig. 1c**), shortly before the development of neutralization breadth. The major escape pathway from 42–119 weeks was a 169I mutation, and thereafter 169E dominated. Toggling was also observed at position 166 (**Fig. 1d**), although this occurred later, with the wild-type 166R immunotype

[1]Centre for HIV and STIs, National Institute for Communicable Diseases (NICD) of the National Health Laboratory Service (NHLS), Johannesburg, South Africa. [2]Faculty of Health Sciences, University of the Witwatersrand, Johannesburg, South Africa. [3]Institute of Infectious Disease and Molecular Medicine, University of Cape Town, Cape Town, South Africa. [4]Vaccine Research Center, National Institute of Allergy and Infectious Diseases, National Institutes of Health, Bethesda, Maryland, USA. [5]Department of Biochemistry and Systems Biology, Columbia University, New York, New York, USA. [6]Centre for the AIDS Programme of Research in South Africa (CAPRISA), University of KwaZulu Natal, Durban, South Africa. [7]National Health Laboratory Services, Johannesburg, South Africa. Correspondence should be addressed to P.L.M. (pennym@nicd.ac.za).

Received 20 May; accepted 3 September; published online 12 October 2015; doi:10.1038/nm.3963

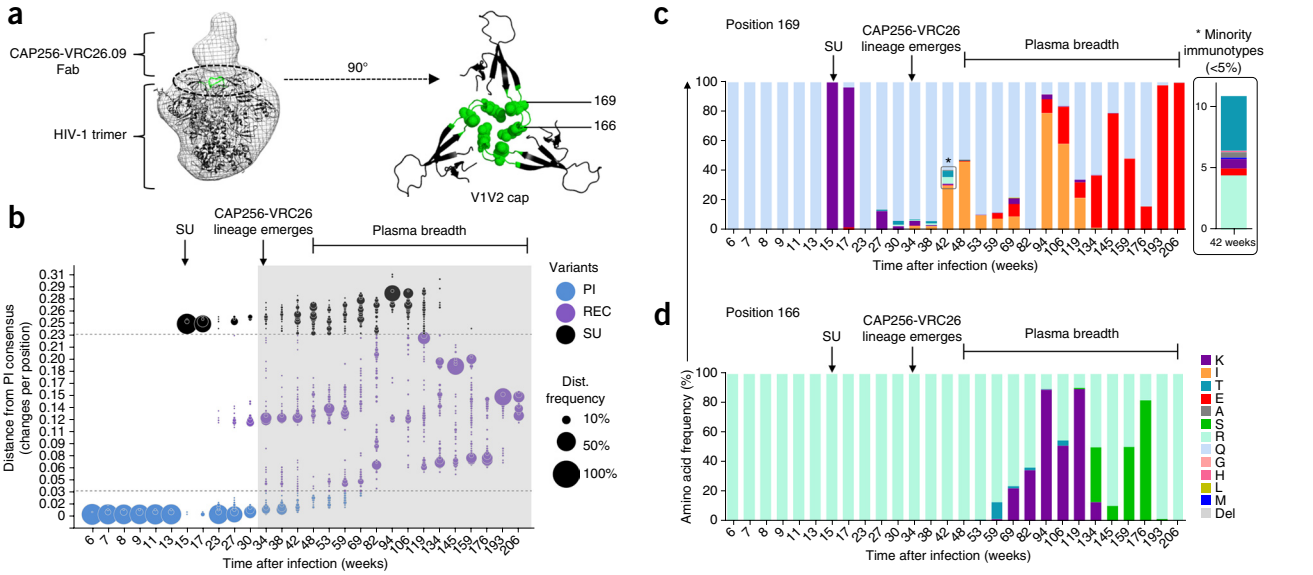


Figure 1 Viral diversification over time in CAP256 HIV-1 Env V1V2. (**a**) BG505 SOSIP.664 trimer structure (PDB: 4TVP) fitted into a 3D reconstruction of the CAP256-VRC26.09 fragment antigen-binding (Fab)-trimer complex (EMD-5856, left). BG505 V1V2 cap with residues 166 and 169 shown as spheres and the C-strand highlighted in green (right). (**b**) Hamming distance from the PI sequence (*y* axis) versus weeks after infection (*x* axis) for all next-generation V1V2 consensus sequences. Values <0.03 and >0.23 were used to distinguish PI-like (blue) and SU-like (black) viruses respectively, whereas those sequences with an intermediate distance (0.03–0.23) were classified as PI-SU recombinant viruses (purple, REC). Hamming distances were normalized for sequence length, and the relative frequency of sequences with a given distance are indicated by the size of the circle (normalized for depth of sequencing, but not for viral load; see **Supplementary Fig. 1**). CAP256-VRC26 next-generation transcript detection in the blood is shown by gray shading. (**c**,**d**) The frequency of amino acids (*y* axis) at positions 169 (**c**) and 166 (**d**) are shown as stacked bars, with each bar representing a single time point from 6 to 206 weeks after infection (*x* axis). Amino acids are colored as indicated, with Del representing a deletion. The inset (*) in **c** expands the 42-week time point (when nine immunotypes are present), to highlight the minority immunotypes present at frequencies of <5%. The time of SU, the emergence of CAP256-VRC26 NGS transcripts and onset of plasma breadth are shown.

© 2015 Nature America, Inc. All rights reserved.

(present in both the PI and SU viruses) occurring in more than 98% of sequences until 53 weeks. At 59 weeks, the virus sampled four amino acids (166R, T, K or S), and thereafter 166K, followed by 166S, became prevalent. By 159 weeks, all viral sequences contained the mutually exclusive K169E or R166S mutations. As both the K169E and R166S mutations abrogate neutralization by the CAP256-VRC26 mAbs[7,13] it is unclear why it took two years for these escape pathways to dominate despite their low-level presence early in the development of the CAP256-VRC26 family (**Supplementary Fig. 2**).

The CAP256-VRC26 UCA was unable to neutralize any of 196 HIV-1 isolates (**Supplementary Fig. 4**), suggesting that Env variants able to engage this UCA may be rare. Because CAP256-VRC26 NGS transcripts were first detected in blood 19 weeks after superinfection (**Supplementary Fig. 3**), we analyzed contemporaneous (34-week) viral sequences to identify a bNAb-initiating Env. Neutralization of the SU virus, but not the PI virus, by the CAP256-VRC26 UCA indicated that an SU-like variant elicited this lineage[7]. Although 8% (75/937) of V1V2 next-generation sequences at the 34-week time point were SU-like, none were identical to the SU virus (**Fig. 2a** and **Supplementary Fig. 5**). Single-genome amplification was therefore used to isolate six functional 34-week Env clones, which differed from the SU virus by 2–8 amino acids in V1V2 and by up to 26 changes across the entire Env (**Fig. 2b**). We observed evidence of early immune pressure, with three of six clones containing K169I or K169E mutations, and four of six clones deleting or shifting the glycan at residue 139 (**Fig. 2c**). As expected, the clones with 169I or 169E mutations were resistant to neutralization by the UCA; however, the three clones containing a wild-type 169K were 5–17-fold better neutralized than the SU virus (**Fig. 2d**). Thus, the 34-week viral variants that evolved from the CAP256 SU T/F virus (but differed from the T/F virus by at least 12 amino acids) provided a stronger stimulus for the CAP256-VRC26 lineage.

We next sought to define how this lineage matured to acquire neutralization breadth in the context of CAP256 viral diversification. A heavy chain phylogenetic tree of 33 isolated CAP256-VRC26 mAbs (12 previously described[7] and 21 recently isolated mAbs[14]) and CAP256-VRC26 NGS transcripts from 34 to 206 weeks showed an early bifurcation[7] (**Fig. 3a**). A small sublineage of 34–59-week sequences, including the CAP256-VRC26.01 and 0.24 mAbs, exhibited restricted evolution. A second larger sublineage, containing transcripts from all time points as well as most of the mAbs (**Fig. 3a**), displayed extensive evolution, suggesting adaption in response to emerging viral escape mutations, such as K169T/I/Q/R and R166K (**Fig. 1c**,**d**). To test this hypothesis, we introduced these immunotypes into the SU virus and assayed them against 32 mAbs (CAP256-VRC26.20 does not neutralize SU and was excluded). The CAP256-VRC26.01 and 24 mAbs, from the smaller sublineage with limited breadth, both neutralized the SU virus at 0.04 μg/ml (**Fig. 3b**). However, SU viruses containing the 166 or 169 immunotypes were either neutralization resistant or showed a >670-fold reduction in neutralization sensitivity (**Fig. 3b**). Thus, the inability of mAbs in this dead-end sublineage to tolerate viral escape mutations was likely to be responsible for limiting their evolution and capacity to become broadly neutralizing.

Among the 30 CAP256-VRC26 mAbs from the evolving sublineage that showed a range of neutralization breadth (2–63%), the 169T, 169I or 169Q mutations abolished or reduced the activity of mAbs with limited breadth (**Fig. 3c**). In contrast, the neutralizing activity of broader family members was largely unaffected. This observation was

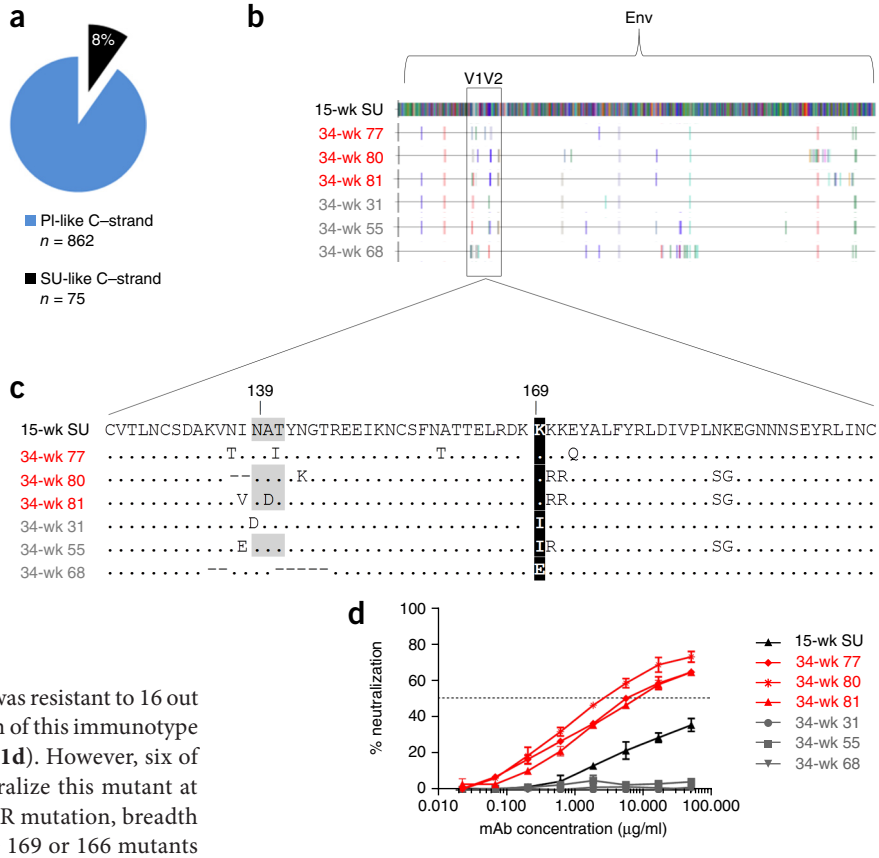


Figure 2 Characterization of the CAP256 34-week Envs. (**a**) Frequency of 34-week next-generation V1V2 consensus sequences possessing a C-strand derived from the PI (blue, $n = 862$) or SU (black, $n = 75$) viruses. (**b**) Amino acid highlighter plot of single-genome amplification (SGA)-derived Env, comparing six SU-like 34-week clones (77, 80, 81, 31, 55 and 68) to the SU virus (designated as the master). Mismatches from the SU are shown as colored ticks and the V1V2 region is boxed. (**c**) Amino acid sequence alignment of the V1V2 region (HXB2 residues 126–196) comparing the SU and the six SGA-derived SU-like 34 week sequences. Red font denotes clones with a wild-type K169, whereas gray font indicates sequences with 169I or 169E mutations. Amino acid identity to the SU virus is represented by dots, deletions are shown as dashes and glycosylation sequons are shaded in gray. (**d**) CAP256-VRC26 UCA neutralization (*y* axis) of the SU virus (black) and the 34-week clones with 169K (red) and 169I or 169E (gray). UCA mAb concentration is shown on the *x* axis. Bars indicate s.e.m. (triplicate).

more pronounced for the R166K mutant, which was resistant to 16 out of 30 mAbs (**Fig. 3c**), consistent with the selection of this immunotype during later stages of bNAb development (**Fig. 1d**). However, six of the nine broadest mAbs were still able to neutralize this mutant at titers <1 μg/ml. With the exception of the K169R mutation, breadth was correlated with the ability to neutralize the 169 or 166 mutants (**Fig. 3c** and **Supplementary Fig. 6**). Overall mAbs with limited neutralization breadth were most severely affected by variation at positions 169 and 166, whereas the broadest mAbs were able to tolerate these early viral escape mutations, thus providing a mechanism for the evolution of neutralization breadth within this lineage.

Because high levels of SHM are often required for HIV-1 broad neutralization[15,16], we investigated the relationship between SHM and neutralization breadth in the CAP256-VRC26 family (**Fig. 4a**). As expected, the nine mAbs with >40% breadth were 17–22% mutated from the UCA; however, three 'off-track' mAbs with a similar level of

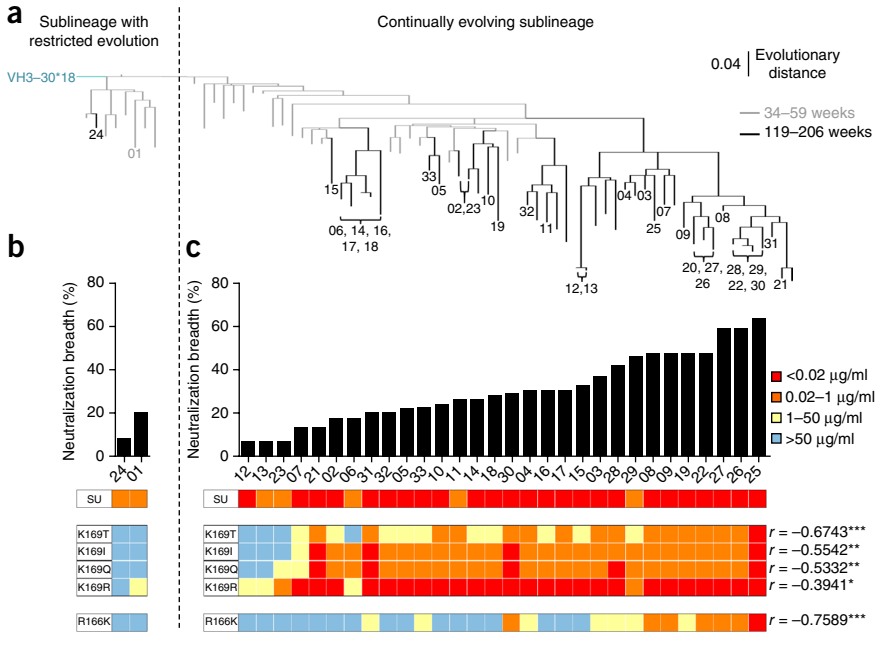


Figure 3 Relationship between bNAb phylogeny, neutralization breadth and tolerance of multiple immunotypes at positions 169 and 166. (**a**) A condensed heavy chain phylogenetic tree, rooted on the VH3-30*18 germline gene and displaying the positions of the 33 CAP256-VRC26 mAbs. Antibody and mAbs are colored according to whether they were isolated from 34–59 weeks (gray) or 119–206 weeks (black). The tree bifurcates into two sublineages (separated by a dashed line); one showing restricted evolution (left) contains only antibody transcripts from early time-points, whereas a continually evolving sublineage (right) contains transcripts from all time points. Scale shows the rate of nucleotide change between nodes. (**b**) Dead-end mAbs in the sublineage with restricted evolution are ranked according to percentage neutralization breadth in the histogram. Neutralization of the SU virus and 169- and 166-mutant viruses by CAP256-VRC26.01 and 24 are shown as a heat map, with shading showing neutralization potency, as indicated in the key. (**c**) Thirty mAbs in the continually evolving sublineage are ranked according to neutralization breadth in the histogram. Neutralization of the SU virus and 169- and 166-mutant viruses by CAP256-VRC26 mAbs are shown as a heat map, with shading showing neutralization potency, as indicated in the key. Correlations (*r*) between neutralization breadth and the IC_{50} titers of each mutant virus are indicated on the right of the heat map. $^{*}P < 0.05$; $^{**}P < 0.005$; $^{***}P < 0.0001$, calculated using a two-tailed non-parametric Spearman correlation.

© 2015 Nature America, Inc. All rights reserved.

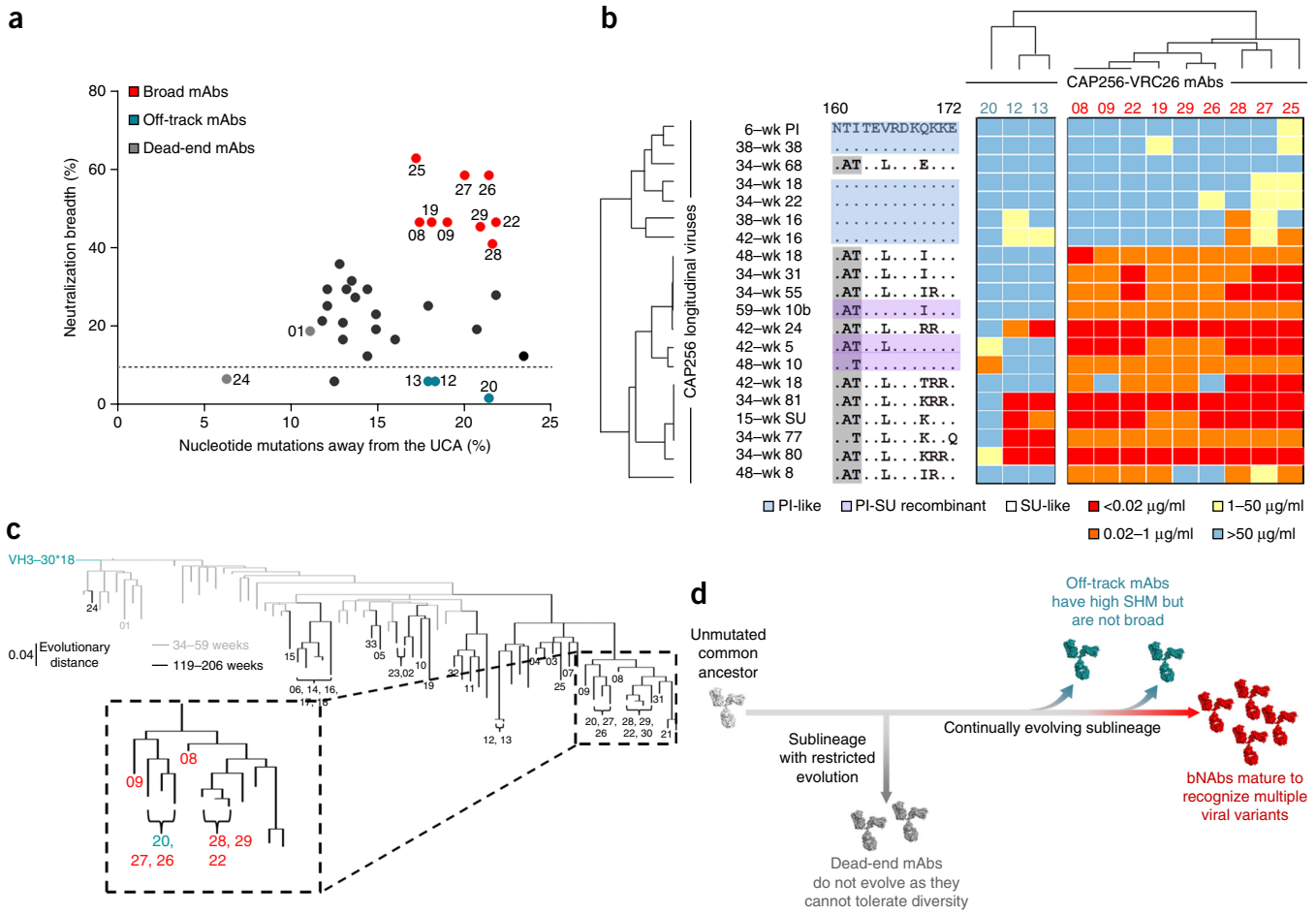


Figure 4 Viral variants that shaped the maturation of broad and off-track antibodies. (**a**) Relationship between neutralization breadth of CAP256-VRC26 mAbs (%, *y* axis) and mutations away from the UCA (%, *x* axis). Broad mAbs with >40% neutralization breadth, off-track mAbs with limited neutralization breadth (<6%) and dead-end mAbs are shown in red, turquoise and gray respectively. The remaining 19 mAbs are shown in black. (**b**) CAP256-VRC26 mAbs and longitudinal CAP256 viruses isolated between 6–59 weeks are hierarchically clustered by their neutralization profiles. Neutralization sensitivity is shown as a heat map with potency indicated in the key. The sequence alignment shows viral C-strand amino acid residues between positions 160–172 (HXB2 numbering), shaded to designate sequences that are PI derived (blue shading), PI-SU recombinants (purple shading) or SU derived (no shading). Off-track (turquoise) and broad (red) mAbs are clustered separately, whereas longitudinal viral variants are clustered by neutralization sensitivity, largely segregated on the basis of an SU-derived V1V2 C-strand. (**c**) A condensed heavy chain phylogenetic tree (**Fig. 3**) with a single clade expanded to illustrate the phylogenetic relatedness of an off-track mAb (turquoise) to seven broad mAbs (red). (**d**) Schematic depicting how CAP256 viral evolution results in the engagement of the CAP256-VRC26 UCA (light gray) and the subsequent development of two distinct mAb sublineages. The sublineage with restricted evolution contains dead-end mAbs (dark gray), which cannot tolerate viral escape mutations. The continually evolving sublineage contains bNAbs (red) and off-track mAbs (turquoise). Although both bNAbs and off-track mAbs have high levels of SHM, only the former mature to recognize multiple immunotypes, and thus acquire breadth.

SHM (17–21%) had only 2–6% breadth (**Fig. 4a**). Therefore, as observed in several families of HIV-specific antibodies[17–20] and influenza-specific antibodies[21], high levels of SHM in the CAP256-VRC26 lineage were not sufficient to confer breadth. To determine whether different viral variants drove the evolution of broad versus off-track mAbs, we tested both groups of mAbs against longitudinal CAP256 viruses (**Fig. 4b**). Hierarchical clustering analysis of mAbs and viruses on the basis of their neutralization profiles showed a clear phenotypic separation between broad and off-track mAbs, with the latter neutralizing substantially fewer autologous viruses, but we could not attribute this to any genetic features of the mAbs. Both groups neutralized viruses with an SU-like C-strand, including the bNAb-initiating 34-week clones. All viruses neutralized by off-track antibodies were also sensitive to at least one broad mAb, suggesting that viral variants associated with the development of neutralization breadth also selected off-track mAbs. Indeed, clustering of broad and off-track mAbs within a single phylogenetic branch highlights the stochastic nature of mAb maturation toward breadth (**Fig. 4c**).

In conclusion, we identified 34-week viral variants, which we have termed bNAb-initiating Envs, that effectively engaged the UCA of the CAP256-VRC26 V1V2 lineage. Although low-frequency viral escape mutations at 27–30 weeks may suggest that CAP256-VRC26 antibodies were present earlier, the 34-week Envs nonetheless represent optimal priming immunogens for this lineage. Identification of rare bNAb-initiating Envs is likely to be of particular importance for V1V2 bNAb precursors, which are derived from a pool of rare B cells with long CDRH3 regions[8,18,22–26]. Second, we have defined a new mechanism for how accumulating viral variants contribute to bNAb development. Thus, viral escape creates multiple immunotypes, and in parallel SHM generates antibodies with differential abilities to engage these epitope variants. Those antibody sublineages that are able to tolerate variability at key epitope contacts will develop breadth (**Fig. 4d**). We note,

© 2015 Nature America, Inc. All rights reserved.

however, that viral diversity may also limit the evolution of less-tolerant mAbs (dead-end sublineages), or it may divert maturation of mAbs toward strain specificity (off-track mAbs) (**Fig. 4d**). This process, which provides a framework for vaccine design (**Supplementary Fig. 7**), is distinct from the multi-lineage cooperative pathway described for a CD4–binding site bNAb lineage[10], highlighting the complex and varied pathways to breadth. Future immunization strategies should therefore aim to include bNAb-initiating Envs to prime bNAb precursor B cells, as well as rationally verified Env variants as sequential boosts to mature the response to neutralization breadth.

METHODS

Methods and any associated references are available in the online version of the paper.

Accession codes. Antibody 454 sequencing reads have been deposited in the National Center for Biotechnology Information (NCBI) Sequence Read Archive (SRA) under the accession numbers SRR2126754 and SRR2126755. Viral V1V2 Illumina MiSeq sequencing reads have been deposited in the NCBI SRA under the BioProject accession number PRJNA294363. CAP256 34-week viral envelope sequences have been have been deposited with GenBank under the accession numbers KT698223–KT698227.

Note: Any Supplementary Information and Source Data files are available in the online version of the paper.

ACKNOWLEDGMENTS

We thank the participants in the CAPRISA 002 cohort for their commitment to attending the CAPRISA clinics in South Africa. Thanks to the CAPRISA 002 study team (including N. Naicker, V. Asari, N. Majola, T. Cekwane, N. Samsunder, Z. Mchunu, D. Nkosi, H. Shozi, S. Ndlovu, P. Radebe, K. Leask and M. Upfold) for managing the cohort and providing specimens. We are grateful to C. K. Wibmer for useful discussions. We thank P. Labuschagne, D. Matten and T. York for assistance with viral next-generation sequence analysis, R. Bailer and M. Louder for the CAP256-VRC26 UCA neutralization data against the large virus panel and J. Mulllikin and the US National Institutes of Health (NIH) Intramural Sequencing Center (NISC) Comparative Sequencing Program for antibody NGS data at 34 weeks. We are grateful to J. Baalwa, D. Ellenberger, F. Gao, B. Hahn, K. Hong, J. Kim, F. McCutchan, D. Montefiori, J. Overbaugh, E. Sanders-Buell, G. Shaw, R. Swanstrom, M. Thomson, S. Tovanabutra and L. Zhang for contributing the HIV-1 envelope plasmids used in our neutralization panel. The JC53bl-13 (TZM-bl) and 293T cell lines were obtained through the NIH AIDS Reagent Program, Division of AIDS, NIAID, NIH from J.C. Kappes, X. Wu and Tranzyme, Inc., and A. Rice, respectively. We acknowledge research funding from the Centre for the AIDS Programme of Research (CAPRISA) (S.S.A.K.), the South African Medical Research Council (MRC) SHIP program (P.L.M.), the NIH through a U01 grant (AI116086-01) (P.L.M.), the intramural research programs of the Vaccine Research Center and the National Institute of Allergy and Infectious Diseases (NIAID) (J.R.M.). CAPRISA is funded by the South African HIV/AIDS Research and Innovation Platform of the South African Department of Science and Technology, and was initially supported by the US NIAID, NIH, US Department of Health and Human Services grant U19 AI51794 (S.S.A.K.). Funding was received by J.N.B. and C.A. from the Columbia University-Southern African Fogarty AIDS International Training and Research Program through the Fogarty International Center, NIH grant 5 D43 TW000231 (to Quarraisha Abdool Karim). Additional fellowships included a University of the Witwatersrand Postgraduate Merit Award (J.N.B.), a Poliomyelitis Research Foundation PhD Bursary (J.N.B.), a National Research Foundation of South Africa Innovation PhD Bursary (J.N.B.), a National Research Foundation of South Africa Postdoctoral Fellowship (C.A.), and a Wellcome Trust Intermediate Fellowship in Public Health and Tropical Medicine, grant 089933/Z/09/Z (P.L.M.).

AUTHOR CONTRIBUTIONS

J.N.B., L.M. and P.L.M. designed the study, analyzed data and wrote the manuscript. C.A. and C.W. designed and performed viral NGS and analysis and edited the manuscript. N.A.D.-R. led the isolation of CAP256 mAbs. J.N.B. and O.K. performed neutralization experiments. C.A.S. and L.S. generated and analyzed antibody NGS data. J.N.B. and T.K. expressed and purified monoclonal antibodies. J.N.B. and D.K. generated single-genome sequences and viral envelope clones. G.B. developed computational tools to analyze NGS data, and assisted in the NGS analysis. J.G. assessed CAP256-VRC26 UCA neutralization of heterologous viruses. N.J.G. and the CAPRISA Study Team managed the CAPRISA cohort and contributed samples and data for CAP256. S.S.A.K., C.W. and L.M. established and led the CAPRISA cohort. C.W., N.A.D.-R., L.S., P.D.K., and J.R.M. contributed to data analysis and edited the manuscript.

COMPETING FINANCIAL INTERESTS

The authors declare no competing financial interests.

Reprints and permissions information is available online at http://www.nature.com/reprints/index.html.

1. Gray, E.S. *et al.* HIV-1 neutralization breadth develops incrementally over 4 years and is associated with CD4+ T cell decline and high viral load during acute infection. *J. Virol.* **85**, 4828–4840 (2011).
2. Hraber, P. *et al.* Prevalence of broadly neutralizing antibody responses during chronic HIV-1 infection. *AIDS* **28**, 163–169 (2014).
3. Piantadosi, A. *et al.* Breadth of neutralizing antibody response to human immunodeficiency virus type 1 is affected by factors early in infection but does not influence disease progression. *J. Virol.* **83**, 10269–10274 (2009).
4. Sather, D.N. *et al.* Factors associated with the development of cross-reactive neutralizing antibodies during human immunodeficiency virus type 1 infection. *J. Virol.* **83**, 757–769 (2009).
5. Euler, Z. *et al.* Longitudinal analysis of early HIV-1-specific neutralizing activity in an elite neutralizer and in five patients who developed cross-reactive neutralizing activity. *J. Virol.* **86**, 2045–2055 (2012).
6. Walker, L.M. *et al.* A limited number of antibody specificities mediate broad and potent serum neutralization in selected HIV-1 infected individuals. *PLoS Pathog.* **6**, e1001028 (2010).
7. Doria-Rose, N.A. *et al.* Developmental pathway for potent V1V2-directed HIV-neutralizing antibodies. *Nature* **509**, 55–62 (2014).
8. Liao, H.X. *et al.* Co-evolution of a broadly neutralizing HIV-1 antibody and founder virus. *Nature* **496**, 469–476 (2013).
9. Mascola, J.R. & Haynes, B.F. HIV-1 neutralizing antibodies: understanding nature's pathways. *Immunol. Rev.* **254**, 225–244 (2013).
10. Gao, F. *et al.* Cooperation of B cell lineages in induction of HIV-1-broadly neutralizing antibodies. *Cell* **158**, 481–491 (2014).
11. Wibmer, C.K. *et al.* Viral escape from HIV-1 neutralizing antibodies drives increased plasma neutralization breadth through sequential recognition of multiple epitopes and immunotypes. *PLoS Pathog.* **9**, e1003738 (2013).
12. Moore, P.L. *et al.* Evolution of an HIV glycan-dependent broadly neutralizing antibody epitope through immune escape. *Nat. Med.* **18**, 1688–1692 (2012).
13. Moore, P.L. *et al.* Multiple pathways of escape from HIV broadly cross-neutralizing V2-dependent antibodies. *J. Virol.* **87**, 4882–4894 (2013).
14. Doria-Rose, N.A. *et al.* A new member of the V1V2-directed CAP256-VRC26 lineage that shows increased breadth and exceptional potency. *J. Virol.* (in the press).
15. Klein, F. *et al.* Antibodies in HIV-1 vaccine development and therapy. *Science* **341**, 1199–1204 (2013).
16. Kwong, P.D., Mascola, J.R. & Nabel, G.J. Broadly neutralizing antibodies and the search for an HIV-1 vaccine: the end of the beginning. *Nat. Rev. Immunol.* **13**, 693–701 (2013).
17. Sok, D. *et al.* Recombinant HIV envelope trimer selects for quaternary-dependent antibodies targeting the trimer apex. *Proc. Natl. Acad. Sci. USA* **111**, 17624–17629 (2014).
18. Walker, L.M. *et al.* Broad neutralization coverage of HIV by multiple highly potent antibodies. *Nature* **477**, 466–470 (2011).
19. Scheid, J.F. *et al.* Broad diversity of neutralizing antibodies isolated from memory B cells in HIV-infected individuals. *Nature* **458**, 636–640 (2009).
20. Mouquet, H. *et al.* Memory B cell antibodies to HIV-1 gp140 cloned from individuals infected with clade A and B viruses. *PLoS ONE* **6**, e24078 (2011).
21. Pappas, L. *et al.* Rapid development of broadly influenza neutralizing antibodies through redundant mutations. *Nature* **516**, 418–422 (2014).
22. Walker, L.M. *et al.* Broad and potent neutralizing antibodies from an African donor reveal a new HIV-1 vaccine target. *Science* **326**, 285–289 (2009).
23. Briney, B.S., Willis, J.R. & Crowe, J.E. Jr. Human peripheral blood antibodies with long HCDR3s are established primarily at original recombination using a limited subset of germline genes. *PLoS ONE* **7**, e36750 (2012).
24. Wardemann, H. *et al.* Predominant autoantibody production by early human B cell precursors. *Science* **301**, 1374–1377 (2003).
25. Jardine, J. *et al.* Rational HIV immunogen design to target specific germline B cell receptors. *Science* **340**, 711–716 (2013).
26. McGuire, A.T. *et al.* Engineering HIV envelope protein to activate germline B cell receptors of broadly neutralizing anti-CD4 binding site antibodies. *J. Exp. Med.* **210**, 655–663 (2013).

© 2015 Nature America, Inc. All rights reserved.

ONLINE METHODS

Study participant. CAP256 was part of the CAPRISA 002 Acute Infection study, a cohort of 245 high-risk, HIV-negative women that was established in 2004 in Durban, South Africa, for follow-up and subsequent identification of HIV seroconversion[27]. This HIV-infected individual was among the seven women in this cohort who developed neutralization breadth[1]. The CAPRISA 002 Acute Infection study was reviewed and approved by the research ethics committees of the University of KwaZulu-Natal (E013/04), the University of Cape Town (025/2004) and the University of the Witwatersrand (MM040202). CAP256 provided written informed consent. Randomization and blinding were not performed in this study.

V1V2 next-generation sequence library preparation. RNA extraction, cDNA synthesis and subsequent amplification were carried out as described previously[28], with the following modifications: A minimum of 5,000 HIV-1 RNA copies were isolated from longitudinal plasma, spanning 4 years of infection, using the QIAamp Viral RNA kit (Qiagen, Germany). The cDNA synthesis primer was designed to bind to the C3 region of the envelope (HXB2 gp160 position 1,094–1,118) and included a randomly assigned 9-mer tag (Primer ID method) to uniquely label each cDNA molecule, followed by a universal primer binding site to allow out-nested PCR amplification of cDNA templates (primers listed in **Supplementary Table 1**). First-round amplification primers were designed to amplify the V1 to V3 region of the envelope (HXB2 gp160 positions 332–358) and contained a template-specific binding region, followed by a variable-length spacer of 0–3 randomly assigned bases to increase sample complexity. In addition, PCR primers contained 5′ overhangs, introducing binding sites for the Nextera XT indexing primers (Illumina, CA) (**Supplementary Table 1**). The nested PCRs were carried out using the Nextera XT indexing kit. After indexing, samples were purified using the MinElute PCR Purification Kit (Qiagen, Germany), quantified using the Quant-iT PicoGreen dsDNA assay (Life Technologies, NY) and pooled in equimolar concentrations. The pooled amplicons were gel extracted using the QIAquick gel purification kit (Qiagen, Germany) to ensure primer removal and the final library submitted for sequencing on an Illumina MiSeq (San Diego, CA), using 2 × 300 paired-end chemistry.

V1V2 next-generation sequence analysis. Raw reads were processed using a local instance of Galaxy[29–31], housed within the University of Cape Town High-Performance Computing core. Read quality was assessed using fastqc (http://www.bioinformatics.babraham.ac.uk/projects/fastqc). Short reads (<150 bp) and low-quality data were filtered out using the Filter FASTQ (version 1.0.0) tool[32] with a minimum quality of Q35 for 3′ base trimming. Forward and reverse reads were joined using FASTQ joiner (version 2.0.0)[32]. A custom python script was used to bin all reads containing an identical Primer ID tag, to align the reads within each bin using MAFFT[33] and to produce a consensus sequence based on a majority rule. Sequences with just one Primer ID representative, as well as consensus sequences derived from less than three reads and those containing degenerate bases, were excluded and the remaining sequences from each time point were aligned with MAFFT, Muscle[34] or RAMICS[35]. The calculation of amino acid frequencies and Hamming distances (for each sequence relative to the consensus sequence from the first time point–inferred PI virus), were performed using custom python scripts. Amino acid frequency distributions were plotted using Prism 6 (GraphPad), whereas Hamming distances were plotted using the python library Matplotlib[36]. All custom scripts used in these analyses, including the Primer ID binning script, are available upon request from Gordon Botha (gbot300@gmail.com).

Single-genome amplification and sequencing. HIV-1 RNA was isolated from plasma using the Qiagen QIAamp Viral RNA kit and reverse transcribed to cDNA using SuperScript III Reverse Transcriptase (Invitrogen, CA). The envelope genes were amplified from single-genome templates[37], and amplicons were directly sequenced using the ABI PRISM BigDye Terminator Cycle Sequencing Ready Reaction kit (Applied Biosystems, Foster City, CA) and resolved on an ABI 3100 automated genetic analyzer. The full-length *env* sequences were assembled and edited using Sequencher version 4.5 software (Genecodes, Ann Arbor, MI). Multiple sequence alignments were performed using Clustal X (version 1.83) and edited with BioEdit (version 7.0.9.0) Sequence alignments were visualized using Highlighter for Amino Acid Sequences version 1.1.0 (beta). Selected amplicons were cloned into the expression vector pcDNA 3.1 (directional) (Life Technologies) by reamplification of SGA first-round products using Fusion enzyme (Stratagene) with the EnvM primer[38] and the directional primer EnvAStop[39]. Cloned *env* genes were sequenced to confirm that they exactly matched the sequenced amplicon, and assayed for function by transfection in 293T cells, as described below.

Site-directed mutagenesis. CAP256 15-wk SU was mutated at positions 169 and 166 by site-directed mutagenesis using the Stratagene QuikChange II kit (Stratagene) as described by the manufacturer. Mutations were confirmed by sequencing.

Antibody next-generation sequence analysis. NGS reads from each time point were processed with an antibodyomics approach described previously[7]. Reads with successfully assigned V and J genes, an in-frame junction and no stop codons were clustered at 97.25% nucleotide sequence identity with CD-HIT to account for possible sequencing error and singletons were discarded. For those remaining reads assigned to VH3-30, divergence from VH and identity to the previously determined UCA[7] were calculated with Clustalw2. Density plots for these sequences were generated using the kde2d function in R. A maximum likelihood tree was built using FastML as described[7]. The tree was collapsed for display by clustering CDRH3 sequences as described[7] using a 90% identity threshold and a minimum of three sequences to define a major branch.

Antibody expression. Equal quantities of antibody heavy and light chain plasmids were co-transfected into FreeStyle 293F cells (Life Technologies) using the PEIMAX transfection reagent (Polysciences). Monoclonal antibodies were purified from cell-free supernatants after 6 d using protein A affinity chromatography.

Neutralization assays. The JC53bl-13 (TZM-bl) and 293T cell lines, confirmed to be free of *Mycoplasma*, were cultured in DMEM (Gibco BRL Life Technologies) containing 10% heat-inactivated FBS and 50 μg/ml gentamicin (Sigma). Cell monolayers were disrupted at confluency by treatment with 0.25% trypsin in 1 mM EDTA (Gibco BRL Life Technologies). Env-pseudotyped viruses were obtained by co-transfecting the Env plasmid with pSG3ΔEnv[40], using the FuGENE transfection reagent (Roche) as previously described[1]. Neutralization was measured as described by a reduction in luciferase gene expression after single-round infection of JC53bl-13 cells with Env-pseudotyped viruses[1]. Titers were calculated as the reciprocal plasma dilution (ID_{50}) causing 50% reduction of relative light units (RLU). Viral and antibody hierarchical clustering based on neutralization profiles was performed using the Heatmap Hierachical Clustering tool on the LANL HIV sequence database http://www.hiv.lanl.gov/content/sequence/HEATMAP/heatmap.html.

Images. Electron microscopy and protein structure representations were created with Chimera 1.5.3rc and The PyMOL Molecular Graphics System, Version 1.3r1edu, Schrödinger LLC. Neutralization images were created in GraphPad Prism6, sequence alignments were made with BioEdit[41] and phylogenetic trees were edited in FigTree 1.4.2.

27. van Loggerenberg, F. *et al.* Establishing a cohort at high risk of HIV infection in South Africa: challenges and experiences of the CAPRISA 002 acute infection study. *PLoS ONE* **3**, e1954 (2008).
28. Jabara, C.B., Jones, C.D., Roach, J., Anderson, J.A. & Swanstrom, R. Accurate sampling and deep sequencing of the HIV-1 protease gene using a Primer ID. *Proc. Natl. Acad. Sci. USA* **108**, 20166–20171 (2011).
29. Goecks, J., Nekrutenko, A., Taylor, J. & Galaxy, T. Galaxy: a comprehensive approach for supporting accessible, reproducible, and transparent computational research in the life sciences. *Genome Biol.* **11**, R86 (2010).
30. Blankenberg, D. *et al.* Galaxy: a web-based genome analysis tool for experimentalists. *Curr. Protoc. Mol. Biol.* **89**, 19.10.1–19.10.21 (2010).

© 2015 Nature America, Inc. All rights reserved.

31. Giardine, B. *et al.* Galaxy: a platform for interactive large-scale genome analysis. *Genome Res.* **15**, 1451–1455 (2005).
32. Blankenberg, D. *et al.* Manipulation of FASTQ data with Galaxy. *Bioinformatics* **26**, 1783–1785 (2010).
33. Katoh, K. & Standley, D.M. MAFFT multiple sequence alignment software version 7: improvements in performance and usability. *Mol. Biol. Evol.* **30**, 772–780 (2013).
34. Edgar, R.C. MUSCLE: multiple sequence alignment with high accuracy and high throughput. *Nucleic Acids Res.* **32**, 1792–1797 (2004).
35. Wright, I.A. & Travers, S.A. RAMICS: trainable, high-speed and biologically relevant alignment of high-throughput sequencing reads to coding DNA. *Nucleic Acids Res.* **42**, e106 (2014).
36. Hunter, J.D. Matplotlib: A 2D graphics environment. *Comput. Sci. Eng.* **9**, 90–95 (2007).
37. Salazar-Gonzalez, J.F. *et al.* Deciphering human immunodeficiency virus type 1 transmission and early envelope diversification by single-genome amplification and sequencing. *J. Virol.* **82**, 3952–3970 (2008).
38. Gao, F. *et al.* Molecular cloning and analysis of functional envelope genes from human immunodeficiency virus type 1 sequence subtypes A through G. The WHO and NIAID Networks for HIV Isolation and Characterization. *J. Virol.* **70**, 1651–1667 (1996).
39. Kraus, M.H. *et al.* A rev1-vpu polymorphism unique to HIV-1 subtype A and C strains impairs envelope glycoprotein expression from rev-vpu-env cassettes and reduces virion infectivity in pseudotyping assays. *Virology* **397**, 346–357 (2010).
40. Wei, X. *et al.* Antibody neutralization and escape by HIV-1. *Nature* **422**, 307–312 (2003).
41. Hall, T.A. BioEdit: a user-friendly biological sequence alignment editor and analysis program for Windows 95/98/NT. *Nucl. Acids. Symp. Ser.* **41**, 95–98 (1999).

© 2015 Nature America, Inc. All rights reserved.

doi:10.1038/nm.3963

Paper 3: Supplementary Information

SUPPLEMENTARY MATERIAL

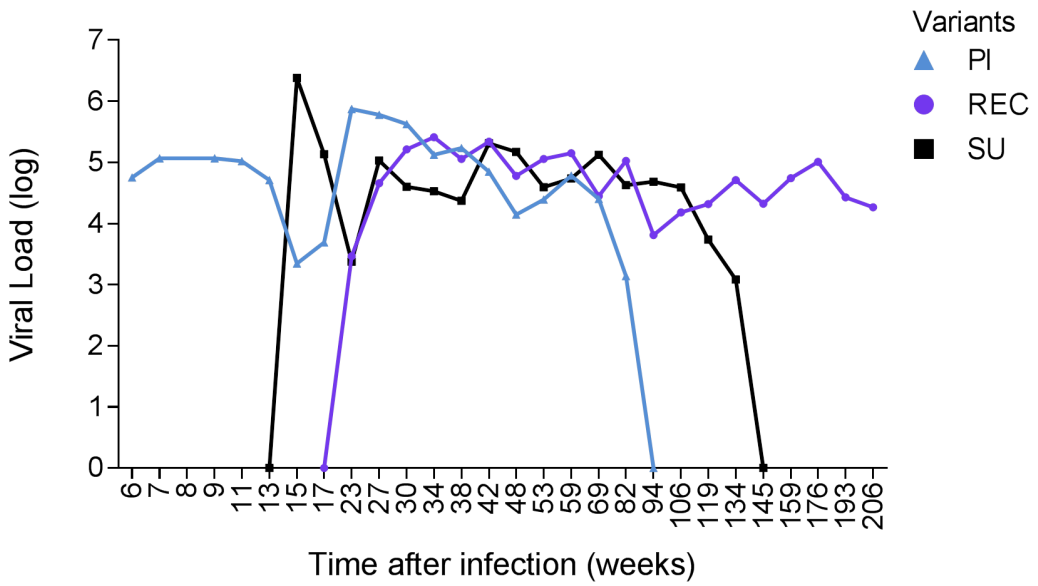
Viral variants that initiate and drive maturation of V1V2-directed HIV-1 broadly neutralizing antibodies

Jinal N. Bhiman[1,2], Colin Anthony[3], Nicole A. Doria-Rose[4], Owen Karimanzira[1], Chaim A. Schramm[5], Thandeka Khoza[1], Dale Kitchin[1], Gordon Botha[3], Jason Gorman[4], Nigel J. Garrett[6], Salim S. Abdool Karim[6],Lawrence Shapiro[4,5], Carolyn Williamson[3.6,7], Peter D. Kwong[4], John R. Mascola[4], Lynn Morris[1,2,6] and Penny L. Moore[1,2,6]

Nature Medicine: doi:10.1038/nm.3963

Primer name	Sequence
env_C3_cDNA primer	5'-GCCTTGCCACACGCTCAGNNNNNNNNNGTTGTAAYTTCTAGRTCCCCTCCTG-3'
env_V1V2_F1_1	5'-TCGTCGGCAGCGTCAGATGTGTATAAGAGACAGTATGGGATSAAAGYCTMAARCCATGTG-3'
env_V1V2_F1_2	5'-TCGTCGGCAGCGTCAGATGTGTATAAGAGACAGNTATGGGATSAAAGYCTMAARCCATGTG-3'
env_V1V2_F1_3	5'-TCGTCGGCAGCGTCAGATGTGTATAAGAGACAGNNTATGGGATSAAAGYCTMAARCCATGTG-3'
env_V1V2_F1_4	5'-TCGTCGGCAGCGTCAGATGTGTATAAGAGACAGNNNTATGGGATSAAAGYCTMAARCCATGTG-3'
Univ_i7_Rev_1	5'-GTCTCGTGGGCTCGGAGATGTGTATAAGAGACAGGCCTTGCCACACGCTCAG-3'
Univ_i7_Rev_2	5'-GTCTCGTGGGCTCGGAGATGTGTATAAGAGACAGNGCCTTGCCACACGCTCAG-3'
Univ_i7_Rev_3	5'-GTCTCGTGGGCTCGGAGATGTGTATAAGAGACAGNNGCCTTGCCACACGCTCAG-3'
Univ_i7_Rev_4	5'-GTCTCGTGGGCTCGGAGATGTGTATAAGAGACAGNNNGCCTTGCCACACGCTCAG-3'

Supplementary Table 1 PCR primers used to prepare V1V2 amplicons for MiSeq next-generation sequencing.



Supplementary Figure 1 Change in viral load over time in CAP256. Sequences were classified as PI-like (black), SU-like (blue) or REC (purple) based on their relative Hamming distance away from PI, as described in Fig 1a. The number of viral copies for each population was derived from its relative proportion of the total viral load per time point (y-axis) and is shown versus weeks after infection (x-axis).

Nature Medicine: doi:10.1038/nm.3963

a

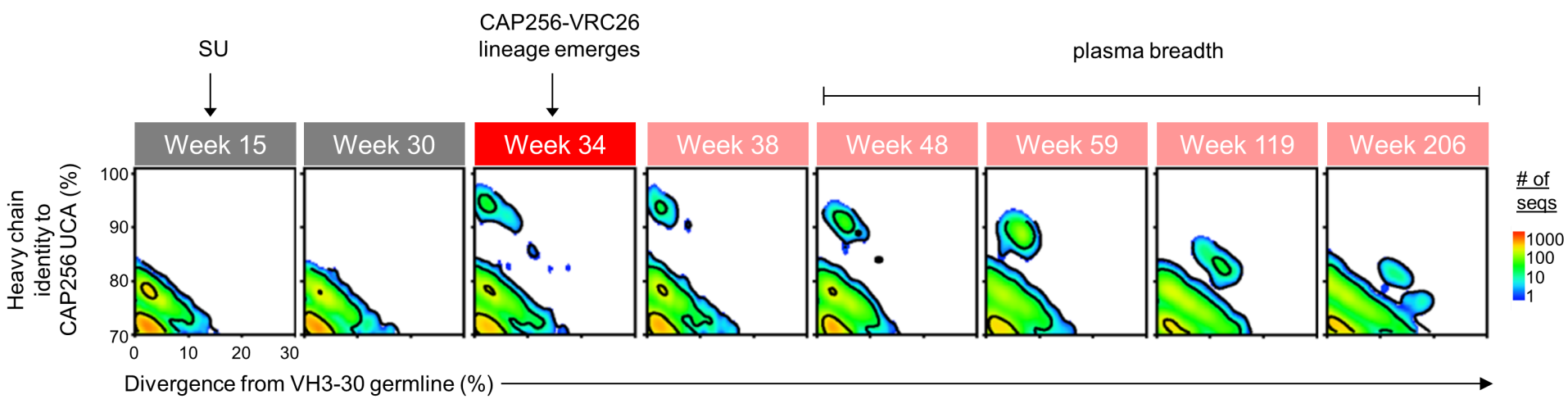
Weeks p.i.	Read count (post quality filter)	Number of consensus sequences	Amino acid frequenices at positon 169 (%)											
			-	A	E	G	H	I	K	L	Q	R	T	M
6	39105	1108	0	0	0	0	0	0	0	0	100	0	0	0
7	92828	1280	0	0	0	0	0	0	0	0	100	0	0	0
8	76182	689	0.1	0	0	0	0	0	0	0.1	99.6	0.1	0	0
9	56436	551	0.4	0	0	0	0	0	0	0	99.5	0.2	0	0
11	59209	563	0	0	0	0	0	0	0	0	100	0	0	0
13	38617	541	0	0	0	0	0	0	0	0	99.8	0.2	0	0
15	139026	3228	0	0	0	0	0	0	99.8	0	0.1	0	0	0
17	21526	405	0	0	2	0	0	0	94	0	3	0	0	0
23	64451	2839	0	0	0	0	0	0	0.2	0	99.6	0	0	0
27	80750	2515	0	0	0.2	0	0	0	13	0	86	0	1	0
30	35354	195	0	0	1	0	0	0	3	0	93	1	3	0
34	92614	937	0	0	0.3	0	0	3.2	3	0	92	0.5	0.4	0
38	96949	815	0	0	0	0	0.1	3	1	0	93	1	2	0
42	62527	906	0	0.4	1	0	0.1	30	1	0	59	4	4	0.1
48	49555	498	0	0	1	0.2	0	47	0	0	52	0	1	0
53	59529	567	0	0	0	0	0	10	0.4	0	89	0	0	0
59	43827	546	0	0	4	0	0	8	0.2	0	88	0	0	0
69	20937	261	0	0	8	0	0	10	4	0.4	78	0	0	0
82	32402	218	0	0	1	0	0	0	0	0	99	0	0	0
94	23847	265	0.4	0	10	0	0	79	3	0	8	0	0	0
106	22058	220	0	0	25	0	0	58	0.5	0	16	0	0	0
119	32228	503	0	0	11	0	0	22	2	0	66	0	0	0
134	16784	262	0	0	35	0	0	2	0.4	0	62	0	0	0
145	30809	421	0	0	79	0	0	0.2	0.2	0	21	0	0	0
159	36680	316	0	0	49	0	0	0	0	0	51	0	0	0
176	30745	305	0	0	16	0	0	0	0	0	84	0	0	0
193	54263	724	0	0	98	0	0	0	0	0	2	0	0	0
206	29435	386	0	0	99.7	0	0	0	0	0	0.3	0	0	0

b

Weeks p.i.	Read count (post quality filter)	Number of consensus sequences	Amino acid frequencies at position 166 (%)					
			-	G	K	R	S	T
6	39105	1108	0	0	0	100	0	0
7	92828	1280	0	0	0	100	0	0
8	76182	689	0.1	0	0	99.9	0	0
9	56436	551	1	0.4	0	99.1	0	0
11	59209	563	0	0	0	100	0	0
13	38617	541	0	0	0	100	0	0
15	139026	3228	0	0	0	100	0	0
17	21526	405	0	0	0	100	0	0
23	64451	2839	0	0	0	100	0	0
27	80750	2515	0	0	0	100	0	0
30	35354	195	0	0	0	100	0	0
34	92614	937	0	0	0.1	99.9	0	0
38	96949	815	0	0.1	0.1	99.8	0	0
42	62527	906	0	0	0.3	99.6	0.1	0
48	49555	498	0	0	0.2	99	0	0.4
53	59529	567	0	0	0.2	98	0	1
59	43827	546	0	0	2	86	0.2	11
69	20937	261	0	0	23	76	0	2
82	32402	218	0	0	35	63	0	2
94	23847	265	0.4	0	89	10	0	0.4
106	22058	220	0	0	52	45	0	4
119	32228	503	0	0	90	9	1	0
134	16784	262	0	0	13	49	37	0
145	30809	421	0	0	1	89	10.2	0
159	36680	316	0	0	0	49	51	0
176	30745	305	0	0	0	18	82	0
193	54263	724	0	0	0	98	2	0
206	29435	386	0	0	0	99.7	0.3	0

50 -100%
10 - 49%
0.01 - 9%
0%

Supplementary Figure 2 Frequency of amino acids or immunotypes (%) at positions (a) 169 and (b) 166 in V1V2 next-generation consensus sequences between 6 and 206 weeks after infection. Read depth after quality filtering is shown for each time-point. Green, blue, or purple shading indicates ranges of amino acid frequencies, as shown in the key.



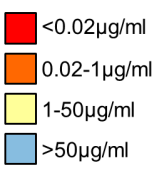
Supplementary Figure 3 Detection of the CAP256-VRC26 lineage in the periphery. Heat map plots show sequence identity to the UCA (y-axis) versus germline divergence (x-axis) for all VH3-30*18 sequences identified in antibody next-generation sequences (NGS) from 15 to 206 weeks. The time of superinfection (SU), the emergence of the CAP256-VRC26 NGS transcripts and onset of plasma breadth are shown. Frequency of sequences is coloured as indicated by the key. Previously published data7 did not include this 34-week time-point.

Nature Medicine: doi:10.1038/nm.3963

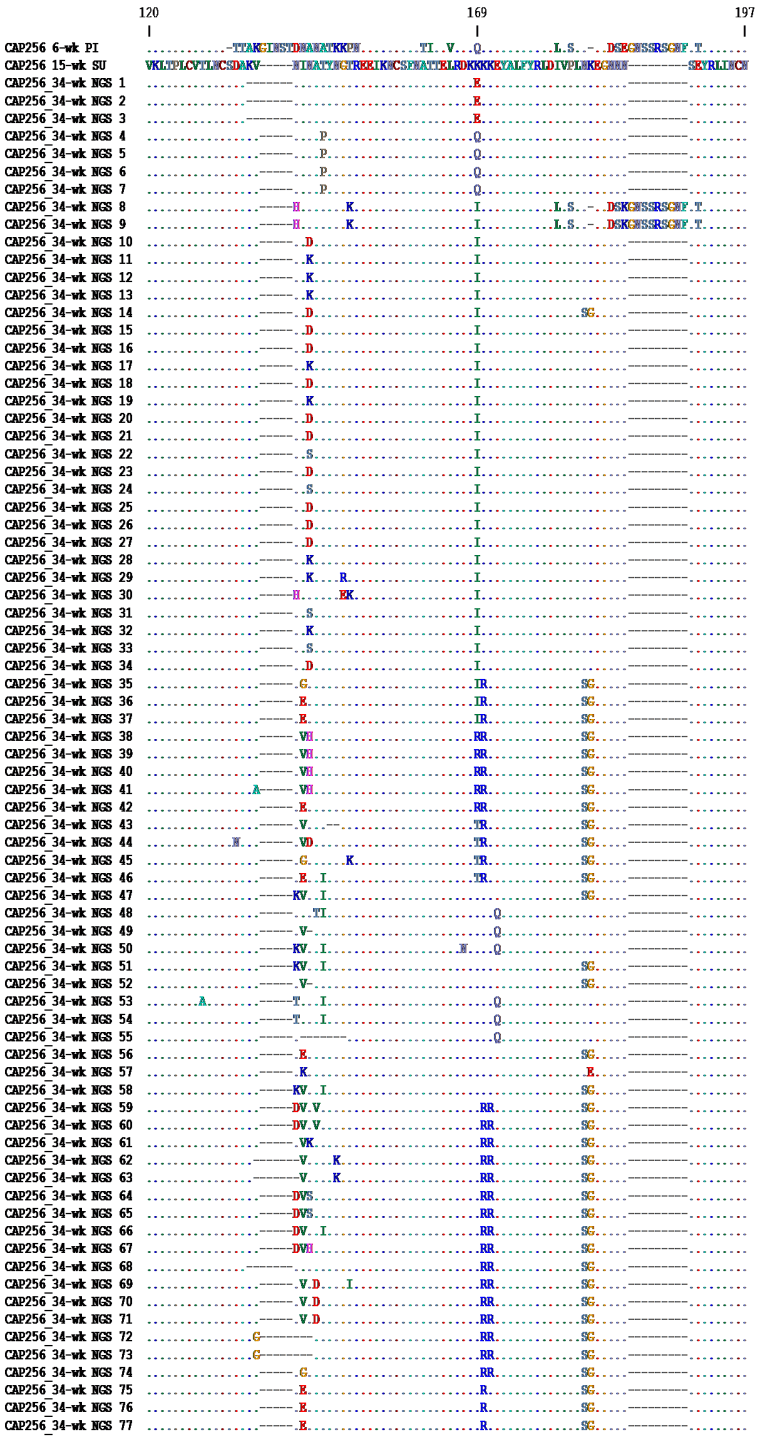
Virus	Clade	IC_{50}
0260.v5.c36	A	>50
0330.v4.c3	A	>50
0439.v5.c1	A	>50
3365.v2.c20	A	>50
3415.v1.c1	A	>50
3718.v3.c11	A	>50
BB201.B42	A	>50
BI369.9A	A	>50
BS208.B1	A	>50
KER2008.12	A	>50
KER2018.11	A	>50
KNH1209.18	A	>50
MB201.A1	A	>50
MB539.2B7	A	>50
MI369.A5	A	>50
MS208.A1	A	>50
Q23.17	A	>50
Q259.17	A	>50
Q769.d22	A	>50
Q769.h5	A	>50
Q842.d12	A	>50
QH209.14M.A2	A	>50
RW020.2	A	>50
UG037.8	A	>50
246-F3.C10.2	AC	>50
3301.V1.C24	AC	>50
3589.V1.C4	AC	>50
6540.v4.c1	AC	>50
6545.V4.C1	AC	>50
0815.V3.C3	ACD	>50
6095.V1.C10	ACD	>50
3468.V1.C12	AD	>50
Q168.a2	AD	>50
Q461.e2	AD	>50
620345.c1	AE	>50
BJOX009000.02.4	AE	>50
BJOX010000.06.2	AE	>50
BJOX025000.01.1	AE	>50
BJOX028000.10.3	AE	>50
C1080.c3	AE	>50
C2101.c1	AE	>50
C4118.09	AE	>50
CNE3	AE	>50
CNE5	AE	>50
CNE55	AE	>50
CNE56	AE	>50
CNE59	AE	>50
CNE8	AE	>50
M02138	AE	>50
R1166.c1	AE	>50
R2184.c4	AE	>50
TH966.8	AE	>50
TH976.17	AE	>50
235-47	AG	>50
242-14	AG	>50
263-8	AG	>50
269-12	AG	>50
271-11	AG	>50
928-28	AG	>50
DJ263.8	AG	>50
T250-4	AG	>50
T251-18	AG	>50
T253-11	AG	>50
T255-34	AG	>50
T257-31	AG	>50
T266-60	AG	>50

Virus	Clade	IC_{50}
T278-50	AG	>50
T280-5	AG	>50
T33-7	AG	>50
3988.25	B	>50
5768.04	B	>50
6101.10	B	>50
6535.3	B	>50
7165.18	B	>50
45_01dG5	B	>50
89.6.DG	B	>50
AC10.29	B	>50
ADA.DG	B	>50
Bal.01	B	>50
BaL.26	B	>50
BG1168.01	B	>50
BL01.DG	B	>50
BR07.DG	B	>50
BX08.16	B	>50
CAAN.A2	B	>50
CNE10	B	>50
CNE12	B	>50
CNE14	B	>50
CNE4	B	>50
CNE57	B	>50
HO86.8	B	>50
HT593.1	B	>50
HXB2.DG	B	>50
JRCSF.JB	B	>50
JRFL.JB	B	>50
MN.3	B	>50
PVO.04	B	>50
QH0515.01	B	>50
QH0692.42	B	>50
REJO.67	B	>50
RHPA.7	B	>50
SC422.8	B	>50
SF162.LS	B	>50
SS1196.01	B	>50
THRO.18	B	>50
TRJO.58	B	>50
TRO.11	B	>50
WITO.33	B	>50
X2278.C2.B1	B	>50
YU2.DG	B	>50
BJOX002000.03.2	BC	>50
CH038.12	BC	>50
CH070.1	BC	>50
CH117.4	BC	>50
CH119.10	BC	>50
CH181.12	BC	>50
CNE15	BC	>50
CNE20	BC	>50
CNE21	BC	>50
CNE40	BC	>50
CNE7	BC	>50
286.36	C	>50
288.38	C	>50
0013095-2.11	C	>50
001428-2.42	C	>50
0077_V1.C16	C	>50
00836-2.5	C	>50
0921.V2.C14	C	>50
16055-2.3	C	>50
16845-2.22	C	>50
16936-2.21	C	>50
25710-2.43	C	>50

Virus	Clade	IC_{50}
25711-2.4	C	>50
25925-2.22	C	>50
26191-2.48	C	>50
3168.V4.C10	C	>50
3637.V5.C3	C	>50
3873.V1.C24	C	>50
6322.V4.C1	C	>50
6471.V1.C16	C	>50
6631.V3.C10	C	>50
6644.V2.C33	C	>50
6785.V5.C14	C	>50
6838.V1.C35	C	>50
96ZM651.02	C	>50
BR025.9	C	>50
CAP210.E8	C	>50
CAP244.D3	C	>50
CAP45.G3	C	>50
Ce1176.A3	C	>50
CE703010217.B6	C	>50
CNE30	C	>50
CNE31	C	>50
CNE53	C	>50
CNE58	C	>50
DU123.06	C	>50
DU151.02	C	>50
DU156.12	C	>50
DU172.17	C	>50
DU422.01	C	>50
MW965.26	C	>50
SO18.18	C	>50
TV1.29	C	>50
TZA125.17	C	>50
TZBD.02	C	>50
ZA012.29	C	>50
ZM106.9	C	>50
ZM109.4	C	>50
ZM135.10a	C	>50
ZM176.66	C	>50
ZM197.7	C	>50
ZM214.15	C	>50
ZM215.8	C	>50
ZM233.6	C	>50
ZM249.1	C	>50
ZM53.12	C	>50
ZM55.28a	C	>50
3326.V4.C3	CD	>50
3337.V2.C6	CD	>50
3817.v2.c59	CD	>50
191821.E6.1	D	>50
231965.c1	D	>50
247-23	D	>50
3016.v5.c45	D	>50
57128.wrc15	D	>50
6405.v4.c34	D	>50
A03349M1.wrc4a	D	>50
NKU3006.ec1	D	>50
UG021.16	D	>50
UG024.2	D	>50
P0402.c2.11	G	>50
P1981.C5.3	G	>50
X1193.c1	G	>50
X1254.c3	G	>50
X1632.S2.B10	G	>50
X2088.c9	G	>50

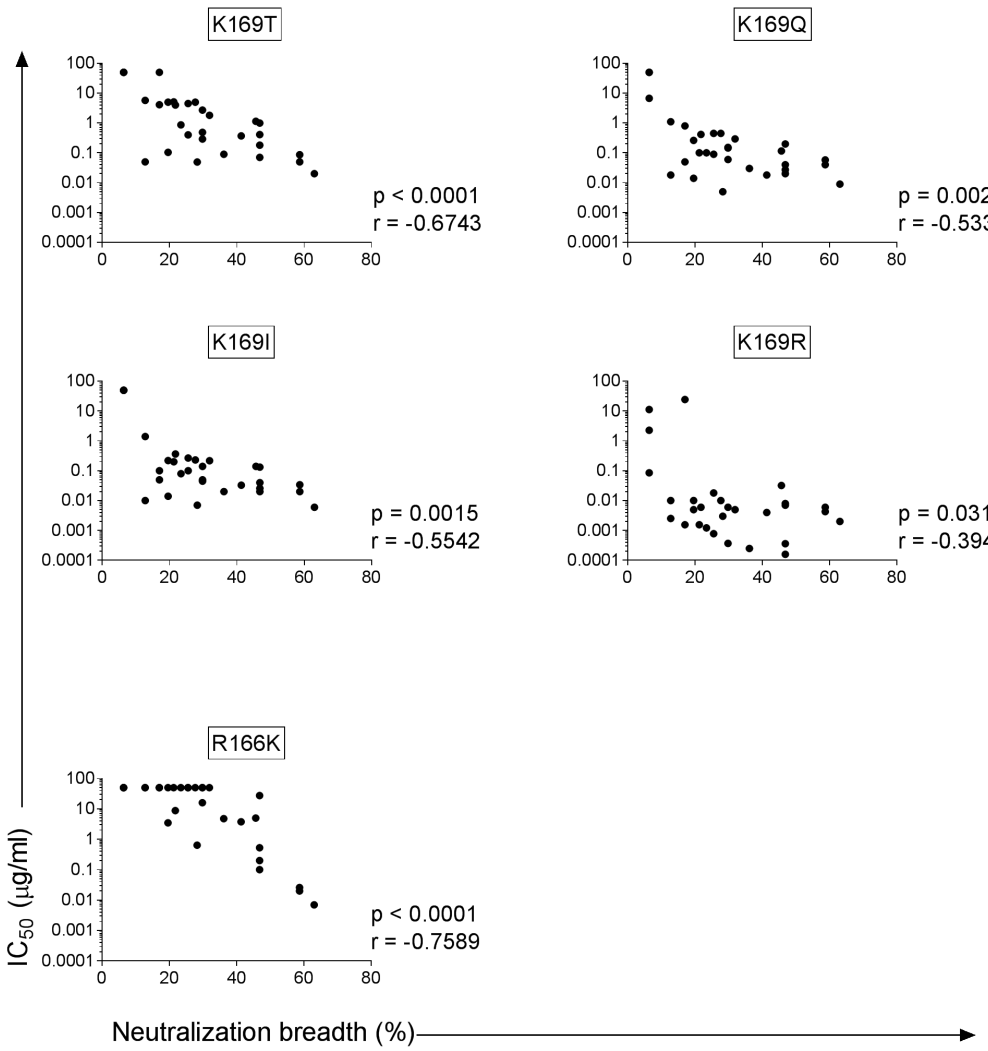


Supplementary Figure 4 CAP256-VRC26 UCA neutralization of a panel of 196 heterologous HIV-1 viruses from multiple subtypes. Values shown are IC50 values with a starting concentration of 50 µg/ml, and >50 indicating no neutralization, as indicated in the key.



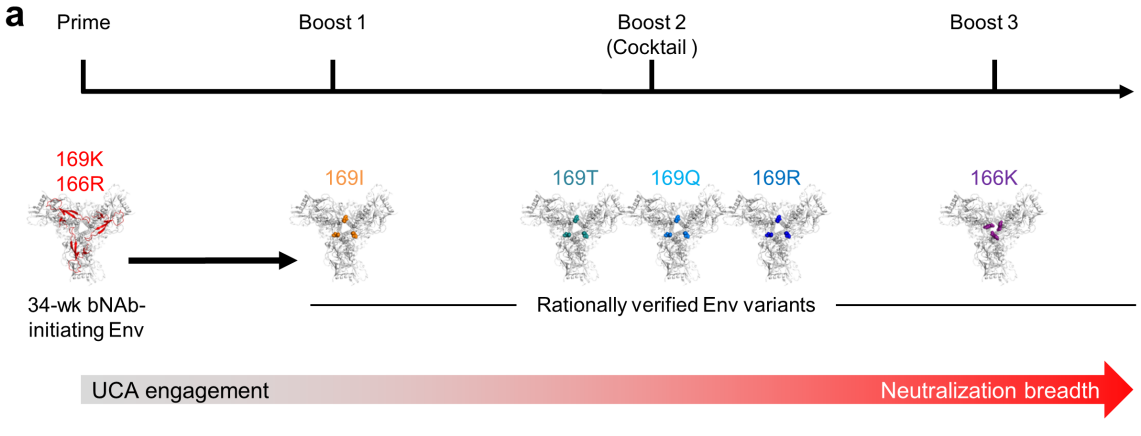
Supplementary Figure 5 Amino acid alignment of the 34-week V1V2 next-generation consensus sequences (HXB2 positions 120-197). Amino acid identity to the superinfecting virus (15-wk SU) is shown as dots, while deletions are shown as dashes. The primary infecting virus (6-wk PI) is also included in the alignment. Residues are coloured according to BioEdit amino acid assignments.

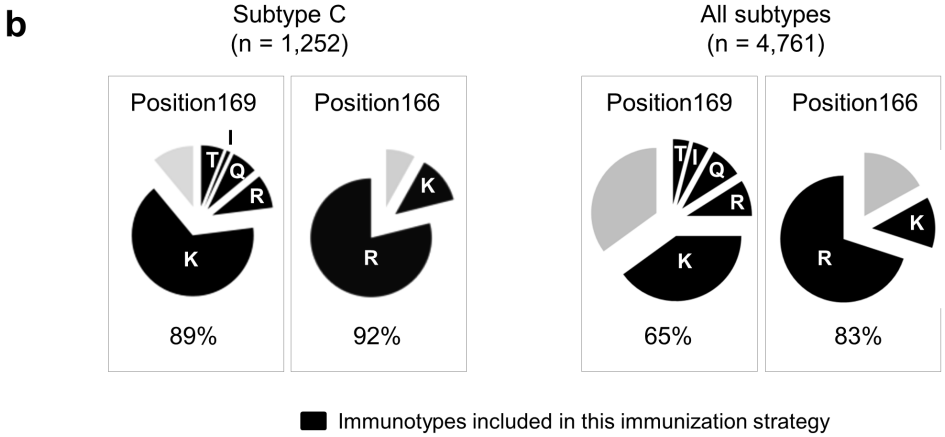
Nature Medicine: doi:10.1038/nm.3963



Supplementary Figure 6 CAP256-VRC26 mAb neutralization of 169/166 mutants and correlation with neutralization breadth. A two-tailed Spearman rank test was used to calculate the *r* and *P* values between IC_{50} neutralization titers of K169T/Q/I/R or R166K mutants (IC_{50} titres on the y-axis) and heterologous neutralization breadth (percentage on the x-axis).

Nature Medicine: doi:10.1038/nm.3963





Supplementary Figure 7 Recapitulating viral evolution for vaccine design. (**a)** A proposed prime-sequential boost immunization strategy to elicit V1V2-directed bNAbs, based on the key viral events that initiated and drove neutralization breadth in the CAP256-VRC26 lineage. A CAP256 34-week bNAb-initiating Env (red), which has the 169K and 166R immunotypes, would be used as a prime to engage UCAs with long CDRH3s. This would be followed by three sequential boosts using immunogens with varying immunotypes to mimic the viral diversification in CAP256 that drove bNAb development. The 169I boost (orange) would be administered first, followed by a cocktail of 169T/Q and R immunogens (blue) and a final boost to expose vaccine-induced mAbs to the 166K immunotype (purple). (**b**) Prevalence of major immunotypes among subtype C and all global viruses are shown in pie charts, with those included in the proposed immunization schedule shaded black. The proposed schedule is tailored towards subtype C viruses using experimentally validated immunotypes. However, vaccine coverage may potentially be enhanced for subtype B viruses by addition of a 169V immunotype.

Nature Medicine: doi:10.1038/nm.3963

Appendix 1: Letter of Support

NATIONAL INSTITUTE FOR COMMUNICABLE DISEASES
Division of the National Health Laboratory Service

Centre for HIV & STI's: HIV Virology Section
1 Modderfontein Road, Sandringham, 2031
Tel: +27 (0)11 386 6331 Fax: +27 (0)11 386 6333
Email: pennym@nicd.ac.za

25 February 2016

To whom it may concern,

Published papers included in PhD thesis: Jinal N Bhiman

We are writing to confirm Jinal Bhiman's substantial role in the three multi-authored papers (one of which is a first author paper) that form part of her PhD thesis.

1. Doria-Rose *et al*, Nature, 2014

Jinal was extensively involved in the data generation for this paper, performing antibody isolation and characterization as well as viral genome amplification and sequencing and viral mutant generation. As such Jinal directly contributed to three of the six main figures and four of the nine extended data figures. In addition she was involved in all stages of writing the paper making substantial intellectual contributions. For these reasons, Jinal is second author (after co-first authors) on an extremely high impact paper with 46 co-authors.

2. Doria-Rose *et al*, Journal of Virology, 2016

Jinal is the second author on this paper as she isolated eight of the 21 antibodies described in the paper, performed some of the characterisation of all of the antibodies, and contributed to four of the eight main figures. Jinal did not write this paper, but made edits to all drafts, including addition of results and discussion points.

3. Bhiman *et al*, Nature Medicine, 2015

Jinal led all laboratory aspects of this paper. She generated 80% of the data with great independence. Together with her supervisors, she created all figures and wrote the manuscript and as is therefore the first author on this paper.

Jinal's significant contribution to these high impact peer-reviewed papers are testament to the high quality of her research.

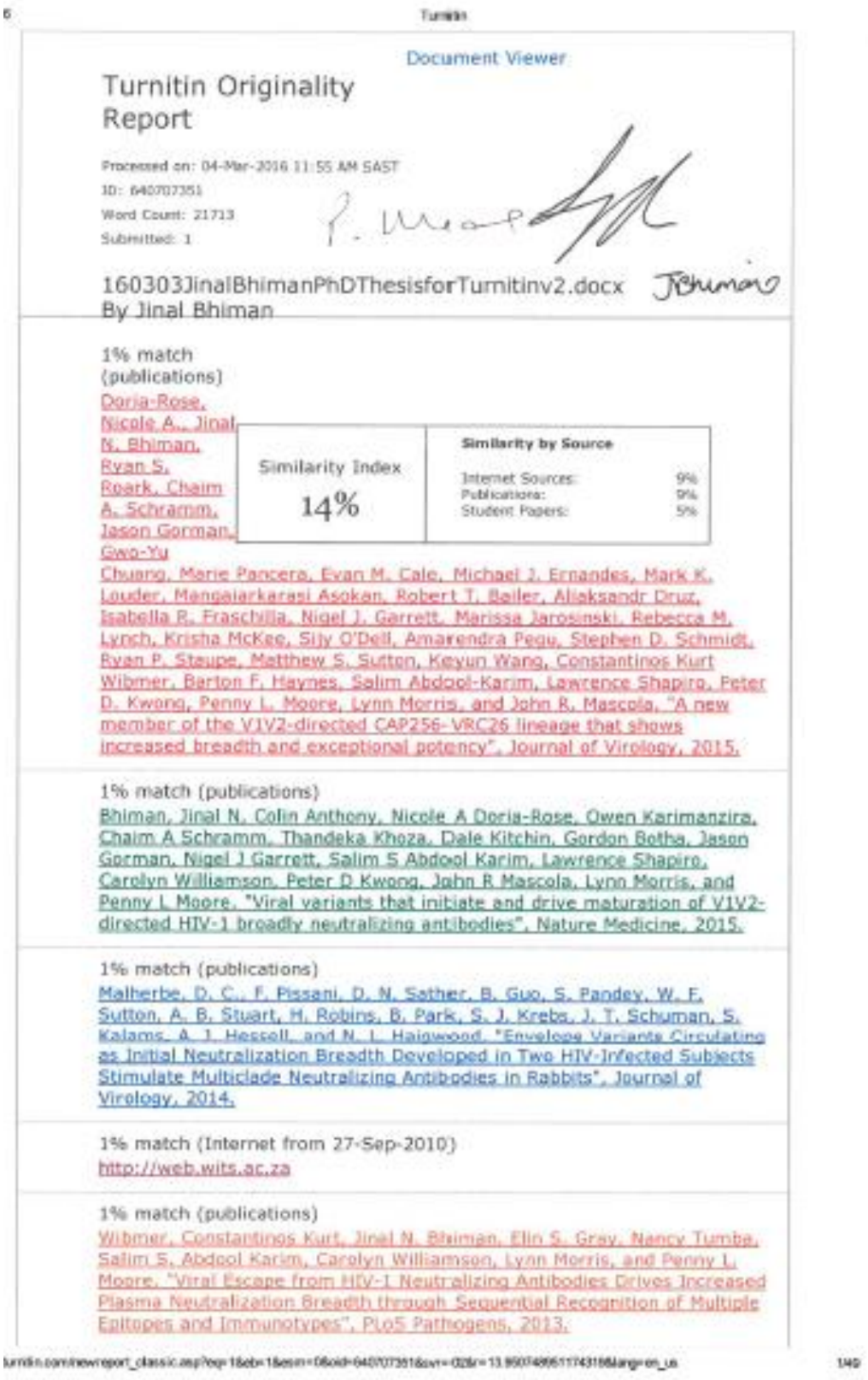
Yours Sincerely,

Prof Penny Moore
Supervisor
SARChI Chair and Reader

Prof Lynn Morris
Co-Supervisor
Research Prof. and HOD

Dr Nicole Doria-Rose
Chief, Humoral Immunology Core
Vaccine Research Center

Appendix 2: Turnitin Report



6 Turnitin

Document Viewer

Turnitin Originality Report

Processed on: 04-Mar-2016 11:55 AM SAST
ID: 640707351
Word Count: 21713
Submitted: 1

160303JinalBhimanPhDThesisforTurnitinv2.docx
By Jinal Bhiman

Similarity Index	Similarity by Source	
14%	Internet Sources:	9%
	Publications:	9%
	Student Papers:	5%

1% match (publications)
Doria-Rose, Nicole A., Jinal N. Bhiman, Ryan S. Roark, Chaim A. Schramm, Jason Gorman, Gwo-Yu Chuang, Marie Pancera, Evan M. Cale, Michael J. Ernandes, Mark K. Louder, Mangaiarkarasi Asokan, Robert T. Bailer, Aliaksandr Druz, Isabella R. Fraschilla, Nigel J. Garrett, Marissa Jarosinski, Rebecca M. Lynch, Krisha McKee, Siny O'Dell, Amarendra Pegu, Stephen D. Schmidt, Ryan P. Staupe, Matthew S. Sutton, Keyun Wang, Constantinos Kurt Wibmer, Barton F. Haynes, Salim Abdool-Karim, Lawrence Shapiro, Peter D. Kwong, Penny L. Moore, Lynn Morris, and John R. Mascola, "A new member of the V1V2-directed CAP256-VRC26 lineage that shows increased breadth and exceptional potency", Journal of Virology, 2015.

1% match (publications)
Bhiman, Jinal N., Colin Anthony, Nicole A Doria-Rose, Owen Karimanzira, Chaim A Schramm, Thandeka Khoza, Dale Kitchin, Gordon Botha, Jason Gorman, Nigel J Garrett, Salim S Abdool Karim, Lawrence Shapiro, Carolyn Williamson, Peter D Kwong, John R Mascola, Lynn Morris, and Penny L Moore, "Viral variants that initiate and drive maturation of V1V2-directed HIV-1 broadly neutralizing antibodies", Nature Medicine, 2015.

1% match (publications)
Malherbe, D. C., F. Pissani, D. N. Sather, B. Guo, S. Pandey, W. F. Sutton, A. B. Stuart, H. Robins, B. Park, S. J. Kreba, J. T. Schuman, S. Kalams, A. J. Hessell, and N. L. Haigwood, "Envelope Variants Circulating as Initial Neutralization Breadth Developed in Two HIV-Infected Subjects Stimulate Multiclade Neutralizing Antibodies in Rabbits", Journal of Virology, 2014.

1% match (Internet from 27-Sep-2010)
http://web.wits.ac.za

1% match (publications)
Wibmer, Constantinos Kurt, Jinal N. Bhiman, Elin S. Gray, Nancy Tumba, Salim S. Abdool Karim, Carolyn Williamson, Lynn Morris, and Penny L. Moore, "Viral Escape from HIV-1 Neutralizing Antibodies Drives Increased Plasma Neutralization Breadth through Sequential Recognition of Multiple Epitopes and Immunotypes", PLoS Pathogens, 2013.

turnitin.com/newreport_classic.asp?oid=640707351&lang=en_us 1/40

Appendix 3: Change of Title

UNIVERSITY OF THE WITWATERSRAND, JOHANNESBURG

Private Bag 3 Wits, 2050
Fax: 027117172119
Tel: 02711 7172076

Reference: Ms Thokozile Nhlapo
E-mail: thokozile.nhlapo@wits.ac.za

30 October 2015
Person No: 0408743N
TAA

Ms JN Bhiman
Box 32269
Braamfontein
2017
South Africa

Dear Ms Bhiman

Doctor of Philosophy: Change of title of research

I am pleased to inform you that the following change in the title of your Thesis for the degree of **Doctor of Philosophy** has been approved:

From:	**Affinity maturation of strain-specific neutralising antibodies in HIV-1 subtype C infection as a prerequisite for neutralisation breadth**
To:	**Defining virus-antibody interplay during the development of HIV-1 neutralization breadth to inform vaccine design**

Yours sincerely

Mrs Sandra Benn
Faculty Registrar
Faculty of Health Sciences

Appendix 4: Ethics Clearance

R14/49 Ms Jinal Nomathemba Bhiman et al

HUMAN RESEARCH ETHICS COMMITTEE (MEDICAL)

CLEARANCE CERTIFICATE NO. M130829

NAME: (Principal Investigator)	Ms Jinal Nomathemba Bhiman et al
DEPARTMENT:	Virology School of Pathology HIV Virology Section, Centre for HIV and STI
PROJECT TITLE:	Affinity Maturation of Strain-Specific Neutralising Antibodies in Human Immunodeficiency Virus Type 1 (HIV-1) Subtype C Infection as a Prerequisite for Neutralisation Breadth
DATE CONSIDERED:	30/08/2013
DECISION:	Approved unconditionally
CONDITIONS:	
SUPERVISOR:	Dr Penny L Moore and Prof Lynn Morris
APPROVED BY:	Professor PE Cleaton-Jones, Chairperson, HREC (Medical)
DATE OF APPROVAL:	30/08/2013

This clearance certificate is valid for 5 years from date of approval. Extension may be applied for.

DECLARATION OF INVESTIGATORS

To be completed in duplicate and **ONE COPY** returned to the Secretary in Room 10004, 10th floor, Senate House, University.
I/we fully understand the conditions under which I am/we are authorized to carry out the above-mentioned research and I/we undertake to ensure compliance with these conditions. Should any departure be contemplated, from the research protocol as approved, I/we undertake to resubmit the application to the Committee. **I agree to submit a yearly progress report**.

Principal Investigator Signature Date

PLEASE QUOTE THE PROTOCOL NUMBER IN ALL ENQUIRIES

Appendix 5: Copyright Permissions

1. Nature and Nature Medicine

"Ownership of copyright in original research articles remains with the Authors…"

http://www.nature.com/reprints/permission-requests.html

Permission requests



On this page

Nature Publishing Group grants permission for authors, readers and third parties to reproduce material from its journals and online products as part of another publication or entity. This includes, for example, the use of a figure in a presentation, the posting of an abstract on a web site, or the reproduction of a full article within another journal. Certain permissions can be granted free of charge; others incur a fee.

For answers to frequently asked questions click here

- Type of permission request
- Permission request options

Types of permission request

Permission can be obtained for re-use of portions of material - ranging from a single figure to a whole paper - in books, journals/magazines, newsletters, theses/dissertations, classroom materials/academic course packs, academic conference materials, training materials (including continuing medical education), promotional materials, and web sites. Some permission requests can be granted free of charge, others carry a fee.

Nature Publishing Group rarely grants free permission for PDFs of full papers to be reproduced online, however e-print PDFs can be purchased as commercial reprints. If you wish to purchase multiple stand-alone copies of a Nature Publishing Group paper, which is then printed and shipped to you, please go to commercial reprints.

Permission request options

Permission requests from authors

The authors of articles published by Nature Publishing Group, or the authors' designated agents, do not usually need to seek permission for re-use of their material as long as the journal is credited with initial publication. For further information about the terms of re-use for authors please see below.

Author Requests

If you are the author of this content (or his/her designated agent) please read the following. Since 2003, ownership of copyright in in original research articles remains with the Authors*, and provided that, when reproducing the Contribution or extracts from it, the Authors acknowledge first and reference publication in the Journal, the Authors retain the following non-exclusive rights:

a. To reproduce the Contribution in whole or in part in any printed volume (book or thesis) of which they are the author(s).

b. They and any academic institution where they work at the time may reproduce the Contribution for the purpose of course teaching.

c. To reuse figures or tables created by them and contained in the Contribution in other works created by them.

d. To post a copy of the Contribution as accepted for publication after peer review (in Word or Tex format) on the Author's own web site, or the Author's institutional repository, or the Author's funding body's archive, six months after publication of the printed or online edition of the Journal, provided that they also link to the Journal article on NPG's web site (eg through the DOI).

NPG encourages the self-archiving of the accepted version of your manuscript in your funding agency's or institution's repository, six months after publication. This policy complements the recently announced policies of the US National Institutes of Health, Wellcome Trust and other research funding bodies around the world. NPG recognizes the efforts of funding bodies to increase access to the research they fund, and we strongly encourage authors to participate in such efforts.

Authors wishing to use the published version of their article for promotional use or on a web site must request in the normal way.

2. Journal of Virology

“Authors also retain the right to reuse the full article I his/her dissertation or thesis.”

http://journals.asm.org/site/misc/reprints.xhtml



Copyright Clearance Center RightsLink®

Home | Create Account | Help | Live Chat

AMERICAN SOCIETY FOR MICROBIOLOGY

Title: New Member of the V1V2-Directed CAP256-VRC26 Lineage That Shows Increased Breadth and Exceptional Potency

Author: Nicole A. Doria-Rose, Jinal N. Bhiman, Ryan S. Roark et al.

Publication: Journal of Virology

Publisher: American Society for Microbiology

Date: Jan 1, 2016

Copyright © 2016, American Society for Microbiology

LOGIN

If you're a copyright.com user, you can login to RightsLink using your copyright.com credentials. Already a RightsLink user or want to learn more?

Permissions Request

Authors in ASM journals retain the right to republish discrete portions of his/her article in any other publication (including print, CD-ROM, and other electronic formats) of which he or she is author or editor, provided that proper credit is given to the original ASM publication. ASM authors also retain the right to reuse the full article in his/her dissertation or thesis. For a full list of author rights, please see: http://journals.asm.org/site/misc/ASM_Author_Statement.xhtml

BACK | CLOSE WINDOW

Copyright © 2016 Copyright Clearance Center, Inc. All Rights Reserved. Privacy statement. Terms and Conditions.
Comments? We would like to hear from you. E-mail us at customercare@copyright.com